

<http://researchspace.auckland.ac.nz>

ResearchSpace@Auckland

Copyright Statement

The digital copy of this thesis is protected by the Copyright Act 1994 (New Zealand).

This thesis may be consulted by you, provided you comply with the provisions of the Act and the following conditions of use:

- Any use you make of these documents or images must be for research or private study purposes only, and you may not make them available to any other person.
- Authors control the copyright of their thesis. You will recognise the author's right to be identified as the author of this thesis, and due acknowledgement will be made to the author where appropriate.
- You will obtain the author's permission before publishing any material from their thesis.

To request permissions please use the Feedback form on our webpage.

<http://researchspace.auckland.ac.nz/feedback>

General copyright and disclaimer

In addition to the above conditions, authors give their consent for the digital copy of their work to be used subject to the conditions specified on the [Library Thesis Consent Form](#) and [Deposit Licence](#).

Pharmacokinetic and Pharmacodynamic Modelling to Advance Perioperative Anaesthesia and Analgesia

Jacqueline Amy Hannam

*A thesis submitted in partial fulfilment of the requirements for the degree of
Doctor of Philosophy in Anaesthesiology, The University of Auckland, 2013.*

Abstract

The practice of anaesthesia involves creating profound drug effects (i.e. lack of awareness and sensation) and then reversing these rapidly. Endpoints are achieved by combining drugs that collectively contribute to desired effects. This requires an understanding of the pharmacological profile of drugs when given alone and alongside others. Pharmacokinetic (PK) and pharmacodynamic (PD) models summarise complex drug relationships so they may be better understood and capitalised on. I report my investigations into using PKPD models to describe combined drug responses for applications in anaesthesia.

I investigated analgesia in children using paracetamol with two non-steroidal anti-inflammatory drugs. Diclofenac dosing in children is currently extrapolated from adult data. I modelled paracetamol and diclofenac analgesia using a modified E_{MAX} model with placebo effects and interval censored dropout. Diclofenac and paracetamol effects were additive. Diclofenac analgesia had a maximal effect (E_{MAX}) of 4.8 cm (visual analogue pain scale 0-10), an equilibration half-life 0.23 h and Ce_{50} of 1.20 mg. Γ^1 in children after adeno-tonsillectomy. The hazard of dropping out was 1.36 for each unit in pain. This interaction model can be used to guide combination diclofenac and paracetamol dosing in children, and future study design of analgesics in similar populations.

I then developed a model describing processed electroencephalograph (EEG) response, using Bispectral Index (BIS), for multiple drug classes. I aimed to establish a model that could be used to simulate EEG response, as a cue of anaesthetic depth, in a human patient simulator (HPS). I developed a model for propofol-alfentanil BIS effects using response surface methodology, and established generalisability of this model to remifentanil. I investigated the use of a combined propofol-remifentanil PKPD model for BIS targeted infusion in surgical patients. Finally, I developed a model describing BIS effects for: propofol (an intravenous anaesthetic); midazolam (a sedative), alfentanil, fentanyl, remifentanil (phenyl-piperidine opioids); desflurane, isoflurane and sevoflurane (inhalation anaesthetics). This is the first study to describe propofol-midazolam BIS effects, which were additive. I discuss how the model might be used in the HPS with attention to creating realistic variability in response, and correlating BIS to manikin eye closure during induction. I anticipate that this work will improve our currently limited simulation of depth of anaesthesia, and enhance our anaesthetic-based simulations for students and experienced clinicians alike.

Acknowledgements

Completing this thesis has been a great experience. I attribute this entirely to the calibre of my supervisors and advisors, colleagues and workmates, and friends and family. Unfortunately this makes for quite a list of acknowledgements!

I gratefully acknowledge my supervisors Professor Alan Merry, Associate Professor Timothy Short and Associate Professor Ross Kennedy for their guidance and expertise.

I would like to thank Associate Professor Short for his enthusiasm and support throughout my studies. He also provided me with some ‘big ideas’ that laid the framework for a large part of my thesis.

I credit Professor Merry with my writing skills; this has been a hard fought battle over many years! His expertise in simulation, general oversight and attention to detail, have been great assets.

I also acknowledge my advisors Professors Brian Anderson and Nick Holford. Dr Anderson’s enthusiasm for modelling has been infectious, and he has spent many hours sharing his considerable knowledge on modelling and providing feedback on my work. The practical support and teaching I have received from Professor Holford has been invaluable.

I was lucky to inherit two datasets to analyse; Professors Anderson and Holford shared their diclofenac/paracetamol data; and Associate Professor Short shared his propofol/alfentanil data. The generosity of my supervisors and advisors in this regard has been outstanding. I would also like to acknowledge those who have shared their published data for pooled analyses: Dr Joseph Standing, Dr Steven Shafer and Rosemount Pharmaceuticals.

I gratefully acknowledge the Green Lane Research and Educational Fund who provided me with a doctoral stipend, and also Aspect Medical Systems who provided me with a grant to purchase study consumables. I also received travel grants from the Royal Society of New Zealand, and the FMHS Postgraduate Students' Association (PGSA) to attend conferences and workshops.

I would like to thank the staff on Levels 4 and 8 of Auckland City Hospital for welcoming me into their theatres. I particularly thank Dr Chris Chambers for letting me convert his laptop into a dedicated study computer, and my study ‘champions’ Drs Doug Campbell, Lara Hopley, Martin Misur and Stephen Laurent. They have consistently made my research a priority, often at their own inconvenience, and shown a genuine interest in my work.

Several individuals have volunteered their expertise. Dr David Cumin provided thoughtful feedback and code for extracting data from electronic records. Dr Matthew Pawley provided statistical advice and helped me to write R code for graphics and data management. Professor Stephen Duffull and his lab have been a great source of NONMEM and modelling support. Kaylene Henderson introduced me to the simulator.

I have had great support from within our department. I cannot thank Associate Professor Simon Mitchell, Dr Guy Warman and Debbie Beaumont enough for their help and encouragement. This also goes for my workmates and friends at the hospital: David, Elaine, James, Mat, Kylie and Nicole, and of course, Ani, my partner in all crimes.

A huge thanks goes to my friends at home, and to my wonderful family, for their endless support. In particular I acknowledge my parents, Noel and Robyn Douglas, and Dale and Ruth Hannam.

Finally, I would like to thank my partner Drew. I suspect there are few men who could cope with four years of high stress and spontaneous ranting about “that program NONMEM”. Somehow, you have!

Publications, Abstracts and Data

The following publications have arisen during the course of my doctoral research:

Journal articles:

Hannam JA, Anderson BJ. Explaining the acetaminophen-ibuprofen analgesic interaction using a response surface model. *Paediatric Anaesthesia*. 2011;21(12):1234-40.

Case reports and correspondence:

Hannam JA, Anderson BJ. Contribution of morphine and morphine-6-glucuronide to respiratory depression in a child [Case report]. *Anaesthesia and Intensive Care*. 2012;40(5):861-6.

Hannam JA, Anderson BJ, Veyckemans F. Tears at breakfast [Correspondence]. *Paediatric Anaesthesia*. 2012;22(4):419

Book chapters:

Short TG, Hannam JA. Pharmacodynamic drug interactions. In: Hemmings H, Egan T, editors. *Pharmacology and Physiology for Anesthesia: Foundations and Clinical Application*. Philadelphia, PA: Elsevier Saunders 2013.

Co-authorship forms are provided for each of the above publications that appear in this thesis. The analyses that I present in chapters 3 and 4 of this thesis use pre-existing datasets collected by my supervisors several years ago. I describe the manner of data collection in both instances, but for clarity, I have separated this text from the main body text of my thesis using boxes. This distinguishes those data that I have collected myself from those data that I have (gratefully) inherited during my research.

Table of Contents

Abstract	ii
Acknowledgements	iii
Publications, Abstracts and Data	v
Table of Contents	vi
List of Figures	x
List of Tables	xvii
List of Abbreviations	xxii
List of Definitions	xxvi
Chapter 1. Introduction	1
1.1. Thesis outline	3
1.2. Anaesthesia	6
1.3. Pharmacology modelling for anaesthesia	7
1.3.1 Population methods.....	7
1.3.2 An illustrative example of combined effects: morphine and its active metabolite	10
1.3.2.1. Methods.....	10
1.3.2.2. Results	14
1.3.2.3. Discussion	17
1.4. Drug classes in anaesthesia	19
1.4.1 Paracetamol (analgesic)	19
1.4.2 Midazolam (sedative).....	21
1.4.3 Propofol (intravenous anaesthetic).....	24
1.4.4 Morphine and the phenyl-piperidines (opioids).....	28
1.4.5 Inhalation anaesthetics	34
1.5. Interactions in anaesthesia	35
1.5.1 Working definitions	35
1.5.2 Studying interactions in anaesthesia	39
1.5.2.1. Response surface models in anaesthesia.....	40
1.5.3 Propofol and midazolam	43
1.5.3.1. Propofol and the opioids	46
1.5.3.2. Propofol and the inhalation anaesthetics.....	47
1.5.3.3. Inhalation anaesthetics and the opioids.....	47
1.6. Summary	49
Chapter 2. Explaining the paracetamol-ibuprofen analgesic interaction using a response surface model	50
2.1. Introduction.....	51
2.2. Methods.....	53
2.2.1 Data	53

2.2.2 Modelling methods	54
2.2.2.1. Model parameterisation.....	54
2.2.2.2. Parameter estimation.....	56
2.2.2.3. Simulation	57
2.3. Results.....	57
2.4. Discussion	63
Chapter 3. A pharmacokinetic-pharmacodynamic model of analgesia for diclofenac and paracetamol in children.....	67
3.1. Introduction.....	68
3.2. Methods.....	69
Box 1. How these data were collected (study 1).....	70
Participants	70
Anaesthetic and postoperative care.....	70
Study drug.....	71
Study measurements.....	71
Box 2. Study 2.....	72
Box 3. Study 3.....	72
3.2.1 Modelling methods	73
3.2.1.1. Pharmacokinetic model.....	73
3.2.1.2. Effect compartment model.....	73
3.2.1.3. Pharmacodynamic model.....	74
3.2.1.4. Placebo effect.....	75
3.2.1.5. Study dropout.....	75
3.2.1.6. Parameter estimation.....	77
3.3. Results.....	77
3.4. Discussion	86
Chapter 4. Propofol and alfentanil pharmacokinetics and pharmacodynamics	92
4.1. Introduction.....	93
4.2. Methods.....	95
Box 4. How these data were collected.....	96
Ethics.....	96
Participants	96
Study phase.....	97
Study drugs.....	97
Blood sampling	97
Effect measurements	98
Intraoperative and recovery phases.....	98
4.2.1 Modelling methods	99

4.2.1.1. Pharmacokinetic analysis	99
4.2.1.2. Pharmacodynamic analysis	99
4.2.1.3. Simultaneous pharmacokinetic-pharmacodynamic analysis	101
4.2.1.4. Population parameter estimates	101
4.3. Results	103
4.3.1 Pharmacokinetics	103
4.3.2 Pharmacodynamics	108
4.4. Discussion	113
Chapter 5. Generalisability of the propofol-opioid relationship for BIS.....	119
5.1. Introduction	120
5.2. Methods.....	120
5.2.1.1. Simulation	121
5.2.1.2. Population parameter estimates	122
5.3. Results.....	123
5.4. Discussion	128
Chapter 6. Predictive performance of a response surface model for target controlled infusion during surgery	131
6.1. Introduction	132
6.2. Methods.....	133
6.2.1 Participants.....	133
6.2.2 Anaesthesia and study drugs	133
6.2.3 Effect measurements	134
6.2.4 Data analysis	135
6.2.4.1. Model performance measures	135
6.2.4.2. Retrospective model performance	136
6.3. Results.....	137
6.3.1 Prospectively tested model.....	137
6.3.2 Retrospectively tested parameter combinations.....	147
6.4. Discussion	151
Chapter 7. A model of combined BIS response for opioid, intravenous and inhalation anaesthetics	156
7.1. Introduction.....	157
7.1. Methods.....	157
7.1.1 Participants.....	158
7.1.2 Data collection	158
7.1.3 Data analysis	159
7.1.3.1. Modelling methods	161
7.1.3.2. Population parameter estimates	163
7.2. Results.....	163

7.3. Discussion.....	171
Chapter 8. Using complex models to simulate anaesthesia.....	181
8.1. Introduction.....	182
8.2. Methods.....	184
8.2.1 The model.....	184
8.2.2 Method of simulation.....	190
8.3. Simulations.....	191
8.3.1 Patient 1: TIVA followed by an inhalation anaesthetic.....	191
8.3.2 Patient 2: Bolus induction followed by inhalation anaesthetic.....	195
8.4. Discussion.....	202
Chapter 9. General discussion.....	208
9.1. Main findings and contributions to knowledge.....	209
9.1.1 Paracetamol and NSAIDs for postoperative analgesia in children.....	209
9.1.2 Intraoperative drug classes and BIS effects.....	211
9.2. Directions for future research.....	215
Appendices.....	218
Appendix 1. Model code for morphine-M6G respiratory effects.....	219
Appendix 2. Model code for ibuprofen-paracetamol analgesia.....	221
Appendix 3. Model code for diclofenac-paracetamol analgesia.....	224
Appendix 4.1 Model code for alfentanil-propofol: loop collapsing.....	230
Appendix 4.2 Model code for alfentanil-propofol: simultaneous PKPD analysis.....	233
Appendix 4.3 PK covariate screening summary.....	237
Appendix 5. Ethics approval for the study described in Chapter 6.....	238
Appendix 6. Ethics approval for the study described in Chapter 7.....	241
Appendix 7. Model code for BIS response for multiple drug classes.....	242
References.....	247

List of Figures

Figure 1.1 Theoretical sigmoidal ‘ E_{MAX} ’ curves for varying γ (or slope) parameters. Baseline effect is given by E_0 and maximum observable effect is given by E_{MAX} . Drug effect approaches but cannot reach E_{MAX} . The curves intersect at the concentration at which 50% E_{MAX} is achieved (C_{e50}). For each curve depicted only the γ parameter is varied; increasing γ parameters describe steeper curves..... 12

Figure 1.2 Observed and predicted respiratory rate for a 12 year old, male child with end-stage renal failure given intravenous morphine *via* a PCA pump for postoperative pain. Predicted respiratory rates are for morphine only, M6G only, and combined morphine M6G effect. Observed partial pressure of CO_2 (kPa) is also given. Dialysis began at 45 h postoperatively (indicated by the arrow) and continued for 3 h. It can be seen that the solid line, depicting predicted respiratory rate for the combined model, more closely follows observations in the 0-15 h time period than do lines depicting predictions using the morphine alone and M6G alone models. Similar predictions following onset of dialysis are made for the M6G alone and combined effect models..... 15

Figure 1.3 Visual predictive check for A) the morphine alone model and B) the combined morphine and M6G effect model. The plots show median and 90% intervals (solid and dashed lines respectively). Prediction percentiles (10%, 50%, and 90%) for predictions (black lines) are overlaid with those of the observations (red lines with symbols). Grey shaded areas are 95% confidence intervals for the prediction percentiles. An improvement in fit can be seen for early and late respiratory rates in the combined effect model (panel B), although little difference is seen between 15 h and 40 h..... 16

Figure 1.4 Sigmoid E_{MAX} curves describing propofol pharmacodynamics for anaesthetic endpoints: loss of consciousness (LOC), measured by ability to open eyes on command; sedation, measured by response to shouting and shaking; lack of response to laryngoscopy; and lack of response to intubation. The influence of age on propofol response is demonstrated for LOC where curves are given for 25 year old (solid line, open circles) and 75 year old patients (solid line, closed circles). Figure adapted from Kern *et al.* and constructed using parameter estimates reported in the literature.[55, 60, 69]..... 28

Figure 1.5 The influence of infusion duration on drug washout for alfentanil, fentanyl and remifentanyl. Curves show the minutes, from cessation of infusion, required for plasma concentrations to decline by half their peak. Half times in this instance are considered ‘in context’ of the duration of infusion, termed context sensitive half times (CSHT). Remifentanyl washout is unaffected by the duration of infusion, unlike alfentanil and fentanyl. Figure adapted from Shafer and Varvel 1991,[72] using parameter estimates reported in the literature.[71, 75]..... 30

Figure 1.6 Isobologram of dose or concentration pairs for two drugs (drug A and drug B) that together cause a single level of effect. A) Line of additivity (or no interaction). The effect is equal for all parts of the line. B) infra-additivity where drug doses required for the effect are greater than expected. C) Supra-additivity, where the drug doses required for the effect are smaller than expected. Isobolograms have long been used to assess interactions in anaesthesia, and also to identify interactions between anti-microbial agents..... 37

Figure 1.7 Hypothetical isobologram and response surface. A) Isobologram of concentration (or dose) pairs of drug 1 with drug 2 that together cause a single level of effect. B) Response surface where additivity exists. C) Response surface where supra-additivity exists. Isoboles are visible as horizontal lines within the response surface. Note that where the concentration of drug 2 is equal to 0, the dose response curve for drug 1 alone can be seen (and vice versa).41

Figure 2.1 Theoretical response surface of effect between paracetamol and ibuprofen. Concentrations are those in the effect compartment. PRID score: mean change from baseline in pain relief and pain intensity difference score (0-8).60

Figure 2.2 Quality of fit of pharmacodynamic data. (A) Population predictions are compared to observed PRID scores. (B) Individual Bayesian predictions, based on adjusted parameters for the specific individual, are compared to observed PRID scores.61

Figure 2.3 Simulated PRID scores (presented as difference from baseline PRID score) for a 5 year old, 20 kg child given single and combination paracetamol-ibuprofen therapy.62

Figure 3.1 Pooled raw plasma concentrations of A) diclofenac and B) paracetamol. Paracetamol concentrations are from children (study 1), and diclofenac concentrations are from children and adults (study 2). Observations for each individual are linked with unsmoothed lines.79

Figure 3.2 Visual predictive check (VPC) plots for (A) diclofenac pharmacokinetics and (B) paracetamol pharmacokinetics predictions. The plots show median and 90% intervals (solid and dashed lines respectively). Prediction percentiles (10%, 50%, and 90%) for predictions (black lines) are overlaid with those of the observations (red lines with symbols). Grey shaded areas are 95% confidence intervals for the prediction percentiles.84

Figure 3.3 Visual predictive check (VPC) plots for predicted pain scores over time. The left panel (A) gives the original VPC plot for analgesia before inclusion of a model of study dropout, and the right panel (B) gives the VPC plot for analgesia the final model (including placebo and dropout models). The plots show median and 90% intervals (solid and dashed lines respectively). Prediction percentiles (10%, 50%, and 90%) for predictions (black lines) are overlaid with those of the observations (red lines with symbols). Grey shaded areas are 95% confidence intervals for the prediction percentiles. A persistent over-prediction of pain scores is visible in the left panel of plot A.84

Figure 3.4 Theoretical surface of response for analgesia using paracetamol with diclofenac. Concentration-response curves individual drugs are given on the outer planes of the surface. The shape of the curves is identical for both drugs (slope parameter=1). C_e is the concentration of drug in the effect site compartment. Baseline pain is fixed at 10 cm on a VAS (0-10 cm).85

Figure 3.5 Simulated response profile for a 20 kg child following a single dose of paracetamol alone and in combination with diclofenac. The black line gives response following 600 mg paracetamol (30 mg.kg^{-1}), as is typically used at Starship Children’s Hospital. The red line gives response following half this dose of paracetamol (15 mg.kg^{-1}) with 20 mg (1 mg.kg^{-1}) diclofenac. Pain scores over time are similar for both dosing strategies despite halving the dose of paracetamol.86

Figure 3.6 Isoboles of concentration pairs that together cause a 1 cm, 2 cm, 3 cm and 4 cm reduction in pain from baseline. C_e is the concentration in the effect site compartment. A 2 cm reduction in pain score can be achieved with C_e paracetamol 11.75 mg.l^{-1} , or C_e diclofenac 1.07 mg.l^{-1} . Alternatively this C_e of paracetamol may be halved to 5.88 mg.l^{-1} , and combined with 0.54 mg.l^{-1} of diclofenac to achieve the same effect.	87
Figure 3.7 Changes in baseline pain over 8 postoperative hours, as predicted by placebo models. The placebo model used in this analysis was similar to that used by Anderson <i>et al.</i> 2001,[29] although the predicted peak effect is larger and occurs later in the current study. Björnsson <i>et al.</i> used an exponential model to describe changes in baseline pain for adults undergoing wisdom tooth extractions.	88
Figure 4.1 Relationships for BIS between phenyl-piperidine opioids, intravenous anaesthetic and inhalation anaesthetic drug classes. Response surface models have been reported for drug combinations representing all three drug class pairs: propofol-sevoflurane models represent intravenous anaesthetic-inhalation anaesthetic combinations;[129, 143] propofol-remifentanyl models represent intravenous anaesthetic-opioid combinations;[59, 146] and sevoflurane-alfentanil and sevoflurane-remifentanyl represent phenyl-piperidine opioid-inhalation anaesthetic combinations.[76, 128] Additivity was found to exist in each of the cited studies for BIS response. A model describing BIS response for propofol-alfentanil is the objective of the work I present in this chapter.	95
Figure 4.2 Raw propofol plasma concentrations; observations for each individual are linked with unsmoothed lines. Samples collected during the study period (approximately 1 h duration) and during anaesthesia were pooled.	104
Figure 4.3 Raw alfentanil plasma concentrations; observations for each individual are linked with unsmoothed lines. Samples collected during the study period (approximately 1 h duration) and during anaesthesia were pooled.	104
Figure 4.4 Quality of fit of propofol and alfentanil pharmacokinetic models. (A) Population alfentanil predictions are plotted against observed alfentanil concentrations. (B) Individual Bayesian alfentanil predictions based on adjusted parameters for the specific individual are plotted against observed alfentanil concentrations. (C) Population propofol predictions are plotted against observed propofol concentrations. (D) Individual Bayesian propofol predictions based on adjusted parameters for the specific individual are plotted against observed propofol concentrations. Units of concentrations are ng.ml^{-1} for all plots.	107
Figure 4.5 Visual predictive check for A) alfentanil pharmacokinetics and B) propofol pharmacokinetics. The plot shows median and 90% intervals (solid and dashed lines respectively). Prediction percentiles (10%, 50%, and 90%) for predictions (black lines) are overlaid with those of the observations (red lines with symbols). Grey shaded areas are 95% confidence intervals for the prediction percentiles.	108
Figure 4.6 Quality of fit of the pharmacodynamic model describing BIS response for propofol with alfentanil. (A) Population predictions for BIS are plotted against observed BIS values. (B) Individual Bayesian predictions for BIS based on adjusted parameters for the specific individual are plotted against observed BIS values. Units are BIS units (0-100, where 100 is resting and awake, and < 60 is	

recommended for surgical stimuli). Some under-prediction of BIS response ranging between 0 and 20 units is visible in the plots as a result of the E_{MAX} parameter. 110

Figure 4.7 Visual predictive check (VPC) plots for the final pharmacodynamic model describing BIS response following propofol with alfentanil. The left panel gives the uncorrected VPC plots, and the right panel gives the prediction corrected VPC (PC-VPC). Prediction percentiles (10%, 50%, and 90%) for predictions (black lines) are overlaid with those of the observations (red lines with symbols). Grey shaded areas are 95% confidence intervals for the prediction percentiles. BIS units are 0-100 (where 100 is resting and awake, and < 60 is recommended for surgical stimuli). 111

Figure 4.8 Surface of response following propofol and alfentanil for BIS. C_e is the concentration in the effect compartment. BIS response is displayed as % effect (note a maximal effect of 79%, which corresponds to a reduction in BIS from 98 to 18 units). The grey surface is that predicted by the model parameters, while red points are observations. Observations that fall on the outer edges of the surface are depicted as half circles; those that fall under the surface can also be seen. 112

Figure 4.9 BIS, blood pressure and loss of consciousness. The figure shows the concentration pairs in the effect site (C_e) required to produce a BIS of 60 (light blue solid line), a BIS of 50 (dark blue solid line) and BIS of 40 (purple solid line) as predicted by the model. The 5%, 50% and 95% isoboles for BIS response are also given (broken black lines). The propofol concentration associated with a reduction in systolic blood pressure (SBP) from 120 mmHg to 100 mmHg is overlaid in red (as estimated by Kato *et al.*, $4.61 \text{ SE} \pm 0.51 \text{ mcg.ml}^{-1}$). [168] The propofol C_{e50} required for loss of consciousness (LOC) when given alone, and with 100 ng.ml^{-1} of alfentanil, is given by the yellow and green circles respectively. [247] Note that the clinically used range of alfentanil is much lower than that depicted here (usually < 200 ng.ml^{-1}). 117

Figure 5.1 Quality of fit of the pharmacodynamic model developed for propofol-alfentanil anaesthesia (chapter 4) when used to predict BIS response for propofol with remifentanil. The quality of fit in study 2 only (propofol-remifentanil data, red circles) [59] can be seen in the left panels. These are overlaid by the residuals for the model when used to predict response in the alfentanil-propofol dataset (chapter 4, open circles) in the right panels. (A) Population predictions for BIS are plotted against observed BIS values. Units are BIS units (0-100, where 100 is resting and awake, and < 60 is recommended for surgical stimuli). (B) Prediction error (PE, %) is plotted against time. Some under-prediction can be seen in panel A reflecting the negative bias reported in Table 5.1. 124

Figure 5.2 Simulated *versus* observed BIS response following propofol-remifentanil anaesthesia, using model parameters developed for propofol-alfentanil anaesthesia (chapter 4). Solid lines are predictions, open circles are observations. BIS units are 0-100 (where 100 is resting and awake, and < 60 is recommended for surgical stimuli). 125

Figure 6.1 Performance error (PE, %) over time for the prospectively tested model (combination 1: standard pharmacokinetic models teamed with the response surface model reported by Bouillon *et al.*). Plots are: (A) PE during the early phase of anaesthesia (0-20 min post infusion start); (B) PE during the recovery phase (from when the infusion is halted at the end of the anaesthetic until the participant opens their eyes); (C) PE during the maintenance phase of anaesthesia (20 min post infusion start to the end of infusion, plot is truncated here at 60 min); and (D) PE during the

maintenance and recovery phase of anaesthesia (20 min post infusion start to the end of data collection). Note the differences in scale of the y-axes (plot A)..... 141

Figure 6.2 Quality of model predictions for the prospectively tested model (combination 1: standard pharmacokinetic models teamed with the response surface model reported by Bouillon *et al.*). Plots give: (A) predicted *versus* observed BIS, where units are BIS units 0-100 (BIS of 100 is resting and awake, BIS < 60 is recommended for surgical stimuli); and (B) performance error (PE, %) against the ratio of the normalised concentrations of propofol (U_P) to remifentanyl (U_R). The ratio, ' Θ ', is calculated as $U_P / (U_P + U_R)$. A Θ value equal to 0 means only remifentanyl is present, while a value of 1 means only propofol is present. The data predominantly fall in the upper range of Θ 142

Figure 6.3 Plots of observed and predicted response over time for individuals. Open circles are observations and solid lines are the model predictions. Model predictions are made using the prospectively tested model (combination 1: standard pharmacokinetic models teamed with the response surface model reported by Bouillon *et al.*). BIS units are 0-100 (where 100 is resting and awake, and <60 is recommended for surgical stimuli). 143

Figure 7.1 Quality of fit of the pharmacodynamic model for BIS response. Plots give (A) Population predictions for BIS against observed BIS values, and (B) individual Bayesian predictions for BIS based on adjusted parameters for the specific individual against observed BIS values. Units are BIS units (0-100, where 100 is resting and awake, and < 60 is recommended for surgical stimuli). A systematic trend in the population predictions can be seen (plot A) as a result of the maximal drug effect, E_{MAX} , which was estimated to be 76 BIS units..... 169

Figure 7.2 Prediction corrected visual predictive checks (PC-VPC) for pharmacodynamic model of BIS response. Plots give A) response over the first 20 min of anaesthesia (i.e. during the induction phase) and B) response from 20 min post induction to 120 min. The plots show median and 90% intervals (solid and dashed lines respectively). Prediction percentiles (10%, 50%, and 90%) for predictions (black lines) are overlaid with those of the observations (red lines with symbols). Grey shaded areas are 95% confidence intervals for the prediction percentiles..... 170

Figure 7.3 Predicted plasma concentrations of midazolam for different pharmacokinetic parameter sets. Concentration curves are for a single 2 mg bolus dose of midazolam in a 70 kg adult given at time=0 and assuming no co-administration of propofol. Concentration profiles are similar for pharmacokinetic models given by Albrecht *et al.*,[39] Greenblatt *et al.*,[40] and Maitre *et al.*,[43] with the exception of that described by Lichtenbelt *et al.* (see text for discussion).[142]..... 173

Figure 7.4 The effect of the keo parameter on the onset of BIS effect for propofol. Concentrations and effects are for a 70 kg, 170 cm, 40 y male given a 200 mg bolus of propofol (at time=0 min). A) Simulated effect site concentrations using the parameter set given by Schnider *et al.*,[54] for various keo estimates.[55, 239, 262] Simulated plasma concentrations are depicted also (solid black line in plot A). B) Simulated BIS effect corresponding to each effect site concentration profile. Time to peak effect is indicated by the broken line in plot B for keo parameters as given by Schnider *et al.* ($T_{peak}=1.6$ min),[54] and by Sepúlveda *et al.* ($T_{peak}=2.45$ min).[262] A T_{peak} of 2.2 min is calculated for this study. 176

Figure 8.1 Simulated pharmacokinetic profiles for (A) propofol, (B) sevoflurane and (C) remifentanyl for patient 1. Concentrations in the plasma (coloured lines in bold) and in the effect site (coloured broken lines) compartments are given. Probability of loss of responsiveness (LOR) and return of responsiveness (ROR) are overlaid on plots A and B (shaded areas). LOR and ROR are predicted from propofol-remifentanyl concentrations and sevoflurane-remifentanyl concentrations respectively.[131, 287] Propofol effect site concentrations as used for LOR predictions are given in plot A (grey broken lines), where the impact of the different keo values (0.19 min^{-1} BIS, 0.51 min^{-1} LOR) is visible. 193

Figure 8.2 Simulated BIS response for patient 1. Plot (A) gives the contributions of each drug alone as well as the total combined response for all drugs (indicated on figure). The combined response is given in black. Plot (B) gives simulated response for the population (solid black line), with probability of loss of responsiveness (LOR) and return of responsiveness (ROR) overlaid on the plot (indicated on figure). LOR and ROR probabilities are predicted from propofol-remifentanyl concentrations (green shaded area) and sevoflurane-remifentanyl concentrations (purple shaded area) respectively and correspond to those given in Figure 8.1.[131, 287] During wash-out of propofol concentrations and wash-in of sevoflurane concentrations both drug pairs contribute to the probability that the patient is unresponsive (overlapping area). The point at which 50% of patients are expected to have lost responsiveness is shown by the vertical broken grey line on the left (plot B), while that at which 50% of patients are expected to have regained responsiveness is given by the vertical broken grey line on the right. 194

Figure 8.3 Simulated pharmacokinetic profiles for midazolam, propofol, fentanyl and sevoflurane for patient 2. Bold lines give the plasma concentration and broken lines give the effect site concentrations. 196

Figure 8.4 Simulated BIS response for patient 2. The contributions of each drug alone are depicted as well as the total combined response for all drugs (indicated on figure). The combined response is given in black. 197

Figure 8.5 The contributions of midazolam and propofol to BIS response for patient 2. Note the small contribution of midazolam alone (given in red) but the increase in response for the combination (given in black) compared with propofol alone. 197

Figure 8.6 Simulated pharmacokinetic profiles for midazolam, propofol, fentanyl and sevoflurane for patient 2 assuming 20% between-subject variability. Solid lines give the plasma concentration and broken lines give the effect site concentrations. Population predictions (no variability) are given in black while those of the five simulations are given in colour. 200

Figure 8.7 Simulated BIS response for patient 2 with variability. The plots show A) simulated response for population predictions of drug concentrations (given in Figure 8.6, black lines) assuming additive unknown error of 8 units only, and B) simulated response for predictions of drug concentrations with between-subject pharmacokinetic variability of 20% (given in Figure 8.6, coloured lines), between-subject pharmacodynamic variability of 30% and additive unknown error of 8 units. No variability is included on keo parameters. Response predictions for the population (no variability) are given in solid lines. 201

Figure 8.8 Simulated BIS response for patient 2 for twenty simulations each. Both plots are analogous to plot B of Figure 8.7 (five simulations) except that variability is also included on the keo parameters. This figure demonstrates the wide range of BIS response profiles possible when between-subject variability of just 20% is included on pharmacokinetics, 30% is included on pharmacodynamic parameters and a residual unknown error of 8 units is included on response predictions. Plot A gives one iteration of twenty simulations, all of which follow roughly a similar pattern. Plot B also gives one iteration of twenty simulations but a subset of these give a higher BIS trace (plus 20-30 units) which might become clinically important during the induction or recovery phases. Response predictions for the population (no variability) are given by the solid black lines.201

Figure 9.1 BIS levels associated with propofol-midazolam concentration pairs. The figure shows the concentration pairs in the effect site (C_e) required to produce a BIS of 60 (green line), a BIS of 70 (black line) and BIS of 80 (red line) as predicted by the model. BIS values between 70 and 80 are associated with an OAA/S scale > 2 and < 3 suitable for light sedation.[38, 299] The propofol C_{e50} for anti-emesis in adults ($0.343 \text{ mcg.ml}^{-1}$),[300] and systolic blood pressure changes in patients aged 70-85 y,[135] are indicated by the broken vertical lines.....213

List of Tables

Table 1.1 Summary of data analysis options for population derived pharmacokinetic (PK) and pharmacodynamic (PD) data. Attributes of the naïve pooled fit, standard two-stage approach and population approach are given. This table is adapted from Anderson <i>et al.</i> [6]	9
Table 1.2 Five most commonly used intravenous drugs during anaesthesia at our centre, in order of frequency of use. *Taken from a random sample of 100 anaesthetic cases at Auckland City Hospital. This table is adapted from Al-Tiay.[36].....	22
Table 1.3 Standardised* model parameter estimates for midazolam pharmacokinetics. *Standardised for a 70 kg, 175 cm, 50 year old male. Covariate models for parameter adjustments are given in square brackets, where applicable. WT=weight (kg), BSA=body surface area. †Model developed in young subjects. ‡Model developed in elderly subjects.....	23
Table 1.4 Standardised* model parameter estimates for propofol pharmacokinetics. *Standardised for a 70 kg, 175 cm, 50 year old male. Covariate models for parameter adjustments are given in square brackets, where applicable. ^ If age < 60, else $CL1=1.44 \cdot (TBW/70)^{0.75} - (AGE-60) \cdot 0.05$. TBW=total body weight (kg), HT=height (cm), AGE=age (y), LBM=lean body mass, <i>bol</i> =1 if bolus and 0 if infusion, <i>ven</i> =1 if venous sampling and 0 if arterial sampling. †Model developed in obese patients. ‡Model developed in paediatric patients.	26
Table 1.5 Standardised* model parameter estimates for alfentanil pharmacokinetics. *Standardised for a 70 kg, 175 cm, 50 year old male.	31
Table 1.6 Standardised* model parameter estimates for fentanyl pharmacokinetics. *Standardised for a 70 kg, 175 cm, 50 year old male.	32
Table 1.7 Standardised* model parameter estimates for morphine pharmacokinetics. *Standardised for a 70 kg, 175 cm, 50 year old male.	32
Table 1.8 Standardised* model parameter estimates for remifentanil pharmacokinetics. *Standardised for a 70 kg, 175 cm, 50 year old male. ^Model developed for obese patients. †Model developed for bolus administration.....	33
Table 1.9 Studies detailing response surface models development in anaesthesia. AAI=auditory evoked potential index, OAA/S=observer assessment of alertness / sedation, BP=blood pressure, HR=heart rate. ‡binary data, †continuous data, N=sample size.....	44
Table 1.10 Required propofol plasma Ce_{50} for common anaesthetic endpoints when given alone and in combination with opioids. Interaction classifications are given for each. * Ce_{50} for propofol alone often cannot be estimated for the endpoint of intubation, as opioids are required to ablate response to this stimulus. Although one study has estimated a propofol concentration of 17.4 mcg.ml^{-1} for ablation of response to intubation using propofol alone,[170] propofol 7.3 mcg.ml^{-1} with remifentanil 1.2 mcg.ml^{-1} is more clinically appropriate. One study found no change was observed in BIS values for propofol supplemented with fentanyl over propofol given alone, suggesting no interaction at the concentrations investigated.[172] LOC=loss of consciousness.	48

Table 2.1 Parameter estimates for the drug interaction model investigating the paracetamol-ibuprofen response surface (CV is the coefficient of variability; SE is the standard error; CI is the confidence interval; Tbase and tabs describe the half times to achieve the effect observed in the placebo group and for absorption, respectively; Err additive is residual unknown variability). CL/F_{oral} and V/F_{oral} are the apparent clearance and volume of distribution respectively following oral dosing.....59

Table 3.1 Pharmacokinetic parameter estimates for the drug interaction model investigating the paracetamol-diclofenac response surface. BOV is the between-occasion variability, population parameter variability expressed as a coefficient of variation (square root of NONMEM omega estimate x 100); CI is the bootstrap confidence interval; tabs is the half-life for absorption for oral paracetamol (tab_{SPARA,O}), rectal paracetamol (tab_{SPARA,R}) and oral diclofenac (tab_{SDICL}); Lag_{PARA,R} is the lag time for rectal formulation paracetamol. V/F and CL/F are the apparent volume and clearance respectively. Err_{add} and Err_{pro} are the additive and proportional residual variability estimated for drug concentrations. *A total of 170 bootstraps were completed in the time available. 80

Table 3.2 Correlation of population parameter variability for pharmacokinetic parameters. V/F and CL/F are the apparent volume and clearance respectively. Tab_{SDICL} is the half-life for absorption for oral diclofenac. BOV is between-occasion variability..... 81

Table 3.3 Pharmacodynamic parameter estimates for the drug interaction model investigating the paracetamol-diclofenac response surface. Population parameter variability expressed as a coefficient of variation (CV, square root of NONMEM omega estimate x 100); CI is the bootstrap confidence interval; λ is the baseline hazard and β_{pain} is the effect of current pain score on hazard; Err_{add} is the additive residual variability estimated for pain score measurements. *A total of 170 bootstraps were completed in the time available. 82

Table 3.4 Correlation of population parameter variability for pharmacodynamic and placebo parameters..... 83

Table 4.1 Pharmacokinetic parameter estimates for propofol and alfentanil. CV=coefficient of variability; CI=confidence interval; Err_{pro}=proportional residual variability term; Err_{add}=additive residual variability term; η_{RUV,i}=variability associated with Err_{add}. *A total of 300 bootstraps were completed in the time available. 106

Table 4.2 Correlation of population parameter variability for pharmacokinetic parameters. 106

Table 4.3 Pharmacodynamic model development. All models were initially run with additive interaction terms, representing the simplest scenario. The structural model selected for further investigation was that by Minto *et al.* with an estimated E_{MAX} parameter and additive interaction term (β=0). OBJ=NONMEM's objective function. 109

Table 4.4 Pharmacodynamic parameter estimates for the model investigating the propofol-alfentanil response surface. CV=coefficient of variability; CI=confidence interval; Err_{add}=residual variability estimated for BIS measurements using an additive error model; η_{RUV,i}=variability associated with Err_{add}; Ce_{50,x}=effect site concentration of drug that causes 50% maximal drug effect; t_{1/2keo,x}=equilibration half-time; keo_x=equilibration rate constant (or 0.69/t_{1/2keo,x}) for drug moving

between plasma and effect site compartments. * A total of 300 bootstraps were completed in the time available.	109
Table 4.5 Correlation of population parameter variability for pharmacodynamic parameters.	110
Table 5.1 Measures of model performance: model bias, given as the median prediction error (MDPE); model precision, given as the median absolute prediction error (MDAPE); and model wobble, given as the PE - MADPE. Values are median percentage bias (10 th :90 th percentile).	123
Table 5.2 Pharmacodynamic parameter estimates for pooled propofol-opioid dataset: CV is the coefficient of variability; CI is the confidence interval; Err _{add} is the residual variability estimated for BIS measurements using an additive error model; and Ce _{50,x} is the effect site concentration of drug that causes 50% maximal drug effect. Parameter and variance estimates reported in chapter 4 for the propofol-alfentanil model are given for ease of comparison.	127
Table 5.3 Estimates of relative potency for the phenyl-piperidine opioids remifentanil and alfentanil. EEG=electroencephalogram.	130
Table 6.1 Tested parameter set combinations. Combination 1 was implemented in the TCI software and tested prospectively, while models 2-4 were assessed retrospectively. *Keo value is adjusted for age, i.e. 0.595 - 0.007• (AGE - 40).[73] PK is pharmacokinetics, PD is pharmacodynamics. Keo values for combination 3 were calculated in PK-PD Tools for Excel© 2009 using the TTPE method and Tpeak estimates reported in the literature. [55, 73] Predicted effect site concentrations of remifentanil were converted to alfentanil equivalents for combinations 2 and 4 using a potency ratio of remifentanil: alfentanil of 1:33 (as estimated in chapter 5).	139
Table 6.2 Measures of model performance for the prospectively tested model for each stage of anaesthesia. Measures are: median bias, given as the median performance error (MDPE); median precision, given as the median absolute performance error (MDAPE); and median wobble, given as the PE-MDPE. Values are median percentage bias (10 th -90 th percentile). The prospectively tested model was standard pharmacokinetic models teamed with the response surface model reported by Bouillon <i>et al.</i>	140
Table 6.3 Measures of model performance by body mass index (BMI, BMI<35 kg.m ⁻² versus BMI≥35 kg.m ⁻²) and by age (Age≥60 y versus Age<60 y) for the prospectively tested model. Measures are: bias, given as the median performance error (MDPE); precision, given as the median absolute performance error (MDAPE); and wobble, given as the PE-MDPE. Values are median percentage bias (10 th -90 th percentile). The prospectively tested model was standard pharmacokinetic models teamed with the response surface model reported by Bouillon <i>et al.</i>	140
Table 6.4 Measures of model performance for each stage of anaesthesia for retrospectively tested combinations. Measures are: median bias, given as the median performance error (MDPE); median precision, given as the median absolute performance error (MDAPE); and median wobble, given as the PE-MDPE. Values are median percentage bias (10 th -90 th percentile). R indicates remifentanil pharmacokinetic parameter set, P indicates propofol pharmacokinetic parameter set, and PD indicates	

pharmacodynamic parameter set. *Note that model performance for the prospectively tested model is reiterated here for ease of comparison. 148

Table 6.5 Measures of model performance by body mass index (BMI, BMI<35 kg.m⁻² versus BMI≥35 kg.m⁻²) for retrospectively tested combinations. Measures are: bias, given as the median performance error (MDPE); precision, given as the median absolute performance error (MDAPE); and wobble, given as the PE-MDPE. Values are median percentage bias (10th-90th percentile). Poor performance is seen for combination 4 (developed in chapter 4) for those individuals with a BMI ≥ 35 kg.m⁻². Measures of bias, precision and wobble for all patients across all time points, as given in Table 6.4, are repeated here for ease of comparison. R indicates remifentanyl pharmacokinetic parameter set, P indicates propofol pharmacokinetic parameter set, and PD indicates pharmacodynamic parameter set. *Note that model performance for the prospectively tested model is reiterated here for ease of comparison. 149

Table 6.6 Measures of model performance by age (Age≥60 y versus Age<60 y) for retrospectively tested combinations. Measures are: bias, given as the median performance error (MDPE); precision, given as the median absolute performance error (MDAPE); and wobble, given as the PE-MDPE. Values are median percentage bias (10th-90th percentile). Under-prediction (in the form of negative bias) is seen for all models in participants aged 60 years and older. Measures of bias, precision and wobble for all patients across all time points, as given in Table 6.4, are repeated here for ease of comparison. R indicates remifentanyl pharmacokinetic parameter set, P indicates propofol pharmacokinetic parameter set, and PD indicates pharmacodynamic parameter set. *Note that model performance for the prospectively tested model is reiterated here for ease of comparison. 150

Table 7.1 Parameter sets selected from the literature and used to predict plasma and effect site concentrations from dosing information. *The three drug classes (and their representative drugs) are defined for this thesis as 1) intravenous anaesthetic (propofol); phenyl-piperidine opioids (alfentanil, fentanyl and remifentanyl); and inhalation anaesthetics (desflurane, isoflurane and sevoflurane). 160

Table 7.2 Patient demographics and drug administrations. ‘Cases’ are the total number of cases in which each drug was administered and ‘Administrations’ gives the total number of administrations for all patients and the final column. NMBD=Neuromuscular blockade drugs. BMI=Body mass index. Ce=concentration in the effect site compartment. Midazolam was given to 75% of patients. NMBD were atracurium (31 cases), rocuronium (2 cases), suxamethonium (8 cases) and vecuronium (3 cases). Thirteen individuals did not receive NMBD. 164

Table 7.3 Pharmacodynamic model development. OBJ is NONMEM’s objective function. †Predicted effect site concentrations were calculated in the data file using Excel (see methods) and used in modelling. ‡Midazolam dosing information was included in the data file and pharmacokinetic parameters and variability estimates reported by Albrecht *et al.* were used to make concentration predictions in NONMEM.[39] *Additional parameters entered for the pharmacokinetic model were not estimated but fixed at values in the literature. 167

Table 7.4 Pharmacodynamic parameter estimates. CV is the coefficient of variability; CI is the confidence interval; Err_{add} is the residual variability estimated for BIS measurements using an additive error model; Ce_{50,x} is the effect site concentration of drug that causes 50% maximal drug effect; t_{1/2keo,x} is the equilibration half-time; and keo_x is the equilibration rate constant (or 0.69/ t_{1/2keo,x}) for

drug moving between plasma and effect site compartments. Note the small effect of age on the Ce_{50} estimate for fentanyl. * A total of 224 bootstraps were completed in the time available..... 168

Table 7.5 Correlation of population parameter variability for the pharmacodynamic model.
..... 169

Table 8.1 Parameter sets used to describe the pharmacokinetics of each drug allowed in the model. †End-tidal concentrations were calculated using a two-compartment model as described by Rietbrock *et al.* for this study,[286] although end-tidal concentrations generated by the METI® HPS™ might be fed directly into the model (as was done in chapter 7 using observed end-tidal concentrations). I assumed for the simulation that: fresh gas flow>tidal volume so that the concentration of inhalation anaesthetic delivered=the concentration inspired by the patient; respiratory rate=10 breaths.min⁻¹; tidal volume=8 ml.kg⁻¹; and alveolar ventilation=tidal volume minus the dead space volume (set at 2.0 ml.kg⁻¹).[286] I also assumed that end-tidal concentrations of inhalation anaesthetic roughly represent the concentration in the plasma compartment. HT=height (cm), WT=weight (kg) and LBM=lean body mass (kg). *Albrecht *et al.* investigated midazolam pharmacokinetics in two age groups (24-28 y and 67-81 y), and gave two separate pharmacokinetic parameter sets; that given for the older age group was used in this analysis, see chapter 7 for discussion. 187

Table 8.2 The pharmacokinetic parameters and covariate effects used for simulations. *Values given are for a 70 kg individual; note there is no clearance from the central compartment included in the model for inhalation anaesthetics (inter-compartmental clearance between compartments1 and 2 is included only). 188

Table 8.3 The pharmacodynamic parameters and covariate effects used for simulations. $Ce_{50,x}$ is the effect site concentration of drug that causes 50% maximal drug effect; and keo_x is the rate constant (or $0.69/ t_{1/2}keo_x$) for drug moving between plasma and effect site compartments. Baseline BIS (E_0) was 98 units. 189

Table 8.4 Proposed method of using complex models to simulate depth of anaesthesia. Ce_{50} =effect site concentration associated with 50% the maximal effect. *Variability is included or adjusted to suit the requirements of the simulation or scenario. 190

Table 8.5 Anaesthetic protocol for patient 1. *Given *via* a target controlled infusion (TCI) pump used in plasma mode. †Given *via* a target controlled infusion (TCI) pump used in effect site mode. C_e is the concentration in the effect site compartment. 192

Table 8.6 Anaesthetic protocol for patient 2.
..... 195

Table 8.7 Variability associated with the pharmacokinetic parameters used for simulations. CV is the coefficient of variability (%). *Authors reported pharmacokinetic models in terms of V_1 , CL_1 and rate constants so variability associated with peripheral compartment volumes and clearances is unknown. Wissing *et al.* reported the range of individual parameter estimates across individuals for their analysis of desflurane, isoflurane and sevoflurane pharmacokinetics only.[103] 199

List of Abbreviations

AAI	Auditory evoked potential index
ASA	American Society of Anesthesiologists' physical status score
AUC	Area under the curve
BETA _{PL}	Nominal placebo dose
BIS	Bispectral Index
BMI	Body mass index
BP	Blood pressure
BSV	Between-subject variability
C _e	Concentration in the effect site compartment
C _{e50}	Concentration in the effect site compartment that causes 50% of E _{MAX}
C _{ET}	End-tidal concentration
CI	Confidence interval
CL1	Clearance
CL2	Inter-compartmental clearance (between model compartments 1 and 2)
CL3	Inter-compartmental clearance (between model compartments 1 and 3)
CV	Coefficient of variation
CUMH	Cumulative hazard
EEG	Electroencephalogram
E _{MAX}	The maximal drug response
Err _{add}	Residual additive error
Err _{pro}	Residual proportional error
E ₀	Baseline level of the effect/physiologic variable of interest

F	Bioavailability (or the fraction of drug that is available unchanged in the plasma)
FIX	Indicates that a parameter has been fixed at the given value during analysis
GA	General anaesthesia
GABA	γ -aminobutyric acid
h	Hours
HR	Heart rate
HPS	Human patient simulator
IDAS	Integrated drug administration system
Ka	Absorption rate constant
keo	Rate constant describing drug transfer between plasma and effect compartments
keq	Equilibration rate constant
LBM	Lean body mass
LLOQ	Lower limit of quantification
LOR	Loss of responsiveness
MAC	Minimum alveolar concentration of an inhalation agent required to ablate movement to noxious stimuli in 50% of patients
MADPE	Median absolute performance error (or 'precision')
MDPE	Median performance error (or 'bias')
min	Minutes
M3G	Morphine-3-glucuronide
M6G	Morphine-6-glucuronide
NMDA	<i>N</i> -methyl-D-aspartate
NMBD	Neuromuscular blocking drug
NONMEM	Non-linear mixed effects modelling program

NSAID	Non-steroidal anti-inflammatory drug
OAAS/S	Observer assessment of alertness / sedation
OBJ	NONMEM's objective function
PCA	Patient controlled analgesia
PE	Performance error
P _i	Parameter adjusted for the individual
P _p	Parameter for the population
PRID	Pain relief and pain intensity difference score
R	Response
ROR	Return of consciousness
RUV	Residual unknown variability
SE	Standard error
SQI	Signal quality index (of the BIS monitor)
tabs	Absorption half-life
TBW	Total body weight
TCI	Target controlled infusion
TIVA	Total intravenous anaesthesia
TTPE	Time-to-Peak-Effect
t _{1/2} keo	Keo expressed as an equilibration half-time (0.693/keo)
U	Normalised units of drug (see equations for calculation)
V ₁	Central volume of distribution
V ₂	Peripheral volume of distribution (model compartment 2)
V ₃	Peripheral volume of distribution (model compartment 3)
VAS	Visual analogue scale

VPC	Visual predictive check
β	A parameter describing the interaction between modelled drugs
β_G	A scale parameter describing a Gompertz distribution
β_W	A scale parameter describing a Weibull distribution
β_{pain}	A scale parameter for the effect of pain on study dropout
γ	A parameter describing the shape of a sigmoidal curve
θ	Concentration ratio of normalised drug units
η	Random effect variables describing between-subject variability
ω^2	Variance

List of Definitions

Additivity	No interaction, for example, half the dose of two drugs given together produces the same effect as giving the whole dose of either drug alone
Antagonism	A negative interaction where there is an absolute reduction in the effect of one drug in the presence of the other, e.g. the analgesic effect of fentanyl is reduced in the presence of naloxone
Between-subject variability	Variability existing between individuals that arises from biological differences
Covariate	Characteristics of an individual that is used to explain predictable sources of variability
C_{e50}	The concentration in the effect site compartment that causes 50% of the maximal drug response (E_{MAX})
EC_{50}	The concentration in the plasma compartment that causes 50% of the maximal drug response (E_{MAX})
E_{MAX}	The maximal drug response
General anaesthesia	A drug induced state of unconsciousness of the brain, coupled with inhibition of arousal in response to noxious stimuli
Hypnosis	For the purposes of this thesis, hypnosis is taken to mean light sedation (or loss of response to verbal command) although in general the word sedation is preferred
Infra-additivity	A negative interaction, for example, half the dose of two drugs given together produces a smaller effect than is expected from additivity

Response surface model	A term used in this thesis to mean pharmacodynamic interaction models that describe a 'surface' of effect for two or more drugs
Sedative	A drug that causes hypnosis but is unable to cause a state of anaesthesia when given alone (for example, midazolam)
Supra-additivity	A positive or 'synergistic' interaction, for example, half the dose of two drugs given together produces a greater effect than is expected from additivity
Within-subject variability	Variability arising between occasions within a single individual

Co-Authorship Form

This form is to accompany the submission of any PhD that contains research reported in published or unpublished co-authored work. **Please include one copy of this form for each co-authored work.** Completed forms should be included in all copies of your thesis submitted for examination and library deposit (including digital deposit), following your thesis Acknowledgements.

Please indicate the chapter/section/pages of this thesis that are extracted from a co-authored work and give the title and publication details or details of submission of the co-authored work.

An extended version of the following case report appears in the Introduction, Section 1.3.2 of this thesis, entitled "An illustrative example of combined effects: Morphine and its active metabolite."

Nature of contribution by PhD candidate: JH wrote initial model codes and contributed to modelling, wrote first draft of the manuscript, contributed to editing and revising of the manuscript.

Extent of contribution by PhD candidate (%): 90

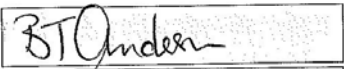
CO-AUTHORS

Name	Nature of Contribution
Professor Brian J Anderson	BJA collected the data in 1997, contributed to modelling, contributed to editing and revising manuscript, provided general oversight.

Certification by Co-Authors

The undersigned hereby certify that:

- ❖ the above statement correctly reflects the nature and extent of the PhD candidate's contribution to this work, and the nature of the contribution of each of the co-authors; and
- ❖ in cases where the PhD candidate was the lead author of the work that the candidate wrote the text.

Name	Signature	Date
BRIAN ANDERSON		Click here 15/5/13
		Click here

Co-Authorship Form

This form is to accompany the submission of any PhD that contains research reported in published or unpublished co-authored work. **Please include one copy of this form for each co-authored work.** Completed forms should be included in all copies of your thesis submitted for examination and library deposit (including digital deposit), following your thesis Acknowledgements.

Please indicate the chapter/section/pages of this thesis that are extracted from a co-authored work and give the title and publication details or details of submission of the co-authored work.

Extended/revised parts of the following book chapter appear in Section 1.5.1 of this thesis (entitled Working definitions, pg 36) and in Section 1.5.2 (entitled Studying interactions in anaesthesia, pg 39).

Short TG, Hannam JA. Pharmacodynamic drug interactions. In: Hemmings H, Egan T, editors. Pharmacology and Physiology for Anesthesia: Foundations and Clinical Application. Philadelphia, PA: Elsevier Saunders 2013 (pg 71 and 73).

Nature of contribution by PhD candidate	JH contributed to writing the initial draft, editing and revising manuscript of relevant sections
Extent of contribution by PhD candidate (%)	50%

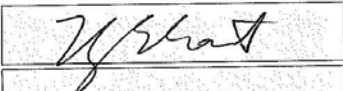
CO-AUTHORS

Name	Nature of Contribution
Associate Professor Timothy G Short	TGS contributed to writing the initial draft, editing and revising the published manuscript. TGS was also the supervising and first author.

Certification by Co-Authors

The undersigned hereby certify that:

- ❖ the above statement correctly reflects the nature and extent of the PhD candidate's contribution to this work, and the nature of the contribution of each of the co-authors; and
- ❖ in cases where the PhD candidate was the lead author of the work that the candidate wrote the text.

Name	Signature	Date
T. G. SHORT		Click here 14/5/2013
		Click here

Co-Authorship Form

This form is to accompany the submission of any PhD that contains research reported in published or unpublished co-authored work. **Please include one copy of this form for each co-authored work.** Completed forms should be included in all copies of your thesis submitted for examination and library deposit (including digital deposit), following your thesis Acknowledgements.

Please indicate the chapter/section/pages of this thesis that are extracted from a co-authored work and give the title and publication details or details of submission of the co-authored work.

An extended version of the following article appears in Chapter 2 of this thesis, entitled Explaining the paracetamol-ibuprofen analgesic interaction using a response surface model.

Hannam JA, Anderson BJ. Explaining the acetaminophen-ibuprofen analgesic interaction using a response surface model. *Paediatric Anaesthesia*. 2011;21(12):1234-40.

Nature of contribution by PhD candidate

JH extracted the data, wrote the initial model codes, wrote the initial manuscript draft, contributed to modelling, and editing and revising the manuscript.

Extent of contribution by PhD candidate (%)

80

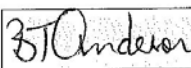
CO-AUTHORS

Name	Nature of Contribution
Professor Brian J Anderson	BJA conceived the study, contributed to modelling, and to editing and revising the manuscript and figures. BJA also provided general oversight of this work.

Certification by Co-Authors

The undersigned hereby certify that:

- ❖ the above statement correctly reflects the nature and extent of the PhD candidate's contribution to this work, and the nature of the contribution of each of the co-authors; and
- ❖ in cases where the PhD candidate was the lead author of the work that the candidate wrote the text.

Name	Signature	Date
BRIAN ANDERSON		Click here 15/5/13
		Click here

Last updated: 25 March 2013

Chapter 1. Introduction

Anaesthesia is a setting in which combinations of drugs, and the interactions between those drugs, are routinely used to achieve clinical goals. These drug combinations are used to create sedation, reduce the likelihood of awareness and modulate response to surgical incision. Using smaller doses of multiple drugs minimises those dose-dependent adverse drug effects associated with the larger doses required when a single drug is used. In modern anaesthesia practice, few anaesthetics involve just one drug. Likewise, postoperative pain can be managed using combinations of analgesics to minimise nausea, vomiting and respiratory depression. Knowledge of a drug's pharmacological profile helps guide dosing decisions, often through pharmacokinetic models that describe dose-concentration relationships, and pharmacodynamic models that describe concentration-effect (or sometimes dose-effect) relationships. Pharmacokinetic and linked pharmacokinetic-pharmacodynamic models form the basis of model controlled delivery systems (e.g. infusion pumps) and recommended drug therapy guidelines in anaesthesia, but those models in common usage are predominantly for single drugs. Recent attention towards modelling drugs in combination reflects the manner in which anaesthetic and analgesic agents are commonly used today.

The term 'response surface model' refers to pharmacodynamic interaction models that describe concentration-effect relationships between two or more drugs that contribute to the same endpoint. They take their name from the surface of response that is achieved when effect observations are plotted against the concentration axis of the study drugs. Advantages of response surface modelling methods include the ability to link these models with existing pharmacokinetic models, to make effect predictions for the entire dosing range of each drug, to estimate the size of an interaction and to describe interactions existing between two or more drugs. Parameter estimates that describe response surface models have been published for commonly used two-drug combinations in anaesthesia, such as intravenous anaesthetic with inhalation anaesthetic, intravenous anaesthetic with opioid, and inhalation agent with opioid. They have yet to be applied to combinations of drugs relevant to anaesthesia used outside the intraoperative period, notably during the postoperative period.

Response surface models are useful tools for modelling anaesthetic drug action:

- they can be used to re-evaluate current perceptions of commonly used drug combinations for which previous analyses may have been restricted or overly simple;
- they might be used to form hypotheses or plan future studies;
- they might be used to drive infusions of drugs in combination to a targeted effect (e.g. depth of anaesthesia determined by electroencephalographic monitoring) selected by anaesthetists, using knowledge of interactions;
- they can be used to describe interactions between three co-administered drugs, as opposed to those occurring between just two drugs.

Few studies investigate combined effects resulting from co-administration of three major anaesthetic drug classes (opioids, intravenous and inhalation agents) for anaesthesia. The absence of a suitable model describing the interaction between these drug classes is illustrated by one recently available anaesthetic monitor (Navigator Applications Suite, GE Healthcare, Finland) which displays predicted effect profiles in real time for commonly used two drug combinations, but is unable to model the administration of a third drug class.

Many anaesthetics involve more than three drugs and numerous interactions may exist between any or all of them. A three drug interaction model in this context may be considered too simple. However, response surface methods are an improvement over the methods traditionally employed for *in vivo* studies in anaesthesia that describe two drug relationships for limited dose combinations or effect targets. An example of this is isobolographic analysis whereby the dose pairs of two drugs that together produce a single effect level are established. Investigations into how response surface models might be extrapolated between similar drug combinations, for example, within drug classes, may lead to improved use of these drugs in clinical settings. Anaesthetic trainees are commonly taught to recognise crises using simulation rather than real patients. Simulation is one setting in which a simplified model of anaesthetic interactions would be useful. A model describing opioid, intravenous and inhalation anaesthetic relationships is

applicable in medical simulators where pharmacokinetic and dynamic models are used to drive simulated ‘patient’ responses to a wide range of drug interventions by the user.

1.1. Thesis outline

In this thesis, I report my investigations into the use of pharmacokinetic and pharmacodynamic models to describe combined drug responses for applications relevant to anaesthesia. In the first part of this thesis, I present models describing the combined analgesic effect of two popular postoperative analgesics, ibuprofen and diclofenac, when given with paracetamol. These combinations are frequently used in cardiac and paediatric settings for postoperative analgesia. In the second part of this thesis, I present work towards developing a three drug-class interaction model for application in the sophisticated patient simulator, the METI[®] Human Patient Simulator (HPS)[™] (Medical Education Technologies, Inc; Sarasota, FL) which is currently used in our institution for anaesthesia based teaching.

This chapter: I begin by illustrating the importance of considering drug interactions using the effects of morphine and its active metabolite on respiratory depression as an example. I then give a brief overview of some drug classes central to anaesthetic management that are commonly used in combination to achieve similar endpoints. Drugs were selected from those frequently used at our institution (a major tertiary teaching hospital) and include some intraoperative drug classes that contribute to the state of anaesthesia, as well as some popular postoperative analgesics. Pharmacological profiles are reviewed and patient characteristics known to influence pharmacokinetic and pharmacodynamic profiles are outlined for each drug class. Interactions between these drugs are summarised, and modelling methods for describing interactions in anaesthesia are briefly reviewed. Finally, I review current literature pertaining to response surface models in anaesthesia.

Chapter 2: Chapters two and three outline novel uses of response surface modelling. Paracetamol with ibuprofen, and paracetamol with diclofenac, are two analgesic combinations used frequently in our teaching hospital. I review discrepancies existing in the current literature between studies investigating the benefits of using paracetamol in combination with ibuprofen for postoperative analgesia, over using

either drug alone. Response surface methods are used to generate a testable hypothesis as to why this may be.

Chapter 3: I then go on to describe the use of response surface methods to determine the combined analgesic effect of paracetamol and diclofenac in children following tonsillectomy, and give a model for postoperative pain relief. Placebo effects and the effects of missing data (or study ‘dropout’) are included in the analysis. Missing data are a common problem in analgesic studies that occurs when participants drop out of studies early because of reasons such as uncontrolled pain or need for rescue medication.

Chapter 4: This is the first in a series of sub-studies that work towards establishing a model describing opioid, intravenous and inhalation anaesthetic relationships. The modelled response (or effect) is processed electroencephalograph (EEG) in the form of the Bispectral Index (BIS) monitor (Covidien Medical, Boulder, CO, USA) used as a surrogate measure for sedation and depth of anaesthetic. I begin by developing a pharmacokinetic-linked response surface model describing BIS effect for propofol with alfentanil (using an existing dataset). The interaction between propofol and alfentanil is investigated.

Chapter 5: I investigate the feasibility of extrapolating a model for BIS response between opioids of the phenyl-piperidine class. An existing dataset derived using propofol and remifentanil to induce anaesthesia in healthy volunteers was available for pooling with the data from chapter 4. The response surface model developed for propofol and alfentanil is used to predict BIS response in the pooled dataset. Model performance is assessed, and parameters are refined. A dose equivalence factor is proposed for conversion between alfentanil and remifentanil effect site concentrations.

Chapter 6: I describe a prospective study of a linked pharmacokinetic-pharmacodynamic model to control the intravenous infusion of two drugs in anaesthesia. This proof-of-concept study investigates the use of response surface model driven infusions of propofol (intravenous anaesthetic) and remifentanil (opioid) to achieve selected BIS levels. Model performance is assessed and retrospective analysis

undertaken to compare response surface models additional to that which was tested prospectively. Model performance is compared to that reported for other models given in the literature.

Chapter 7: I describe an observational study in which collected data are used to develop a model of BIS response for three major anaesthetic drug classes; opioids, and intravenous and inhalation anaesthetics. The sedative midazolam is also included in the model. The intention of this work is to begin development of a generalised drug model suitable for use in a high fidelity, model driven patient simulator.

Chapter 8: I discuss how the model developed in chapter 7 might be used to simulate realistic BIS response in our human patient simulator (METI[®] HPS[™], Medical Education Technologies, Inc; Sarasota, FL). I use simulation of some simple anaesthetic scenarios to illustrate how the model might provide a useful measure of depth of anaesthesia for experienced clinicians, and how it might be linked to some simulated clinical endpoints (specifically, closing of the manikin eyes during induction of anaesthesia). I also provide some initial discussion around simulating realistic variability for simulation purposes.

Chapter 9: I present a general discussion of my work. My conclusions are reviewed in the light of current knowledge and potential areas for future research are outlined.

1.2. Anaesthesia

William T. Morton successfully demonstrated the use of di-ethyl ether on a patient undergoing removal of a vascular lesion in the neck in October 1846.[1] Before this pain and awareness were accepted as inevitable consequences of surgery. The practical implications for surgery were immediately obvious. The induced state was called ‘anaesthesia’ by Oliver Wendell Holmes, the term meaning “temporarily without sensation”. General anaesthesia can be defined as a drug induced state of unconsciousness of the brain, coupled with inhibition of arousal in response to noxious stimuli activating pain pathways.[2]

General anaesthesia was originally produced using single inhalational agents. However, when single drugs are used the dosing range within which adequate anaesthesia can be achieved tends to be narrow; too little drug results in responsiveness, awareness or movement, while too much drug is associated with negative effects such as profound cardiac and respiratory depression, slow recovery or even death. In 1926, Lundy proposed using smaller doses of a number of anaesthetic agents in combination to cause unconsciousness, coupled with ample local anaesthetic to block pain signals and subsequent arousal.[3] He termed his approach to anaesthesia ‘balanced’. The concept was extended in 1952 and three factors fundamental to providing balanced general anaesthesia were identified: narcosis, analgesia and muscle relaxation.[4] Although muscle relaxation does not add to the state of anaesthesia specifically through suppression of consciousness or sensation, its inclusion as a supplement to anaesthesia was important. Muscle relaxation sufficient for abdominal surgery was only achieved using high doses of inhalation anaesthetics before the introduction of neuromuscular blocking drugs (NMBDs). The addition of NMBDs meant that muscle relaxation could be controlled independently of inhalation agent dose, respiration could be fully controlled and laryngeal spasm prevented, all while using only minimal doses of other anaesthetic agents and thus minimising their dose-dependent adverse effects.[5]

Combining drugs also allows a degree of independent control over patients’ physiological variables such as blood pressure, sedation and response to pain; this is an important advantage when dealing with diverse patient populations typical of hospital settings. Mathematical equations (modelling) help enable understanding of a drug’s pharmacological profile, and more specifically, its dose-concentration-effect

relationships. This understanding supports dosing decisions and improves the ability of clinicians to achieve desired anaesthetic endpoints or influence physiological variables in individual patients.

1.3. Pharmacology modelling for anaesthesia

Pharmacological profiles guide drug dosing but individual responses to standardised drug doses vary widely. Pharmacokinetic (PK) and pharmacodynamic (PD) models summarise these profiles, and can be used to titrate dose and predict drug effects. Such models are descriptions of an average individual typical for the population studied.

1.3.1 Population methods

The simplest way in which population data may be modelled is to treat all data points as if they were collected from a single individual. This is known as the naïve pooled fit and may be suitable when there are many observations per individual. The main limitation of this approach is that each individual's information is treated as equally important and so outlier individuals or missing data have greater potential to bias model estimates. A two-stage fit involves estimating parameters for each individual and averaging these individual parameter estimates to establish a typical parameter value for the population as a whole. The range of estimates associated with each population parameter roughly represents between-subject variability. Between-subject variability refers to variability between individuals that arises from biological differences. Some of this variability may be explainable by identifiable factors (known as covariates) but some factors are not always easily identifiable. A second source of variability also exists; that arising between occasions within a single individual (within-subject variability). Within-subject variability is observed when taking repeated measurements and may arise from measurement inaccuracies, but may also come from unknown differences in the individual over time (e.g. attributable to circadian rhythms). Between-subject variability in the two-stage fit may be inflated because covariates remain unidentified and within subject variability is not considered.

Therefore a “mixed effects” approach is more often used. This method copes with missing or sparse data and variable sampling times by borrowing information between individuals (a Bayesian approach). It also recognises the different sources of variability. “Mixed effects” refers to the presence of both predictable and unpredictable variability. Predictable variability is that occurring between subjects that is attributable to, or explainable by, patient characteristics or covariates such as age, weight or pathology. A covariate model describes how much an individual will differ from the population average on account of that covariate. Inclusion of covariate effects helps to reduce estimates of (unexplained) between-subject variability. Parameters describing structural pharmacokinetic or pharmacodynamic models are estimated alongside those describing error and covariate models. A mixed effects approach makes use of all the data available for an individual, unlike the naïve pooled fit or two-stage fit, in which some information about individuals and how they differ from the rest of the population is lost. The differences between these approaches are summarised in Table 1.1.

Understanding sources of variability allows us to better predict how an individual’s profile will differ from that describing the ‘typical’ patient. This makes models more representative of a wider range of individuals. Drugs are often given in combination in anaesthesia. The influence of one drug on the pharmacological profile of another is a potential source of variability which is often overlooked. A model’s ability to predict observed drug effects may be improved by considering other agents that also contribute towards that effect. These concepts are illustrated briefly below using the opioid morphine as an example.

	Naïve pooled	Standard two-stage	Population
Method of analysis	All data points pooled and treated as if derived from a single individual	Individual profiles analysed independently, parameters are then are combined to give summary measures for population	All data are analysed together but data are recognised as belonging to individuals. Each individual's data contributes to population parameters and estimates of variability (that show how individuals differ from the 'typical' patient due to random and identifiable sources of variability)
Data required	Rich from few individuals; a full dataset is required from each	Rich from few individuals; individuals for which data are truncated or missing must often be excluded from analysis	Sparse data from many individuals; data may be pooled from various sources, individuals for whom data are truncated or missing can be included in the analysis
Sampling times	Taken at the exact same time for each individual	Taken within a sampling window	Sampling times can vary
Covariate analysis	Not possible	Possible but requires good estimates of each individual's parameters	Covariate analysis is standard practice
Variability	No information on between subject variability is gained	Between subject variability and residual variability is not distinguished	Between-subject variability, within-subject variability and residual variability are estimated

Table 1.1

Summary of data analysis options for population derived pharmacokinetic (PK) and pharmacodynamic (PD) data. Attributes of the naïve pooled fit, standard two-stage approach and population approach are given. This table is adapted from Anderson *et al.*[6]

1.3.2 An illustrative example of combined effects: morphine and its active metabolite

Morphine is an analgesic that is commonly used in adult and paediatric patients and is associated with respiratory depression. There is a direct relationship between morphine concentration and this effect; morphine plasma concentrations above 20 ng.ml^{-1} depress carbon dioxide (CO_2) response in 70% of children (2-570 days postnatal age) following cardiac surgery, and are associated with hypercapnia in 67% of children. Respiratory depression persists after ceasing morphine infusions with morphine concentrations over 15 ng.ml^{-1} associated with hypercapnia in 46% of children, and concentrations less than 15 ng.ml^{-1} in 13%.[7] Morphine's respiratory effects may be confounded by those of its active metabolite. Approximately 55% of morphine is converted to morphine-3-glucuronide (M3G), with a further 10% converted to morphine-6-glucuronide (M6G). M6G has analgesic and respiratory depressant effects and is cleared predominantly by the kidneys.[8] Consequently, M6G accumulates due to little or no clearance in patients with poor renal function and its effects may compound with those of the parent drug. In these patients, models of morphine effect on respiratory rate may be improved by also considering M6G effects.

1.3.2.1. Methods

Data were available from a 12 year old, male child (27 kg) with end-stage renal failure, hyperparathyroidism and congestive heart failure who received treatment at Starship Children's Hospital in 1997. Data (morphine dose and respiratory rate) were collected by Professor Brian Anderson, who was the attending clinician at the time. Ethics committee review was not required for these observational data as they were collected as part of standard clinical care and audit by the attending physician.[9] The patient and his parents gave written permission to analyse and publish data, both at the time of treatment (1997) and again in 2011. The patient was scheduled for parathyroid resection and intravenous morphine, delivered by a Patient Controlled Analgesia (PCA) pump, was prescribed for postoperative pain. PCA was restricted to morphine 0.5 mg as a bolus, with a five minute lockout period before subsequent dosing. Hourly morphine dose was recorded directly from the PCA pump, and respiratory rate recorded by nursing staff, for two postoperative days. The child was receiving regular haemodialysis and this treatment was scheduled postoperatively on day two, but was delayed until 45 h because of heavy weekend service commitments on attending hospital staff.

Plasma concentrations of morphine and M6G were estimated from morphine doses using a published model of morphine pharmacokinetics in children.[10] This was a one-compartment, first order elimination model with an estimated morphine volume of distribution (V) of 136 l.70kg⁻¹, M3G formation clearance (CL) 64.3 l.h⁻¹.70kg⁻¹ and V1 23 l.70kg⁻¹, M6G formation CL 3.6 l.h⁻¹.70kg⁻¹ and V1 30 l.70kg⁻¹, and morphine clearance by other routes 3.1 l.h⁻¹.70kg⁻¹. [10] As this child had severe renal dysfunction, metabolite clearances were fixed at 0.001 l.h⁻¹.70kg⁻¹ until dialysis began, reflecting renally dependent clearance pathways for these metabolites. A delayed effect compartment model was used to describe morphine and M6G concentrations causing respiratory depression; the temporal relationship between predicted concentrations in plasma and effect siteⁱ compartments was described by an equilibration rate constant (keo), derived from an estimated equilibration half-time (t_{1/2}keo) i.e.

$$t_{1/2\text{keo}} = \frac{\text{Ln}(2)}{\text{keo}}$$

Equation 1.1

The relationship between estimated morphine effect site concentrations (C_{eM}) and observed respiratory rate was described using a sigmoidal equation i.e.

$$E_M = E_0 - (E_0 - E_{\text{MAX}}) * \frac{C_{eM}^\gamma}{(C_{eM}^\gamma + C_{e50,M}^\gamma)}$$

Equation 1.2

where E_M is the effect of morphine, E₀ is baseline respiratory rate (the lowest possible respiratory rate was assumed as zero), E_{MAX} is the maximal reduction in respiratory rate, C_{e50,M} is the concentration of morphine in the effect site that produces 50% of E_{MAX} and γ is a parameter describing the sigmoidal curve shape. This model was used by Hill to describe the oxygen dissociation curve.[12] A sigmoidal curve is often used to describe drug effect because it adheres to a number of properties true of most drugs: some threshold concentration must be surpassed before any drug effect is seen; effect is non-linearly related to drug concentration; and saturation of the system must occur at which point additional increases in drug

ⁱ The temporal delay between drug plasma concentrations and corresponding drug effect can be described using a hypothetical ‘effect site’ compartment in which drug binds receptors.[11] Rate constants describe equilibration of drug concentrations between the plasma and effect site compartments, while drug effect is assumed to be proportional to effect site concentrations.

concentration no longer produce increases in effect. This is demonstrated below in Figure 1.1 where the influence of the slope parameter (which is estimated and gives the curve its sigmoidal shape at values greater than 1) is visible. It is important to note that some portions of the pharmacodynamic relationship can be approximated by linear models, for example, in the central region. The use of a linear model may be appropriate in situations where the concentration range studied is limited (as is often the case in clinical studies where higher doses of drug are associated with intolerable negative drug effects) and relates to one such area on the effect curve.

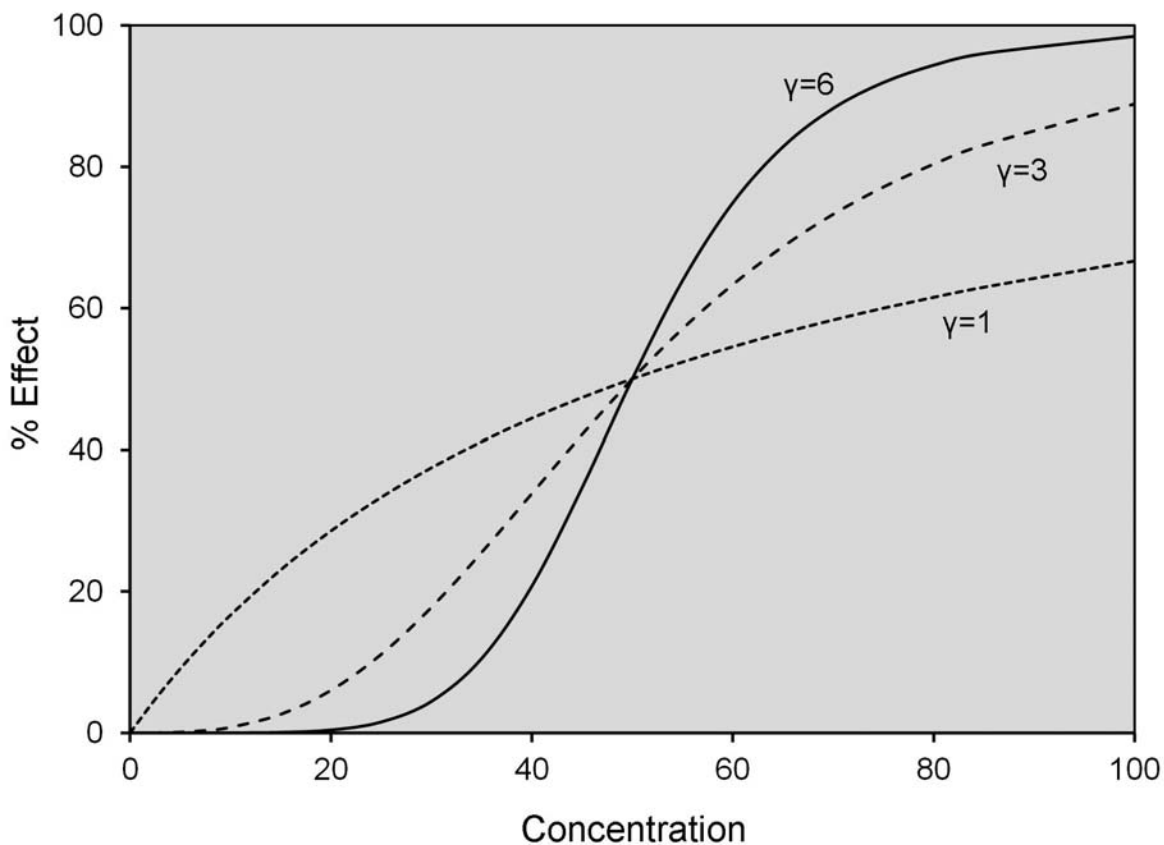


Figure 1.1

Theoretical sigmoidal ' E_{MAX} ' curves for varying γ (or slope) parameters. Baseline effect is given by E_0 and maximum observable effect is given by E_{MAX} . Drug effect approaches but cannot reach E_{MAX} . The curves intersect at the concentration at which 50% E_{MAX} is achieved (C_{E50}). For each curve depicted only the γ parameter is varied; increasing γ parameters describe steeper curves.

The model described above was repeated for the effect of M6G (E_{M6G}) alone, using an equilibration rate constant (keo) for M6G transfer to the M6G effect compartment i.e.

$$E_{M6G} = E_0 - (E_0 - E_{MAX}) * \frac{C_{eM6G}^{\gamma}}{(C_{eM6G}^{\gamma} + C_{e50,M6G}^{\gamma})}$$

Equation 1.3

where C_{eM6G} is the concentration of M6G, $C_{e50,M6G}$ is the concentration of M6G producing 50% of E_{MAX} . Finally, a third model describing combined effects of morphine and M6G was tested, where total effect on respiratory rate was calculated as $E_M + E_{M6G}$, where E_M is morphine effect and E_{M6G} is M6G effect as described using Equation 1.2.

Data were analysed using nonlinear mixed effects models (NONMEM VI, Globomax LLC, Hanover, MD, USA). Residual unknown error was described using an additive error model for each observation prediction (Err_{ADD}). Parameters and residual variance were estimated using the first order conditional estimate method. Equations were integrated within ADVAN=4 with TRANS=4. Convergence criterion was 3 significant digits. The NONMEM code used for the three models is given in Appendix 1. The fit of each model to the data was assessed using NONMEM's objective function value (OBJ) and visual examination of plots of observed *versus* predicted respiratory rates. Models were nested and an improvement in the OBJ was referred to the Chi-squared distribution to assess significance (e.g. a decrease of 6.64 is significant at $\alpha=0.01$). A visual predictive check (VPC), [13] a modelling tool that estimates prediction intervals and graphically superimposes these on observed respiratory rates, was used to evaluate how well the model predicted the distribution of observed respiratory rates.

1.3.2.2. Results

The combined effect model for morphine with M6G was better than those using either morphine (Δ OBJ = -47.7, $P < 0.001$) or M6G alone (Δ OBJ = -4.8, $P = 0.03$) (Figure 1.2). Baseline respiratory rate was 20.7 breaths.min⁻¹ and E_{MAX} assumed as zero. The Ce_{50} for both morphine and M6G was 16.9 ng.ml⁻¹; individual parameters did not improve the OBJ. Similarly morphine and M6G shared a slope parameter of 2.35 as individual parameters did not significantly improve the fit of our model. The $t_{1/2keo}$ for morphine was 16 min while that for M6G was considerably larger at 6.7 h. Err_{ADD} was estimated as 2.2 breaths.min⁻¹. A VPC for the final combined effect model is shown in Figure 1.3. VPCs, showing observed and predicted respiratory rates over time, are given in Figure 1.3 for the morphine alone model and the combined morphine with M6G model.

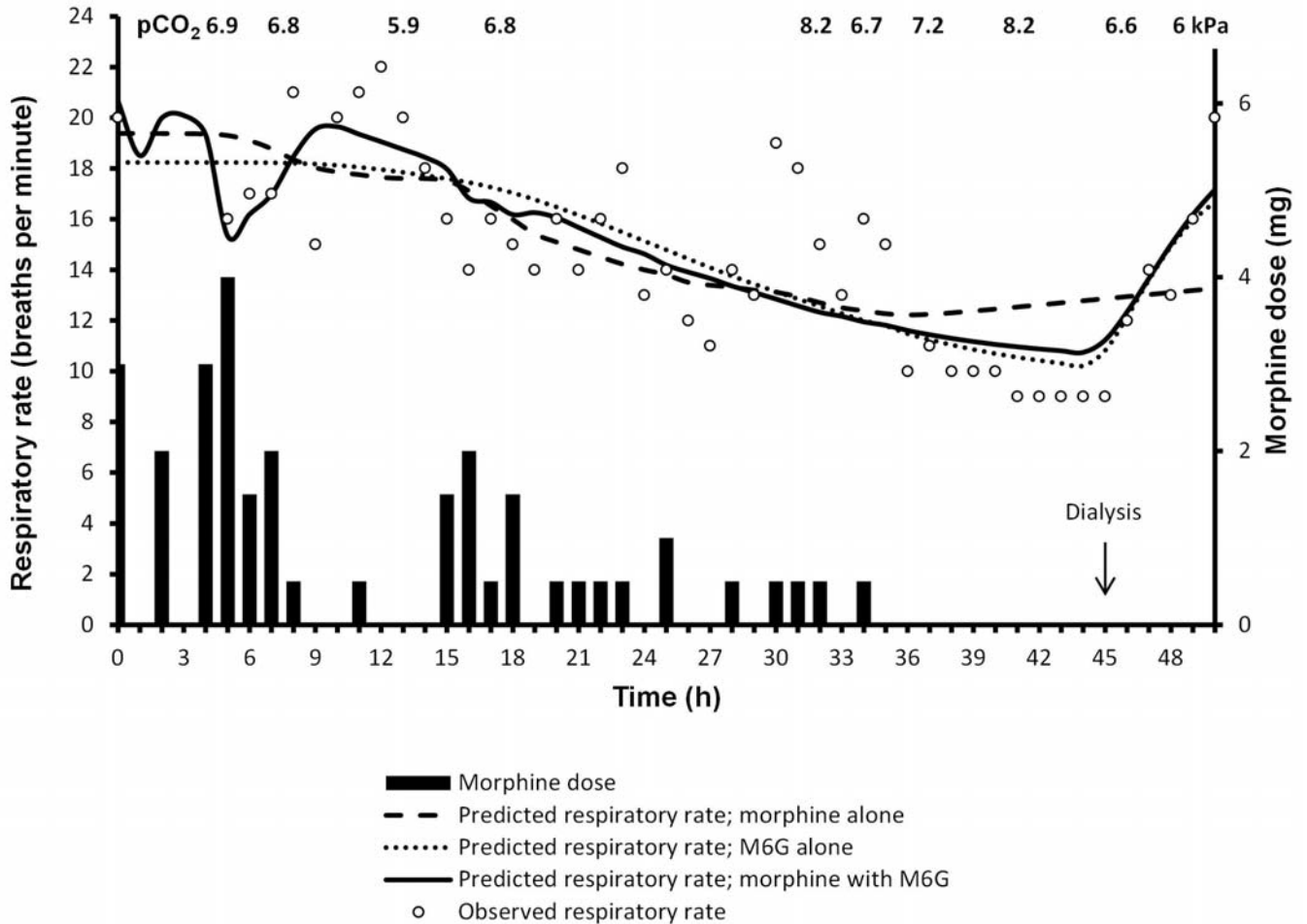


Figure 1.2

Observed and predicted respiratory rate for a 12 year old, male child with end-stage renal failure given intravenous morphine *via* a PCA pump for postoperative pain. Predicted respiratory rates are for morphine only, M6G only, and combined morphine M6G effect. Observed partial pressure of CO₂ (kPa) is also given. Dialysis began at 45 h postoperatively (indicated by the arrow) and continued for 3 h. It can be seen that the solid line, depicting predicted respiratory rate for the combined model, more closely follows observations in the 0-15 h time period than do lines depicting predictions using the morphine alone and M6G alone models. Similar predictions following onset of dialysis are made for the M6G alone and combined effect models.

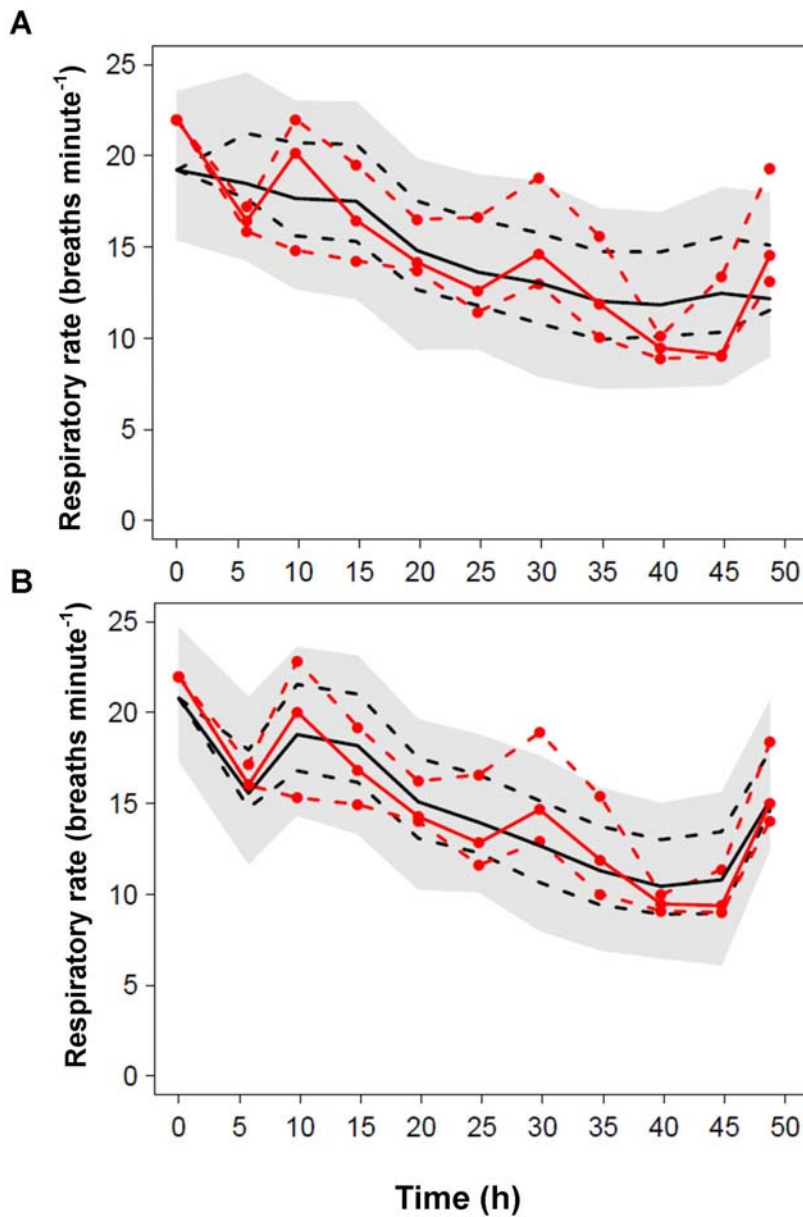


Figure 1.3

Visual predictive check for A) the morphine alone model and B) the combined morphine and M6G effect model. The plots show median and 90% intervals (solid and dashed lines respectively). Prediction percentiles (10%, 50%, and 90%) for predictions (black lines) are overlaid with those of the observations (red lines with symbols). Grey shaded areas are 95% confidence intervals for the prediction percentiles. An improvement in fit can be seen for early and late respiratory rates in the combined effect model (panel B), although little difference is seen between 15 h and 40 h.

1.3.2.3. Discussion

Models for morphine alone, M6G alone, and combined morphine and M6G were used to describe observed respiratory rates over 50 h in a child with end-stage renal failure. Observations were more consistent with contributions from both morphine and M6G to respiratory effect. Peak respiratory depression has been observed to occur considerably later than would be expected from peaks in morphine concentrations [14] and it is likely this reflects the process of morphine metabolism to M6G and subsequent movement of M6G from plasma to an effect site where it acts to depress respiration. Little or no clearance of M6G due to poor renal function allowed assessment of M6G respiratory effects in this child.

A model of morphine effect alone inadequately described initial changes in respiration and late respiratory depression at 35 h in this child (Figure 1.2). A model using just M6G alone better described late respiratory depression but failed to track observed respiratory rates in the first 10 h. A model describing additive effects of both morphine and M6G improved the fit for early and late respiratory rates (Figure 1.3), although there were still some differences between the predictions and observations at some time points.

This is as one might expect because pharmacokinetic predictions were estimated using a population model and consequently these may not be typical for the index child.[15] Respiratory changes due to external stimulation are not accounted for (e.g., acute pain from intravenous cannula insertion at approximately 31 h). The model cannot estimate between-subject variability. Results of this simulation study fit with those observed by others, despite these limitations. Morphine pharmacodynamics appear to be similar for respiratory depression and analgesia.[16] An estimated morphine $t_{1/2keo}$ of 16 min for respiratory depression is the same as that reported for analgesia[17, 18] and a M6G $t_{1/2keo}$ estimate of 6.7 h is within the 4-8 h range reported for delayed M6G analgesic effect.[18] The Ce_{50} of morphine was not distinguishable from that of its metabolite using these data, although the Ce_{50} for morphine of 16.9 ng.ml^{-1} is consistent with clinical observations for both analgesic concentrations ($10\text{-}20 \text{ ng.ml}^{-1}$)[19-21] and respiratory depression (hypercapnia in 46% children with concentration $>15 \text{ ng.ml}^{-1}$).[7]

Others have also reported that hypercapnic ventilator responses for both parent and metabolite are similar (Ce_{50} 10-18 $ng.ml^{-1}$). [16, 18, 22] The response curve steepness (represented by the slope parameter γ) for morphine and M6G were also indistinguishable; this has been noted by others examining the hypercapnic ventilator [18] and pupillary responses to morphine and M6G. [23]

This example illustrates a number of important points. Firstly, we see how models may be used to interpret trends observed in clinical practice. Morphine is metabolised to active M6G through hepatic UGTB27 and this metabolite is cleared by the kidney; the plasma concentration increases in those with renal impairment. Contribution of accumulating M6G due to poor clearance may explain unexpected or persistent respiratory depression in some patients; indeed fentanyl, which is metabolised predominantly by hepatic pathways, is now preferred for repeat dosing over time in patients with renal impairment.

This example also illustrates how identifying factors that describe how an individual varies from the population can improve model predictions. The final model, in which M6G clearance before dialysis is fixed at $0.001\ l.h^{-1}.70kg^{-1}$ and that during dialysis is estimated, gives an OBJ value of 121. Rerunning this model with M6G clearance fixed at a population estimate of $5.8\ l.h^{-1}$ [10] results in a 47 point increase in OBJ. This represents a much poorer fit and we can see that the M6G clearance of this patient varies widely from that of the population.

Finally, we see the importance of considering combined drug effects on the endpoint in question. Early and late respiratory rate predictions in this example were improved by including parent and metabolite drug effects, as compared to tested single drug models (Figure 1.2). Models that are developed to describe drug effects in the clinical setting may be improved by incorporating the effects of concomitant drugs. This may be particularly important in anaesthesia where multiple agents are used together to achieve clinical endpoints.

1.4. Drug classes in anaesthesia

I will summarise key information about some drugs commonly used in anaesthetic practice, and central to this thesis, in the remainder of this chapter. I will begin with the analgesic paracetamol, and then consider the opioid, intravenous and inhalation anaesthetic drugs most prominently used during anaesthesia at Auckland City Hospital. Pharmacokinetic and pharmacodynamic parameter estimates reported in the literature will be given where available. The way in which these drugs are combined to achieve desired anaesthetic endpoints, and the interactions existing between them, will also be discussed.

1.4.1 Paracetamol (analgesic)

Pain control, both intraoperatively and postoperatively, is an important aspect of anaesthetic management. Aside from patient comfort, analgesia also plays a role in suppressing the body's surgical stress response.ⁱⁱ Postoperative pain control may begin during surgery, or even preoperatively for short cases. Agents that provide analgesia over a number of hours may be given at the end of surgery, contributing to postoperative analgesia. Drug side effects that are manageable (or even beneficial) during anaesthesia may become unfavourable during recovery. An example of this is opioid induced respiratory depression. Patients are mechanically ventilated and drugs are used to give anaesthetists complete control over respiration during surgery, but postoperatively patients resume spontaneous breathing. Drugs that cause respiratory depression may inhibit recovery in spontaneously breathing patients, and so those agents with fewer propensities to cause this effect are preferred.

Paracetamol (acetaminophen) is considered first line treatment for pain and is often used for antipyresis. It may be given alone and in combination for postoperative pain control. Paracetamol's mechanisms of action are not fully understood,[25] though its antipyretic and analgesic effects are of a similar magnitude to those of aspirin and the wider non-steroidal anti-inflammatory drug (NSAID) group. NSAIDs act *via* inhibition of cyclooxygenase site of the Prostaglandin (PG) H2 Synthetase enzyme leading to inhibition of various prostaglandins (PGI₂, PGE₂, PGF₂) and thromboxane (other mechanisms may also exist).[26]

ⁱⁱ A number of physiological changes resulting from endocrine, inflammatory and metabolic responses to tissue injuries caused during surgery.[24]

Paracetamol lacks any significant anti-inflammatory or anti-platelet properties and acts *via* different pathways, probably the peroxidase site of the same enzyme.[26] A central action is postulated and multiple possible pathways for this have been proposed, including *N*-methyl-D-aspartate (NMDA), substance P, cannabinoid, nitric oxide synthase inhibition and serotonergic pathways.[25-28]

A central action for paracetamol is supported by animal data and through concentration-effect modelling. A concentration in a central 'effect site' of 10 mg.l^{-1} has been related to a reduction in pain of 2.6 cm on a visual analogue scale, (0-10) after tonsillectomy; comparable concentrations have been detected in the cerebrospinal fluid (used as a surrogate for a central effect site),[29] better describing paracetamol pharmacodynamics than plasma concentrations.[26, 30] Paracetamol is one of the most popular over-the-counter analgesics [31] and is used in oral, rectal and intravenous formulations. Pharmacokinetics are usually described by a single compartment with a V_1 ranging between 56 and 70 l , and CL_1 between 12 and 21 l.hr^{-1} for a 70 kg adult.[32] Absorption half-lives (t_{abs}) for oral dosing range from 2.7 to 4.5 minutes and are associated with a lag time (t_{lag}) of 4.2 minutes.[33, 34]

Paracetamol within dosing recommendations is not associated with respiratory depression or increased nausea and vomiting, making it ideal for spontaneously breathing surgical patients recovering from general anaesthesia. Paracetamol when used as monotherapy at common doses ($10\text{-}15 \text{ mg.kg}^{-1}$) may be insufficient for severe pain. It is often combined with other analgesics such as tramadol, low dose opioid or an NSAID, or supplemented with techniques such as nerve blocks and local anaesthetic placement. Paracetamol with an NSAID is a common combination in the perioperative period, for example it is often used after paediatric adeno-tonsillectomy. Analgesic and anti-inflammatory effects of NSAIDs are offset by the potential for adverse effects on gastrointestinal, renal and cardiovascular systems and consequently dosing is restricted. Many studies have sought to compare analgesia efficacies of combination therapy over monotherapy using either paracetamol or a single NSAID. However, results are often conflicting. This problem is considered further in chapters 2 and 3 where pharmacokinetic models are linked to response surface models to describe combined drug effects over time.

1.4.2 Midazolam (sedative)

Midazolam hydrochloride is a benzodiazepine that has sedative, anxiolytic and amnesic properties. Midazolam acts as an agonist at the benzodiazepine site (located between the γ_2 and α_1 subunits) of the GABA_A receptor.[35] Midazolam has many uses ranging from prevention of seizures to treatment of insomnia. Midazolam is often given intravenously as a premedication to facilitate anaesthetic induction because it contributes to sedation, relaxes patients and prevents recall. Midazolam is the only sedative that appears in the top five administered intravenous drugs during anaesthesia at Auckland City Hospital (Table 1.2).[36] Midazolam has an onset of action between three and five minutes. Pharmacokinetics of intravenously administered midazolam are best described by a three compartment model. Parameter estimates obtained from various pharmacokinetic studies are given in Table 1.3. Midazolam causes sedation at doses of 0.14 mg.kg^{-1} [37] with an estimated EC_{50} of 270 ng.ml^{-1} (Ce_{50} in the plasma) at steady state,[38] although it cannot produce anaesthesia alone. Age influences midazolam pharmacodynamics, with a Ce_{50} of 522 ng.ml^{-1} estimated in the effect site for EEG measures in adults aged 25 years, as opposed to 223 ng.ml^{-1} estimated in elderly (70 years of age).[39] These estimates are associated with keo values of 0.11 and 0.08 min^{-1} ($t_{1/2keo}$ 6.3-8.7 min) respectively.[39]

Drug Name	Drug Class	Common usage	Mean (SD) administrations per patient*
Fentanyl	Opioid	Intraoperative and postoperative analgesia	1.71 (1.63)
Propofol	Intravenous anaesthetic	Induce and maintain state of anaesthesia	0.86 (1.02)
Cefazolin	Antibiotic	Prevention of infection	0.48 (0.67)
Midazolam	Sedative	Reduce anxiety, facilitate induction of anaesthesia	0.49 (0.65)
Morphine	Opioid	Postoperative analgesia	0.54 (0.95)

Table 1.2

Five most commonly used intravenous drugs during anaesthesia at our centre, in order of frequency of use.

*Taken from a random sample of 100 anaesthetic cases at Auckland City Hospital. This table is adapted from Al-Tiay.[36]

Study	V1 (l)	V2 (l)	V3 (l)	CL1 (l.min ⁻¹)	CL2 (l. min ⁻¹)	CL3 (l. min ⁻¹)
Greenblatt 1989 [40]	29.60	99.40	-	0.34	0.99	-
Bar 2001 [41]	51.73	131.00	-	0.25	0.60	-
	[1.57·(63-AGE)+0.32·(WT-78)+33.90]	131.00	-	[0.006·(WT-78)+0.30]	0.60	-
Albrecht 1999 [†] [39]	7.90	21.94	47.45	0.33	1.32	0.39
Albrecht 1999 [‡] [39]	8.50	18.57	63.03	0.30	0.95	0.44
Bührer 1990 [42]	3.30	17.56	96.76	0.54	2.01	0.83
Maitre 1989 [43]	10.30	27.80	65.50	0.25	0.38	0.11
Zomorodi 1998 [44]	33.00	[(32.1·BSA)+3.32]	365.00	[(0.15·BSA)+0.09]	0.62	0.26

Table 1.3

Standardised* model parameter estimates for midazolam pharmacokinetics. *Standardised for a 70 kg, 175 cm, 50 year old male. Covariate models for parameter adjustments are given in square brackets, where applicable. WT=weight (kg), BSA=body surface area. [†]Model developed in young subjects. [‡]Model developed in elderly subjects.

1.4.3 Propofol (intravenous anaesthetic)

An anaesthetic agent is defined for this thesis as a drug which is able to induce a state of anaesthesia when given alone. Examples of intravenous anaesthetics include propofol and thiopentone, while sevoflurane is an example of an inhalational anaesthetic. The most commonly used intravenous anaesthetic in our study hospital is propofol (refer Table 1.2).[36]

Propofol has sedative and amnesic properties. It is thought to create its effect by increasing cerebral levels of the inhibitory γ -aminobutyric acid (GABA) neurotransmitter, most likely *via* the ligand gated GABA_A receptor. It was initially formulated with a surfactant (Cremophor EL) because of its high lipid solubility. However this formulation was abandoned because of the high incidence of pain on injection and anaphylactic reactions. Today, a propofol emulsion with soya bean oil and egg lecithin is used. Propofol is favoured over traditional induction agents such as thiopentone because of its fast onset and offset of effect with minimal residual ‘hangover’ after awakening. Clearance is greater than that of thiopentone, contributing to its comparatively quicker offset, although redistribution is the principle determinant of anaesthetic offset. Propofol is administered by both bolus and continuous infusion, and can be used for conscious sedation and total intravenous anaesthesia (TIVA). TIVA is often given through automated infusion pumps pre-programmed with population models that predict plasma concentrations, or effect site concentrations.

Propofol pharmacokinetics are best described by a three compartment model. Covariates of particular importance include age and body size. The best size descriptor remains uncertain (e.g. fat free mass, lean body mass, total body weight).[45] There are several different parameter sets available that can be used to describe propofol pharmacokinetics. A summary of these is given in Table 1.4 (adult data). A number of automated infusion pumps are programmed to infuse propofol using published parameter sets. These parameter sets are often labelled as “models” and take their name from a principle investigator or a company. Diprifusor® (AstraZeneca, Macclesfield, UK) uses that derived from adult data analysed by Marsh *et al.*[46] The parameter set was adjusted from earlier parameter estimates by Gepts *et al.*[47] and although volume parameters are scaled proportionally to an individual’s weight, no adjustment was made for gender or age. White *et al.* reinvestigated propofol pharmacokinetics to account for these additional

covariates.[48] The Diprifusor® consistently under-predicts plasma concentrations when used to infuse propofol to selected plasma concentrations, although model performance improves during recovery [49] and is considered to be within clinically acceptable limits of accuracy.[50] There are few linked pharmacokinetic-pharmacodynamic models available and determination of an appropriate keo parameter is commonly based on subsequent studies using Tpeak methodology.[51] Consequently, estimated keo rate constants for use with the Marsh model range from 0.20 to 1.2 min⁻¹ (t_{1/2}keo 0.6-3.5 min).[52, 53] The keo estimate is only specific for the data from which it was determined. The Schnider model was derived from a linked pharmacokinetic-pharmacodynamic study allowing direct estimation of keo at 0.46 min⁻¹ (t_{1/2}keo 1.5 min).[54, 55] Covariate effects of weight, height, lean body mass (LBM) and age were also estimated by Schnider *et al.* with increasing age reducing the Ce₅₀ for loss of consciousness from 2.35 mcg.ml⁻¹ in a 25 year old to just 1.25 mcg.ml⁻¹ in a 75 year old (Figure 1.4). The inclusion of age improves model performance in elderly patients in whom plasma concentrations may be underestimated, potentially leading to overdosing. Onset of drug effect is quicker with decreasing age in children. We might expect a shorter propofol t_{1/2}keo with decreasing age based on size models,[56] and this is exactly what has been described by Jeleazcov *et al.*[57] Similar results have been demonstrated for sevoflurane and BIS.[58] If unrecognised, this will result in excessive dose in a young child if a concentration in the effect site is targeted and peak effect (Tpeak) is anticipated to be later than it actually is because it was determined in a teenager or adult. Estimates for propofol Ce₅₀ for ablation of response to noxious stimuli, such as skin incision or laryngoscopy, range from 5.4-5.6 mcg.ml⁻¹. [59-61]

Study	V1 (l)	V2 (l)	V3 (l)	CL1 (l.min ⁻¹)	CL2 (l. min ⁻¹)	CL3 (l. min ⁻¹)
Shafer 1988 [62]	25.20	146.71	-	2.03	1.56	-
Bouillon 2002 [63]	5.55	30.90	209.0	2.96	2.55	1.00
Cortínez 2010 [†] [45]	4.47	26.60	53.8	2.25	3.20	0.52
Gepts 1987 [47]	16.92	39.90	230.00	1.77	1.52	0.62
Kataria 1994 [‡] [64]	36.40	70.70	574.00	2.38	4.06	1.82
Marsh 1991 [‡] [46]	15.96	33.16	203.15	1.90	1.82	0.67
Schuttler 2000	7.62	44.20	266.00	1.44	2.25	0.92
[65]	$[9.30 \cdot (TBW/70)^{0.71} \cdot (AGE/30)^{-0.39} \cdot (1+bol \cdot 1.16)]$	$[44.2 \cdot (TBW/70)^{0.61} \cdot (1+bol \cdot 0.73)]$		$[1.44 \cdot (TBW/70)^{0.75}]^{\wedge}$	$[2.25 \cdot (TBW/70)^{0.62} \cdot (1+ven \cdot -0.40) \cdot (1+bol \cdot 2.02)]$	$[0.92 \cdot (TBW/70)^{0.55} \cdot (1+bol \cdot -0.48)]$

Table 1.4

Standardised* model parameter estimates for propofol pharmacokinetics. *Standardised for a 70 kg, 175 cm, 50 year old male. Covariate models for parameter adjustments are given in square brackets, where applicable. [^] If age < 60, else CL1=1.44·(TBW/70)^{0.75}-(AGE-60)·0.05. TBW=total body weight (kg), HT=height (cm), AGE=age (y), LBM=lean body mass, bol=1 if bolus and 0 if infusion, ven=1 if venous sampling and 0 if arterial sampling. [†]Model developed in obese patients. [‡]Model developed in paediatric patients.

Study	V1 (l)	V2 (l)	V3 (l)	CL1 (l.min ⁻¹)	CL2 (l. min ⁻¹)	CL3 (l. min ⁻¹)
Schnider 1998 [54]	4.27	20.07	238.00	1.69	1.36	0.83
		[18.90+0.39·(AGE-53)]		[1.89+((TBW - 77)·0.046)+((LBM-59)·0.07)+(HT-177)·0.02]	[1.29+0.02·(AGE-53)]	
Servin 1993† [66]	17.90	42.30	66.00	1.70	2.99	0.21
Shafer 1988 [62]	8.40	43.65	185.95	1.96	1.59	0.81
Short 1994‡ [67]	16.66	24.30	178.00	2.03	0.68	0.80
Tackley 1989 [68]	22.40	36.75	144.94	1.85	2.35	0.49
White 2008 [48]	12.45	25.81	158.45	1.78	1.42	0.52
	[0.18+46.0E6·AGE]			[0.03+29.0E6·AGE]		

Table 1.4 continued.

Standardised* model parameter estimates for propofol pharmacokinetics. *Standardised for a 70 kg, 175 cm, 50 year old male. Covariate models for parameter adjustments are given in square brackets, where applicable. ^ If age < 60, else $CL1=1.44 \cdot (TBW/70)^{0.75} - (AGE-60) \cdot 0.05$. TBW = total body weight (kg), HT=height (cm), AGE=age (y), LBM=lean body mass, *bol*=1 if bolus and 0 if infusion, *ven*=1 if venous sampling and 0 if arterial sampling. †Model developed in obese patients. ‡Model developed in paediatric patients.

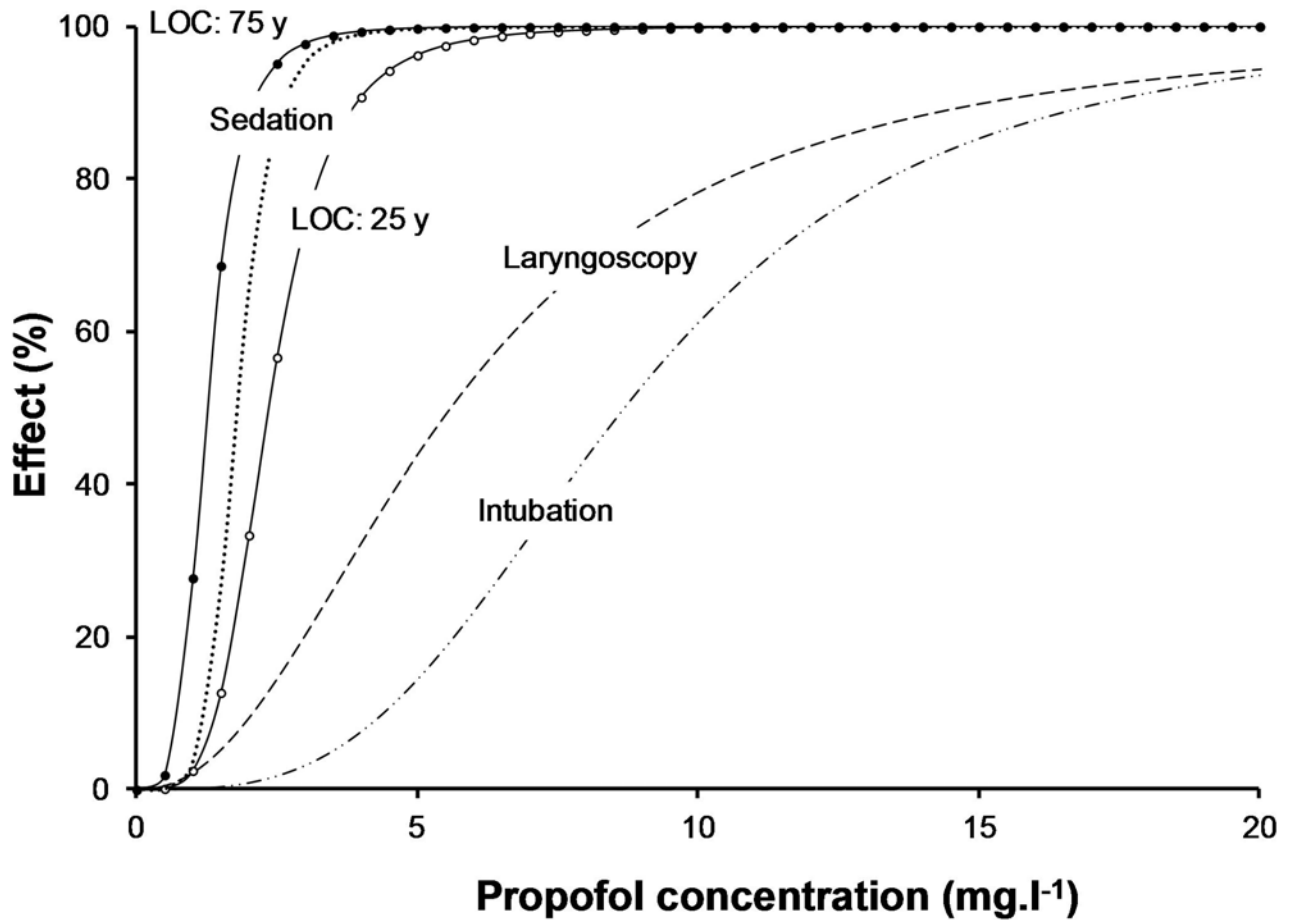


Figure 1.4

Sigmoid E_{MAX} curves describing propofol pharmacodynamics for anaesthetic endpoints: loss of consciousness (LOC), measured by ability to open eyes on command; sedation, measured by response to shouting and shaking; lack of response to laryngoscopy; and lack of response to intubation. The influence of age on propofol response is demonstrated for LOC where curves are given for 25 year old (solid line, open circles) and 75 year old patients (solid line, closed circles). Figure adapted from Kern *et al.* and constructed using parameter estimates reported in the literature.[55, 60, 69]

1.4.4 Morphine and the phenyl-piperidines (opioids)

Drugs of the opioid class bind to opioid receptors, which are found throughout the body in both the peripheral and central nervous systems. Opioid effects are determined by the type of opioid receptor bound. For example, μ opioid receptor binding is characterised by analgesia and respiratory depression, while sedation and dysphoria are typical of κ receptor binding. The opioids fentanyl and morphine are frequently given as boluses to deliver analgesia during anaesthesia at our hospital (refer

Table 1.2),[36] and remifentanyl is preferred for long infusions, for example during TIVA with propofol.

Morphine is a commonly used postoperative analgesic often used for PCA. It has a slower onset ($t_{1/2keo}$ 16 min), and longer duration of action (half-life $t_{1/2}$ 2 h) than other opioids.[17, 18] Negative effects associated with morphine use, such as nausea, vomiting and peripheral vasodilatation caused by histamine release, led to the development of other opioid derivatives with improved side effect profiles and shorter onsets and durations of action.[70] Fentanyl ($t_{1/2keo}$ 4.6 min) and alfentanil ($t_{1/2keo}$ 1 min) are commonly given during anaesthesia for analgesia.[71] They are typically administered as bolus doses to supplement intravenous anaesthetic agents that, when given alone, do not provide sufficient pain relief for surgery. The duration of effect for fentanyl is relatively short following bolus doses and brief infusions (attributed to redistribution with a half-life 19 min) but it rapidly increases when infused for over 30 minutes (Figure 1.5).[72] Remifentanyl may be a more appropriate choice for infusions that exceed this duration. Remifentanyl has similar potency to fentanyl but is characterised by a much shorter offset of action that is independent of the duration of infusion.[72]

The pharmacokinetics and dynamics of opioids have been well studied. Multiple compartment models are favoured to describe pharmacokinetics (Table 1.5 to Table 1.8). Age and the size descriptors total body weight and lean body mass have been identified as significant covariates for alfentanil and remifentanyl pharmacokinetics (Table 1.5 and Table 1.8 respectively). Volume and clearance from the central compartment decreases with increasing age.[73, 74] Ce_{50} estimates for processed EEG are alfentanil 376-479 ng.ml⁻¹, fentanyl 7.8 ng.ml⁻¹ and remifentanyl 11.2-19.9 ng.ml⁻¹. [71, 73, 75] Corresponding keo values are reported to be 0.72-1.4 min⁻¹ ($t_{1/2keo}$ 0.5-1 min), 0.15 min⁻¹ ($t_{1/2keo}$ 4.6 min), and 0.43-0.52 min⁻¹ ($t_{1/2keo}$ 1.3-1.6 min) respectively.[71, 73, 75] Opioid effects on EEG measures are generally accepted to be small and Ce_{50} estimates for opioid effect on EEG may be unidentifiable.[59, 76] Age is a significant covariate for remifentanyl pharmacodynamics, decreasing both Ce_{50} and keo estimates with increasing age and contributing to reduced dosing requirements in elderly.[73] One study found remifentanyl Ce_{50} estimates for processed EEG decreased from 16 ng.ml⁻¹ in 20 year olds to 7.9 ng.ml⁻¹ in 75 year olds.[73] Corresponding keo estimates were 0.61 min⁻¹ and 0.57 min⁻¹ ($t_{1/2keo}$ 1.14-1.22 min) respectively. Gender related differences in morphine

analgesia have been demonstrated with increased efficacy in women, though whether this observation holds for other opioids remains unclear.[77, 78]

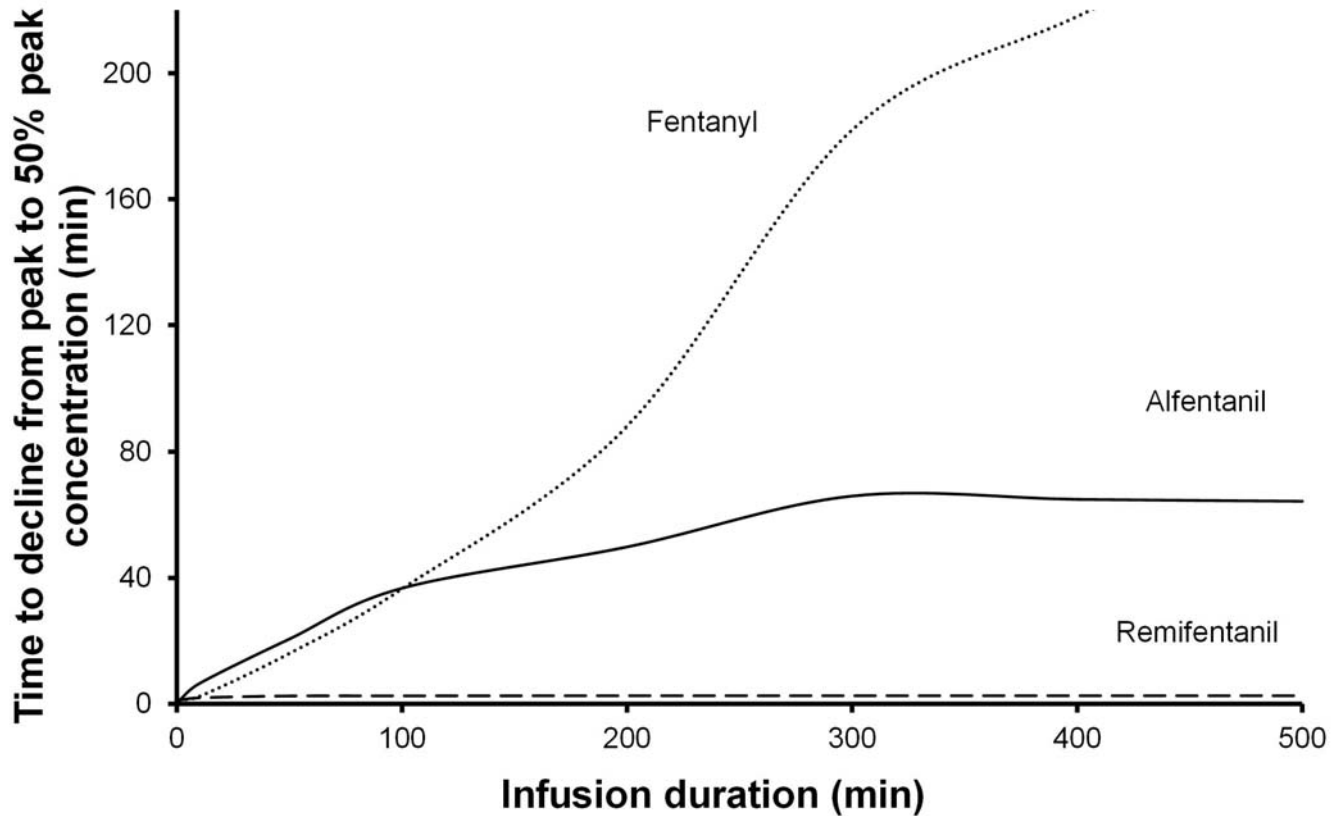


Figure 1.5

The influence of infusion duration on drug washout for alfentanil, fentanyl and remifentanil. Curves show the minutes, from cessation of infusion, required for plasma concentrations to decline by half their peak. Half times in this instance are considered 'in context' of the duration of infusion, termed context sensitive half times (CSHT). Remifentanil washout is unaffected by the duration of infusion, unlike alfentanil and fentanyl. Figure adapted from Shafer and Varvel 1991,[72] using parameter estimates reported in the literature.[71, 75]

Study	V1 (l)	V2 (l)	V3 (l)	CL1 (l.min ⁻¹)	CL2 (l.min ⁻¹)	CL3 (l.min ⁻¹)
Barvais <i>et al.</i> 1993 [79]	11.1	13.4	-	0.2	0.3	-
Bouillon <i>et al.</i> 1999 [80]	5.4	10.4	-	0.4	0.5	-
Bower <i>et al.</i> 1982 [81]	11.0	16.9	-	0.2	0.6	-
Burm <i>et al.</i> 1993 [82]	10.0	21.0	-	0.3	0.6	-
Fragen <i>et al.</i> 1983 [83]	9.1	14.5	-	0.2	0.4	-
Maitre <i>et al.</i> 1987 [74]	10.1	27.5	-	0.3	0.6	-
Meistelman <i>et al.</i> 1987 [84]	13.1	18.6	-	0.3	0.4	-
Persson <i>et al.</i> 1988 [85]	13.8	18.9	-	0.2	0.3	-
Shafer <i>et al.</i> 1986 [86]	14.0	9.8	-	0.3	1.0	-
Van Beem <i>et al.</i> 1989 [87]	10.3	21.0	-	0.3	0.5	-
Bovill <i>et al.</i> 1982 [88]	5.6	7.5	14.7	0.4	2.0	0.3
Camu <i>et al.</i> 1982 [89]	15.4	6.5	18.5	0.6	0.9	0.4
Egan <i>et al.</i> 1996 [75]	4.1	12.2	17.8	0.4	2.5	0.3
Maitre <i>et al.</i> 1987 [74]	7.9	11.9	17.4	0.3	0.9	0.2
Mertens <i>et al.</i> 2001 [90]	7.1	20.2	8.7	0.4	22.8	0.2
Petros <i>et al.</i> 1995 [91]	1.5	1.7	12.6	0.2	0.2	0.1
Scott <i>et al.</i> 1987 [71]	2.2	5.6	14.1	0.2	1.3	0.2

Table 1.5

Standardised* model parameter estimates for alfentanil pharmacokinetics. *Standardised for a 70 kg, 175 cm, 50 year old male.

Study	V1 (l)	V2 (l)	V3 (l)	CL1 (l.min ⁻¹)	CL2 (l.min ⁻¹)	CL3 (l.min ⁻¹)
Bower and Hull 1982 [81]	59.70	275.70	-	1.68	6.17	-
McClain and Hug 1980[92]	26.91	48.30	190.00	1.10	4.98	3.79
Scott and Stanski 1987 [71]	12.70	49.34	296.88	0.71	4.74	2.29
Shafer <i>et al.</i> 1990 [93]	7.35	31.22	235.90	0.59	3.32	1.39

Table 1.6

Standardised* model parameter estimates for fentanyl pharmacokinetics. *Standardised for a 70 kg, 175 cm, 50 year old male.

Study	V1 (l)	V2 (l)	V3 (l)	CL1 (l.min ⁻¹)	CL2 (l.min ⁻¹)	CL3 (l.min ⁻¹)
Lötsch <i>et al.</i> 2002 [94]	17.80	87.30	199.00	1.26	2.27	0.33 · (BSA/1.83) ⁴
Olofsen <i>et al.</i> 2010 [95]	5.11	10.0	114.0	1.57	0.90	1.53
Romberg <i>et al.</i> 2004 [96]	3.64	4.76	4.69	0.13	0.56	0.07

Table 1.7

Standardised* model parameter estimates for morphine pharmacokinetics. *Standardised for a 70 kg, 175 cm, 50 year old male.

Study	V1 (l)	V2 (l)	V3 (l)	CL1 (l.min ⁻¹)	CL2 (l.min ⁻¹)	CL3 (l.min ⁻¹)
2 compartments						
Bouillon <i>et al.</i> 2002 [63]	10.50	8.22	-	2.34	0.82	-
Egan <i>et al.</i> 1998 [97]	6.80	7.60	-	2.70	1.20	-
Egan <i>et al.</i> 1998 [^] [97]	7.50	8.70	-	3.10	1.30	-
Egan <i>et al.</i> 2004 [†] [97]	5.60	10.90	-	4.10	1.50	-
3 compartments						
Egan <i>et al.</i> 1993[98]	7.10	15.60	10.10	2.80	2.30	0.16
Egan <i>et al.</i> 1996 [75]	7.60	9.40	4.70	2.92	1.95	0.10
Minto <i>et al.</i> 1997 [73]	5.10-.02·(Age-40)+0.07·(LBM-55)	9.82-.08·(Age-40)+0.11·(LBM-55)	5.42	2.60-.02·(Age-40)+0.02·(LBM-55)	2.05-.03·(Age-40)	0.08-.001·(Age-40)

Table 1.8

Standardised* model parameter estimates for remifentanyl pharmacokinetics. *Standardised for a 70 kg, 175 cm, 50 year old male. [^]Model developed for obese patients. [†]Model developed for bolus administration.

1.4.5 Inhalation anaesthetics

Inhalation anaesthetics are those given in the form of a gas or vapour, usually through an anaesthetic vaporiser within a delivery system. Early inhalation anaesthetics included chloroform and ether. Use of chloroform was associated with fatal cardiac arrhythmias, while ether was prone to igniting and tended to produce high rates of nausea and vomiting. These early inhalation anaesthetics were replaced with halothane. Halothane use has since declined because of its association with infrequent but severe liver damage ('halothane hepatitis'), its propensity to cause bradycardia at high concentrations and its slower onset and recovery than seen for more modern agents. Today, isoflurane, sevoflurane and desflurane are commonly used in the teaching hospital at our institution. Sevoflurane is particularly popular because its less irritating smell makes it suitable for gas inductions. These drugs have faster onset and offset times with decreased anaesthetic hangover than earlier inhalation agents. The standard measurement of inhalation anaesthetic potency is the minimum alveolar concentration required to prevent movement in response to noxious stimuli in 50% of patients (MAC). MAC values for desflurane, isoflurane and sevoflurane are 6.60, 1.17 and 1.80 vol% respectively, for a 40 year old adult.[99] MAC values decline with increasing age (after the age of 1-2 years) and this relationship is consistent between inhalation anaesthetic agents.[99]

Models of inhalation anaesthetic kinetics vary. Some include a series of compartments reflecting anaesthetic machine components, and lung and other body tissues.[100-102] Others have shown that two compartment pharmacokinetic models are sufficient to describe most inhalation anaesthetics.[103] Pharmacokinetic models of isoflurane and sevoflurane are included in our high fidelity patient simulator at the Clinical Skills Centre, University of Auckland. Work in our own department has been directed towards establishing a similar model for desflurane. Modern anaesthetic machines measure end tidal concentrations. These are used as a proxy for arterial concentrations which may be correlated to concentrations in the hypothetical effect site, negating the need to model pharmacokinetics.

For example, the rate of drug transfer from plasma to effect site may be estimated using a keo rate constant i.e.

$$\frac{dC_{\text{eff}}}{dt} = k_{\text{eo}} [C_{\text{et}} - C_{\text{e}}]$$

Equation 1.4

where C_{et} is the end tidal concentration and C_{e} is the effect site concentration of the inhalation anaesthetic. These methods are sufficient for many applications and keo estimates for processed EEG measures range between $0.54\text{-}0.61\text{ min}^{-1}$ ($t_{1/2\text{keo}}$ 1.1-1.3 min) for desflurane,[104, 105] $0.16\text{-}0.29\text{ min}^{-1}$ ($t_{1/2\text{keo}}$ 2.4-4.3 min) for isoflurane,[104, 105] and $0.20\text{-}0.48\text{ min}^{-1}$ ($t_{1/2\text{keo}}$ 1.4-3.5 min) for sevoflurane.[58, 104-110] Mostly, a sigmoid E_{MAX} curve is used to describe effect. $C_{\text{e}50}$ estimates obtained using this method and for EEG effects are 3.48 vol% for desflurane, 0.66 vol% for isoflurane, and 1.12-1.70 vol% for sevoflurane.[105-109, 111] Age dependent sensitivity to inhalation anaesthetic effects is also seen for EEG measures.[58, 112] For example isoflurane 0.82 vol%, or sevoflurane 1.28 vol%, is required to maintain a BIS below 50 in patients of 30 years while in patients aged 75 years these values are reduced to 0.56 vol% and 0.87 vol% respectively.[112]

1.5. Interactions in anaesthesia

A brief explanation of common pharmacodynamic interactions, and how they are studied in anaesthesia, is provided in the following section. This is followed by a summary of the interactions existing between the drugs described above for relevant anaesthetic endpoints.

1.5.1 Working definitions

Drug interactions may occur at a pharmacokinetic or pharmacodynamic level. Pharmacokinetic interactions alter the dose-concentration relationship, while pharmacodynamic interactions alter the concentration-effect relationship.

Pharmacodynamic interactions are those that modify the body's response to a drug without altering that drug's concentration at its site of action. For example, a drug's receptor binding, activation or signalling

processes may be modulated by a second drug, resulting in a change in the magnitude or duration of effect normally observed for the first drug when given alone. *In vivo* studies of these interactions in anaesthesia usually involve observing effects of drugs given alone and in combination with some other agent, and are most often presented for clinical application in terms of change in dose or change in concentration.

Classification of interactions is often debated, so some general working definitions are required for this thesis. These definitions are best illustrated using a simple hypothetical experiment. Consider the dose of two drugs that alone cause a predefined effect (say, that which produces 50% of the maximum observable effect). If no interaction exists, we would expect half the dose of each given together to produce the same effect as giving the whole dose of either drug alone.[113] This is defined as additivity (see Figure 1.6). The ‘expected’ effects for various dose combinations (or in other words, the effects predicted by an additive relationship) are used as the benchmark against which the presence (or absence) of a positive or negative interaction is assessed. If the dose combination is tested and the observed effect is greater than expected then supra-additivity (synergy) exists. On the other hand if the observed effect was less than expected then infra-additivity exists.

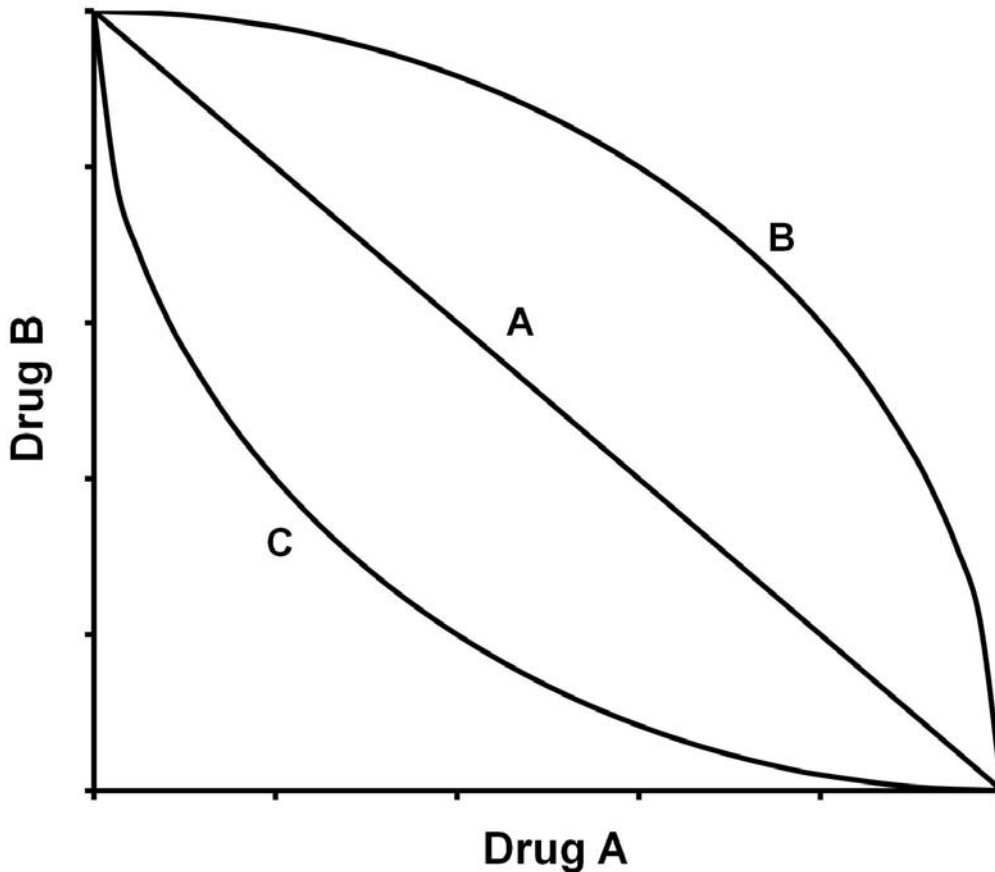


Figure 1.6

Isobologram of dose or concentration pairs for two drugs (drug A and drug B) that together cause a single level of effect. A) Line of additivity (or no interaction). The effect is equal for all parts of the line. B) infra-additivity where drug doses required for the effect are greater than expected. C) Supra-additivity, where the drug doses required for the effect are smaller than expected. Isobolograms have long been used to assess interactions in anaesthesia, and also to identify interactions between anti-microbial agents.

Clearly, classification of any drug interaction will depend on how additivity is defined. The definition of additivity is often called the reference model. Disparities in additivity definitions have long given rise to debate over drug interaction classifications. Of the numerous reference models described, two are most commonly cited: Bliss independence,[114] and Loewe additivity.[113]

The Bliss independence model gives the fractional response for a combination of two drugs at a specific dose combination as the sum of the fractional response seen for each when given alone, minus their product i.e.

$$Fa_{12} = Fa_1 + Fa_2 - Fa_1 \cdot Fa_2$$

Equation 1.5

where Fa_{12} is the fractional response (of the total possible response) that results from d_1 and d_2 , where d_1 and d_2 are the doses of drug 1 and drug 2. Fa_1 and Fa_2 are the fractional effects of d_1 and d_2 when given alone, respectively. The use of fractional responses means that the effect of drug 2 will be a fraction of the total possible effect remaining after the effect of drug 1 has been considered.

Bliss independence implies distinct and independent mechanisms of actions of both drugs to create a common response, and is based on probabilities of independent events. However, drugs may act at the same receptor to create response. Loewe additivity instead calculates an interaction index, based on the assumption that a drug cannot interact with itself. The Loewe interaction index indicates the interaction type: <1 denotes supra-additivity; >1 denotes infra-additivity; and 1 denotes additivity i.e.

$$\text{Interaction Index} = \frac{d_1}{D_1} + \frac{d_2}{D_2}$$

Equation 1.6

where D_1 and D_2 are the doses of drug 1 and 2 respectively that create a given effect alone, while d_1 and d_2 are the doses of drug 1 and 2 respectively that create that same effect in combination.

Loewe additivity is taken to be the working definition of additivity for this thesis.

1.5.2 Studying interactions in anaesthesia

Numerous techniques for evaluating pharmacodynamic interactions *in vivo* have been described in the anaesthetic literature.[115-119] Simple investigations involve characterising dose response curves for one drug given alone and in the presence of steady concentrations of a second drug. A standard sigmoidal E_{MAX} curve is often used. The effect of fixed doses of a second drug on the dose response curve of the first is visible as shifts in the curve along the concentration axis. Reductions or increases in dose relevant to markers of potency such as the Ce_{50} provide important information for clinical use of combinations. A common example of this is the reduction in the MAC of an inhalation agent when a bolus dose of an opioid, such as fentanyl, is given (identifiable through a shift to the left in the dose response curve of the inhalation anaesthetic). This method gives an idea of the direction of interaction but it does not quantify the magnitude of that interaction and is restricted to comparing changes in the dose response curve at a single concentration of the first drug.

An alternative method is to construct isoboles of the dose pairs for two drugs that together produce a single level of effect (Figure 1.6). Comparison of the plotted dose pairs with the line of additivity signals the interaction type; plots that bow in towards the origin indicate synergy while those that bow outward indicate infra-additivity. A level of effect that relates to clinical practice is usually studied, such as the Ce_{50} , and often a single ratio of drug *A* to drug *B* is maintained. Overlaying multiple isoboles for different levels of effect goes part way to mitigating this limitation of studying a single effect level and can give an idea of dose pairs across various effect levels. Differences in methods for judging whether deviations from the line of additivity are significant or within margins of variability (less than 10% is often classed as additivity for clinical endpoints), and in additivity definitions, may lead to disparate results between studies. Isobolographic methods work well when both drugs can independently achieve the study endpoint because the potency ratio of the two drugs remains constant across all dose pairs in keeping with the assumptions of the standard isobologram (given above in Figure 1.6). Where individual dose-response curves reach different levels of maximum effect this may not be the case, and consequently the line of additivity may appear curved. An extension of the standard isobologram is required in this instance to avoid mistakenly classifying additivity as synergism.[120]

The approaches described here are simple to implement and are informative for clinical use but have disadvantages. Information gained about interactions is applicable only to those dose combinations and effect levels investigated, and distinguishing an interaction from additivity is confounded by variability. It is often the case in anaesthesia that one drug is unable to produce the studied endpoint when given alone. Dose (or concentration) response relationships established for two drugs in combination may not hold true in the presence of other drugs. These disadvantages limit the use of these methods for applications in anaesthesia beyond simple comparisons of potency alone and in combination.

1.5.2.1. Response surface models in anaesthesia

A more flexible method of investigating interactions is by using response surface methods. Response surface models incorporate the information presented in both dose response curves (visible as vertical slices in the plotted surface of effect) and isoboles (visible as horizontal slices) (Figure 1.7). They can be used to describe the type and magnitude of an interaction for all possible dose pairs, enabling identification of optimal dose pairs for clinical endpoints. For example, the optimal dose combination of propofol and remifentanyl to ablate response to laryngoscopy without respiratory depression has been identified.[121] Response surface methods are predominantly used to describe interactions between two drugs in the current anaesthetic literature, but they are also extensible to a three drug interaction model.[122] Some of these models may theoretically be extended to describe more than three drugs, although this has not been reported in the anaesthetic literature. Response surface models are developed using population modelling methods and can be linked to existing pharmacokinetic models to describe drug response over time. Model parameters have an associated variability and may be statistically evaluated for significance.[117] Evaluating an interaction parameter in this way removes ambiguity in defining non-additive interactions and in quantifying the magnitude of an interaction. Synergy is depicted visually by outward bowing of the surface on the horizontal plane (Figure 1.7).

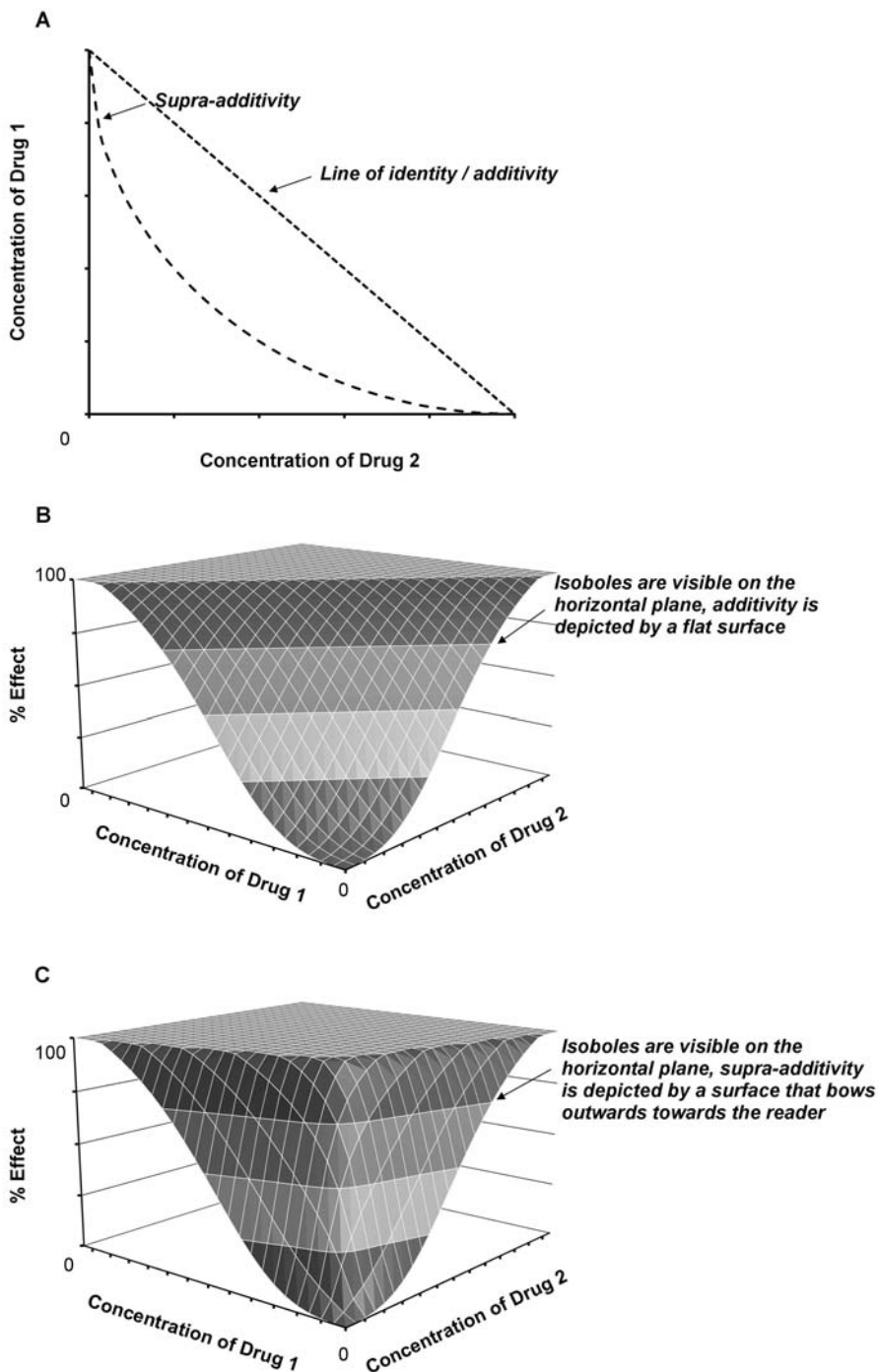


Figure 1.7

Hypothetical isobologram and response surface. A) Isobologram of concentration (or dose) pairs of drug 1 with drug 2 that together cause a single level of effect. B) Response surface where additivity exists. C) Response surface where supra-additivity exists. Isoboles are visible as horizontal lines within the response surface. Note that where the concentration of drug 2 is equal to 0, the dose response curve for drug 1 alone can be seen (and vice versa).

A number of articles describe response surface model development for interactions in anaesthesia. Early approaches such as those described by Carter *et al.*,[123] Gennings *et al.*,[124] and Plummer and Short[125] used logarithmic transformations of the E_{MAX} model. However, models built on this premise always predict some drug effect as the curve can approach but not equate to zero. Some baseline commonly does exist for variables in biology (for example, consider blood pressure in a healthy adult for which baseline systolic/diastolic values may typically be 120/80 mmHg) but this baseline is not a function of the drug itself. Approaches based on the concept of Loewe additivity that preserve the sigmoidal shape of the E_{MAX} curve are more popular, for example those described by Machado *et al.* and Greco *et al.*[126, 127] Greco's model has often been applied to anaesthetic data for anaesthetic studies,[60, 69, 128, 129] although its inflexible parameterisation may force some datasets to conform to its predefined surface shape. More flexible models have been proposed, like that by Minto *et al.*[122] They applied a quadratic function to the parameters of a modified E_{MAX} model, allowing the shape of the dose response curve to be influenced by the ratio of the modelled drugs present and their degree of interaction. Certain response surface models may be better suited to specific drug class combinations. For example, opioids alone are unable to achieve induction of anaesthesia and this may cause difficulties in identifying opioid effect parameters for a model describing this endpoint. Bouillon *et al.* developed the 'Hierarchical' model to describe combined drug effects for propofol-remifentanyl anaesthesia using sequential processing of drug effects, beginning with opioid components.[59] Reductions of both Greco and Hierarchical models that express opioid Ce_{50} as a proportion of that of the other drug have been identified as suitable for intravenous anaesthetic-opioid and intravenous-inhalation anaesthetic combinations where the interaction is known to be strongly synergistic (or supra-additive).[59, 60, 130] Specifics of those models discussed above and used in this work appear in the methods sections of the relevant chapters of this thesis.

A summary of studies using response surface methods for endpoints relevant to anaesthesia is given in Table 1.9. Studies in the past have focused on identifying the type and size of interactions; focus in the literature is now on identifying optimal dose combinations for specific anaesthetic endpoints or targets and validating previously established models for clinical use in real time. This has been done for combinations of remifentanyl with sevoflurane and isoflurane with fentanyl for emergence from anaesthesia.[131-133] Interactions existing between the reviewed drugs, and for key anaesthetic endpoints, are outlined below.

1.5.3 Propofol and midazolam

Propofol tends to be associated with dose dependent hypotension [134-136] and this adverse effect limits dose. Midazolam alone is incapable of producing immobility to a noxious stimulus.[37] However, premedication with midazolam contributes to sedation and reduces the propofol dose required to induce anaesthesia.[137] The combination is thought to be synergistic, as the effect observed when combining these drugs is greater than that expected from the effect observed from either drug alone. Synergism between propofol and midazolam is thought to exist for both hypnosis (defined by the authors as loss of response to verbal command),[37, 137-140] and ablation of response to noxious stimuli.[37, 122, 137, 138] Propofol clearance is reduced in the presence of midazolam,[141] while midazolam clearance and distribution out of the plasma compartment is reduced by propofol.[142] The mechanisms for these observations remain uncertain but both result in increases in drug concentrations and, therefore, in drug effect.

Study drugs			N	Study endpoint (continuous or bivariate)	Reference
Intravenous anaesthetic - inhalation anaesthetic	Propofol	Sevoflurane	60 patients	BIS, State and response entropy †, and response to shake, tetany, laryngeal mask insertion and laryngoscopy ‡	Schumacher 2009 [129]
			24 patients	BIS †	Diz 2010[143]
Intravenous anaesthetic - opioid	Propofol	Remifentanil	24 volunteers	Respiratory depression †, OAA/S and response to oesophageal instrumentation †	LaPierre 2011 [121]
			45 patients	Response to laryngoscopy ‡	Luginbuhl 2012[144]
			70 patients	Responses to electrical tetanus ‡	Yang 2010 [145]
			20 volunteers	Response to shouting and laryngoscopy ‡, raw and processed EEG (BIS) †	Bouillon 2004 [59]
			24 volunteers	OAA/S, response to algometry, tetany and laryngoscopy ‡	Kern 2004 [60]
			22 volunteers	Invasive BP, HR and BIS †	Nieuwenhuijs 2003 [146]
			20 volunteers	OAA/S, response to laryngoscopy and intubation ‡, processed EEG (BIS) †	Bruhn 2003 [147]
			30 patients	Response to laryngoscopy and intubation, and return to consciousness ‡	Mertens 2003 [69]
	Alfentanil	400 patients	Failure to open eyes to verbal command ‡	Minto 2000 [122]	

Table 1.9

Studies detailing response surface models development in anaesthesia. AAI=auditory evoked potential index, OAA/S=observer assessment of alertness / sedation, BP=blood pressure, HR=heart rate. ‡binary data, †continuous data, N=sample size.

Study drugs			N	Study endpoint (continuous or bivariate)	Reference
Intravenous anaesthetic-sedative	Propofol	Midazolam	400 patients	Failure to open eyes to verbal command ‡	Minto 2000 [122]
Inhalation anaesthetic-opioid	Sevoflurane	Alfentanil	9 volunteers	Normoxic resting ventilation, hypoxic ventilation, HR and BIS †	Dahan 2001 [76]
		Remifentanil	40 patients	Response to shouting, tetany, LMA insertion and laryngoscopy ‡	Heyse 2012[130]
			16 volunteers	OAA/S, response to algometry, tetany and thermal stimulation ‡	Manyam 2006 [148]
			20 patients	OAA/S (as return to consciousness) and response to tibial pressure ‡	Johnson 2009 [131]
			24 volunteers	OAA/S ‡, BIS and AAI †	Manyam 2007 [128]
65 patients	OAA/S ‡ and BIS †	Wang 2012[149]			
	Isoflurane	Fentanyl	25 patients	OAA/S (as return to consciousness)	Syroid 2010[132]
Sedative-opioid	Midazolam	Alfentanil	400 patients	Failure to open eyes to verbal command ‡	Minto 2000 [122]

Table 1.9 continued.

Studies detailing response surface models development in anaesthesia. OAA/S=observer assessment of alertness / sedation, BP=blood pressure, HR=heart rate. ‡binary data, †continuous data, N=sample size.

1.5.3.1. Propofol and the opioids

Propofol lacks analgesic effect and so supplementary analgesia with opioids is generally required for surgery. Opioids reduce the propofol dose required for hypnosis, loss of consciousness and ablation of response to noxious stimuli. The relationship between propofol dose and opioids for EEG measures such as BIS is cited as additive.[59, 150] This observation is probably as expected given EEG provides a measure of ‘wakefulness’ or consciousness, and noxious stimuli from surgical processes that would otherwise increase consciousness are ablated by opioids.[150] The relationship between propofol and opioids, and indeed midazolam and opioids, appears to be fairly consistent across various anaesthetic endpoints,[138] as demonstrated in Table 1.10.

The combination of propofol and alfentanil is synergistic for sedation,[122, 137, 139] as is the combination of midazolam and alfentanil.[122, 137, 139] Some of this interaction is likely to be pharmacokinetic, as Pavlin *et al.* demonstrated an increase of propofol concentrations when combined with alfentanil (between 21 and 22%) compared to propofol concentrations when given alone.[151] These authors also demonstrated a benefit in using the combination whereby the antiemetic effect of propofol reduced nausea and vomiting associated with alfentanil.[151] Two studies have identified the interaction between propofol and fentanyl as synergistic for sedation.[61, 134, 138] One other found the propofol-fentanyl interaction was additive for anaesthetic induction,[152] but the midazolam-fentanyl interaction in the same dataset was synergistic for anaesthetic induction.[153] Propofol and fentanyl are thought to show synergy for ablation of response to noxious stimuli, with 0.6 ng.ml⁻¹ of fentanyl halving the Ce₅₀ of propofol required for ablation of response to skin incision.[61] These relationships are summarised below in Table 1.10.

Although propofol pharmacokinetics appear unchanged in the presence of remifentanil, propofol administered by bolus may affect the volume of distribution and clearance of remifentanil.[63] The effect is not significant when given by infusion[63] and the majority of studies investigating propofol-remifentanil interactions have focused on infusion kinetics for TIVA. Interactions between propofol and remifentanil are thought to be synergistic for ablation of response to noxious stimuli [59, 60, 69, 154] and for reducing propofol requirements for loss of consciousness.[59, 60, 69] Remifentanil is unable to

achieve either endpoint when given alone.[59] The combination is thought to be additive for BIS,[59, 146, 155] although the authors of one study concluded that the interaction for maintenance of a BIS value between 45 and 55 was synergistic during surgery.[156]

1.5.3.2. Propofol and the inhalation anaesthetics

Inhalation anaesthetics are commonly used for maintenance of anaesthesia following propofol induction. Interaction studies involving inhalation anaesthetics generally present findings in terms of a reduction (or increase) in MAC of the inhalation agent when given in combination compared to when given alone. This is a useful way to interpret changes in dose response relationships relative to a recognisable marker of drug potency.

Propofol and sevoflurane are cited as acting additively for endpoints of MAC, sedation and BIS.[129, 143, 157, 158] Additivity is thought to occur *via* separate binding sites at GABA_A receptors.[158-160] Although the propofol-desflurane interaction and propofol-isoflurane interactions have not been studied, these inhalation anaesthetics modulate GABA in a similar manner to sevoflurane so interactions are likely to be similar.[161]

1.5.3.3. Inhalation anaesthetics and the opioids

Morphine has no effect on the concentrations of sevoflurane or isoflurane at which consciousness is regained,[162, 163] but animal data suggest synergism for response to noxious stimuli.[138, 164] Fentanyl and its derivatives have been more widely studied in combination with inhalation anaesthetics. Opioids interact synergistically with sevoflurane to create hypnosis and anaesthesia,[128, 138, 148] but additively for EEG measures.[76, 128, 165] Synergism for ablation of response to noxious stimuli has been well documented for a variety of agents. This has been shown for fentanyl with desflurane,[166] isoflurane[167] and sevoflurane,[168] and for remifentanyl with isoflurane[169] and sevoflurane.[148] Thus, interactions between various opioids and desflurane, isoflurane and sevoflurane appear consistent.

Endpoint	Propofol Ce ₅₀ alone	Propofol Ce ₅₀ (opioid concentration)	Interaction
LOC	3.4 mcg.ml ⁻¹ [69]		
Alfentanil		2.2 mcg.ml ⁻¹ (Alfentanil 122 ng.ml ⁻¹)[136]	Synergistic
Fentanyl		2 mcg.ml ⁻¹ (Fentanyl 3 ng.ml ⁻¹) [61]	Synergistic
Remifentanil		0.5 mcg.ml ⁻¹ (Remifentanil 8 ng.ml ⁻¹) [69]	Synergistic
BIS	4.5 mcg.ml ⁻¹ [59]		
Alfentanil		2 mcg.ml ⁻¹ (Alfentanil 50 ng.ml ⁻¹) [150]	Additive
Remifentanil		4.5 mcg.ml ⁻¹ (Remifentanil 19.3 ng.ml ⁻¹) [59]	Additive
Intubation	17.4* mcg.ml ⁻¹ [170]		
Alfentanil		2.0 mcg.ml ⁻¹ (Alfentanil 280 ng.ml ⁻¹)[171]	Synergistic
Fentanyl		8.5 mcg.ml ⁻¹ (Fentanyl 3.0 ng.ml ⁻¹)[170]	Synergistic
Remifentanil		2.0 mcg.ml ⁻¹ (Remifentanil 4.7 ng.ml ⁻¹) [69]	Synergistic
Incision	9.0 mcg.ml ⁻¹ [69]		
Alfentanil		2.0 mcg.ml ⁻¹ (Alfentanil 259 ng.ml ⁻¹)[171]	
Fentanyl		5.6 mcg.ml ⁻¹ (Fentanyl 1.0 ng.ml ⁻¹) [61]	Synergistic
Remifentanil		2.0 mcg.ml ⁻¹ (Remifentanil 6.3 ng.ml ⁻¹) [69]	Synergistic

Table 1.10

Required propofol plasma Ce₅₀ for common anaesthetic endpoints when given alone and in combination with opioids. Interaction classifications are given for each. *Ce₅₀ for propofol alone often cannot be estimated for the endpoint of intubation, as opioids are required to ablate response to this stimulus. Although one study has estimated a propofol concentration of 17.4 mcg.ml⁻¹ for ablation of response to intubation using propofol alone,[170] propofol 7.3 mcg.ml⁻¹ with remifentanil 1.2 mcg.ml⁻¹ is more clinically appropriate. One study found no change was observed in BIS values for propofol supplemented with fentanyl over propofol given alone, suggesting no interaction at the concentrations investigated.[172] LOC=loss of consciousness.

1.6. Summary

The concept of co-administering drugs that together contribute to achieving clinical endpoints is fundamental to the practice of anaesthesia. However, most pharmacokinetic and pharmacodynamic models commonly used in anaesthesia are for single agents. Response surface methods can be used to describe effects for two or more drugs in combination, and importantly may be linked to existing pharmacokinetic models to describe drug effects over time. They can be used to target optimal doses or concentrations for specific clinical endpoints, or to titrate dosing for individuals (for example, to improve recovery times). They may be useful in simulated environments as educational tools to aid understanding of pharmacokinetic and pharmacodynamic concepts. A model describing the response to those drug classes central to anaesthesia (intravenous anaesthetics, inhalation anaesthetics and phenyl-piperidine opioids) could be used to improve simulation of depth of anaesthetic at our simulation centre.

The work I present in this thesis aims to describe pharmacodynamic relationships for some commonly used anaesthesia drugs when given together, as is common practice. In chapters two and three, I describe the use of response surface models to investigate some commonly combined postoperative analgesics. Current dosing recommendations for diclofenac in children are derived using extrapolation from adult pharmacodynamics. I investigate diclofenac analgesia in children and report pharmacodynamic parameters for diclofenac alone and in combination with paracetamol. I then begin work towards establishing a model for combined BIS effects for some commonly used drug classes. Many authors have now investigated two drug interactions in anaesthesia using response surface methods but few have considered three drug combinations. Just one study, for which a midazolam (sedative)-propofol (intravenous anaesthetic)-alfentanil (opioid) combination was used, has used response surface methods to describe three drug classes in anaesthesia.[122, 139] Models describing intravenous anaesthetic-inhalation anaesthetic-opioid combinations have not yet been developed. The intention of this work has been to fill this gap in our current knowledge. I aimed to establish a model suitable for simulating realistic BIS response and capable of describing effects following doses of drugs from multiple drug classes.

Chapter 2. Explaining the paracetamol-ibuprofen analgesic interaction using a response surface model

Background: The value of paracetamol-ibuprofen combination therapy over single therapy is debated for acute pain management in children. A model describing combined analgesia for these drugs together would be useful for understanding current literature and future study design.

Methods: Published pooled time-effect profiles in adults given combination or single therapy after dental extraction were used to construct a pharmacodynamic model. Pain was measured using pain intensity differences (PRID, 0-8) from 0-8 h postoperatively. Pharmacodynamic parameter estimates in children were assumed to equal those of adults. Pharmacokinetic estimates in children were scaled to size using allometric theory. Curve fitting was performed using nonlinear mixed effects models.

Results: Pooled data were available in adults given eight single and multiple dose combinations as well as placebo. Pharmacodynamic parameter estimates, expressed using a response surface model, were maximum effect (E_{MAX}) 4.06 (95%CI 3.24, 5.51), the concentration associated with 50% of the maximal drug effect was paracetamol ($Ce_{50,PARA}$) 11.9 (95%CI 6.0, 49.5) $mg.l^{-1}$, and ibuprofen ($Ce_{50,IBU}$) 5.07 (95%CI 3.50, 8.26) $mg.l^{-1}$, with slope 2 (95%CI 1.3, 2.8). Drug effects were additive. Simulation showed the addition of paracetamol to ibuprofen was effective when the ibuprofen dose was less than 5 $mg.kg^{-1}$. A more sustained analgesic effect was noted at 4-8 h after combination dosing.

Conclusions: The maximum effect (E_{MAX}) limits analgesic gains from combination therapy when using high doses of both drugs. Differences in effect between single drug therapy and combination therapy should be sought at modest doses and beyond the immediate postoperative period. Combination therapy may prolong the duration of analgesia.

2.1. Introduction

Paracetamol is a first line treatment for postoperative pain and is popular in many settings including paediatrics and cardiac surgery.[173, 174] The pharmacokinetics of paracetamol were discussed in Section 1.5.2. Paracetamol is often combined with other analgesics such as those from the NSAID group. Ibuprofen is a common choice for this. A single compartment has predominantly been used to describe ibuprofen pharmacokinetics, though some investigators have used two compartment models.[175, 176] Estimates for volume of distribution (V) and clearance (CL) after oral dosing are dependent on the bioavailability (F) of the formulation. The fraction of ibuprofen available in the plasma after oral dosing (F_{oral}) is 0.63.[175] Estimates for V/F_{oral} vary between 6.4 and 23.5 $\text{l}\cdot\text{70kg}^{-1}$, and $\text{clearance}/F_{\text{oral}}$ estimates range between 2.9 and 5.9 $\text{l}\cdot\text{hr}^{-1}$ in adults.[175-179] An equilibration half-time ($t_{1/2\text{keo}}$) of around 28 minutes has been reported,[177] and for oral dosing absorption half-life (t_{abs}) estimates range from 24 to 36 minutes.[177, 179]

Many studies have compared the relative effectiveness of these two drugs; a recent meta-analysis identified 54 studies directly comparing the analgesic effect of ibuprofen with that of paracetamol,[180] of which 36 studies related to adults and 18 to children. Twenty-six of the adult studies supported ibuprofen over paracetamol for analgesia, while ten found no difference between the two. Trends are less clear in children.[180, 181] Six studies supported ibuprofen over paracetamol; one supported ibuprofen over paracetamol on the day of surgery only; three suggested ibuprofen over paracetamol without reaching statistical significance; and the remainder found no difference in analgesic efficacy. The authors of this meta-analysis concluded that ibuprofen is at least, if not more so, as effective as paracetamol in both adults and children.[180]

Perhaps unsurprisingly given the lack of consensus on comparative effectiveness of these two drugs, it remains unclear whether combining ibuprofen with paracetamol offers any real benefit over either drug alone. A recent review of randomised controlled studies comparing combined paracetamol NSAID therapy for postoperative pain management against monotherapy identified six studies relating to paracetamol and ibuprofen.[182] Of those studies conducted in adult populations, two supported the

combination over paracetamol alone,[183, 184] two supported the combination over ibuprofen alone[185, 186] and one found no difference between combination therapy and ibuprofen alone.[183] Oral premedication with ibuprofen/paracetamol was supported over paracetamol alone for tonsillectomy pain in children[187] and following tooth extraction,[188] while rectally administered ibuprofen and paracetamol showed no benefit over paracetamol alone for pain following adenoidectomy, although a reduction in rescue analgesia was seen in the combination group once home.[186]

Disparities between results may stem from differences in the endpoint studied (particularly for assessments of analgesia or pain control) and dissimilar dosing regimens, as well as a plethora of other factors relating to study design, conduct and analysis.[189] Although dose-response data are available for a number of commonly used paracetamol and ibuprofen combinations, these data are limited and are not easily applied to clinical use. For example, of the studies identified above comparing combination therapy with monotherapy,[182] just one compared one dose combination of paracetamol with ibuprofen against two doses of paracetamol alone.[188] The remaining studies all compared a single dose against that same dose given in combination.[183-187] Pierce *et al.* noted that 29 of 36 adult studies investigating comparative efficacies of ibuprofen and paracetamol did so using just one dose of each.[180] This illustrates the limited context in which the efficacies of these drugs have been compared. Only limited sections of the full dose response curve are represented and interpretation of observations may not hold true for other dose ranges.

Plasma concentrations are commonly missing in these studies. Plasma concentrations are the link required to explain observed response,[190] making extrapolation of dose to different patient groups difficult when unaccounted for. Due to the limited knowledge of pharmacokinetics and pharmacodynamics for paracetamol-NSAID combinations in children, dosing decisions continue to be dependent on extrapolation from the adult population, individual drug profiles and clinical experience. One study has reported pharmacokinetic parameter estimates in adults for both paracetamol and ibuprofen when given orally alone and in combination.[179] No evidence for a pharmacokinetic interaction was reported. A model describing pharmacodynamics of these drugs when given together would be useful for both understanding current literature, and for design of future studies investigating clinical benefits of the combination over monotherapy.

The aim of the work described in this chapter was therefore to:

1. develop a pharmacodynamic model to describe analgesic effect of paracetamol and ibuprofen, when given alone or in combination (as is common for postoperative pain relief),
2. use this model to interpret discrepancies existing between studies investigating benefits of monotherapy over combination therapy for analgesia.

2.2. Methods

2.2.1 Data

A large, randomised, double blind, placebo controlled trial comparing effectiveness and tolerability of paracetamol and ibuprofen, alone and in combination, for postoperative pain relief following the removal of impacted molars in adults was identified.[191] This study investigated analgesia over a range of dosing levels. Patients were given an oral dose of either paracetamol 250 mg with ibuprofen 100 mg, paracetamol 500 mg with ibuprofen 200 mg, paracetamol 1000 mg with ibuprofen 400 mg, paracetamol 500 mg alone, paracetamol 1000 mg alone, ibuprofen 200 mg alone, ibuprofen 400 mg alone or placebo. Pain intensity was measured using a categorical scale (0-3) and pain relief was measured using a 5 point categorical scale (0=none, 1=a little, 2=some, 3=a lot, 4=complete). The primary endpoint was the pain relief and pain intensity difference score (PRID) from zero to eight hours postoperatively.[191] PRID scores were displayed as mean changes from baseline in PRID (where 0 is no pain relief and 8 is total pain relief) over the eight hour period to account for differences between individuals in baseline pain. Mean time-PRID data were extracted from the published plot using the freeware Graph Extract version 2.1 (Quadtech Associates, Inc).[192] A total of 85 mean observations were extracted from time points 0.25, 0.5, 0.75, 1, 1.5, 2, 3, 4, 5, 6, 7 and 8 h.

2.2.2 Modelling methods

2.2.2.1. Model parameterisation

Plasma concentration sampling was not undertaken in the selected study so these were estimated using first order absorption, one-compartment linear model with first order elimination for both paracetamol and ibuprofen, in accordance with literature reports.[177-179, 193, 194] CL/F_{oral} , V/F_{oral} and absorption were fixed at reported literature estimates.[178, 179, 195] An additional compartment was incorporated into the model to describe the delay observable between drug reaching the plasma and an effect occurring.[11] An equilibration rate constant (k_{eo}) can be used to characterise the temporal relationship between drug in the plasma and movement to this hypothetical compartment of effect, and is parameterised as an equilibration half-time ($t_{1/2k_{eo}}$) i.e.

$$t_{1/2k_{eo}} = \frac{\ln(2)}{k_{eo}}$$

Equation 2.1

For the description of concentration-effect with interactions, a sigmoid based response surface model was investigated. The model, described by Minto *et al.*,[122] requires normalisation of estimated effect compartment concentrations to a relative potency (or unit, U) for each drug i.e.

$$U_{IBU} = \frac{C_{eIBU}}{C_{e50,IBU}} ; U_{PARA} = \frac{C_{ePARA}}{C_{e50,PARA}}$$

Equation 2.2

where C_{eIBU} is the predicted effect site concentration of ibuprofen, $C_{e50,IBU}$ is the concentration of ibuprofen associated with 50% of the maximal drug effect (or E_{MAX}), C_{ePARA} is the predicted effect site concentration of paracetamol, and $C_{e50,PARA}$ is the concentration of paracetamol associated with 50% of E_{MAX} .

The concentration ratio of the two drugs is described by the term θ :

$$\theta = \frac{U_{\text{PARA}}}{U_{\text{IBU}} + U_{\text{PARA}}}$$

Equation 2.3

where θ is equal to 0 if the concentration of both drugs is 0. The term θ is used to calculate the $U_{50}(\theta)$ i.e.

$$U_{50}(\theta) = 1 - \beta \cdot \theta + \beta \cdot \theta^2$$

Equation 2.4

where β is an interaction parameter ($\beta = 0$ denotes additivity; > 0 a supra-additive interaction; and < 0 an infra-additive interaction). In this equation $U_{50}(\theta)$ is a function that modifies the normalised concentrations of both drugs, depending on the ratio of drugs present and the β parameter i.e.

$$U = \frac{U_{\text{IBU}} + U_{\text{PARA}}}{U_{50}(\theta)}$$

Equation 2.5

$U_{50}(\theta)$ takes the value 1 when β equals 0 (representing no interaction, or additivity) and consequently no modification of drug potency occurs. The function gives the surface a flexible nature and may be applied to any or all parameters of the equation (for example, the slope or maximum response parameters). It may also be extended for three drugs, but its use here represents its most simple form. Drug effect, 'Effect(drug)', can then be calculated using a sigmoidal dose response curve:

$$\text{Effect(drug)} = E_{\text{MAX}} \cdot \frac{(U)^\gamma}{(1 + U)^\gamma}$$

Equation 2.6

where E_{MAX} is the maximum response and γ is a coefficient describing the steepness of the relationship between drug concentration and effect.

In the published study PRID scores were available for a placebo group or no drug effect. Baseline (E_0) was equated to this in the model and described using an exponential asymptotic model i.e.

$$E_0 = 1 - \text{EXP}\left(-\text{TIME} \cdot \frac{\ln(2)}{T_{\text{base}}}\right)$$

Equation 2.7

where T_{base} describes the half time to achieve the effect observed in the placebo group. Response (R) including drug and placebo effects may then be calculated, i.e.

$$R = E_0 - \text{Effect}(\text{drug})$$

Equation 2.8

2.2.2.2. Parameter estimation

Data for individuals were unavailable from the publication; data were presented as averaged responses for each treatment group. This did not allow for estimation of sources of population parameter variability (between and within subjects). The coefficients of variability (CV) of model parameters were modelled by an exponential variance term (equivalent to assuming a log-normal distribution) and residual unknown error was characterised using an additive term. Data were analysed using nonlinear mixed effects models (NONMEM VI, Globomax LLC, Hanover, MD, USA). Model parameters, CV and residual variance were estimated using the first order conditional interaction estimation method. Equations were integrated within ADVAN=6 with TOL=5. Convergence criterion was three significant digits. Parameter uncertainty was evaluated by bootstrap methods [196] with a total of 1000 simulations used to estimate confidence intervals. Bootstrap methods provide a distribution-free confidence interval by randomly sampling from the dataset and running NONMEM, then repeating the process (typically 1000 times) to give an indication of model stability. The NONMEM code used for the final model is given in Appendix 2.

2.2.2.3. Simulation

Simulation was used to demonstrate the time-effect profile for a given dosage regimen. Simulation of effect profiles over time was performed using Berkeley Madonna™ modelling and analysis of dynamic systems software (Robert Macey and George Oster of the University of California, Berkeley, USA). The final model and estimated parameters from this current analysis to simulate mean response profiles for a 20 kg child. Pharmacokinetic parameters for the child were estimated using allometric scaling.[56] Allometric scaling recognises elimination kinetics are nonlinearly related to size and parameter values for the typical patient (P_T) are scaled for an individual (P_i) i.e.

$$P_i = P_T \cdot (W_{t_i}/W_{t_T})^s$$

Equation 2.9

where W_{t_i} is an individual's weight, W_{t_T} is the typical weight of the population and s is equal to 1 for volume of distribution, 0.75 for clearance, and 0.25 for equilibration half-time estimates.[56, 194] Simulated doses were chosen to reflect standard clinical practice and to demonstrate effect profiles.

2.3. Results

Final parameter estimates and associated CV, standard error and confidence intervals are given in Table 2.1. The resulting surface of effect for a paracetamol dose range of 500-1000 mg and an ibuprofen dose range of 100-400 mg is given in Figure 2.1. There was imprecision in the estimate of the interaction term ($\beta=0.75$; SE% 143; 95%CI -4.53, 1.94) and fixing this parameter to 0 (additive interaction) did not alter the objective function. Figure 2.2 demonstrates the quality of fit for pharmacodynamic data. Population effect predictions are based on typical parameter and covariate information for the population, while individual effect predictions are calculated from NONMEM's post hoc (posterior individual) step and are based on adjusted parameter values for the specific individual using their observed data and covariate information.

Time-effect profiles in a 20 kg child simulated using model parameter estimates are given in Figure 2.3. Simulation showed the addition of paracetamol to ibuprofen when less than 5 mg.kg⁻¹ was effective; paracetamol had minimal effect when given with ibuprofen at doses greater than 5 mg.kg⁻¹ in the

immediate postoperative period. A more sustained analgesic effect was noted at 4-8 h after combination dosing. Regular dosing revealed similar trends. Ibuprofen 100 mg three times daily contributed a mean PRID score of 3.5; addition of paracetamol 200 mg four times daily improved the PRID score to 4.1. Higher additional paracetamol dosing contributed minimal additional effect e.g. ibuprofen 100 mg and paracetamol 400 mg achieved a mean PRID score 4.3.

Parameter	Estimate	%CV	%SE	95% CI
Pharmacodynamics				
E_{MAX}	4.03	12.90	13.90	3.24, 5.51
Slope (γ)	2.00	-	19.80	1.30, 2.80
Beta (β)	0 FIX	-	-	-
$t_{1/2keO_{PARA}}$ (h)	0.15	-	23.10	0.10, 0.35
$Ce_{50,PARA}$ ($mg.l^{-1}$)	11.90	84.30	58.40	6.00, 49.50
$t_{1/2keO_{IBU}}$ (h)	1.16	-	11.00	0.96, 1.93
$Ce_{50,IBU}$ ($mg.l^{-1}$)	5.07	23.10	18.70	3.50, 8.26
Tbase (h)	0.33	-	47.70	0.10, 0.50
Err additive	0.16	-	26.60	0.08, 0.19
Pharmacokinetics				
CL_{PARA}/F_{oral} ($l.h^{-1}.70kg^{-1}$)	15.00			
V_{PARA}/F_{oral} ($l.70kg^{-1}$)	55.00			
$tabs_{PARA}$ (h)	0.20			
CL_{IBU}/F_{oral} ($l.h^{-1}.70kg^{-1}$)	3.60			
V_{IBU}/F_{oral} ($l.70kg^{-1}$)	10.00			
$tabs_{IBU}$ (h)	0.25			

Table 2.1

Parameter estimates for the drug interaction model investigating the paracetamol-ibuprofen response surface (CV is the coefficient of variability; SE is the standard error; CI is the confidence interval; Tbase and tabs describe the half times to achieve the effect observed in the placebo group and for absorption, respectively; Err additive is residual unknown variability). CL/F_{oral} and V/F_{oral} are the apparent clearance and volume of distribution respectively following oral dosing.

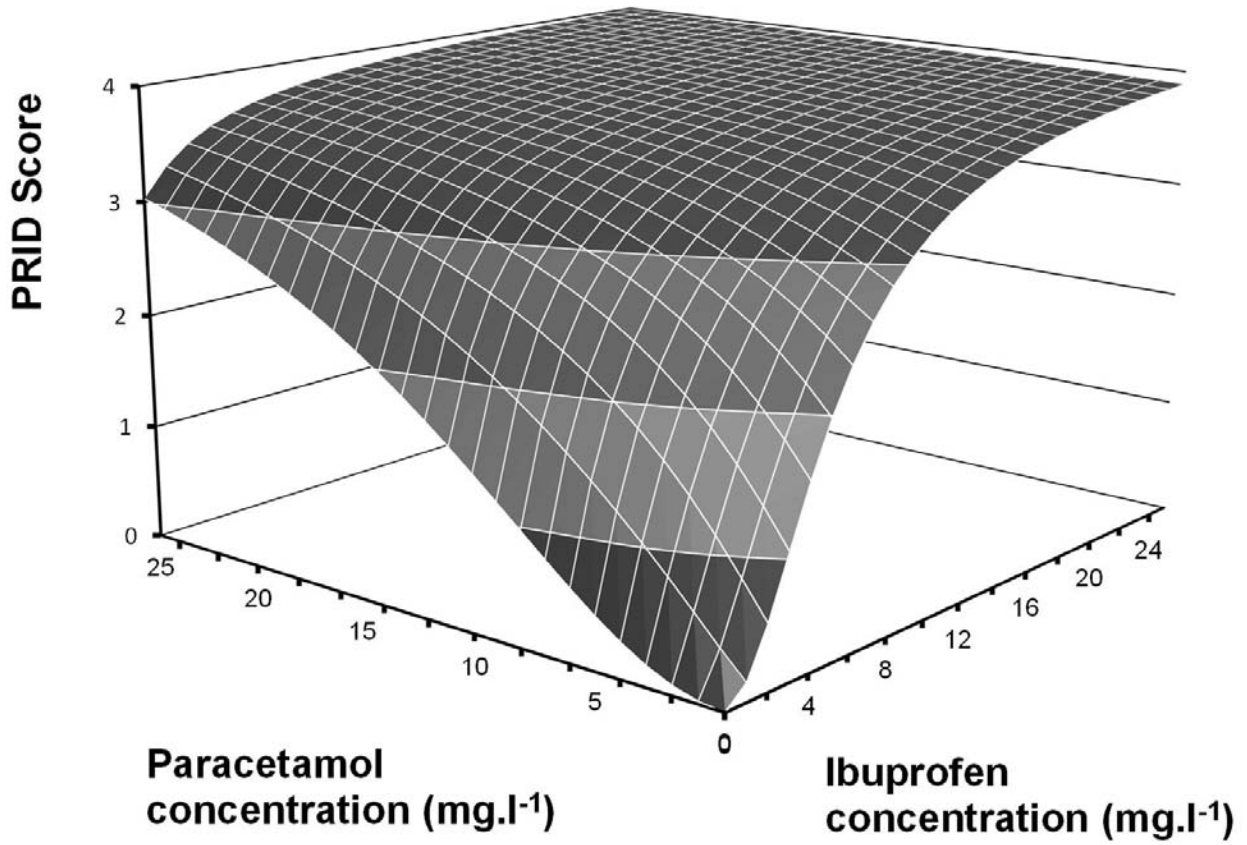


Figure 2.1
Theoretical response surface of effect between paracetamol and ibuprofen. Concentrations are those in the effect compartment.
PRID score: mean change from baseline in pain relief and pain intensity difference score (0-8).

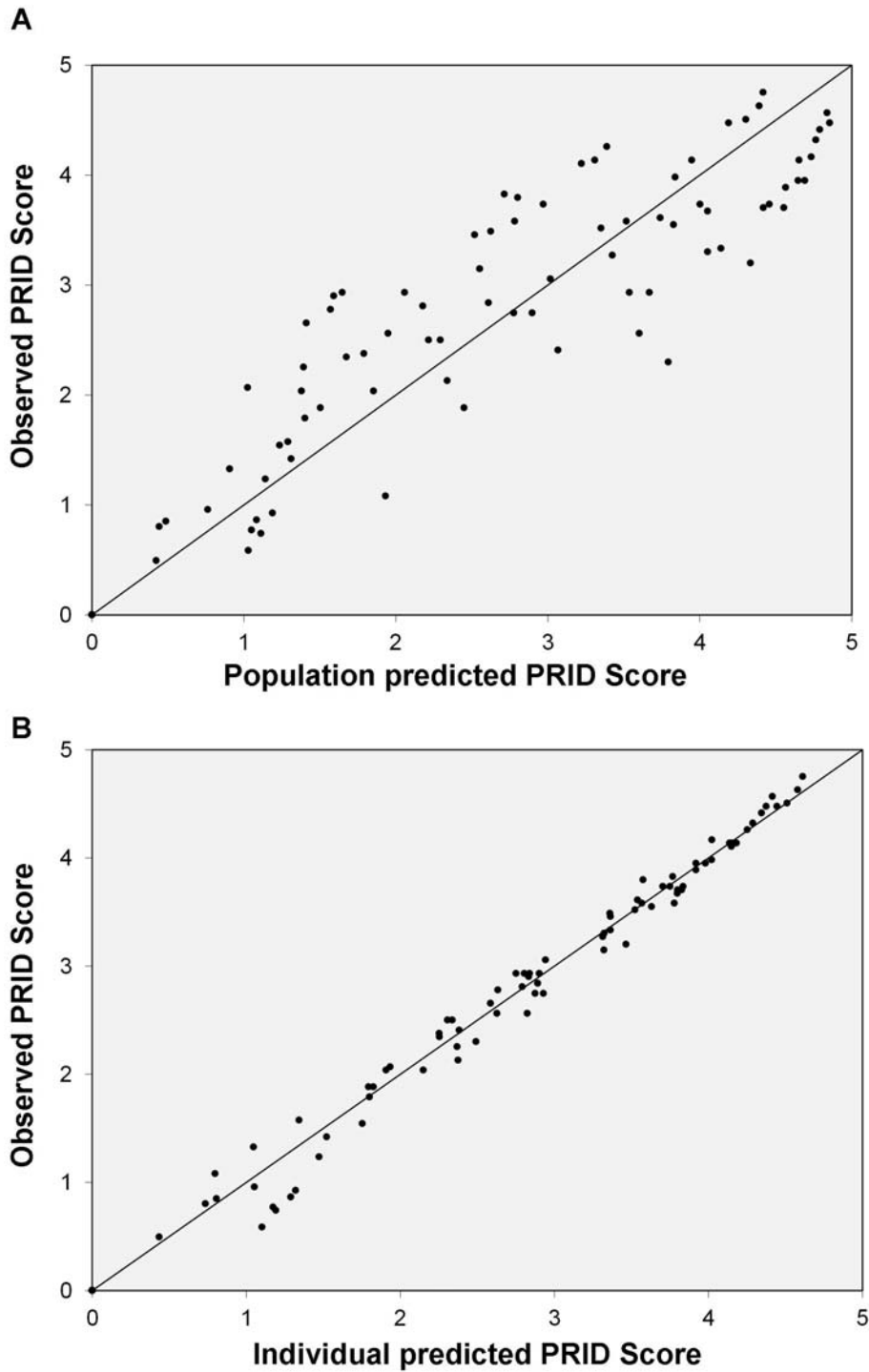


Figure 2.2

Quality of fit of pharmacodynamic data. (A) Population predictions are compared to observed PRID scores. (B) Individual Bayesian predictions, based on adjusted parameters for the specific individual, are compared to observed PRID scores.

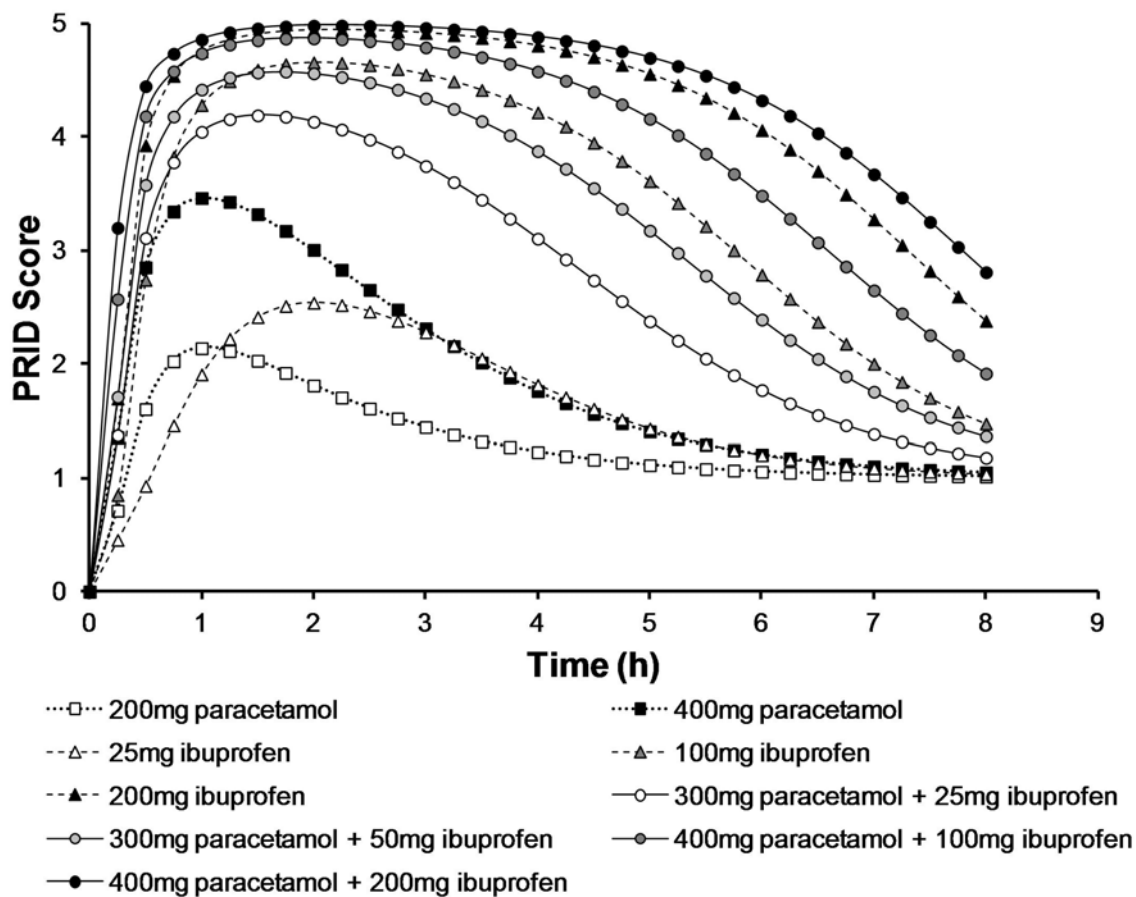


Figure 2.3

Simulated PRID scores (presented as difference from baseline PRID score) for a 5 year old, 20 kg child given single and combination paracetamol-ibuprofen therapy.

2.4. Discussion

Pharmacokinetic and pharmacodynamic analyses improve our knowledge of dose-effect relationships and in some cases may shed new light on old problems. Though a number of studies investigate paracetamol and ibuprofen both alone and in combination, it remains unclear as to which therapy offers better analgesia. In this study, a linked pharmacokinetic-pharmacodynamic model that considers combined drug effects is used to generate hypotheses as to why this may be the case.

This simulation study suggests combination therapy is better for postoperative pain relief than either agent alone when the dose of ibuprofen is less than 100 mg (5 mg.kg^{-1} , single oral dose) (Figure 2.3). Although the simulation given here is for a 5 year old child, similar trends can be expected for adults using this model. The addition of paracetamol has little impact when higher doses of ibuprofen are used. For example, Dahl *et al.* concluded that oral ibuprofen 800 mg three times a day provided better pain relief in adults following orthopaedic surgery than paracetamol 1000 mg, but no further benefit was gained by using the combination.[183] This dose is greater than 11 mg.kg^{-1} , assuming an average adult weight of 70 kg. Likewise, Gazal *et al.* compared oral elixirs of ibuprofen 5 mg.kg^{-1} alone, and in combination with paracetamol 15 mg.kg^{-1} , for tooth extraction in children.[188] They were able to detect improvement of analgesia on recovery from anaesthesia and again after 15 min for ibuprofen alone and in combination over paracetamol monotherapy. No difference between ibuprofen alone and in combination with paracetamol was observed.

The use of more modest doses (paracetamol 500 mg, ibuprofen 150 mg six hourly) after tooth extraction was reported to give greater analgesia in adults when combination therapy was used over monotherapy with either drug.[179] This dose is approximately equivalent to ibuprofen 2 mg.kg^{-1} . In children, Pickering *et al.* reported better analgesia after tonsillectomy with combination therapy (paracetamol 20 mg.kg^{-1} and ibuprofen 5 mg.kg^{-1}) than with paracetamol alone,[187] consistent with Figure 2.3. The observations above suggest that some disparities between studies investigating benefits of the combination over monotherapy may arise from the doses chosen. Studies demonstrating an analgesic benefit of the combination appear to have done so at doses relating to the lower and mid portions of the response curve. Efficacies of single drugs are unlikely to be distinguishable from that of the combination

if the studied doses are those relating to the upper portion of the analgesic curve where response is approaching its maximum. Both paracetamol and ibuprofen are associated with adverse effects at high doses. High dose paracetamol can lead to hepatotoxicity when clearance *via* glucuronide and sulphate pathways becomes saturated and clearance is predominantly shifted to formation of a liver toxic metabolite, N-acetyl-p-benzoquinone imine (NAPQI).[173, 175] High dose NSAID's are associated with reduced renal blood flow and renal dysfunction.[197, 198] Little benefit can be gained through doses of either drug above those associated with maximal analgesic effect as the risk of experiencing a dose dependent adverse effect increases. Analgesic gains seen for the combination in the lower portion of the dosing range may be important in patients susceptible to NSAID adverse effects and in whom higher doses are intolerable. The maximum daily dose of paracetamol is often taken to be 4 g (this information is available on drug packaging and medsafe.govt.nz) but four hourly dosing is required to maintain adequate analgesia for strong pain. In this context the addition of a NSAID such as ibuprofen to supplement analgesia is helpful.

A second hypothesis generated by this simulation study is that a benefit of combination therapy may not be obvious if pain monitoring is only in the post-anaesthetic care unit. Analgesia measured during this period may be similar to monotherapy and differences in effect only become obvious 2-8 h later. This is illustrated by a prolonged analgesic effect clearly visible for combination therapy in Figure 2.3. This suggests benefits of the combination are not related to the maximal effect gained but to time, and perhaps explains why Viitanen *et al.* were only able to observe an improvement in children's pain relief with rectal paracetamol and ibuprofen in combination over either drug alone outside of the immediate postoperative period.[186] Combination therapy may increase the duration of analgesia.

Final parameter estimates were capable of describing the original pooled adult data and enabled extrapolation to children. The $C_{e50,IBU}$ estimate of 5.07 (95% CI 3.50, 8.26) mg.l^{-1} is similar to that associated with fever control (6.18 mg.l^{-1}).[175] Li *et al.* recently reported an ibuprofen $C_{e50,IBU}$ for analgesia for dental pain after molar extraction to be 10.2 SE 0.23 mg.l^{-1} in adults.[177] These authors used a model corrected for the data censoring that arises from the pain assessment intervals and participants dropping out of the study due to poorly controlled pain.[177] An estimated $C_{e50,PARA}$ of 11.9 (95% CI 6.0, 49.5) mg.l^{-1} is similar to the 9.98 mg.l^{-1} obtained from an analysis in children

investigating analgesia after tonsillectomy.[29] The paucity of paracetamol doses explored (500 mg and 1000 mg) contributes to the uncertainty of the $CE_{50,PARA}$ estimate. The E_{MAX} estimate for the combination (4.0 PRID units on a scale of 0-8) is similar to an E_{MAX} of 5.1 cm (visual analogue scale, 0-10) reported for paracetamol after tonsillectomy,[29] although the PRID scores used to measure a combination of pain relief and pain intensity may not be directly comparable to other measures of analgesia. The paracetamol $t_{1/2}$ keo estimate in this study differed from a previous estimate of 0.88 h,[29, 199] although this is unsurprising because data were from averaged time-effect profiles. This $t_{1/2}$ keo parameter is dependent on the data from which it is derived (see Section 1.4.3) and to some extent corrects for inaccuracy of pharmacokinetic parameter estimates.[200] The parameter estimates in this study are comparable with those reported from clinical studies in children, but as this was an exercise in informing future studies (as opposed to defining optimal dosing regimens) the model should not be used as the basis of dosing decisions until it has been validated clinically.

The modelling approach used here is similar to ‘K-PD’ models (as the population pharmacokinetic information is absent), and is useful when plasma concentrations have not been collected.[51, 200, 201] Established literature parameters were used as estimates to predict pharmacokinetics. Estimation of population variability was not possible as response profiles were pooled responses, and the final model is derived from what is essentially a naïve pooled fit (see Section 1.3.1). The authors measured analgesia using PRID scores which may not be comparable to other measures of analgesia commonly reported, for example current pain intensity on a visual analogue scale. However, maximal effects observed here were similar to that observed for paracetamol analgesia measured using VAS (50% reduction in pain),[29] and PRID scores were presented as the difference from initial PRID score to correct for differences between individuals in baseline pain. The pharmacodynamic response surface model used here is overly complex for the simple data available. However, the purpose of this simulation study was not to identify or quantify a possible interaction existing between these two drugs, but instead to better understand dose-effect relationships when given in combination. Accurate portrayal of the ‘true’ response surface (and therefore identification of interactions) involves measuring effect as observed at various ratios of drug 1: drug 2 (i.e. 0:1 through to 1:0), and spanning upper and lower limits of the clinically used range. This makes data collection for response surface investigations aiming to quantify interactions demanding with a minimum of 20 intensively studied individuals required for continuous, quantitative effect endpoints.[202] Response surface methods have been used here with limited data to explain combined

drug response. Although the initial β parameter estimate suggested synergism between paracetamol and ibuprofen, there was considerable uncertainty about this parameter because of the sparse data available; thus an additive interaction ($\beta=0$) was assumed. Synergism has been suggested for this drug pair for acute pain in mice using both intraperitoneal and oral dosing,[203] although this observation has yet to be confirmed in humans. It is unlikely that this model will perform well outside the dosing range from which it was derived and the observations made in this work have yet to be validated by prospective clinical studies. These limitations also limit the ability to extend this model to describe repeat dosing. Despite this, the method provided a useful model of time dependent dose-response data for understanding paracetamol and ibuprofen interactions.

Summary

In this chapter, a model is given for analgesic effects of paracetamol and ibuprofen when administered both alone and in combination. An appreciation of the time-effect profiles generated by this analysis allows greater understanding of the nuances of combination therapy, and their impacts on study design. For example, the work presented here suggests future research designs seeking to demonstrate differences in effect between monotherapy and combination therapy should do so at lower doses and beyond the immediate postoperative period. Combination therapy with modest doses can achieve analgesia as effectively as single drug therapy with higher doses; combination therapy at higher doses (e.g. ibuprofen 10 mg.kg⁻¹ three times daily, and paracetamol 20 mg.kg⁻¹ four times daily) may increase propensity to adverse effects without any perceptible analgesic gains because the maximum effect (E_{MAX}) is approached. Differences in study design, pain measures, pain type, observation intervals and dosing schedules hinder comparison of published study conclusions. Integrated pharmacokinetic-pharmacodynamic studies using population modelling can permit greater insights and prediction of effect than current dose-effect studies.[204]

Chapter 3. A pharmacokinetic-pharmacodynamic model of analgesia for diclofenac and paracetamol in children

Background: Diclofenac dosing in children is limited to extrapolation from adult pharmacodynamic data. A pharmacokinetic-pharmacodynamic model for diclofenac alone and with paracetamol may improve analgesic dosing in children.

Methods: An existing dataset was available for analysis. Children (n=151) undergoing tonsillectomy were randomised to receive paracetamol elixir 40 mg.kg⁻¹ before surgery and 20 mg.kg⁻¹ rectally at the end of surgery, oral diclofenac suspension 0.1 mg.kg⁻¹, 0.5 mg.kg⁻¹ or 2.0 mg.kg⁻¹ before surgery or placebo. A further 93 children were randomised to receive diclofenac 0.1-2.0 mg.kg⁻¹ only. Postoperative pain was assessed in the postoperative care unit at half hourly intervals from waking until discharge. Data were pooled with pharmacokinetic data from a further 182 children and 70 adults. One compartment models with first order absorption and elimination were used to describe the pharmacokinetics of both medicines. Combined drug effects were modelled using a modified E_{MAX} model with an interaction term. An interval censored model described the hazard of early study dropout.

Results: Analgesia onset had an equilibration half-life between plasma and effect site of 0.495 h for paracetamol and 0.23 h for diclofenac. The maximum effect was 4.89 cm (Visual Analogue Score, VAS 0-10 cm). Diclofenac Ce₅₀ was 1.20 mg.l⁻¹ and paracetamol Ce₅₀ was 13.30 mg.l⁻¹. The placebo model (which describes changes in baseline pain) had an equilibration half-life of 2.65 h, elimination half-life of 2.96 h and placebo dose effect of 1.76 cm. This gives a peak 'placebo effect' of 6.8 cm occurring at 4.04 h. Drug effects were additive for analgesia. The hazard of dropping out of the study was related to pain score with a hazard ratio of 1.36 per unit change in pain.

Conclusions: A reduction in pain score of 2 cm can be achieved with either a concentration of paracetamol 11.75 mg.l⁻¹, or paracetamol 5.88 mg.l⁻¹ with diclofenac 0.54 mg.l⁻¹.

3.1. Introduction

A linked pharmacokinetic-pharmacodynamic model was used to describe analgesic effects of paracetamol with ibuprofen in Chapter 2. This work enabled useful observations to be made through an improved understanding of dose-concentration-effect relationships over time, despite limitations (notably, individual time-concentration data were unavailable and these were predicted from literature pharmacokinetic parameter estimates, pharmacodynamic parameters were derived from naïve pooled data). Comparison of effectiveness at doses that approach maximal effects, and failure to study analgesia outside the immediate postoperative period, are possible reasons why some studies have been unable to demonstrate benefits of the combination over either drug alone where others have.[205]

The non-steroidal anti-inflammatory drug (NSAID) diclofenac is also often combined with paracetamol. Diclofenac has been associated with less nausea and vomiting than opioids and so is popular for postoperative pain relief in spontaneously breathing, recovering patients.[206] The combination is particularly useful in paediatric settings where other therapeutic indications exist, such as fever reduction.[173] Oral diclofenac pharmacokinetics are usually described by an initial depot compartment to reflect processes of absorption linked to a single central compartment.[206, 207] Diclofenac has an apparent volume in the central compartment (V/F_{oral}) of $22.8 \text{ l}\cdot\text{70kg}^{-1}$ [207] and apparent clearance (CL/F_{oral}) between $44.8\text{-}52.7 \text{ l}\cdot\text{h}^{-1}\cdot\text{70kg}^{-1}$ for oral formulations in children.[207-209] Recently, pharmacokinetic data were pooled from existing studies and a three compartment model for intravenous, oral and suppository diclofenac formulations in children reported.[206] The clearance from this pooled analysis was $16.5 \text{ l}\cdot\text{h}^{-1}\cdot\text{70kg}^{-1}$.

The pharmacokinetics of diclofenac have been investigated in children,[208] but studies investigating diclofenac pharmacodynamics for analgesia in children are sparse. Rømsing *et al.* studied pharmacokinetics of diclofenac in children for tonsillectomy pain,[209] but their analysis did not extend to describing the relationship between concentration and observed pain score. The authors were unable to identify significant differences between baseline pain scores and those observed at 1 and 5 h after $1\text{-}2 \text{ mg}\cdot\text{kg}^{-1}$ oral diclofenac. Some pharmacokinetic studies have described the relationship between oral diclofenac dose and the subsequent area under the concentration curve (AUC) in children, the idea being that dosing in children may be guided by targeting an AUC

associated with effective analgesia in adults.[206] Standing *et al.* recommended 1 mg.kg^{-1} orally to achieve diclofenac concentrations in children comparative to those concentrations achieved with an effective dose of 50 mg in adults;[206] however, as AUC and analgesia were not studied in children, these recommendations are dependent on the assumption that this relationship is similar to that identified for adults.

Dosing continues to be dependent on extrapolation from adult data because no studies directly describe diclofenac pharmacodynamics for analgesia in children. The aims of the work I describe in this chapter were therefore to:

1. define the pharmacodynamic profile of diclofenac for analgesia in children, as measured by visual analogue scales after tonsillectomy.
2. develop a linked pharmacokinetic-pharmacodynamic model describing dose-effect relationships over time for diclofenac when given alone and in combination with paracetamol (as is common for postoperative care in anaesthesia).

Pharmacodynamic parameters describing diclofenac effects for postoperative analgesia in children have not been published prior to this work, to my knowledge.

3.2. Methods

An existing dataset derived from a randomised, placebo controlled study of oral and rectal dosing of paracetamol and diclofenac for tonsillectomy pain in children was available for analysis. These data were previously unanalysed and have not been published elsewhere. The dataset (study 1) provided only pharmacodynamic data. Existing pharmacokinetic data for paracetamol and diclofenac in children were requested from the authors of two published studies (study 2 and study 3). Data were pooled with those of study 1 to make up for a lack of pharmacokinetic data and to facilitate modelling of the full dose-concentration-response relationship. These studies are described briefly below. My modelling methods are described in detail in Section 3.2.1.

Box 1. *How these data were collected (study 1)*

Data for study 1 were collected by Professor Brian Anderson during a double-blinded, placebo controlled study conducted in the paediatric postoperative care unit (PACU) of Starship Children's Hospital, Auckland, in 1995. Regional ethics approval for study 1 was given by North Health Ethics Committee (reference 95/204).

Participants

Children aged 2-15 years with an American Society of Anesthesiologists physical status (ASA) of 1-2 and who were scheduled for outpatient tonsillectomy with or without adenoidectomy at Starship Children's Hospital were eligible to be studied. Children with hepatic or renal disease, or who had already received paracetamol or diclofenac within 24 hours of surgery, were excluded. A research doctor or nurse explained the study to potential participants. Patients were also given an information sheet and allowed ample time to consider, and discuss with family, their participation. Written informed consent was given by the parents of each participant.

Anaesthetic and postoperative care

All participants received 20 ml.kg⁻¹ of an intravenous balanced salt solution and anaesthesia was induced with either intravenous propofol 3 mg.kg⁻¹, or by inhalation of halothane and 70% nitrous oxide in oxygen. Intravenous atracurium 0.4 mg.kg⁻¹ was given to facilitate insertion of the endotracheal tube, and anaesthesia was maintained using halothane and 70% nitrous oxide in oxygen with controlled ventilation. Neuromuscular blockade was reversed with neostigmine (0.05 mg.kg⁻¹) and atropine (0.02 mg.kg⁻¹) at the end of the procedure. The endotracheal tube was removed following return of spontaneous respiration, and the patient was transported to the recovery room. Participants were offered a flavoured ice block once awake and alert, and a parent was invited to the recovery room. A minimum of four hours of pain observations were made before participants could be discharged.

Study drug

Participants were given paracetamol elixir (250 mg.ml^{-1}) 40 mg.kg^{-1} one hour preoperatively and a further 20 mg.kg^{-1} rectally at the end of surgery to maintain plasma paracetamol concentrations into the postoperative period. No other premedication was given. Participants were randomised to receive a preoperative oral dose of diclofenac. This was given 15 minutes before surgery as an oral suspension dissolved in blackcurrant syrup and was either: (0.5 ml.kg^{-1} blackcurrant syrup without diclofenac); dispersal diclofenac 0.1 mg.kg^{-1} ; 0.5 mg.kg^{-1} ; 2.0 mg.kg^{-1} or placebo. A further group was randomised to receive oral diclofenac $0.1\text{-}2.0 \text{ mg.kg}^{-1}$ only (no paracetamol). Postoperative rescue analgesia in the event of poorly controlled pain was intravenous morphine 0.05 mg.kg^{-1} and participants were subsequently withdrawn from the study. Data up until administration of rescue analgesia were included in the analysis and the reason for study dropout recorded (e.g. inadequate analgesia, adverse drug effects etc.).

Study measurements

Postoperative pain scores (ranging from a maximum pain scored as 10, to no pain scored as 0) were estimated a half hourly intervals from waking in the postoperative care unit until discharge. Pain scores were recorded by a pain nurse practitioner who was blinded to study group randomisation. Pain scores for subjects 5 years and older were assessed using a Visual Analogue Score (VAS 0-10) with smiley faces,[210, 211] while for those under 5 years, pain was assessed by the pain nurse practitioner using an objective scoring system (the Hannallah Objective Pain Scale).[212, 213]

Study 1 had originally been designed as an integrated pharmacokinetic-pharmacodynamic study. Blood was also drawn from a dedicated venous cannula in each participant for paracetamol and diclofenac assay. There were 4-5 samples taken from each participant over the perioperative period. These samples were centrifuged and serum stored at $-20 \text{ }^{\circ}\text{C}$ for later analysis.

Paracetamol concentrations were determined using fluorescence polarisation immunoassay with Abbot TDx (Abbot Laboratories, Abbott Park, Ill, USA). The lower limit of quantification (LLOQ) for this assay was 1.5 mg.l^{-1} . One sample was measured as less than the LLOQ and it was discarded. Unfortunately all diclofenac samples were lost because of refrigeration failure during the 5 week long power outage that affected Auckland City in 1998.[214]

Box 2. Study 2

Data came from a previously published analysis of paracetamol pharmacokinetics and pharmacodynamics.[29, 33] Study 2 was conducted in the paediatric postoperative care unit (PACU) of Starship Children's Hospital, Auckland. Ethics approval was given by North Health Ethics Committee (reference 95/042). Anaesthetic protocol and pain score collection in this study was the same as that in study 1.

Data were available from 152 children, aged 2-15 years with an ASA physical status 1 and 2, who were scheduled to undergo tonsillectomy with or without adenoidectomy. Participants were randomised to receive either 40 mg.kg^{-1} paracetamol elixir (n=12), 100 mg.kg^{-1} paracetamol elixir (n=20) 40 mg.kg^{-1} oral paracetamol (n=20), or 40 mg.kg^{-1} paracetamol rectally (n=100) 0.5-1 h preoperatively. Pain scores were obtained from the time of wakening in the postoperative care unit at half hourly intervals over 4 postoperative hours, and 3 to 4 plasma samples from each participant were taken.

Box 3. Study 3

Data were provided by the authors of a pharmacokinetic study of diclofenac in children.[206, 208] Data were available from 70 children scheduled to undergo minor day stay surgery and who received a single oral dose of diclofenac suspension 1.0 mg.kg^{-1} two hours prior to surgery. Three plasma samples were available from each child. Data from 30 healthy adults who participated in a bioequivalence study conducted by Rosemount Pharmaceuticals were also available.[206, 208] Adults in this study received a single 50 mg dose of diclofenac suspension and plasma samples were taken at 13 time points following dosing.

3.2.1 Modelling methods

The following describes my analysis of the existing datasets outlined above.

3.2.1.1. Pharmacokinetic model

Paracetamol and diclofenac pharmacokinetics were described using first order absorption, one-compartment distribution and first order elimination. Models were parameterised in terms of absorption half time (t_{abs}), apparent clearance (CL/F) and apparent volume (V/F). Initial estimates for CL/F, V/F and absorption were given as those reported in the literature, [29, 194, 208] and theory based allometric scaling was used to scale parameter estimates for size in children.[215] All subjects were older than 2 years for paracetamol studies, and older than 1 year for the diclofenac study, and so no attempt was made to include maturation in the pharmacokinetic model.[13, 14]

3.2.1.2. Effect compartment model

The observed delay in analgesic response was described for each drug by the addition of a hypothetical effect compartment. This effect compartment was given a very small volume by scaling the first order rate constant for drug transfer from the central compartment to the effect compartment to 1/1000 of that describing elimination from the central compartment, so as not to influence the pharmacokinetics of the central compartment. The temporal relationship between concentrations in effect and plasma compartments was described using an equilibration rate constant (k_{eq}), parameterised as an equilibration half-time (t_{1/2}k_{eq}) i.e.

$$t_{1/2}k_{eq} = \frac{\ln(2)}{k_{eq}}$$

Equation 3.1

3.2.1.3. Pharmacodynamic model

Pain scores were treated as if they were continuous variables. Predicted effect site concentrations were related to pain score using an E_{MAX} model modified to express combined drug response as described previously for paracetamol with ibuprofen.[205] Predicted effect site concentrations of both drugs were normalised against their Ce_{50} i.e.

$$U_{DICL} = \frac{Ce_{DICL}}{Ce_{50,DICL}} ; U_{PARA} = \frac{Ce_{PARA}}{Ce_{50,PARA}}$$

Equation 3.2

where Ce_{DICL} is the predicted effect site concentration of diclofenac, $Ce_{50,DICL}$ is the concentration of diclofenac associated with 50% of the maximal drug effect (or E_{MAX}), Ce_{PARA} is the predicted effect site concentration of paracetamol, and $Ce_{50,PARA}$ is the concentration of paracetamol associated with 50% of E_{MAX} . Both the Greco and Minto response surface models were investigated.[122, 127] Drug effect (Effect(drug)) was modelled for the normalised drug concentrations using a modified sigmoidal curve that includes an interaction parameter i.e.

$$\text{Effect(drug)} = E_{MAX} \cdot \frac{(U)^\gamma}{(1 + U)^\gamma}$$

Equation 3.3

where E_{MAX} is the maximum response and γ is a coefficient describing the steepness of the relationship between drug concentration and effect. U is calculated for the Minto model as

$$(U_{DICL} + U_{PARA}) / (1 - \beta \cdot \theta + \beta \cdot \theta^2)$$

Equation 3.4

where θ is $U_{PARA} / (U_{PARA} + U_{DICL})$ and β is the interaction parameter. U is calculated using a first order interaction term for Greco's model i.e.

$$U = U_{DICL} + U_{PARA} + \beta \cdot U_{DICL} \cdot U_{PARA}$$

Equation 3.5

The Greco equation is derived from that describing a simple isobole for 50% of the maximal drug effect, and this is reflected in the surface whereby horizontal planes describing effects for dose pairs are constrained to a single effect level.[127, 216] Interaction parameters were initially fixed at 0 for both models, denoting the simplest scenario; no interaction or 'additivity'. Inclusion of a non-additive

interaction term ($\beta > 0$ =supra-additivity and < 0 =infra-additivity) was tested by looking for a statistically significant improvement in NONMEM's objective function.

3.2.1.4. Placebo effect

Baseline, or no drug effect (E_0), was assumed to be equal to a maximum pain score of 10 as expected for no analgesia. A model for placebo response to describe changes in baseline pain over time was included, using published parameters as initial estimates.[29] Placebo effect onset and offset were parameterised in terms of rate constants for placebo effect onset (keq_{PL}) and offset (kel_{PL}) i.e.

$$t_{1/2}keq_{PL} = \frac{\text{Ln}(2)}{keq_{PL}}, \quad t_{1/2}kel_{PL} = \frac{\text{Ln}(2)}{kel_{PL}}$$

Equation 3.6

where $t_{1/2}keq_{PL}$ is the equilibration half-life for placebo effect onset and $t_{1/2}kel_{PL}$ is an elimination half-life for placebo effect offset. The effect of placebo (Effect(placebo)) is assumed to be equal in all patient groups,[193] i.e.

$$\text{Effect(placebo)} = \text{BETA}_{PL} \cdot keq_{PL} / (keq_{PL} - kel_{PL}) \cdot \exp(-kel_{PL} \cdot t) - \exp(-keq_{PL} \cdot t)$$

Equation 3.7

where t is time and BETA_{PL} is the nominal placebo dose. Total response (R) including drug and placebo effects may then be calculated i.e.

$$R = E_0 - \text{Effect(drug)} \cdot (1 - \text{Effect(placebo)})$$

Equation 3.8

3.2.1.5. Study dropout

A model of study dropout was investigated to describe the flow of participants as poorly controlled pain requiring rescue analgesia resulted in termination of study participation in accordance with the study protocol. This was necessary to avoid confounding the study drug effect measurements with those of the rescue analgesic. However, this in itself may introduce bias as those patients with high pain scores drop out of the study and those with well controlled pain continue to participate.

Hazard of requiring rescue analgesia (h) was investigated using an exponential model i.e.

$$h(t) = \lambda_{\text{base}} \cdot \exp(c)$$

Equation 3.9

where λ_{base} describes baseline hazard with no covariate effects, t is time and c describes the influence of covariates on the baseline hazard. A Gompertz distribution i.e.

$$h(t) = \lambda_{0G} \cdot \exp^{\beta_G \cdot t} \cdot \exp(c)$$

Equation 3.10

where β_G is a scale parameter, and a Weibull function i.e.

$$h(t) = \lambda_{0W} \cdot \exp^{\beta_W \times \ln(t)} \cdot \exp(c)$$

Equation 3.11

where β_W is a shape parameter, were also investigated. Pain score correlated to drug effect was investigated as a covariate effect (c) for hazard i.e.

$$c = \beta_{\text{pain}} \cdot \text{pain}(t)$$

Equation 3.12

where β_{pain} is a scale parameter for pain score. The cumulative hazard (CUMH) was obtained by integrating h from 0 to the time of the dropout event, t . The likelihood of an individual remaining in the study was predicted from the survivor function at the time of the event i.e.

$$S(t) = \exp(-\text{CUMH}(t))$$

Equation 3.13

Pain scores were collected at half hourly intervals and so an interval censored model for hazard was investigated as well as uncensored models. A time-to-event model reflects that participation could theoretically end at any time between rescue analgesic administration and the last time point at which the participant was known to be in the study. The interval censored likelihood (L) is calculated from the survivor function at time t_{end} by subtracting from the survivor function at the time of the last pain score measurement (t_{start}) i.e.

$$L(t_{\text{end}}) = S(t_{\text{start}}) - S(t_{\text{end}})$$

Equation 3.14

3.2.1.6. Parameter estimation

Pooled data from studies 1-3 were analysed using nonlinear mixed effects models (NONMEM 7.1, Globomax LLC, Hanover, MD, USA). Population parameters, covariate effects and variances were estimated using the first order conditional, Laplace estimation method with interaction. Model equations were integrated within ADVAN=13 with TOL=9. The F-FLAG option was used to specify between observation predictions and likelihood predictions (in this case, the model of study dropout). Population parameter variability was described using exponential error models which is equivalent to assuming a log-normal distribution and avoids biologically inappropriate parameter values of zero or less. Additive and proportional error models were used to describe unknown pharmacokinetic residual error. An additive error model was used for pharmacodynamic residual error. Seven subjects were re-admitted for a second surgery on a separate occasion in study 3.[208] Between-occasion variability was estimated for these individuals who received diclofenac on more than one occasion.

Convergence criterion was three significant digits. Model selection required a statistically significant improvement in the NONMEM objective function between nested models, equating to a reduction > 6.64 based on a Chi square distribution ($\alpha < 0.01$). Visual inspection of plots of observed *versus* model predicted concentrations and pain scores, and visual predictive checks (VPC) were used to assess how well the optimal model predicts observed dependent variables. Bootstrap methods were used to evaluate uncertainty associated with parameter estimates.[196] VPCs were used to evaluate how well the model predicted the distribution of observed concentrations and pain scores.[13] VPCs inform on the suitability of both the structural model (for example in pharmacokinetics, a three compartment model) and error models by graphically superimposing model simulations on observations. Median, upper and lower percentile predictions may be compared visually with those of observations. The NONMEM code used for the final model is given in Appendix 3.

3.3. Results

Data were available for 244 children from study 1. Pooled data from 496 individuals were studied (466 children, 30 adults). Children had a mean age of 7.7 (range 1.1-16.0) years with a mean weight of 32.4 (range 9.4-105.0) kg. Adult volunteers, who contributed diclofenac pharmacokinetic data, had a mean age of 21.0 (range 18.0-28.0) years with a mean weight of 71.7 (range 48.0-93.8) kg. There were 218 male and 248 female children, and 14 male and 16 female adult volunteers. Of the

participants in study 1, 151 were randomised to receive paracetamol in combination with diclofenac while 93 were randomised to receive diclofenac alone. All participants who contributed to pain scores (studies 1 and 2) were scheduled for tonsillectomy, providing a comparable pain model between individuals. A total of 1552 pain scores, 829 paracetamol and 911 diclofenac plasma concentrations were available for analysis. No paediatric diclofenac samples were reported as LLOQ in study 3. Measurements that were less than LLOQ were not reported by the laboratory that analysed diclofenac concentrations for the adult bioequivalence data (study 3) and so these could not be included in this analysis.[206] Raw plasma concentrations for diclofenac and paracetamol are given in Figure 3.1.

Minto's model was selected over Greco's model to describe concentration-effect relationships ($\Delta \text{OBJ} = -126, P < 0.001$). The interaction term was zero suggesting effects of diclofenac and paracetamol are simply additive for analgesia ($\Delta \text{OBJ} = +6.77$ with a non-additive interaction term). An interval censored time-to-event model with baseline hazard and no covariate effects (Equation 3.9) had an $\text{OBJ} = 770.70$. Describing baseline hazard using a Weibull distribution (Equation 3.11) gave an $\text{OBJ} = 770.62$, while using a Gompertz distribution (Equation 3.10) gave an $\text{OBJ} = 763.99$ ($\Delta \text{OBJ} = -7$ from the base model, $P = 0.01$). Including current pain score as a covariate effect to describe study dropout reduced the OBJ to 753.5 ($\Delta \text{OBJ} = -16.5$ from the baseline hazard model, $P < 0.0001$). Including a Gompertz distribution at this point did not significantly improve the model ($\text{OBJ} = 750.9$, $\Delta \text{OBJ} = -2.6$ from the hazard model with pain as a covariate, $P = 0.107$) and so a simple baseline hazard with pain as a covariate was selected. The equilibration half-life for placebo effect onset ($t_{1/2\text{eqPL}}$), and for placebo elimination ($t_{1/2\text{elPL}}$), was 2.65 h and 2.97 h respectively. This gave a peak placebo effect of 6.8 cm occurring at 4.04 h.

Parameter and variability estimates are given in Table 3.1 for pharmacokinetic models, while estimates for covariance between population parameter variability (where included) are given for pharmacokinetics in Table 3.2. Parameter and variability estimates are given in Table 3.3 for pharmacodynamic models, while estimates for covariance between population parameter variability are given for pharmacodynamics in Table 3.4. VPCs for diclofenac and paracetamol pharmacokinetics are shown in Figure 3.2, while those for analgesia are given in Figure 3.3. The concentration-response relationships for diclofenac and paracetamol are demonstrated in Figure 3.4.

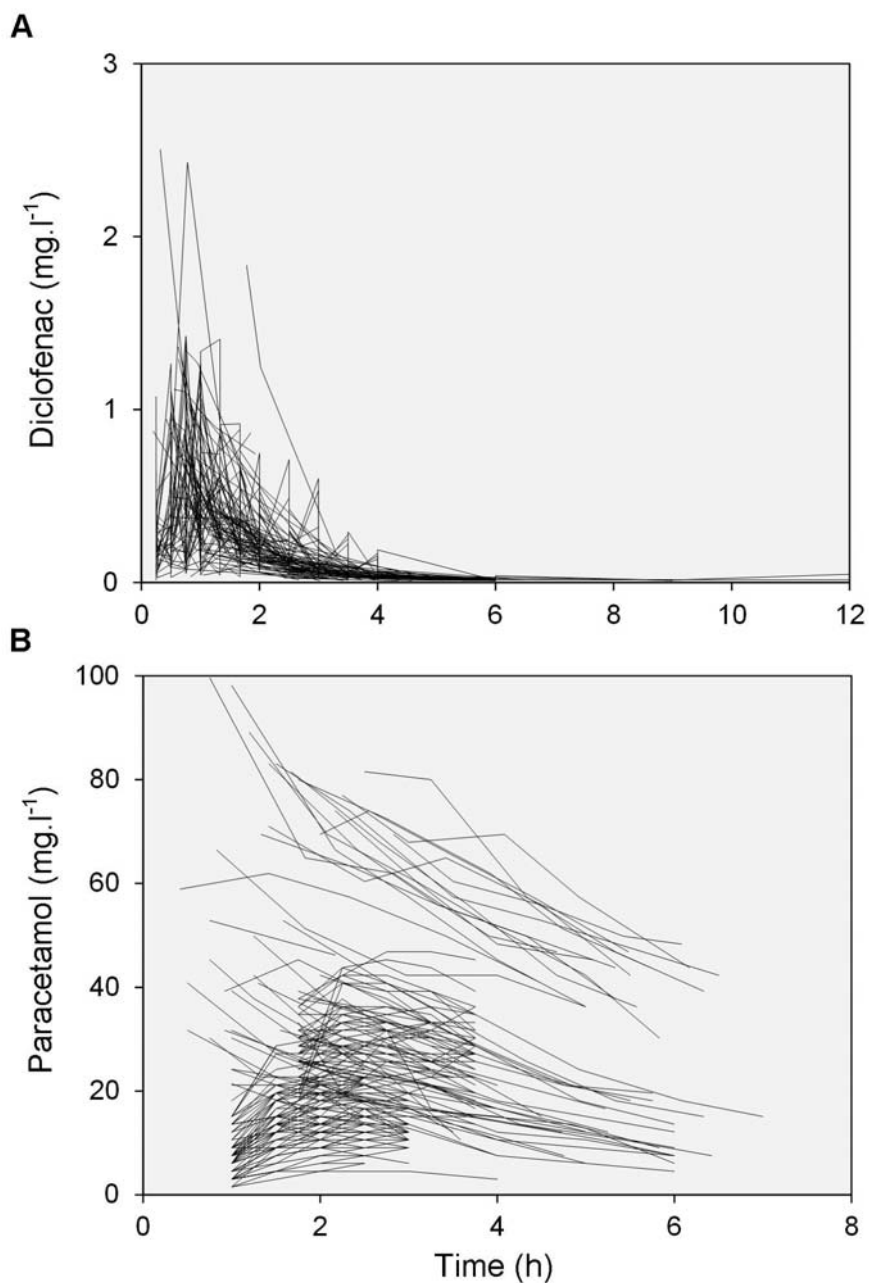


Figure 3.1

Pooled raw plasma concentrations of A) diclofenac and B) paracetamol. Paracetamol concentrations are from children (study 1), and diclofenac concentrations are from children and adults (study 2). Observations for each individual are linked with unsmoothed lines.

Parameter	Estimate	% BOV	% CV	95% CI*
$\text{tabs}_{\text{PARA, O}}$ (h)	0.127	-	25.73	
$\text{tabs}_{\text{PARA, R}}$ (h)	0.538	-	2.00	
$\text{Lag}_{\text{PARA, R}}$ (h)	0.5	-	-	0.496, 0.506
$\text{tabs}_{\text{DICL}}$ (h)	1.09	-	54.50	1.08, 1.09
$\text{CL}_{\text{PARA/F}}$ ($\text{l}\cdot\text{h}^{-1}\cdot 70\text{kg}^{-1}$)	11.7	18.76	44.05	11.6, 11.8
$\text{V}_{\text{PARA/F}}$ ($\text{l}\cdot 70\text{kg}^{-1}$)	56.1	67.97	43.70	55.8, 56.2
$\text{CL}_{\text{DICL/F}}$ ($\text{l}\cdot\text{h}^{-1}\cdot 70\text{kg}^{-1}$)	53.4	-	21.17	52.6, 54.0
$\text{V}_{\text{DICL/F}}$ ($\text{l}\cdot 70\text{kg}^{-1}$)	16.0	-	44.49	15.8, 16.2
$\text{Err}_{\text{add, PARA}}$ ($\text{mg}\cdot\text{l}^{-1}$)	1.17			
$\text{Err}_{\text{pro, PARA}}$ (%)	9.0			
$\text{Err}_{\text{add, DICL}}$ ($\text{mg}\cdot\text{l}^{-1}$)	.01			
$\text{Err}_{\text{pro, DICL}}$ (%)	46.37			

Table 3.1

Pharmacokinetic parameter estimates for the drug interaction model investigating the paracetamol-diclofenac response surface. BOV is the between-occasion variability, population parameter variability expressed as a coefficient of variation (square root of NONMEM omega estimate x 100); CI is the bootstrap confidence interval; tabs is the half-life for absorption for oral paracetamol ($\text{tabs}_{\text{PARA, O}}$), rectal paracetamol ($\text{tabs}_{\text{PARA, R}}$) and oral diclofenac ($\text{tabs}_{\text{DICL}}$); $\text{Lag}_{\text{PARA, R}}$ is the lag time for rectal formulation paracetamol. V/F and CL/F are the apparent volume and clearance respectively. Err_{add} and Err_{pro} are the additive and proportional residual variability estimated for drug concentrations. *A total of 248 bootstraps were completed in the time availableⁱⁱⁱ.

ⁱⁱⁱ Typically around 1000 bootstraps are completed. However run times were slow as a result of the model parameterisation (which used differential equations) so a limited number of bootstraps were performed in the time available.

Paracetamol	$CL_{PARA/F}$	$V_{PARA/F}$		
$CL_{PARA/F}$	1			
$V_{PARA/F}$	-0.084	1		
Diclofenac	$CL_{DICL/F}$	$V_{DICL/F}$	$tabs_{DICL}$	
$CL_{DICL/F}$	1			
$V_{DICL/F}$	0.046	1		
$tabs_{DICL}$	0.825	0.412	1	
Diclofenac BOV	$CL_{DICL/F}$	$V_{DICL/F}$		
$CL_{DICL/F}$	1			
$V_{DICL/F}$	0.064	1		

Table 3.2

Correlation of population parameter variability for pharmacokinetic parameters. V/F and CL/F are the apparent volume and clearance respectively. $tabs_{DICL}$ is the half-life for absorption for oral diclofenac. BOV is between-occasion variability.

Parameter	Estimate	% CV	95% CI*
Pharmacodynamics			
E_0 (cm VAS 0-10)	10.0 FIX		
E_{MAX} (cm VAS 0-10)	4.89	108.6	4.83, 4.93
Slope (γ)	1.0	0 FIX	
Interaction (β)	0 FIX	0 FIX	
$t_{1/2}keq_{PARA}$ (h)	0.49	0 FIX	0.491, 0.5
$Ce_{50,PARA}$ (mg.l ⁻¹)	13.3	137.11	13.2, 13.4
$t_{1/2}keq_{DICL}$ (h)	0.23	0 FIX	0.228, 0.232
$Ce_{50,DICL}$ (mg.l ⁻¹)	1.2	123.29	1.18, 1.22
Placebo effect			
$t_{1/2}keq_{PL}$ (h)	2.65	50.99	2.57, 2.67
$t_{1/2}kel_{PL}$ (h)	2.96	74.03	2.92, 3.0
$BETA_{PL}$ (cm VAS 0-10)	1.76	1.14	1.73, 1.78
Time-to-event model			
λ (h ⁻¹)	0.0152	18.76	0.0148, 0.0154
β_{pain} (cm VAS 0-10)	0.311	67.97	0.277, 0.337
Err_{add} (cm VAS 0-10)	1.18		

Table 3.3

Pharmacodynamic parameter estimates for the drug interaction model investigating the paracetamol-diclofenac response surface. Population parameter variability expressed as a coefficient of variation (CV, square root of NONMEM omega estimate x 100); CI is the bootstrap confidence interval; λ is the baseline hazard and β_{pain} is the effect of current pain score on hazard; Err_{add} is the additive residual variability estimated for pain score measurements. *A total of 248 bootstraps were completed in the time available.

Pharmacodynamics	E_{MAX}	$Ce_{50,PARA}$	$Ce_{50,DICL}$
E_{MAX}	1		
$Ce_{50,PARA}$	0.442	1	
$Ce_{50,DICL}$	0.004	0.029	1
Placebo	$T_{1/2keq_{PL}}$	$T_{1/2kel_{PL}}$	
$t_{1/2keq_{PL}}$	1		
$t_{1/2kel_{PL}}$	-0.109	1	

Table 3.4

Correlation of population parameter variability for pharmacodynamic and placebo parameters.

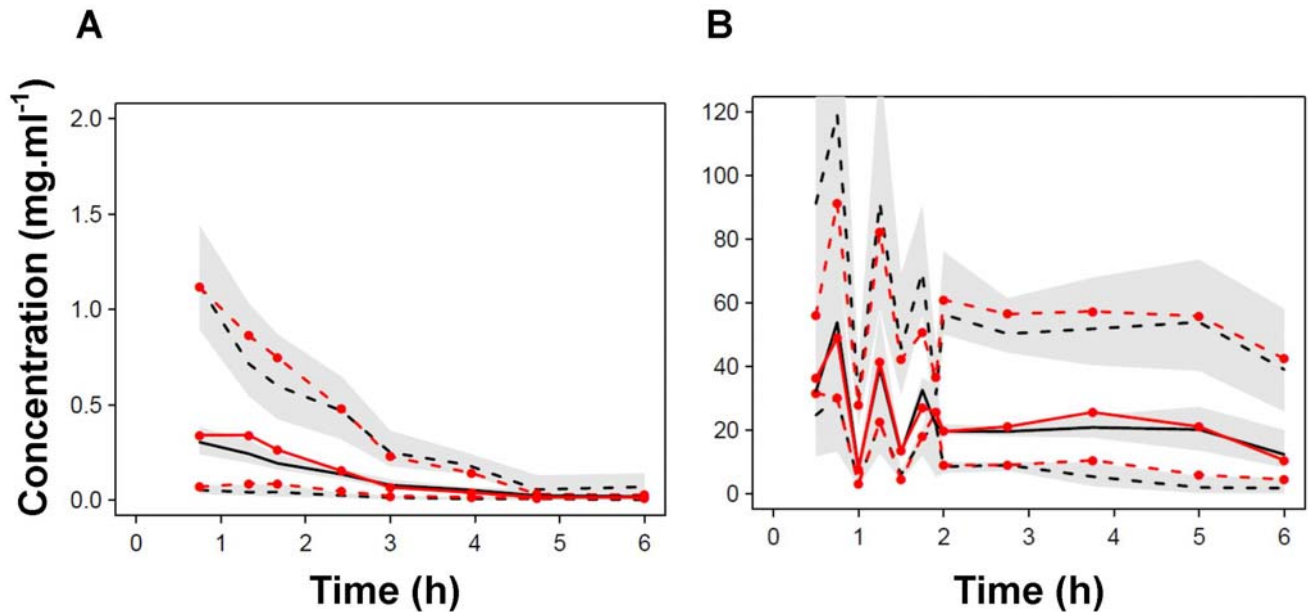


Figure 3.2

Visual predictive check (VPC) plots for (A) diclofenac pharmacokinetics and (B) paracetamol pharmacokinetics predictions. The plots show median and 90% intervals (solid and dashed lines respectively). Prediction percentiles (10%, 50%, and 90%) for predictions (black lines) are overlaid with those of the observations (red lines with symbols). Grey shaded areas are 95% confidence intervals for the prediction percentiles.

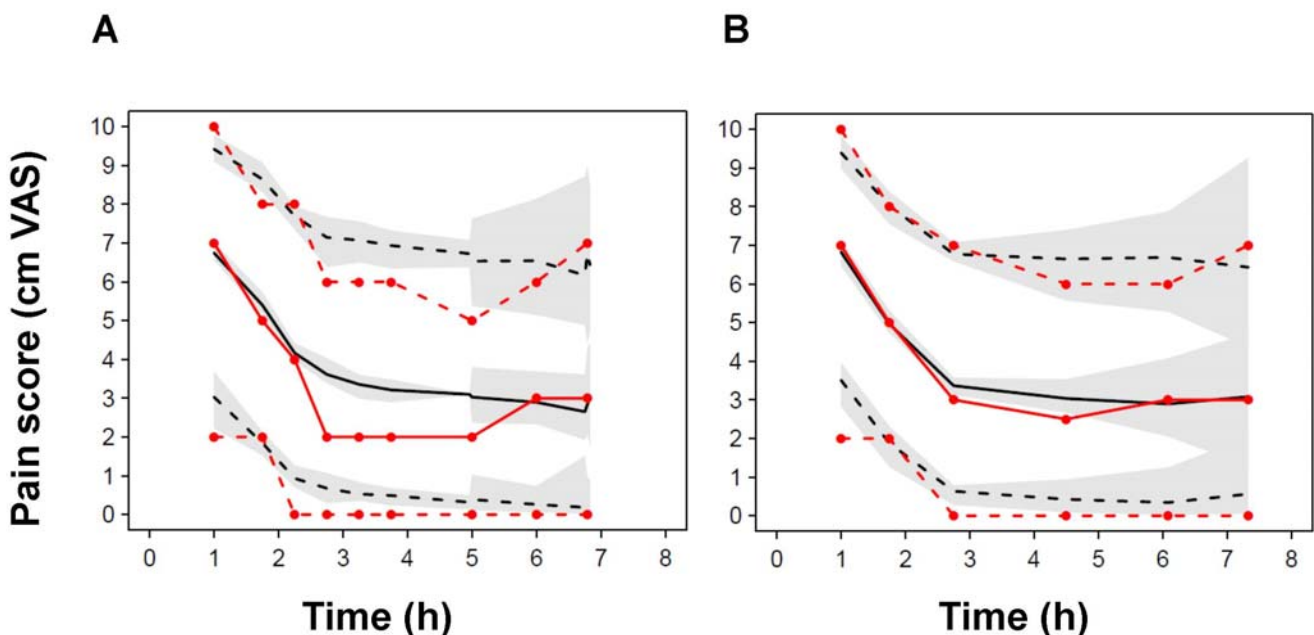


Figure 3.3

Visual predictive check (VPC) plots for predicted pain scores over time. The left panel (A) gives the original VPC plot for analgesia before inclusion of a model of study dropout, and the right panel (B) gives the VPC plot for analgesia the final model (including placebo and dropout models). The plots show median and 90% intervals (solid and dashed lines respectively). Prediction percentiles (10%, 50%, and 90%) for predictions (black lines) are overlaid with those of the observations (red lines with symbols). Grey shaded areas are 95% confidence intervals for the prediction percentiles. A persistent over-prediction of pain scores is visible in the left panel of plot A.

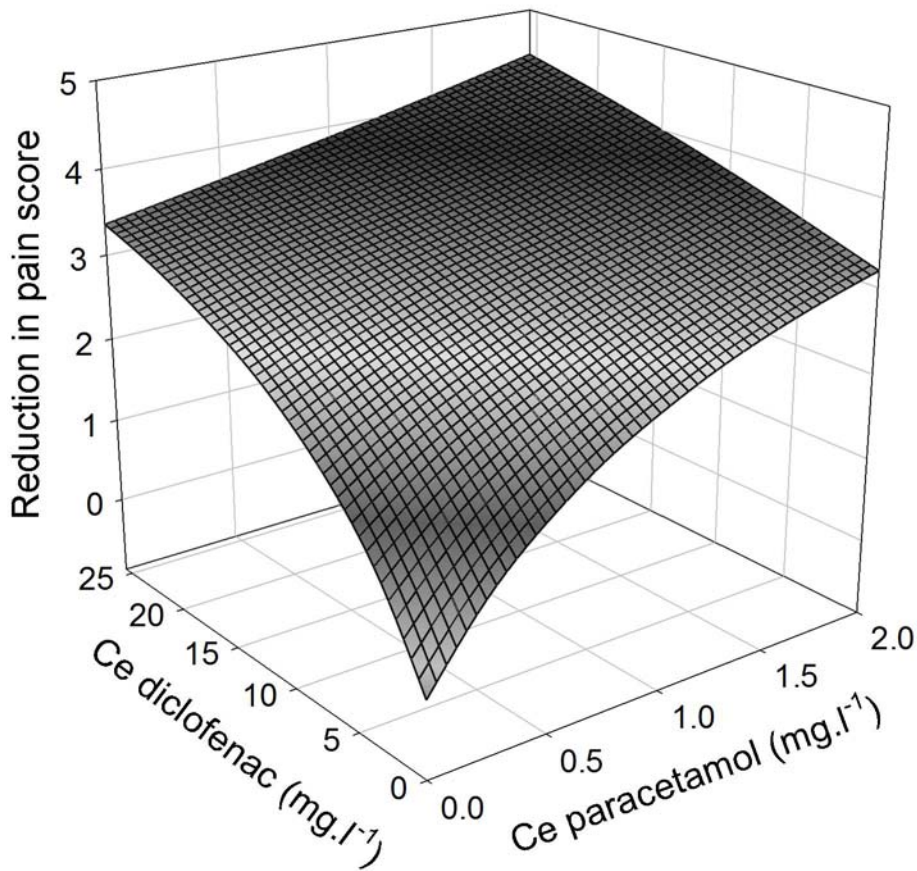


Figure 3.4

Theoretical surface of response for analgesia using paracetamol with diclofenac. Concentration-response curves individual drugs are given on the outer planes of the surface. The shape of the curves is identical for both drugs (slope parameter=1). C_e is the concentration of drug in the effect site compartment. Baseline pain is fixed at 10 cm on a VAS (0-10 cm).

Simulation was used to demonstrate the time-effect profile for a given dosage regimen. Simulation of effect profiles over time was performed using Berkeley MadonnaTM modelling and analysis of dynamic systems software (Robert Macey and George Oster of the University of California, Berkeley, USA).

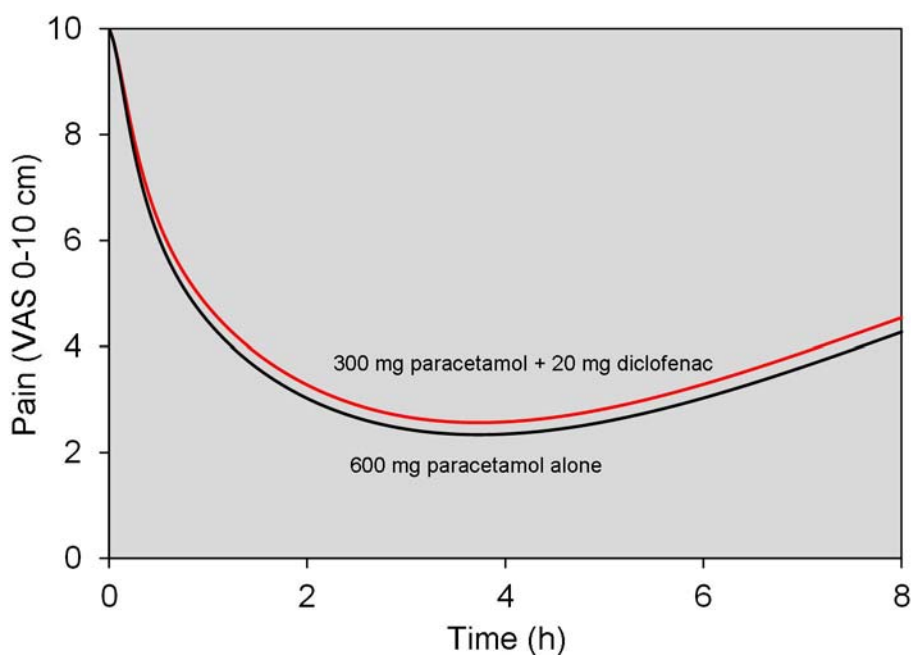


Figure 3.5

Simulated response profile for a 20 kg child following a single dose of paracetamol alone and in combination with diclofenac. The black line gives response following 600 mg paracetamol (30 mg.kg^{-1}), as is typically used at Starship Children's Hospital. The red line gives response following half this dose of paracetamol (15 mg.kg^{-1}) with 20 mg (1 mg.kg^{-1}) diclofenac. Pain scores over time are similar for both dosing strategies despite halving the dose of paracetamol.

3.4. Discussion

Diclofenac is commonly prescribed for postoperative analgesia in children, yet its dosing in this patient group remains largely dependent on extrapolation from adult data. Diclofenac pharmacokinetics have been reported in children, but pharmacodynamics for analgesia in this population have not. A pooled data analysis approach was used in this analysis to develop a pharmacodynamic model for diclofenac in combination with paracetamol for analgesia in children.

Simulation studies have been used to predict the diclofenac dose needed to reach an effective analgesic concentration. An oral dose of 1.0 mg.kg^{-1} of diclofenac is recommended for children aged 1-12 years on the basis of the effective AUC in adults.[206, 208] The current model suggests somewhat better analgesia can be achieved with a dose of 2.0 mg.kg^{-1} . A targeted effect site concentration of 10 mg.l^{-1} paracetamol has been recommended for postoperative pain relief in children, corresponding to a reduction in pain score of 2.2 cm (VAS 0-10).[29] This concentration is

associated with a reduction in pain score of 1.46 cm when the current model is used. A 2 cm reduction in pain score can be achieved with a paracetamol effect site concentration of 11.75 mg.l⁻¹ or a diclofenac effect site concentration of 1.07 mg.l⁻¹. Alternatively, half this concentration of paracetamol (5.88 mg.l⁻¹) may be combined with 0.54 mg.l⁻¹ of diclofenac to achieve the same effect (Figure 3.6).

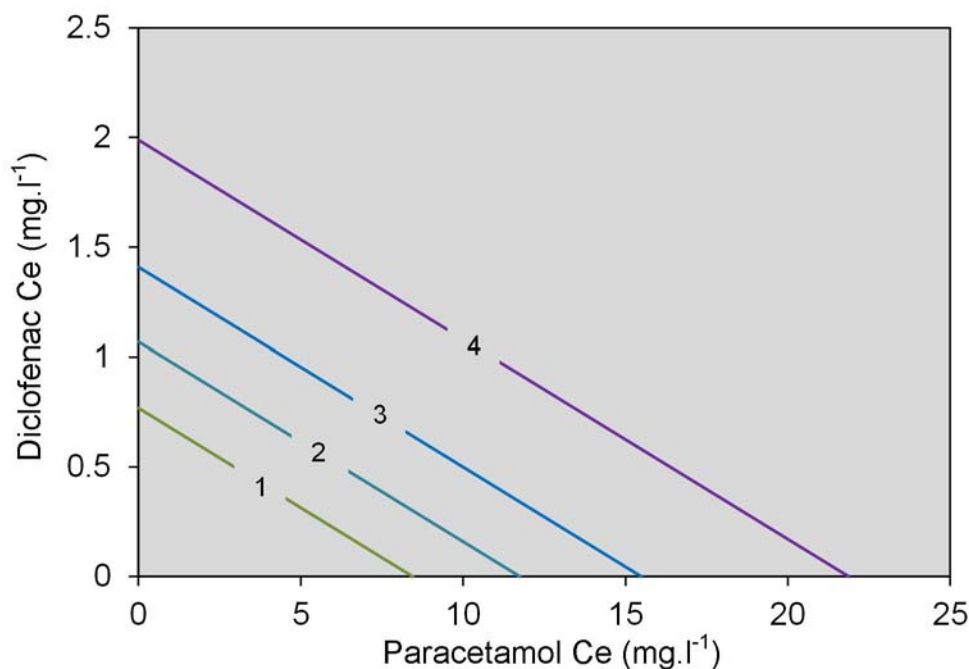


Figure 3.6

Isoboles of concentration pairs that together cause a 1 cm, 2 cm, 3 cm and 4 cm reduction in pain from baseline. Ce is the concentration in the effect site compartment. A 2 cm reduction in pain score can be achieved with Ce paracetamol 11.75 mg.l⁻¹, or Ce diclofenac 1.07 mg.l⁻¹. Alternatively this Ce of paracetamol may be halved to 5.88 mg.l⁻¹, and combined with 0.54 mg.l⁻¹ of diclofenac to achieve the same effect.

The Ce₅₀ parameter estimate for paracetamol (13.3 mg.l⁻¹, 95% CI 13.2, 13.4 mg.l⁻¹) was similar to other estimates. A Ce₅₀ of 11.9 mg.l⁻¹ was estimated in chapter 2 of this thesis for paracetamol analgesia alone and in combination with ibuprofen for wisdom tooth extraction in adults,[217] while a Ce₅₀ of 9.98 mg.l⁻¹ was reported for the data from study 2 in which children received oral and rectal paracetamol for pain following tonsillectomy.[29] Anderson *et al.* (study 1) estimated a maximal effect of paracetamol to be 5.3 cm (VAS 0-10),[29] similar to that obtained in this study.

Anderson *et al.* also included a model of placebo effect to describe changes in baseline pain over time. The placebo model had an equilibration half-life ($t_{1/2eq_{PL}}$) of 2.0 h, an elimination half-life ($t_{1/2el_{PL}}$) of 2.0 h and a potency ($BETA_{PL}$) of 1.5 cm (VAS 0-10).[29] They predicted a peak reduction in pain of 5.6 cm occurring at 2.89 hours (illustrated in Figure 3.7).[29] The maximum reduction in VAS was 6.8 cm for the current analysis, occurring 4 hours postoperatively. This probably coincides with some participants being discharged and taken home, after which baseline pain begins to increase again. Björnsson *et al.* studied pain relief following wisdom tooth extraction using visual analogue pain scores as a measurement of analgesia (0-10).[218] They also included a model for study dropout but chose to incorporate placebo effects as an exponential model. Although they studied the effects of naproxen, the placebo effect can be considered ‘drug independent’.[218] They reported a maximum reduction in baseline pain of 20.2%, equating to 2 cm (VAS 0-10). Conversion of the $t_{1/2keq_{PL}}$ of 2.7 h estimated in this study gives a rate constant for onset of placebo effect of 0.26 h^{-1} . Björnsson *et al.* estimated a rate constant for placebo effect of 0.237 h^{-1} ,[218] again similar to the estimates in this study. The differences in predictions of baseline pain for these studies can be seen in Figure 3.7.

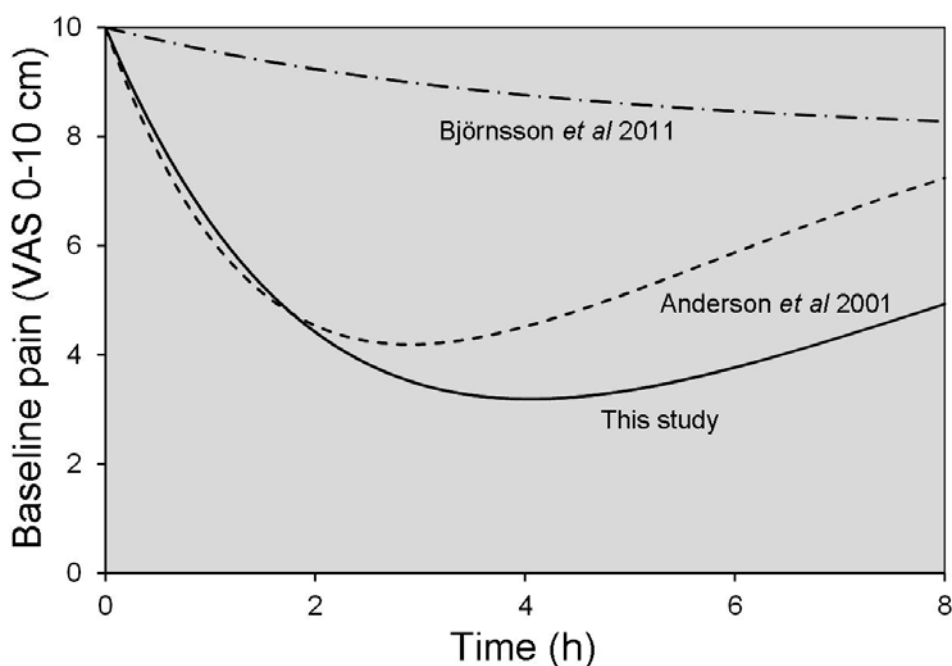


Figure 3.7

Changes in baseline pain over 8 postoperative hours, as predicted by placebo models. The placebo model used in this analysis was similar to that used by Anderson *et al.* 2001,[29] although the predicted peak effect is larger and occurs later in the current study. Björnsson *et al.* used an exponential model to describe changes in baseline pain for adults undergoing wisdom tooth extractions.

There was a persistent over-prediction of pain scores in the initial analysis (left panel, plot A of Figure 3.3). A potential explanation for this observation is that observed pain scores were lower than predicted because those individuals with poorly controlled pain are more likely to request rescue medication and subsequently be excluded from the study. This prompted investigation of a model describing study dropout. A time-to-event hazard model was used to reflect the interval censored nature of pain score measurements. Pain scores were identified as a significant covariate on the hazard model in both this study and that by Björnsson *et al.*,[218] with increasing pain correlating to an increased likelihood of study dropout. Some over-prediction was still observable in the final model (see panel B of Figure 3.3), but this was greatly improved from that of the initial analysis. This is an example of informative study dropout where the reason for discontinued participation is identifiable and predictable. Ignoring dropouts in models categorises all missing data as ‘missing completely at random’,[219] and assumes that dropout is equally likely to occur in all arms of the study. In fact multiple reasons for dropout exist, some of which may be identifiable (for example, poorly controlled pain) and some of which may be non-random but as yet unknown (for example, undocumented adverse effects of the treatment).[219, 220] These types of non-random study dropout can have a large impact on the outcome of a study, both in terms of assessing clinical study outcomes and on the design of future trials.[220] The latter is particularly relevant to paediatrics where study participation may be onerous or daunting for parents and children, and studies are carefully designed to obtain adequate power with small numbers of participants.

This study has a number of limitations. Serum concentrations were unavailable for diclofenac due to an unfortunate loss of frozen samples. Today alternative techniques that are less costly and do not require cold storage are available, such as dried blood spot sampling which has the added benefit of being more tolerable to children than standard blood sampling.[221] To remedy the lack of pharmacokinetic data, data were pooled with those of previously published pharmacokinetic studies in children.[29, 33, 206, 208] It may be that the diclofenac pharmacokinetic profile developed from data contributed by study 3 does not reflect that of the other paediatric populations. Although patient demographics in this study were similar to those of study 2, study 3 included both paediatric and adult participants. Additionally, participants of study 3 received a new suspension of 50 mg.5 ml⁻¹ diclofenac sodium, while those of study 1 were given an oral dose of diclofenac dispersal formulation. The adult participants of study 3 received diclofenac on two occasions and subsequently between-occasion variability in this group was included in the analysis. These factors may have contributed to an under-prediction of diclofenac concentrations visible in the first 1.5 postoperative hours, visible in

panel A of Figure 3.2. Tonsillectomy was used as a pain model for both the current study and study 2, while in study 3 minor day case surgery was used as a pain model. Inconsistencies in pain models and analgesia measurements may contribute to differences between studies. However, as only dosing and plasma concentrations were available for diclofenac, study 3 did not contribute data towards the pharmacodynamic model. Visual analogue scales (0-10) were used to measure pain in both study 1 and study 2. Some difference may exist between self-rated pain scores (using a visual analogue scale with faces) and observer assessed pain scores, although good correlation has been shown between these measures when used in children.[222, 223]

An additive model was used to describe the combined effects of paracetamol and diclofenac for analgesia. This was supported by a poorer fit of the model indicated by NONMEM's objective function when the interaction parameter was estimated. However, the study was designed to identify the pharmacokinetic-pharmacodynamic profiles of paracetamol and diclofenac for analgesia in children; not to assess the presence of an interaction between them. We cannot therefore draw any conclusions from this analysis as to the nature of the interaction. A recent animal study reported a synergistic interaction between paracetamol and diclofenac for analgesia,[203] but there is little in the literature to suggest anything other than an additive effect exists. A number of adult studies comparing doses of roughly 1.4 mg.kg^{-1} diclofenac alone and with paracetamol have failed to demonstrate an improvement in analgesia as measured by pain scores,[224-227] although some noted an improvement over paracetamol alone.[224, 226] A potential reason for these results, as previously mentioned, is that the maximal analgesic effect of these drugs is already approached at the doses used.[217] Others have demonstrated a benefit in pain scores for paracetamol and diclofenac over either drug alone.[228, 229] These conflicting results should not be interpreted as a lack of clinical benefit in using the combination over either drug alone. A clinical benefit exists in situations where reducing the dose of paracetamol is of importance. This can be achieved without significantly impacting analgesia by the addition of an NSAID, such as ibuprofen or diclofenac, at low doses.

Summary

This analysis highlights some of the difficulties in interpreting paediatric analgesic studies. Pain was analysed as a continuous variable.[230] Placebo effects and study dropout caused by the need for rescue analgesia were included in this analysis. The model provides a framework for estimating appropriate dosing in children for both drugs alone, and in combination, as they are commonly prescribed. Models of placebo and study dropout can be considered ‘drug independent’,[218] and may reflect observations in other paediatric populations. I provide an estimate of the C_{e50} (1.2 mg.l^{-1}) and equilibration half-time ($t_{1/2keo}$, 0.2 h) in children for oral dosing of diclofenac suspension, both of which are previously unreported. The current model suggests that doubling the dose currently recommended for children from 1 mg.kg^{-1} to 2 mg.kg^{-1} gives somewhat better analgesia. These previous recommendations were obtained through extrapolation of adult data and use of AUC analyses.[206, 208] A paracetamol concentration (in the effect site compartment) of 11.75 mg.l^{-1} provides a 2 cm reduction in pain score when given alone. The equivalent effect can be achieved with half this concentration when combined with a diclofenac effect site concentration of 0.53 mg.l^{-1} . A dose of 20 mg diclofenac with 300 mg paracetamol achieves equivalent analgesia as 600 mg paracetamol alone, in a 20 kg child.

Chapter 4. Propofol and alfentanil pharmacokinetics and pharmacodynamics

Background: The interaction between propofol and remifentanil, and between propofol and alfentanil, is thought to be additive for BIS. Interaction models using response surface methods have been used to confirm this for propofol with remifentanil. However, a pharmacodynamic response surface model to describe the propofol-alfentanil BIS response has not been reported.

Methods: An existing dataset was available for analysis, in which twenty two adult patients received either propofol or alfentanil as a constant infusion with ramped infusions of alfentanil or propofol, respectively. BIS measurements, and plasma concentrations of propofol and alfentanil, were available. Propofol and alfentanil pharmacokinetics were described using three and two compartment models, respectively. Effect was described using a response surface model with an interaction parameter. Fractional, E_{MAX} and interpolated E_{MAX} parameterisations were investigated.

Results: The response surface method described by Minto et al., with an estimated E_{MAX} parameter, best fit response data. The concentration in the effect site associated with 50% the maximal effect (Ce_{50}) was $646 \text{ ng}\cdot\text{l}^{-1}$ for alfentanil and $2.7 \text{ mg}\cdot\text{l}^{-1}$ for propofol. Baseline BIS was 98 units, maximal effect (E_{MAX}) was a reduction in BIS of 80 units, and slope was 3.1. Estimating the interaction parameter ($\beta \neq 0$) did not improve the model fit, suggesting additivity.

Conclusions: An integrated pharmacokinetic-pharmacodynamic model for effect measured by BIS demonstrated an additive relationship for propofol and alfentanil.

4.1. Introduction

I presented models describing combined effects for paracetamol with ibuprofen, and with diclofenac, for postoperative pain in the first part of this thesis. I now describe a series of studies that work towards establishing a generalised model for opioid, intravenous and inhalation anaesthetic effects on BIS response using similar methodology. There are numerous studies that describe two drug models for interactions between phenyl-piperidine opioids, intravenous and inhalation anaesthetics. [59, 60, 69, 76, 128, 131, 132, 146-148] There are no analyses that describe combined effects for all three drug classes when given together, even though this combination is commonly used in general anaesthetics today.

A model for these three drug classes could be used to improve the current simulation of BIS in our high fidelity, model-driven patient simulator. It could also be used to extend pharmacokinetic-pharmacodynamic display systems that do not currently predict patient response following the introduction of a third drug class. The idea presented here is that the model will be ‘generalised’ in the sense that users may substitute a modelled drug with another from the same class (e.g. replace the phenyl-piperidine opioid remifentanil with another of that class such as fentanyl, or alfentanil).

Generalisability of a model in this manner relies on the assumption that relationships between phenyl-piperidine opioids, intravenous and inhalation anaesthetic drug classes are consistent for the modelled endpoint. As I discussed in chapter 1, this is the case for many combinations (e.g. synergy has been observed for ablating response to noxious stimuli for the opioids fentanyl and remifentanil when given with the inhalation anaesthetics desflurane, isoflurane and sevoflurane, Section 1.5.3.3).[148, 166-169] Concentrations of an administered drug might be converted to equivalent concentrations of another drug that is known to act in a similar manner and is included in the model, on the basis of this assumption. This technique has already been used by Syroid *et al.*, who converted fentanyl effect site concentrations to remifentanil equivalents using a ratio of relative potency (remifentanil: fentanyl=1:1.2).[132] They were able to predict return to consciousness following isoflurane with fentanyl administration using a model originally derived from sevoflurane and remifentanil data.[131] Similarly, other opioids such as alfentanil could be converted to a modelled ‘core’ opioid for inclusion in a three drug model describing opioid, intravenous and inhalation anaesthetic effects.

Model ‘generalisability’ between opioids and inhalation anaesthetics has already been established.[131, 132] Interaction analyses that use response surface methods have been reported for BIS response for alfentanil with sevoflurane, and remifentanil with sevoflurane.[76, 128] The next step is to establish similar data for intravenous anaesthetic-opioid pairs and BIS response (Figure 4.1). The interaction between propofol and remifentanil, and between propofol and alfentanil, has been investigated for multiple endpoints and is thought to be additive for BIS (Section 1.5.3.1). Two studies have used interaction response surface methods to confirm this for propofol with remifentanil.[59, 146] The additive relationship for BIS with propofol and other opioid combinations suggested by less robust methods has yet to be confirmed using interaction response surface methods.[150, 231]

The aim of the work presented in this chapter was therefore to identify an appropriate pharmacodynamic response surface model to describe the propofol-alfentanil BIS response.

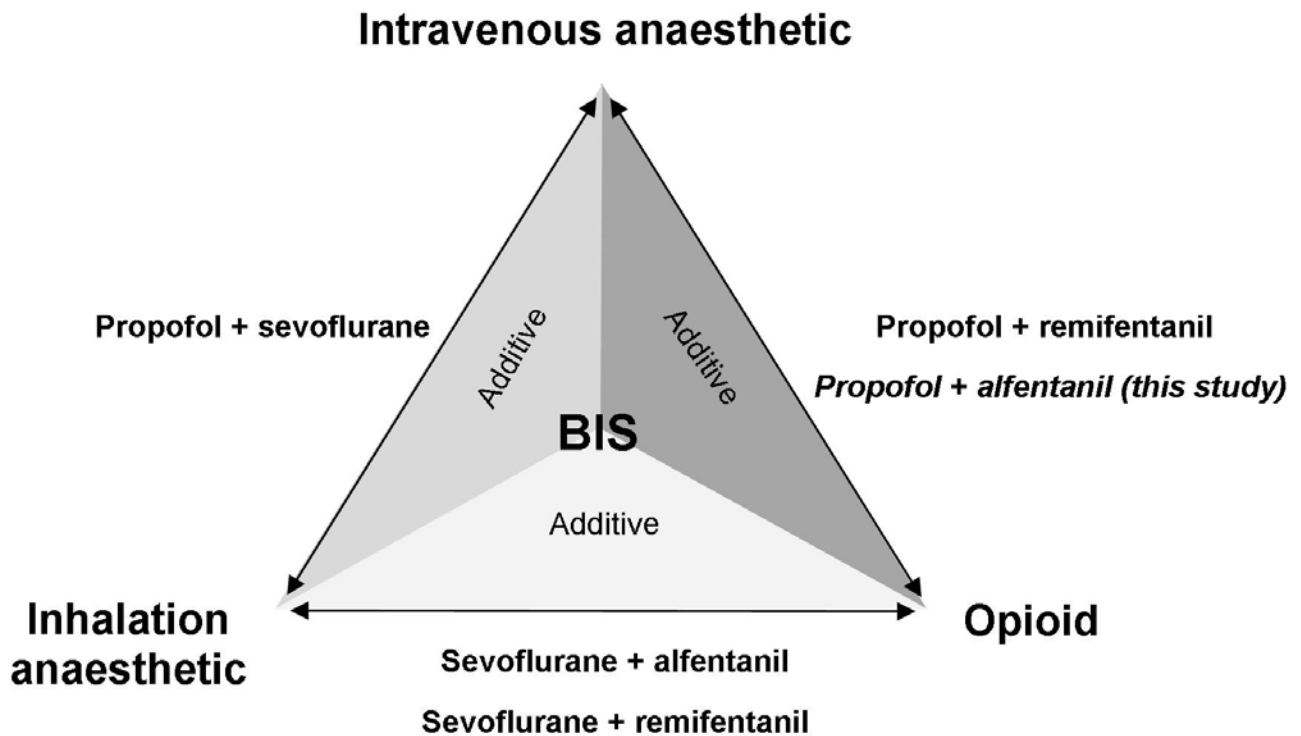


Figure 4.1

Relationships for BIS between phenyl-piperidine opioids, intravenous anaesthetic and inhalation anaesthetic drug classes. Response surface models have been reported for drug combinations representing all three drug class pairs: propofol-sevoflurane models represent intravenous anaesthetic-inhalation anaesthetic combinations;[129, 143] propofol-remifentanil models represent intravenous anaesthetic-opioid combinations;[59, 146] and sevoflurane-alfentanil and sevoflurane-remifentanil represent phenyl-piperidine opioid-inhalation anaesthetic combinations.[76, 128] Additivity was found to exist in each of the cited studies for BIS response. A model describing BIS response for propofol-alfentanil is the objective of the work I present in this chapter.

4.2. Methods

The analysis used an existing pharmacokinetic pharmacodynamic dataset derived from patients receiving total intravenous anaesthesia (TIVA) using propofol and alfentanil. These data were previously unanalysed and have not been published elsewhere.

Box 4. *How these data were collected*

Data were collected by Associate Professor Timothy Short at the Prince of Wales Hospital in Hong Kong between March and September 1996. Data were from an interaction study using the criss-cross study design as proposed by Short *et al.* and BIS as an effect measure.[202] The criss-cross design was developed to maximise efficiency when collecting concentration and effect data across a range of doses for two drugs and using a continuous endpoint such as BIS.[202] Patients are randomised to receive either drug 1 or drug 2 at a constant infusion rate throughout the study, whilst the infusion rate of the other drug is varied. In this way, observations are made for various strategic dose pairs, providing information for all areas of the effect ‘surface’.

Ethics

Regional ethics approval for this study was given by the Research Ethics Committee of the Faculty of Medicine, Chinese University of Hong Kong prior to commencing the study. A research doctor explained the study to potential participants, and written informed consent was given by each adult participant.

Participants

Adult patients, aged 18-50 years with an American Society of Anesthesiologists physical status (ASA) of 1-2 and who were scheduled for elective gynaecologic or orthopaedic surgery at the Prince of Wales Hospital, were studied. Patients whose weight exceeded their ideal body weight by 50% or greater, and those with an allergy or contraindication to the study drugs, were not studied.

Study phase

Each participant was studied for approximately one hour before being transferred to the operating room and anaesthetised for surgery. Forearm venous access was established for infusion of the study drugs. A 22 gauge radial arterial cannula inserted into the opposite arm to that used for study drug administration was used exclusively to collect blood samples. No premedication or NMBDs were given during this time. A second anaesthetist was in attendance and was responsible for the care of the participants during the study.

Study drugs

Participants received a constant infusion of either propofol or alfentanil according to a random schedule designed to reach predefined target plasma concentrations, with ramped infusions of the other study drug. Propofol was given as a 10 mg.ml⁻¹ solution, while alfentanil was given as a 200 mcg.ml⁻¹ solution. Study drugs were infused using Graseby 3400 syringe pumps connected to a single study laptop by the RS232C serial ports. Computer controlled infusion software developed at the Chinese University of Hong Kong was used to drive the syringe pump infusion rates (software author YH Tam).[232] The software uses pharmacokinetic models to drive drug administration to targeted plasma concentrations selected by the user. Target plasma concentrations were designed to achieve a range of effect levels, including maximal drug effects. Infusion rates of the second drug were increased until no further reduction in BIS response was observed, after which infusions were discontinued. Infusion rates and volumes for each participant were saved in a file generated by the software.

Blood sampling

Arterial blood samples were taken using an approximately log-time sampling schedule of 1, 2, 4, 8, 16, 30 minutes during the ramped infusion and 31, 34, 36, 42, 60 minutes during wash-out of the infusion and at 30 minute intervals during subsequent anaesthesia. A maximum of 30 samples were taken per patient. Two ml of blood was drawn from the dedicated sampling cannula at each time point and added to lithium-heparin tubes. These were stored at 4 °C until alfentanil and propofol concentrations were analysed.

Alfentanil concentrations were analysed using an alfentanil radio-immunoassay kit supplied by Janssen Pharmaceutica, Beerse, Belgium, with a lower limit of detection of approximately 1 ng.ml^{-1} . Propofol samples were analysed using a high pressure liquid chromatography assay with fluorescence detection already in use for other projects within the same department.[233] The lower limit of detection of the propofol assay was 2 ng.ml^{-1} .

Effect measurements

BIS response was monitored prior to beginning study drug infusions and throughout both the study and subsequent anaesthesia until recovery. BIS was recorded electronically using an A1000 EEG monitor with BIS software version 3.2 (Aspect Medical Systems, Massachusetts, USA) in 10 second epochs. Physiologic monitoring, including blood pressure and heart rate, was according to standards of practice of the Hong Kong College of Anaesthetists.

Intraoperative and recovery phases

Following completion of the study period, participants were transferred to the operating room. Anaesthesia was induced for surgery and maintained throughout using propofol and alfentanil. All aspects of anaesthetic care and monitoring during this phase were according to standard practice and at the discretion of the attending anaesthetist. Participants were observed for a minimum of one hour in the postoperative unit to ensure adequate recovery from anaesthesia.

4.2.1 Modelling methods

Pharmacokinetic analyses were completed for each drug individually and plasma concentrations for each individual estimated. Predicted plasma concentrations were used to estimate apparent effect site concentrations and a structural pharmacodynamic model for BIS response selected. Parameters for the full integrated pharmacokinetic-pharmacodynamic model describing propofol with alfentanil for BIS were refined using a simultaneous pharmacokinetic-pharmacodynamic analysis.

4.2.1.1. Pharmacokinetic analysis

Blood samples taken during the study period and subsequent anaesthesia were pooled for analysis. Two and three compartment models were investigated. Models were parameterised in terms of clearance and volume of distribution with initial estimates given as those reported in the literature.[54, 75] Allometric scaling (as described previously in chapters 2 and 3) was used to adjust population parameter values (P_P) for the individual patient (P_i) according to their total body weight (TBW_i) i.e.

$$P_i = P_P \cdot (TBW_i/TBW_P)^s$$

Equation 4.1

where TBW_P is the typical TBW of the population (set to 70 kg here according to convention), and the scaling exponent s is equal to 1 for volume of distribution (V) and 0.75 for clearance (CL).[215] Age, gender, weight and co-administration of another drug were investigated for covariate effects.

4.2.1.2. Pharmacodynamic analysis

BIS data were reduced to one minute epochs during induction and five minute epochs for the remaining study time to facilitate modelling. An additional compartment was used to characterise drug concentration at the effect site. A first order rate constant (keo) was used to describe transfer of drug between the plasma and this effect site. This dataset was large and run times were slow, so hysteresis loop collapsing was used to gain some initial estimates for keo and pharmacodynamic parameters. The method given by Schnider *et al.* was used,[55] whereby effect site concentrations (C_e) over time can be described by the convolution of the input function (describing drug movement from the plasma to effect site compartment) and the effect site compartment disposition function (describing distribution and elimination processes of drug in the effect compartment). Individual Bayesian

predictions of plasma concentrations for each individual (established during development of the pharmacokinetic models) were used in this step. The NONMEM code is given in Appendix 4.1.

Pharmacodynamic models were explored at this stage. Minto's model and Greco's model (as given in Equation 3.3 to Equation 3.5, Chapter 3) were investigated. [122, 127] Response (R) was expressed both using fractional parameterisations i.e.

$$R = E_0 * \left(1 - \frac{U^\gamma}{(1 + U)^\gamma} \right)$$

Equation 4.2

and E_{MAX} parameterisations i.e.

$$R = E_0 - \left(E_{MAX} \cdot \frac{U^\gamma}{(1 + U)^\gamma} \right)$$

Equation 4.3

where E_{MAX} is the maximum reduction in BIS, γ is the slope coefficient describing the steepness of the relationship between drug concentration and effect, E_0 is baseline BIS and U is a function of the normalised drug potencies present and the interaction parameter (as calculated according to the structural model, see earlier descriptions of the Greco and Minto models given in Section 3.2.1.3, given in Equation 3.3 to Equation 3.5). A constraint model was used to ensure that E_{MAX} did not result in a negative BIS in each individual (see Appendix 4.1). Additionally, an adaption of Greco's model as described by Schumacher *et al.* was investigated.[129] They replaced the single E_{MAX} parameter with a function that allows different maximal drug effects i.e.

$$R = E_0 - \left(E_{MAX}' \cdot \frac{U^\gamma}{(1 + U)^\gamma} \right)$$

Equation 4.4

E_{MAX}' is dependent both on the relative concentration of the two drugs and on an estimated parameter $REST_0$ describing non-suppressible BIS by opioids i.e.

$$E_{MAX}' = REST_0 \cdot \left(\frac{U_A}{U_A + U_P} \right)^\lambda$$

Equation 4.5

where λ is a parameter to be estimated, U_A is the normalised concentration of alfentanil and U_P is the normalised concentration of propofol. This interpolation approach was applied to both Minto and Greco's models. The possibility of a varying slope parameter for the combination was also explored for the final model, using the methods described by Minto *et al.*[122]

4.2.1.3. Simultaneous pharmacokinetic-pharmacodynamic analysis

A simultaneous analysis in which pharmacokinetic and pharmacodynamic models are estimated together is considered best practice.[234, 235] However run times may be long and good initial parameter estimates help produce stable models. Separate analysis of pharmacokinetic and pharmacodynamic data may lead to inaccuracies in pharmacodynamic parameters and associated variability as parameter estimates are conditioned on the pharmacokinetic model.[235] Pharmacokinetic and pharmacodynamic model parameters established above were refined using a simultaneous analysis. The model code for the final simultaneous fit is given in Appendix 4.2.

4.2.1.4. Population parameter estimates

Data were analysed using nonlinear mixed effects models (NONMEM 7.1, Globomax LLC, Hanover, MD, USA). Between-subject variability was described in terms of random effect variables ('ETA', or η) assumed to have a mean of 0 and a variance (ω^2) to be estimated. An exponential error model was used to relate between subject variability to parameters i.e.

$$P_i = P_p e^{\eta_{individual}}$$

Equation 4.6

Covariance between elements of η , for example between CL and V, was related to their correlation (r) i.e.

$$r = \frac{\text{covariance}}{\sqrt{(\omega_{\text{CL}} \cdot \omega_{\text{V}})}}$$

Equation 4.7

Proportional and additive error models were tested to describe residual unknown error (ε) for concentration predictions, while additive error models were used for response predictions. Variability associated with this residual error ($\eta_{RUV,i}$) was also estimated. Population parameters, covariate effects and variances were estimated using the first order conditional estimation method with interaction option. Equations were integrated within ADVAN=3 for two compartment models and ADVAN=11 for three compartment models. A user defined PRED routine was used for the pharmacodynamic analysis.

Six alfentanil plasma concentrations were recorded as observations occurring below the lower limits of quantification (LLOQ). A common method of dealing with these observations is to remove them from the dataset but this censors data towards zero and as such can bias parameter estimates. Beal's method 3 as described by Ahn *et al.* was used to avoid this. LLOQ observations are treated as censored and the likelihood that each LLOQ data point is a true LLOQ observation is estimated.[236, 237] NONMEM's F_FLAG option was used to differentiate between estimation of a likelihood (F_FLAG=1) for a LLOQ observation and making a model prediction (F_FLAG=0) for those observations above the limit of quantification. No propofol concentrations were recorded as LLOQ observations.

Convergence criterion was three significant digits. Model selection required a statistically significant improvement in the NONMEM OBJ between nested models, equating to a reduction > 6.64 (for one additional parameter) based on a Chi square distribution ($\alpha < 0.01$). The interaction parameter was initially fixed at 0 to denote additivity. Variation of an interaction parameter from 0, or inclusion of a covariate effect, requires a statistically significant improvement in the OBJ.

Plots of observed *versus* model predicted concentrations and BIS values, and visual predictive checks, were used to assess how well models predict observed dependent variables. Bootstrap methods were used to estimate distribution-free parameter confidence intervals (CI) as an indicator of model stability.[196] VPC plots were constructed from 1000 simulations of the subjects to evaluate how well the model predicted the distribution of observed concentrations and BIS values.[13, 238]

4.3. Results

Twenty two patients were studied in total, and one patient was excluded from the analysis because of a computer failure in which infusion data were lost. There were 21 remaining individuals, of whom twenty were female and one was male. The mean age was 37 (range 20-47) years and the mean weight was 55 (range 43-71) kg.

4.3.1 Pharmacokinetics

One propofol concentration was removed as an erroneously high value (more than six times the standard deviation of propofol measurements taken during a two minute bin around the sample). In total, 332 alfentanil and 334 propofol concentrations were available for analysis from the index study. Seven alfentanil concentrations were identified as below the limit of quantification, equating to 2% of the total samples collected. Raw plasma concentrations for propofol and alfentanil are given in Figure 4.2 and Figure 4.3 respectively.

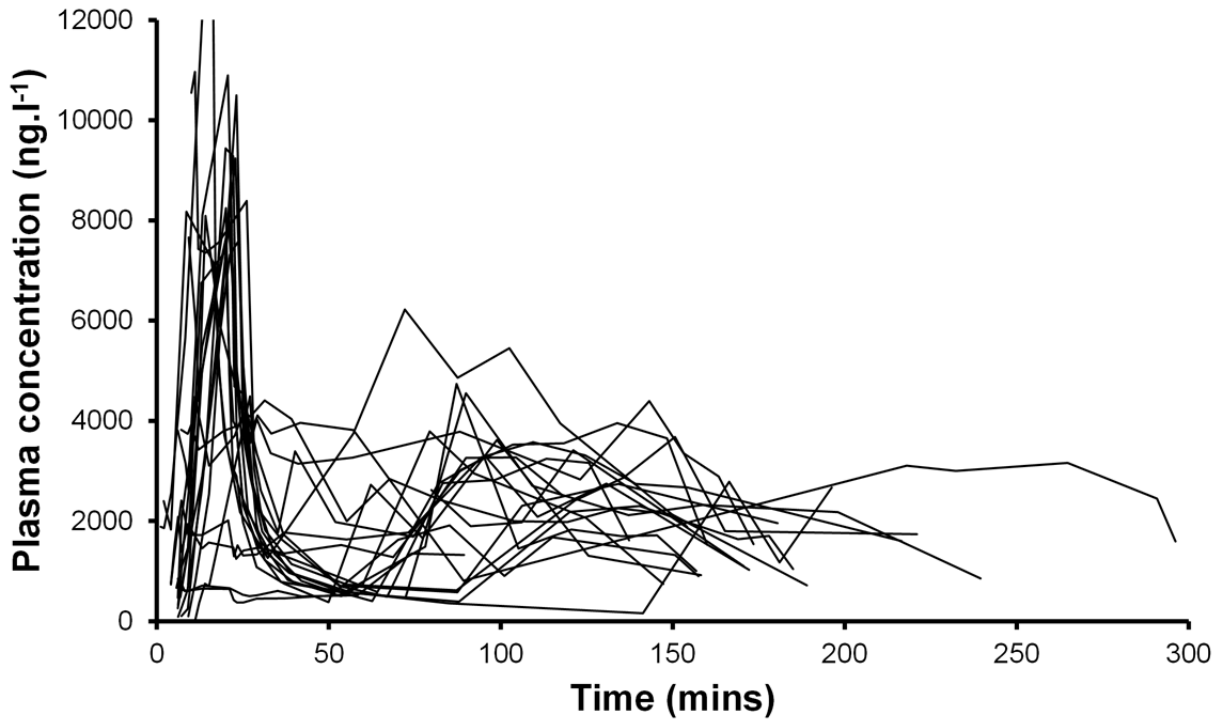


Figure 4.2

Raw propofol plasma concentrations; observations for each individual are linked with unsmoothed lines. Samples collected during the study period (approximately 1 h duration) and during anaesthesia were pooled.

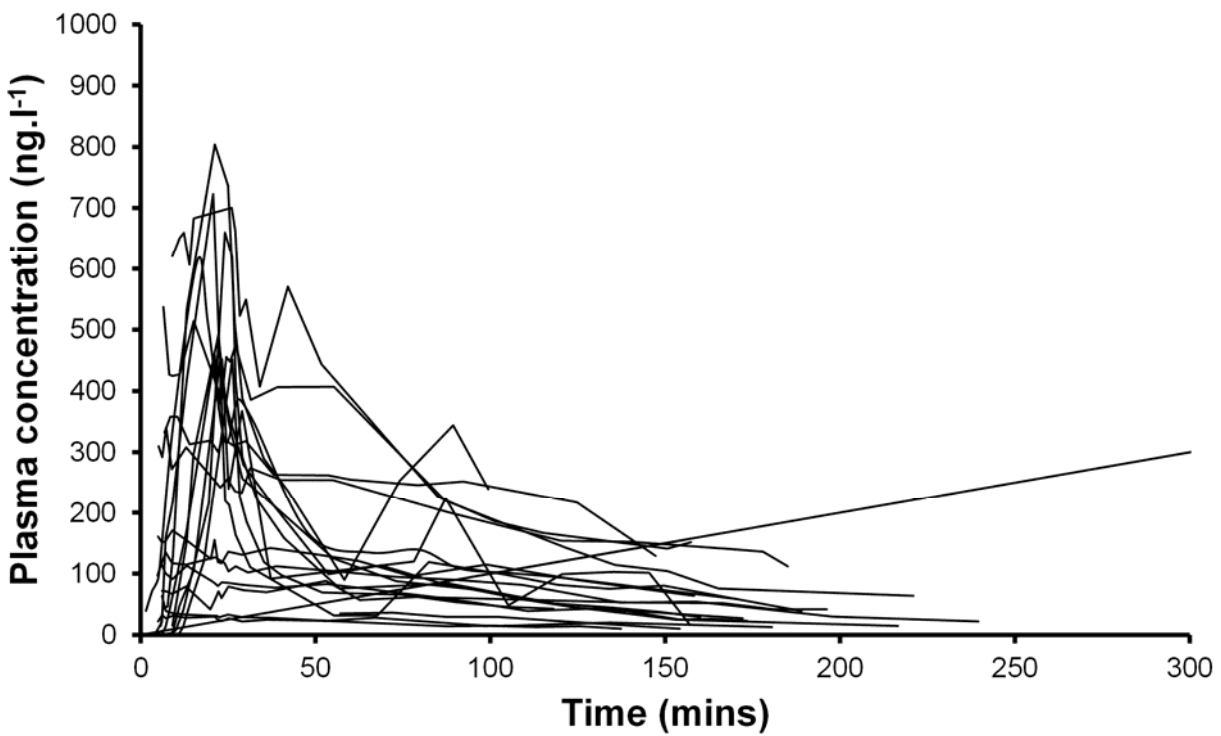


Figure 4.3

Raw alfentanil plasma concentrations; observations for each individual are linked with unsmoothed lines. Samples collected during the study period (approximately 1 h duration) and during anaesthesia were pooled.

A three compartment pharmacokinetic model (OBJ 4719) was selected over a two compartment model (Δ OBJ -19, $P < 0.001$) for propofol pharmacokinetics. Allometric scaling using TBW further reduced the OBJ to 4554 representing a large improvement in model fit (Δ OBJ -165, $P < 0.001$). The difference between two and three compartment models was negligible for alfentanil pharmacokinetics (OBJ 2838 for both models), and so the simplest model was selected for continued development. Allometric scaling using TBW further reduced the OBJ to 2608 (Δ OBJ -203, $P < 0.001$). Covariates of age, height, gender and co-administration of alfentanil or propofol did not improve model fit for either drug. The covariate screening process is summarised in Appendix 4.3.

Final estimates for parameters, associated variances and confidence intervals for propofol and alfentanil pharmacokinetics are given in Table 4.1, while estimates for covariance between population parameter variability (where included) are given for pharmacokinetics in Table 4.2. Graphs of residuals and visual predictive checks are given in Figure 4.4 and Figure 4.5 respectively.

Parameter	Propofol			Alfentanil		
	Estimate	95% CI*	%CV	Estimate	95% CI*	%CV
V1 (l.70kg ⁻¹)	6.8	4.8, 10.9	48.9	6.3	5.1, 7.7	24.2
V2 (l.70kg ⁻¹)	13.3	7.0, 29.7	18.1	15.8	13.0, 18.6	18.0
V3 (l.70kg ⁻¹)	63.2	19.8, 87.9	1.5	-	-	-
CL1 (l.min ⁻¹ .70kg ⁻¹)	2.1	1.95, 2.33	17.0	0.5	0.41, 0.52	26.3
CL2 (l.min ⁻¹ .70kg ⁻¹)	2.1	1.29, 2.25	27.1	0.7	0.52, 0.77	24.6
CL3 (l.min ⁻¹ .70kg ⁻¹)	1.1	0.45, 1.5	15.1	-	-	-
Err _{pro} (%)	23.0		-	18.0		-
Err _{add} (ng.l ⁻¹)	0.01		$\eta_{RUV,i}$ 0.3	0.04		$\eta_{RUV,i}$ 0.6

Table 4.1

Pharmacokinetic parameter estimates for propofol and alfentanil. CV=coefficient of variability; CI=confidence interval; Err_{pro}=proportional residual variability term; Err_{add}=additive residual variability term; $\eta_{RUV,i}$ =variability associated with Err_{add}. *A total of 300 bootstraps were completed in the time available.

Alfentanil	V1	CL1			
V1	1				
CL1	0.758				
Propofol	V1	CL1	V2	CL2	
V1	1				
CL1	0.809	1			
V2	0.017	0.567	1		
CL3	0.958	-0.803	-0.020	1	

Table 4.2

Correlation of population parameter variability for pharmacokinetic parameters.

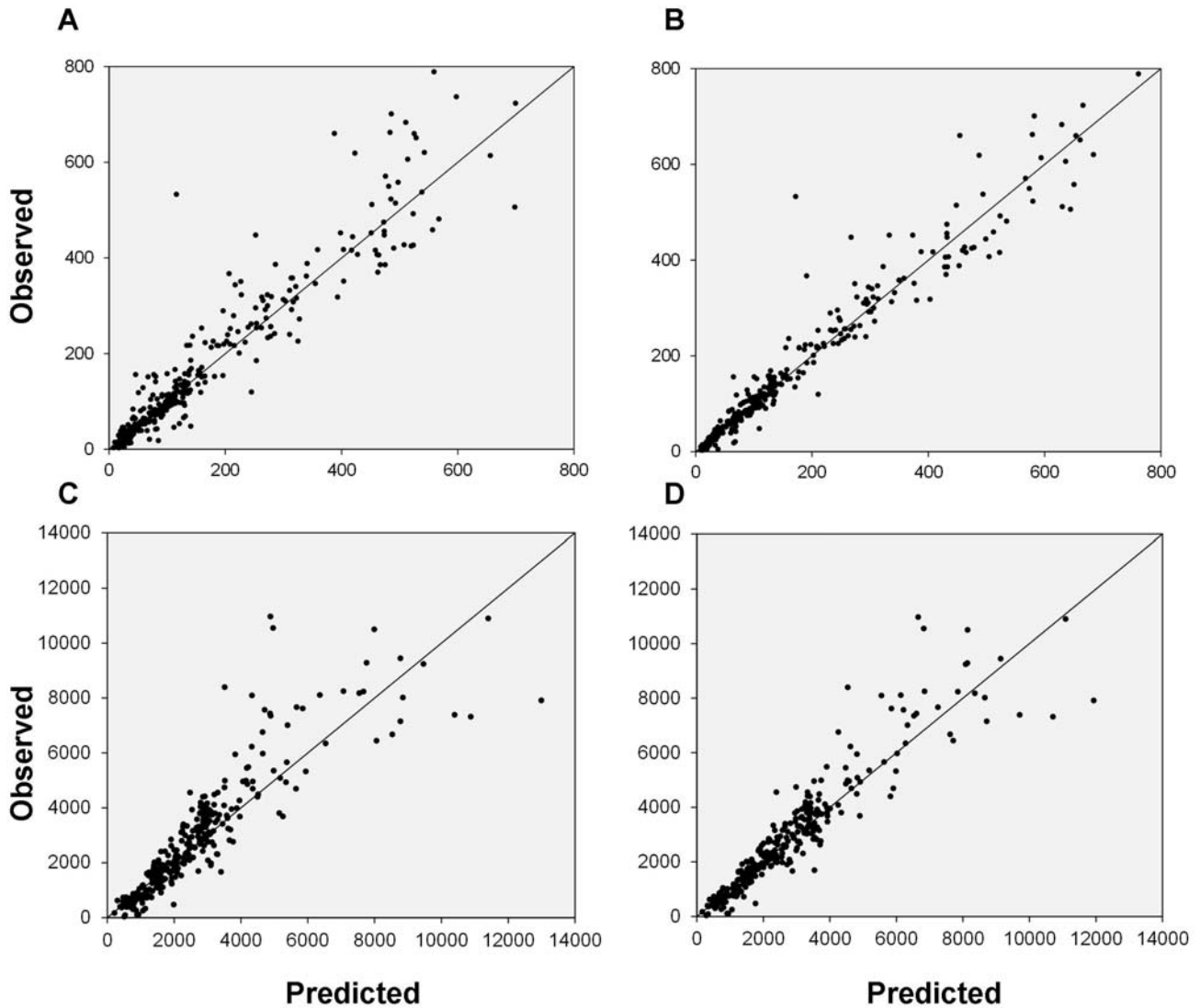


Figure 4.4

Quality of fit of propofol and alfentanil pharmacokinetic models. (A) Population alfentanil predictions are plotted against observed alfentanil concentrations. (B) Individual Bayesian alfentanil predictions based on adjusted parameters for the specific individual are plotted against observed alfentanil concentrations. (C) Population propofol predictions are plotted against observed propofol concentrations. (D) Individual Bayesian propofol predictions based on adjusted parameters for the specific individual are plotted against observed propofol concentrations. Units of concentrations are ng.ml⁻¹ for all plots.

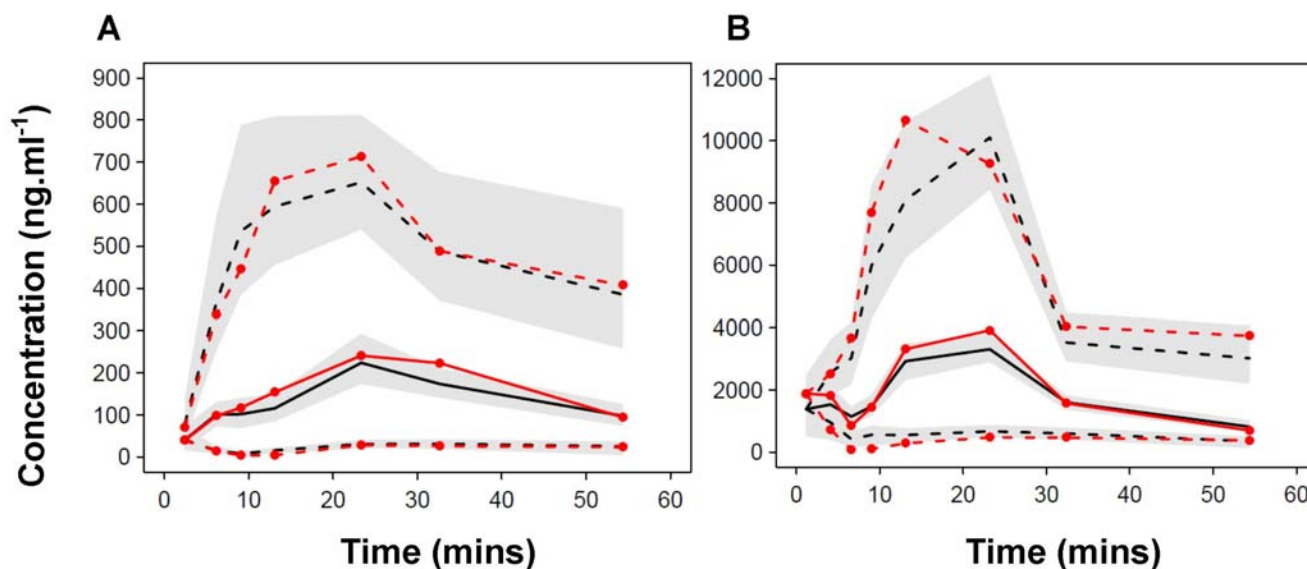


Figure 4.5

Visual predictive check for A) alfentanil pharmacokinetics and B) propofol pharmacokinetics. The plot shows median and 90% intervals (solid and dashed lines respectively). Prediction percentiles (10%, 50%, and 90%) for predictions (black lines) are overlaid with those of the observations (red lines with symbols). Grey shaded areas are 95% confidence intervals for the prediction percentiles.

4.3.2 Pharmacodynamics

Minto's model was selected to describe propofol-alfentanil pharmacodynamics for BIS response over Greco's model (Δ OBJ 13, $P < 0.0003$). Inclusion of an E_{MAX} parameter improved model fit, though allowing this to vary according to the ratio of propofol to alfentanil ('interpolated E_{MAX} ') did not result in further improvements (Table 4.3). A non-additive interaction parameter for potency resulted in a decrease in OBJ of 0.5 points and was associated with a 95% CI -1.6, 0.7 (obtained through bootstrap analysis). This interaction parameter was consequently fixed at 0. The final model was unable to converge successfully when a separate interaction parameter was applied to the slope of the curve. Pharmacodynamic model parameters were further refined using a simultaneous fit. LLOQ data were removed during this final stage; this shortened model run times but did not impact on parameter estimates. Final estimates for parameters and associated variances are given for the final model in Table 4.4, while estimates for covariance between population parameter variability (where included) are given for pharmacokinetics in Table 4.5. Plots of residuals and visual predictive checks are given in Figure 4.6 and Figure 4.7 respectively.

Model	OBJ	N parameters	Δ OBJ
Greco	2626		
Minto	2613		-13 ($P < 0.001$)
E_{MAX} parameter	2585	+ 1	-28 ($P < 0.001$)
Interpolated E_{MAX} parameterisation	2600	+ 1	+15
Minto E_{MAX} model selected for continued development:			
Non-additive interaction	2584	+ 1	-1 ($P = 0.317$)

Table 4.3

Pharmacodynamic model development. All models were initially run with additive interaction terms, representing the simplest scenario. The structural model selected for further investigation was that by Minto *et al.* with an estimated E_{MAX} parameter and additive interaction term ($\beta=0$). OBJ=NONMEM's objective function.

Parameter estimate	Estimate	%CV	95% CI*
E_0	98.0 FIX	0 FIX	-
Beta (β)	0 FIX	-	-
$Ce_{50, Propofol}$ (ng.ml ⁻¹)	2710.0	27.1	2354, 3296
$Ce_{50, Alfentanil}$ (ng.ml ⁻¹)	646.0	62.2	425, 964
Slope (γ)	3.1	52.5	2.1, 4.3
E_{MAX}	79.4	108.6	71.2, 92.6
$t_{1/2keo_P}$ (min)	3.5	5.4	2.3, 4.4
$t_{1/2keo_A}$ (min)	4.0	76.7	1.4, 8.2
keo_P	0.2	-	
keo_A	0.2	-	
Err_{add}	7.72	$\eta_{RUV,i}$ 0.21	

Table 4.4

Pharmacodynamic parameter estimates for the model investigating the propofol-alfentanil response surface. CV=coefficient of variability; CI=confidence interval; Err_{add} =residual variability estimated for BIS measurements using an additive error model; $\eta_{RUV,i}$ =variability associated with Err_{add} ; $Ce_{50,x}$ =effect site concentration of drug that causes 50% maximal drug effect; $t_{1/2keo_x}$ =equilibration half-time; keo_x =equilibration rate constant (or $0.69/t_{1/2keo_x}$) for drug moving between plasma and effect site compartments. *A total of 300 bootstraps were completed in the time available.

	E_{MAX}	$Ce_{50,Alfentanil}$	Slope
E_{MAX}	1		
$Ce_{50,Alfentanil}$	0.907	1	
Slope	0.876	-0.753	1

Table 4.5

Correlation of population parameter variability for pharmacodynamic parameters.

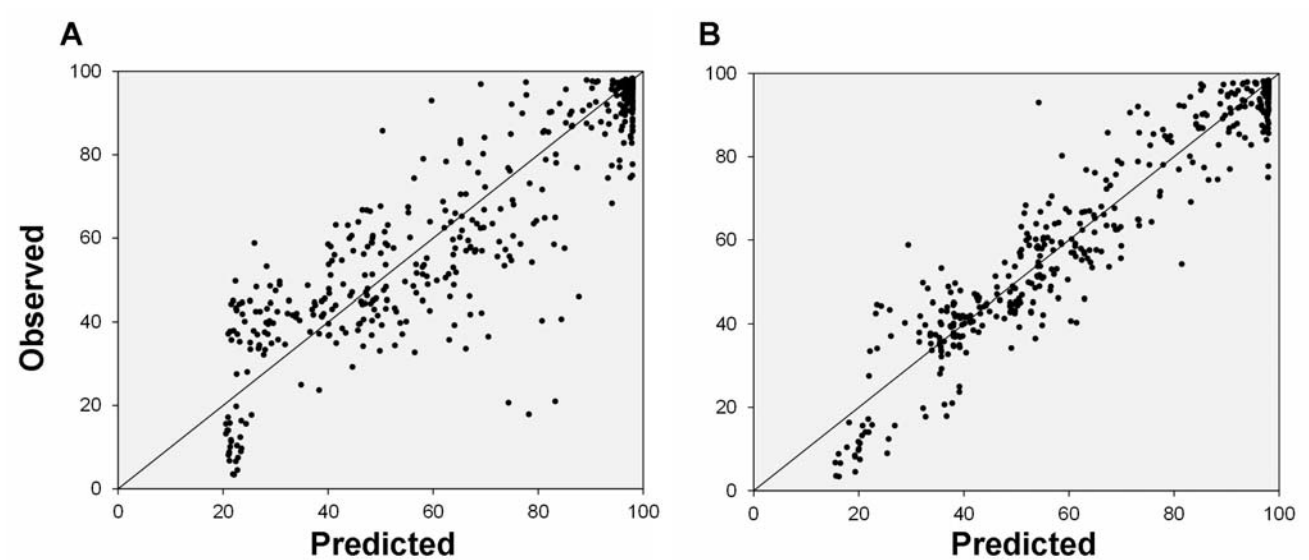


Figure 4.6

Quality of fit of the pharmacodynamic model describing BIS response for propofol with alfentanil. (A) Population predictions for BIS are plotted against observed BIS values. (B) Individual Bayesian predictions for BIS based on adjusted parameters for the specific individual are plotted against observed BIS values. Units are BIS units (0-100, where 100 is resting and awake, and < 60 is recommended for surgical stimuli). Some under-prediction of BIS response ranging between 0 and 20 units is visible in the plots as a result of the E_{MAX} parameter.

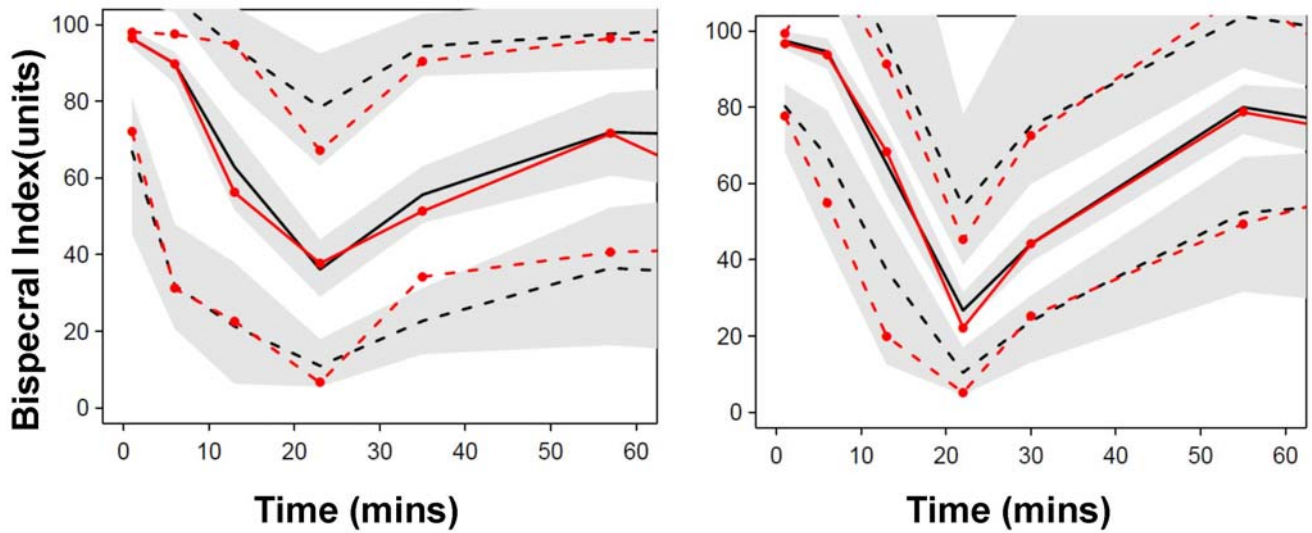


Figure 4.7

Visual predictive check (VPC) plots for the final pharmacodynamic model describing BIS response following propofol with alfentanil. The left panel gives the uncorrected VPC plots, and the right panel gives the prediction corrected VPC (PC-VPC). Prediction percentiles (10%, 50%, and 90%) for predictions (black lines) are overlaid with those of the observations (red lines with symbols). Grey shaded areas are 95% confidence intervals for the prediction percentiles. BIS units are 0-100 (where 100 is resting and awake, and < 60 is recommended for surgical stimuli).

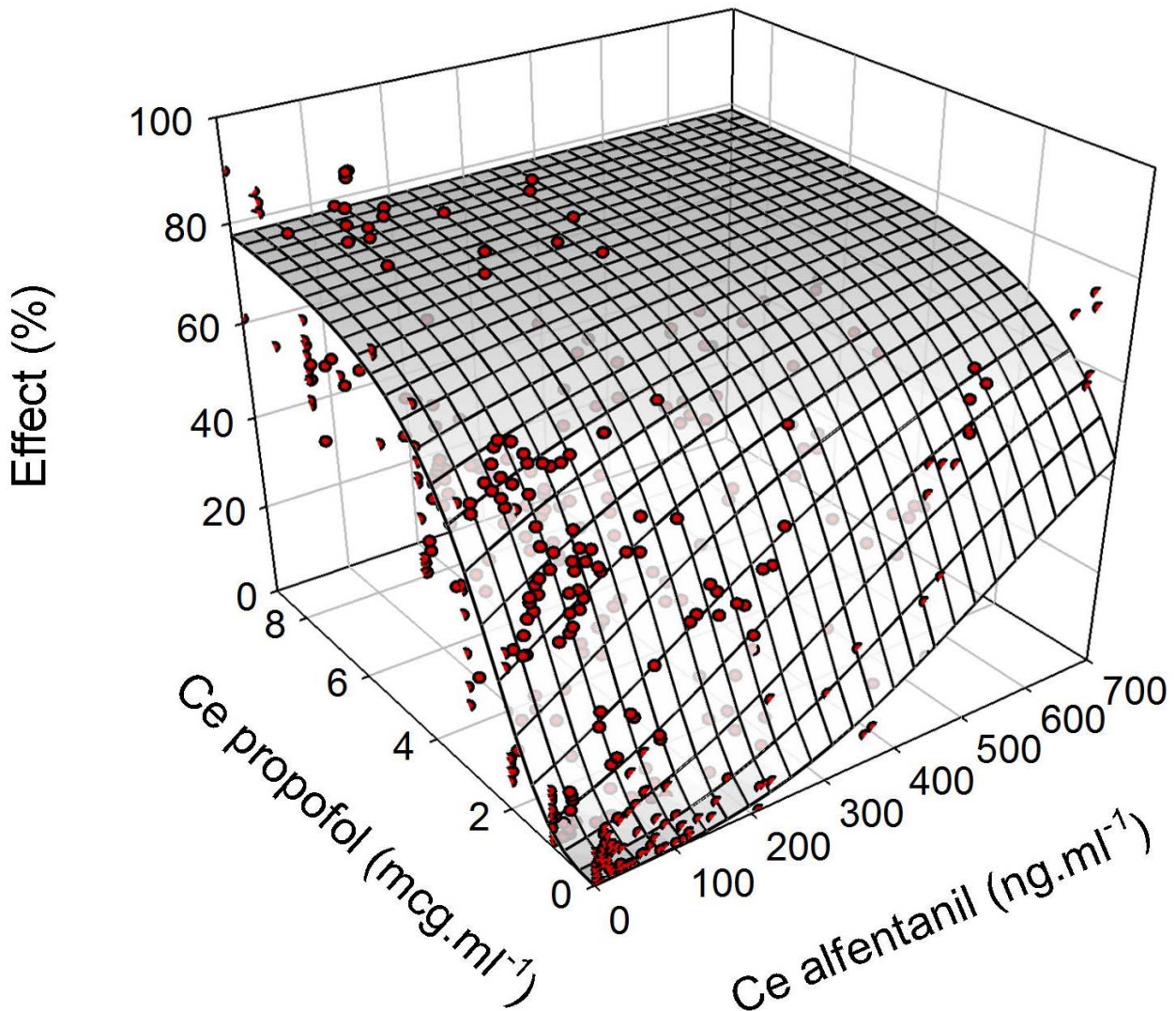


Figure 4.8

Surface of response following propofol and alfentanil for BIS. Ce is the concentration in the effect compartment. BIS response is displayed as % effect (note a maximal effect of 79%, which corresponds to a reduction in BIS from 98 to 18 units). The grey surface is that predicted by the model parameters, while red points are observations. Observations that fall on the outer edges of the surface are depicted as half circles; those that fall under the surface can also be seen.

4.4. Discussion

The concept of model generalisability has already been demonstrated between phenyl-piperidine opioids and inhalation anaesthetic drug pairs,[131, 132] and an additive relationship between drugs of these groups confirmed for BIS using response surface methods.[76, 128] Likewise, additive response surface models have been reported for propofol with remifentanil for BIS response.[59, 146] I report a linked pharmacokinetic-pharmacodynamic model with drug interaction characterised by a response surface for propofol with alfentanil for BIS response, and confirm earlier work suggesting an additive relationship for this drug pair over the clinically used concentration range.[150, 231]

Minto's model, with an estimated E_{MAX} and an additive interaction parameter ($\beta=0$), best fitted observed BIS response. Nested models in which the interaction parameter was allowed to vary (non-additive) did not result in a significant improvement in model fit as judged by a reduction in NONMEM's OBJ value. This was as expected from the literature which generally supports additivity.[59, 146, 147, 150] Only one study found synergism between propofol and a phenyl-piperidine opioid for BIS.[156] This observation might be explained by the choice to pre-medicate all participants with oral midazolam 2 h before anaesthesia with propofol and remifentanil. The slope parameter (γ) was estimated at 3.1. This was higher than other estimates of 1.0-1.4 given for propofol with remifentanil for BIS response in volunteers and using response surface methods,[59, 146] but perhaps better reflects slope estimates for propofol when given alone.[53, 239, 240]

The Ce_{50} (the concentration in the effect site associated with 50% of the maximal response) estimate for propofol in this study was 2.7 mcg.ml^{-1} . Propofol Ce_{50} estimates for BIS range between 2.3 and 3.4 mcg.ml^{-1} . [38, 59, 150, 155, 241, 242] A propofol Ce_{50} of 3.1 mcg.ml^{-1} was estimated for BIS by Bouillon *et al.*[59] Nieuwenhuijs *et al.* reported a Ce_{50} of 2.7 mcg.ml^{-1} for propofol when given with remifentanil.[146] Other authors who have used response surface methods to model BIS response for propofol in combination with inhalation anaesthetics report Ce_{50} estimates of 3.7 to 5.0 mcg.ml^{-1} . [129, 143] The alfentanil Ce_{50} estimated in this study was high at 646.0 ng.ml^{-1} . The inability of opioids alone to cause anaesthesia, and their small impact on BIS, makes estimation of this parameter difficult.[130] For example, an E_{MAX} of just 36 BIS units has been estimated for alfentanil when given alone.[53] EC_{50} (Ce_{50} in the plasma) estimates as high as $1240.0 \text{ ng.ml}^{-1}$ have been reported for alfentanil and EEG effects using isobolographic methods,[231] while other Ce_{50} estimates range from

480.0-634.0 ng.ml⁻¹. [53, 71, 72, 243] Egan *et al.* estimated an Ce₅₀ of 596.7 ng.ml⁻¹ for alfentanil effects on the spectral edge parameter of EEG measures when given as an infusion. [75] Dahan *et al.* used response surface methods to describe alfentanil with sevoflurane for multiple anaesthetic endpoints but was unable to estimate an Ce₅₀ value for alfentanil and BIS effect, possibly due to the low range of concentrations studied. [76] Similarly, Nieuwenhuijs *et al.* was unable to estimate an Ce₅₀ for remifentanil effect on BIS, [146] while Bouillon *et al.* reported a remifentanil Ce₅₀ estimate of 20.1 ng.ml⁻¹. [59]

Variability associated with the alfentanil Ce₅₀ estimate was high and the model was sensitive to initial parameter estimates. The stability of the model and its performance may be improved by using a different structural pharmacodynamic model to describe the propofol-opioid relationship for BIS. For example, remifentanil Ce₅₀ estimates much higher than the concentrations actually investigated have been reported for endpoints of return to consciousness and ablation of response to noxious stimuli when the Greco model was used. [69, 131] Mertens *et al.* handled this issue by reducing the Greco model to express the opioid Ce₅₀ as a ratio against the non-additive interaction parameter ($\alpha' = \alpha / Ce_{50,o}$). [69] Bouillon *et al.* proposed hierarchical processing of first opioid attenuation of noxious stimuli, and then attenuation of the remaining pain signal by an intravenous anaesthetic. [59] This model has since been reduced and two modifications for intravenous anaesthetic-opioid data proposed. [59, 130, 144, 216] However, these models assume a synergistic interaction. [59, 69, 216] They are therefore not appropriate for drug combinations that display additivity for the modelled endpoint, as seen here for propofol with opioids for BIS.

Residual variability was estimated at 7.7 units for BIS predictions. Reported estimates for residual variation in BIS response range from around 6.4 during propofol anaesthesia in adults without surgical stimulus, up to 14 in cardiac patients undergoing surgery. [244, 245] Some have found inclusion of a lag improves model performance for BIS, the hypothesis being that the processing time associated with signal smoothing and artefact removal is usually between 15 and 30 s. [200, 239, 240] A lag was not included in the current model and this is a possible limitation of this analysis, although VPCs suggest a good fit. BIS processing was set to 15 s and this delay is probably 'soaked up' by the t_{1/2} keo parameters. The keo estimate for propofol (keo 0.2 min⁻¹; t_{1/2}keo 3.47 min) was similar to that reported for propofol in adults when a lag of 10 s is included. [239, 240]

A three compartment model best fitted propofol concentrations, consistent with reports in the literature. The estimate for propofol elimination clearance (CL1) was within a reported range of 1.4-3.0 l.min⁻¹.70kg⁻¹, [47, 48, 54, 62, 63, 65, 68] and a similar trend was seen for inter-compartment clearance parameters. The central volume (V1) estimate was within the reported range of 4-22 l.70kg⁻¹ at 7.1 l.70kg⁻¹. [47, 48, 54, 55, 62, 65, 68] However parameter estimates were generally below those previously reported for adults using a three compartment model (Table 1.4, Section 1.4.3). For example, the estimated volume of the rapidly equilibrating peripheral compartment (V2) was 13.3 l.70kg⁻¹, while other estimates range from 20 to 44 l.70kg⁻¹. [47, 48, 54, 62, 63, 65, 68] Likewise, the slowly equilibrating peripheral compartment (V3) had a small volume (63.2 l.70kg⁻¹) compared to reports of 140-266 l.70kg⁻¹. [47, 48, 54, 62, 63, 65, 68]

These differences may stem from the study design, which aimed to determine the pharmacodynamic relationship between propofol and alfentanil. Sampling schedules were developed to allow assessment of pharmacodynamic endpoints across the range of clinically used doses. [202] Propofol is lipid soluble and V3 is often reported as large. Longer infusion durations and sampling windows following cessation of drug administration give more accurate estimates of peripheral compartment parameters by allowing better equilibration between compartments. [246] Here, practical and ethical considerations limited the study period over which the drugs were infused and samples were taken. Another limitation of the pharmacokinetic models developed here is that they assume administered drug is 'well stirred' throughout the central compartment at all times. This assumption might not hold true where drug concentrations are sampled shortly after onset of drug administration as was the case in this study.

There was little difference in fit between two and three compartment models for alfentanil pharmacokinetics and subsequently the simpler two compartment model was selected. Parameter estimates were similar to reported values. The central compartment volume (V1) estimate was 6.3 l.70kg⁻¹ and similar to reported estimates which range from 5.4-14.0 l.70kg⁻¹ for a two compartment model in adults. [74, 79-87] Peripheral compartment volume (V2) estimates range from 9.8-27.5 l.70kg⁻¹ with 15.8 l.70kg⁻¹ estimated in this dataset. [74, 79-87] Clearance (CL1) and inter-compartmental clearance (CL2) were estimated at 0.5 and 0.7 l.min⁻¹.70kg⁻¹ respectively, with reported estimates ranging from 0.2-0.4 l.min⁻¹.70kg⁻¹ for CL1, and 0.3-1.0 l.min⁻¹.70kg⁻¹ for CL2. [74, 79-87]

None of the covariates investigated improved fits for either propofol or alfentanil models despite reported effects of age and gender on opioid pharmacokinetics,[71, 73, 74] and effects of age on propofol pharmacokinetics.[48, 54, 65] However with only one male participant, and participant age and weight ranges encompassing just 27.0 years and 28 kg respectively, these data may be too homogenous for detection of covariate effects. A model derived from a small group of similar participants is unlikely to perform well in a more diverse patient population. A peak in the observed propofol concentrations (Figure 4.5) occurring around 10-15 min post infusion start was at the 95% prediction interval given by the model. Hypotension, causing a reduction in hepatic clearance through reduced hepatic blood flow (perfusion limited clearance), may be a potential reason for the poor fit at this time point. Propofol concentrations in the effect site compartment of 4-7.5 mcg.ml⁻¹ have been correlated to a 30-40% decrease in systolic blood pressure,[134] and the addition of alfentanil may augment this effect.[136] Propofol and alfentanil concentrations were investigated for covariate effects on propofol clearance however this did not improve the model further.

The relationship between BIS, blood pressure and propofol concentration is illustrated in Figure 4.9. The isoboles show the concentration pairs required to reach various BIS levels (i.e. BIS of 40, 50 and 60 units). Lysakowski *et al.* found that loss of consciousness occurred in 50% of patients at an estimated propofol effect site concentration of 2.34 mcg.ml⁻¹ when given alone *versus* 1.65 mcg.ml⁻¹ when given with 100 ng.ml⁻¹ of alfentanil (indicated on the plot).[247] These concentrations corresponded to BIS values of 60.5 and 74.6 units respectively (or BIS predictions of 66.7 and 73.7 units respectively with the current model). Propofol concentrations above 4.10 mcg.ml⁻¹, shaded in red in Figure 4.9, are associated with greater reductions in systolic blood pressure.[168] An estimated 17.4 mcg.ml⁻¹ of propofol is required to ablate response to intubation in 50% of patients when given alone, more than 3 times that indicated on Figure 4.9 for reductions in blood pressure.[170] This concentration can be reduced to 10.6 mcg.ml⁻¹ in the presence of 2 ng.ml⁻¹ of fentanyl, illustrating the advantages of combining propofol with phenyl-piperidine opioids when trying to achieve anaesthetic endpoints. The lower quarter of Figure 4.9 is the most applicable to clinical practice as the alfentanil concentrations depicted here stretch to the upper limits of the clinically used range.[43]

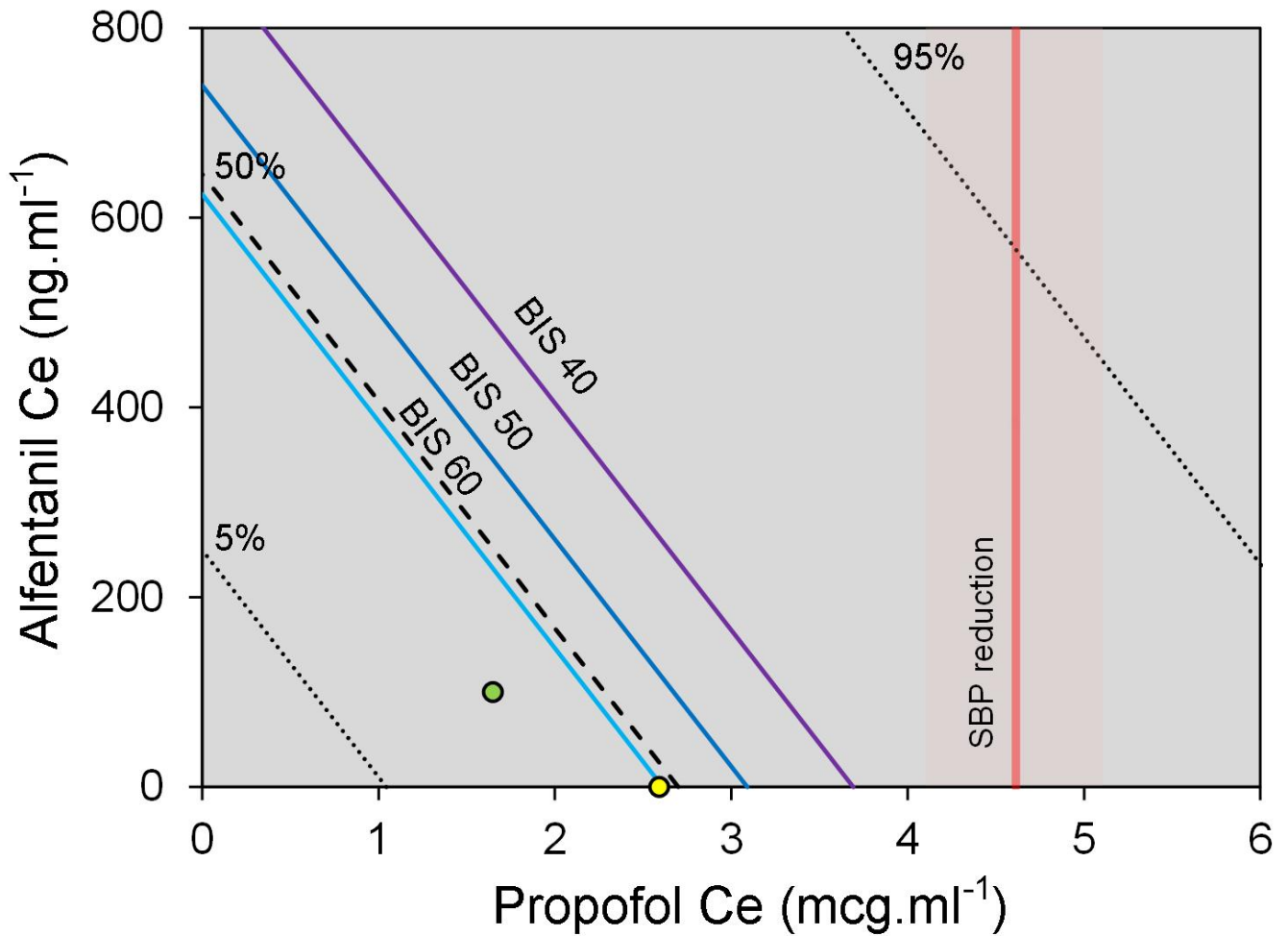


Figure 4.9

BIS, blood pressure and loss of consciousness. The figure shows the concentration pairs in the effect site (C_e) required to produce a BIS of 60 (light blue solid line), a BIS of 50 (dark blue solid line) and BIS of 40 (purple solid line) as predicted by the model. The 5%, 50% and 95% isoboles for BIS response are also given (broken black lines). The propofol concentration associated with a reduction in systolic blood pressure (SBP) from 120 mmHg to 100 mmHg is overlaid in red (as estimated by Katoh *et al.*, $4.61 \text{ SE} \pm 0.51 \text{ mcg.ml}^{-1}$). [168] The propofol C_{e50} required for loss of consciousness (LOC) when given alone, and with 100 ng.ml^{-1} of alfentanil, is given by the yellow and green circles respectively. [247] Note that the clinically used range of alfentanil is much lower than that depicted here (usually $< 200 \text{ ng.ml}^{-1}$).

Summary

I report a pharmacokinetic-linked response surface model of BIS for propofol and alfentanil in non-steady state conditions and confirm an additive relationship for EEG response suggested by other studies for this drug pair.[150, 231] In the subsequent chapter I investigate the idea of model generalisability using the model developed here and an existing dataset derived in volunteers receiving propofol-remifentanil anaesthesia.

Chapter 5. Generalisability of the propofol-opioid relationship for BIS

Background: An additive relationship between propofol and alfentanil for BIS was confirmed in the work I reported in chapter 4. Relationships between propofol and opioids of the phenyl-piperidine class (e.g. alfentanil, remifentanil) may be sufficiently similar that models can be extrapolated between drug pairs.

Methods: A dataset was available on the ANESTHESIOLOGY website (<http://journals.lww.com/anesthesiology>) from a study in which twenty adult volunteers were randomised to receive stepped infusions of either propofol or remifentanil, both alone and alongside a constant infusion of either remifentanil or propofol, respectively. The dataset included individual Bayesian predicted plasma and remifentanil concentrations, and observed BIS response, obtained during steady state conditions. These data (study 2) were pooled with individual Bayesian predicted effect site concentrations of alfentanil and propofol, and observed BIS response, obtained using the dataset and model reported in chapter 4 (study 1). Simulation was used to assess performance of the alfentanil-propofol model reported in chapter 4 when used to predict BIS response in the propofol-remifentanil and pooled opioid datasets. Model performance measures were: bias (median prediction error, MDPE); precision (median absolute prediction error, MDAPE); and wobble (median absolute PE-MDPE). Model parameters were refined in the pooled dataset.

Results: Model performance was similar when the original model was used to predict BIS response for study 1 (MDPE -1%, MDAPE 12%, wobble 12%), study 2 (MDPE -1%, MDAPE 8%, wobble 8%), and the pooled propofol-opioid dataset (MDPE -1%, MDAPE 11%, wobble 10%). Estimated parameters, obtained when the model was applied to the pooled dataset, were similar to those reported for propofol-alfentanil alone. The maximal effect (E_{MAX}) was 80 units (90%CI 74.6-86.8 units) with a slope of 2.6 (90%CI 2.2-2.7). The effect site concentrations associated with 50% of E_{MAX} (Ce_{50}) were alfentanil 606 ng. Γ^1 (90%CI 552.0-887.5 ng. Γ^1) and propofol 2.7 mg. Γ^1 (90%CI 2.2-2.7 mcg. Γ^1). The relative potency of remifentanil to alfentanil is 1:33 for this endpoint.

Conclusions: A model describing the propofol-alfentanil relationship for BIS may be extrapolated to describe that of propofol-remifentanil.

5.1. Introduction

Additivity between propofol with remifentanyl for BIS response has been reported using response surface methods.[59, 146] I confirmed that a similar relationship exists between propofol and alfentanil in chapter 4. The feasibility of extrapolating a model describing remifentanyl-sevoflurane effects to other drugs within the phenyl-piperidine opioid and inhalational anaesthetic drug classes has already been demonstrated using dose equivalents and an endpoint of return to consciousness.[132] Here, I investigate whether a model describing propofol-alfentanil effects on BIS response may be extrapolated between opioid pairs of the phenyl-piperidine class in a similar manner. This will provide a foundation for a generalised model of BIS response for use in simulation or clinical environments.

The aims of the work presented in this chapter were therefore to:

1. test the hypothesis that a pharmacodynamic model describing the propofol-alfentanil relationship for BIS response can be extrapolated to describe that of propofol-remifentanyl for BIS response,
2. identify a ratio of relative potency to convert alfentanil effect site concentrations to remifentanyl equivalents using the model developed in chapter 4.

5.2. Methods

A dataset of BIS response following propofol-remifentanyl infusion was identified. Bouillon *et al.* studied healthy volunteers using ramped infusions based on the criss-cross design proposed by Short *et al.*[59, 202] Arterial samples and effect measurements were taken at intervals following dose adjustments designed to ensure equilibration of drug between plasma and effect site compartments.[59] Bayesian predicted propofol and remifentanyl plasma concentrations were estimated using pharmacokinetic models developed in their dataset.[63] Bouillon *et al.* selected Minto's model to describe the relationship between these concentrations and observed BIS response. Predicted concentrations and response data from this study were available on the ANESTHESIOLOGY website (<http://journals.lww.com/anesthesiology>).[248]

Estimated alfentanil and propofol effect site concentrations were calculated using the final model and dataset described in chapter 4. These concentrations were pooled with individual Bayesian predictions of propofol and remifentanil plasma concentrations at steady state from Bouillon *et al.*[59] Plasma concentrations taken at steady state were assumed to be proxies for effect site concentrations. Units of each opioid (calculated by normalising drug by its Ce_{50}) were summed and modelled as a single opioid alongside normalised propofol effect site concentrations. An Ce_{50} of 20.1 ng.ml⁻¹ (fixed) was used to normalise remifentanil concentrations, according to estimates provided by Bouillon *et al.* for their dataset.[59]

5.2.1.1. Simulation

BIS response at each time point was predicted from concentration data using the model parameters reported in chapter 4 and NONMEM's simulation mode (NONMEM 7.1, Globomax LLC, Hanover, MD, USA). Model performance measures as described by Varvel *et al.* were used to assess how well the model predicted the observed BIS.[249]

Performance error (PE) was calculated at each time point using weighted residuals, i.e.

$$PE(\%) = \frac{Y - \hat{Y}}{\hat{Y}} \cdot 100$$

Equation 5.1

where Y is the measured BIS value and \hat{Y} is the model predicted BIS.[73, 202, 249] For each individual i the median PE (MDPE) was calculated as a measure of bias, i.e.

$$MDPE_i = \text{Median} \{PE_{ij}, j = 1, \dots, N_i\}$$

Equation 5.2

The median absolute PE (MDAPE) was used as a measure of model prediction precision, i.e.

$$\text{MDAPE}_i = \text{Median} \{ |PE_{ij}|, j = 1, \dots, N_i \}$$

Equation 5.3

Wobble, which measures within-individual variation in PE, was calculated as:

$$\text{Wobble}_i = \text{Median} \{ |PE_{ij} - \text{MDPE}_{ij}|, j = 1, \dots, N_i \}$$

Equation 5.4

These measures of model performance were used to assess whether the pharmacodynamic model describing the propofol-alfentanil relationship for BIS response can be extrapolated to describe that of propofol-remifentanil for BIS response. The propofol-alfentanil model was then refined using the pooled opioid dataset in a further step in which population parameter and variances were estimated.

5.2.1.2. Population parameter estimates

Data were analysed using nonlinear mixed effects models (NONMEM 7.1, Globomax LLC, Hanover, MD, USA). Population parameters and variances were estimated using the first order conditional estimation method with interaction option. Between-subject variability was described using proportional error models. Additive error models were tested to describe residual unknown error. Variability associated with this term ($\eta_{RUV,i}$) was also estimated for each study individually. Model selection required a statistically significant improvement in the NONMEM OBJ between nested models, equating to a reduction > 6.64 (for one additional parameter) based on a Chi square distribution ($\alpha < 0.01$). A user-defined PRED routine was used and equations were integrated within ADVAN=11. Convergence criterion was three significant digits.

5.3. Results

Measures of model performance for the propofol-alfentanil model when used to simulate BIS response for the propofol-remifentanil dataset are given in Table 5.1. Measures were similar between each of the datasets. Model predicted *versus* observed plots are given for each individual in Figure 5.2. Pooling of the two datasets and re-estimation of parameters resulted in an OBJ of 3256.3. Estimates for parameters, associated variances and confidence intervals are given for the pooled dataset model in Table 5.2 alongside those reported in chapter 4 for ease of comparison. The estimated relative potency for remifentanil: alfentanil, assuming Ce_{50} values of remifentanil 20.1 ng.ml⁻¹ and alfentanil 606 ng.ml⁻¹ (as given in chapter 4), is 1: 30. Re-estimation of parameters in the pooled dataset gives a relative potency of 1: 33 by the same method.

Measures of model performance	MDPE (%)	MDAPE (%)	Wobble (%)
Study 1	-1 (-27:48)	12 (1:59)	12 (1:59)
Study 2	-1 (-32:18)	8 (0:37)	8 (0:38)
Pooled (all data)	-1 (-28:41)	11 (1:52)	10 (0:51)

Table 5.1

Measures of model performance: model bias, given as the median prediction error (MDPE); model precision, given as the median absolute prediction error (MDAPE); and model wobble, given as the PE - MADPE. Values are median percentage bias (10th:90th percentile).

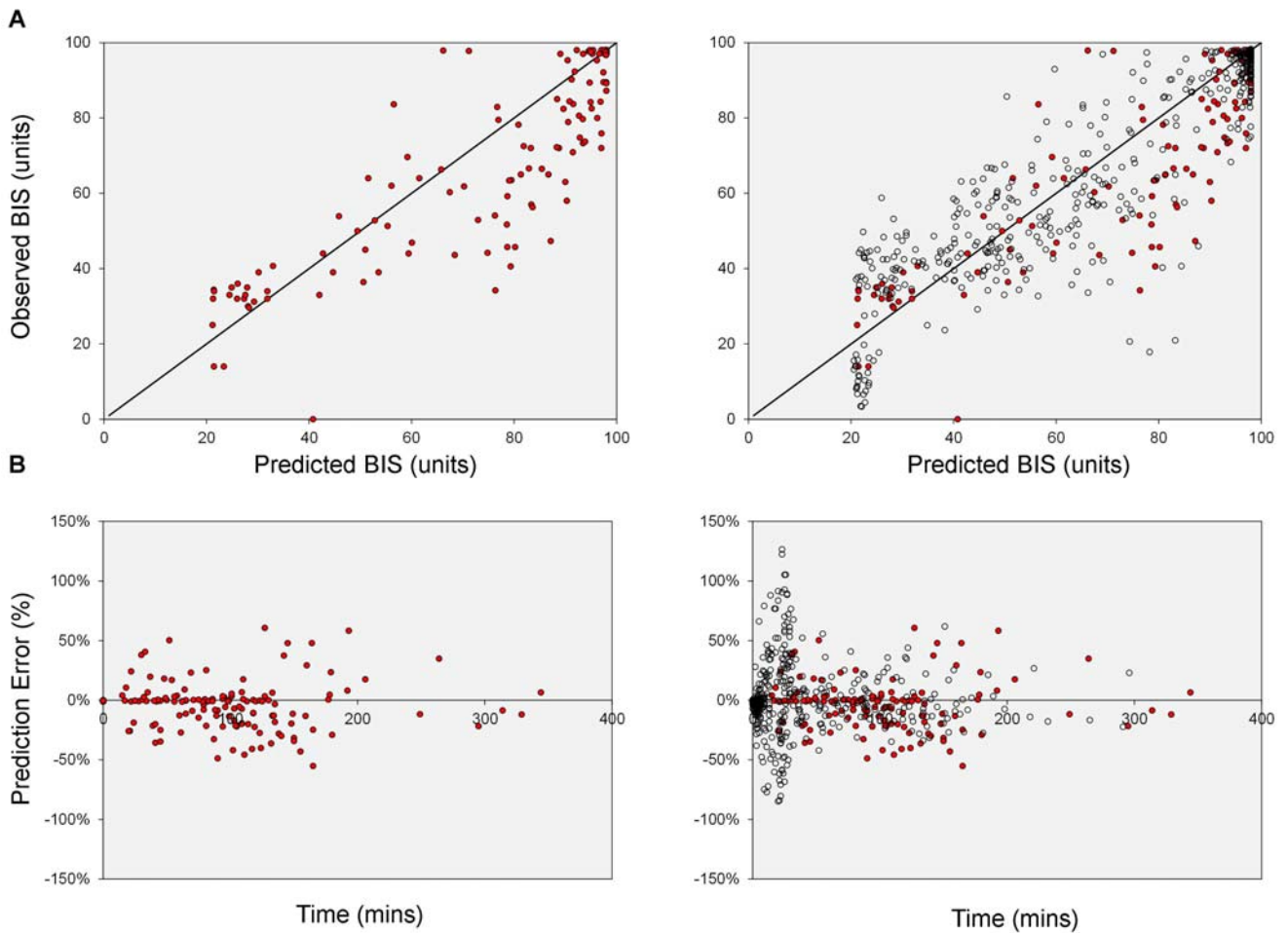


Figure 5.1

Quality of fit of the pharmacodynamic model developed for propofol-alfentanil anaesthesia (chapter 4) when used to predict BIS response for propofol with remifentanil. The quality of fit in study 2 only (propofol-remifentanil data, red circles)[59] can be seen in the left panels. These are overlaid by the residuals for the model when used to predict response in the alfentanil-propofol dataset (chapter 4, open circles) in the right panels. (A) Population predictions for BIS are plotted against observed BIS values. Units are BIS units (0-100, where 100 is resting and awake, and < 60 is recommended for surgical stimuli). (B) Prediction error (PE, %) is plotted against time. Some under-prediction can be seen in panel A reflecting the negative bias reported in Table 5.1.

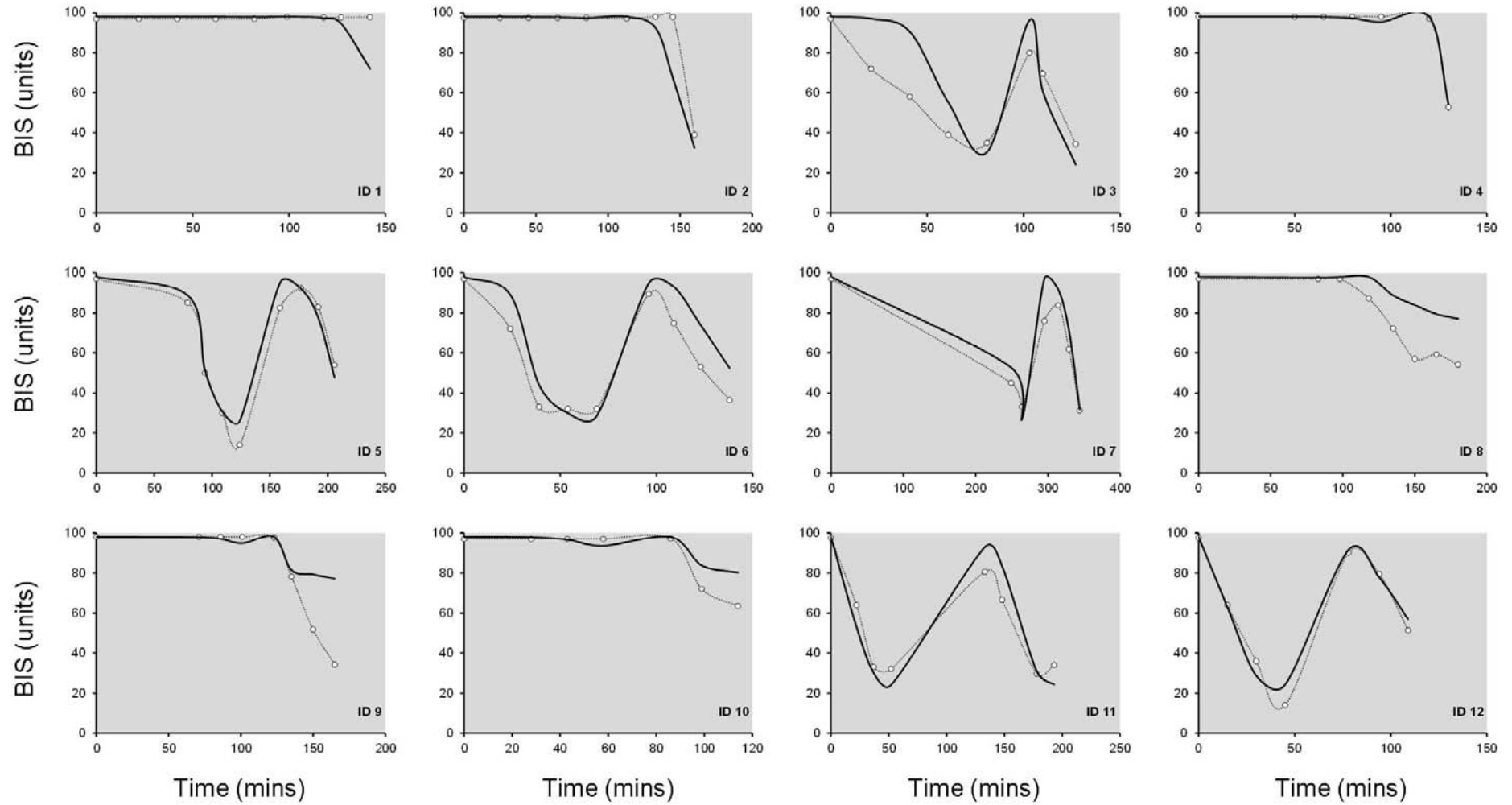


Figure 5.2

Simulated *versus* observed BIS response following propofol-remifentanyl anaesthesia, using model parameters developed for propofol-alfentanil anaesthesia (chapter 4). Solid lines are predictions, open circles are observations. BIS units are 0-100 (where 100 is resting and awake, and < 60 is recommended for surgical stimuli).

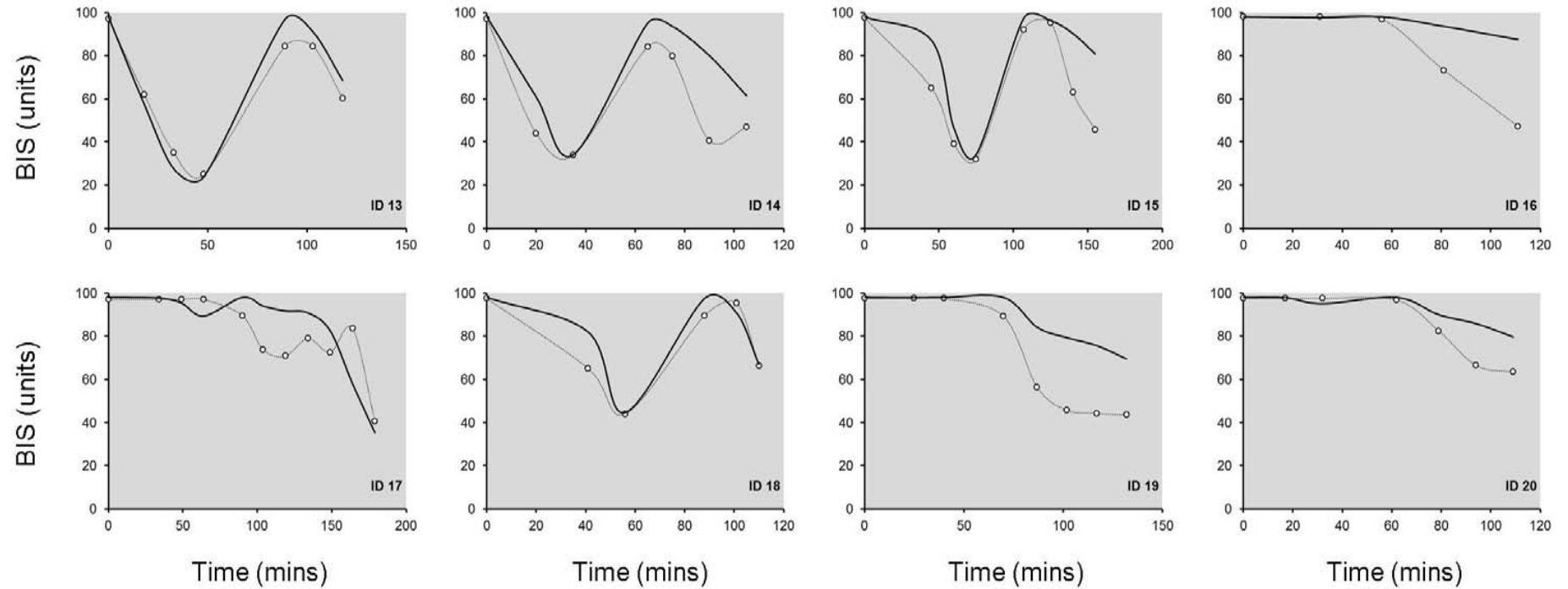


Figure 5.2 continued

Simulated *versus* observed BIS response following propofol-remifentanyl anaesthesia, using model parameters developed for propofol-alfentanil anaesthesia (chapter 4). Solid lines are predictions, open circles are observations. BIS units are 0-100 (where 100 is resting and awake, and < 60 is recommended for surgical stimuli).

Parameter	Propofol-alfentanil model (chapter 4)		Propofol-opioid model (current analysis)		
	Estimate	%CV	Estimate	90% CI	%CV
E ₀	98.1 FIX	0 FIX	98.0 FIX	-	0 FIX
Beta (β)	0 FIX	-	0 FIX	-0.78-0.53	-
Ce _{50,Propofol} (ng.ml ⁻¹)	2710.0	27.1	2440.0	2.2-2.7	19.4
Ce _{50,Alfentanil} (ng.ml ⁻¹)	646.0	62.2	672.0	552.0-887.5	47.6
Ce _{50,Remifentanil} (ng.ml ⁻¹)	-	-	20.1 FIX	-	42.4
Slope (γ)	3.1	52.5	2.6	2.2-3.3	52.2
E _{MAX}	79.4	108.6	80.2	74.6-86.8	84.0
Err _{add}	7.72	$\eta_{RUV,i}$ 0.21	8.0		$\eta_{RUV,i}$ 0.21 study1 $\eta_{RUV,i}$ 0.16 study 2

Table 5.2

Pharmacodynamic parameter estimates for pooled propofol-opioid dataset: CV is the coefficient of variability; CI is the confidence interval; Err_{add} is the residual variability estimated for BIS measurements using an additive error model; and Ce_{50,x} is the effect site concentration of drug that causes 50% maximal drug effect. Parameter and variance estimates reported in chapter 4 for the propofol-alfentanil model are given for ease of comparison.

5.4. Discussion

Relationships between propofol and phenyl-piperidine opioids may be sufficiently similar that models can be extrapolated between drug pairs of this class. An additive relationship between propofol, alfentanil and BIS has now been confirmed (chapter 4). The model reported for propofol-alfentanil was extrapolated to describe response for an existing dataset of propofol-remifentanil anaesthesia in the current simulation study. Measures of model performance were similar for the tested datasets (propofol/alfentanil-chapter 4, propofol/remifentanil and the pooled dataset Table 5.1).[59] and refinement of parameters in the pooled dataset resulted in similar estimates to those reported for propofol with alfentanil. The feasibility of extrapolating pharmacodynamic response surface models between alfentanil and remifentanil has been demonstrated previously for an endpoint of return of responsiveness,[132] and this is confirmed in the current work for an endpoint of BIS response.

Performance has been considered acceptable if MDPE (bias) was between -20% and 20% and if MDAPE (precision) was less than 30% in other reports investigating pharmacokinetic models.[250-252] Measures of model performance were similar between datasets, and are also comparable to those reported in the literature for tested pharmacodynamic models. For example, Minto *et al.* reported a MDAPE of 15.3% (expressed as a percentage of the pharmacodynamic range) for their model describing remifentanil pharmacodynamics for spectral edge frequency.[73] BIS predictions for propofol (using the model reported by Schneider *et al.*)[55] are associated with a MDPE of 2.2% and MDAPE of 14.2% in adults, while in children these values are -1.7% and 21.0%.[200] Estimates of pharmacodynamic model performance are dependent on the underlying pharmacokinetic model (and k_{eo} value) used to predict plasma and effect site concentrations. For example, Rigouzzo *et al.* reported MDPE estimates ranging from -1.57% to 1.91%, and MDAPE estimates ranging from 21.0% to 22.0% for BIS response in children, when different pharmacokinetic parameter sets were used to predict plasma concentrations of propofol.[200]

The model showed negative bias in both datasets meaning that BIS observations were under-predicted (MDPE= -1%). The E_{MAX} parameter was the predominant cause for this in study 1 as, at a maximum reduction in BIS of 80 units, observations nearing zero were not well captured (visible in Figure 5.1). A small increase in the E_{MAX} parameter was seen when model parameters were re-estimated in the pooled dataset (80.2 CV 84%). The slope parameter estimated for propofol with alfentanil was larger

than that estimated by Bouillon *et al.* for propofol with remifentanyl (3.1, CV 52.5% versus 1.4, CV 26.8%).[59] Re-estimation of parameters in the pooled dataset resulted in a slope of 2.6 (CV 52.2%) but this was sensitive to changes in the other model parameters. Estimating separate slope parameters for each opioid reduced the objective function, nearing statistical significance (Δ OBJ -3.641, $P=0.056$). A reduction in OBJ of <4 points represents a small improvement in model fit and the addition of a second slope parameter was rejected in accordance with the *a priori* criteria for model building.

The relative potency for remifentanyl: alfentanil, based on Ce_{50} values of remifentanyl 20.1 ng.ml⁻¹ (literature estimate) and alfentanil 606 ng.ml⁻¹ (from chapter 4), is 1: 30. Pooling of the two datasets resulted in an estimated relative remifentanyl: alfentanil potency of 1:33. Of course, apparent potencies are dependent on a number of factors, such as the underlying pharmacokinetic models used to predict plasma and effect site concentrations, or how the endpoint is measured.[243] The remifentanyl Ce_{50} reported by Bouillon *et al.* for their dataset (20.1 ng.ml⁻¹),[59] and supported by other estimates in the literature for EEG measures,[75] was assumed to be correct for study 2 and therefore was fixed. The conversion factor proposed here may not be appropriate outside of these datasets although others have reported similar potency ratios. Egan *et al.* estimated Ce_{50} parameters of 20 ng.ml⁻¹ and 376 ng.ml⁻¹ for the effects of remifentanyl and alfentanil respectively on EEG measures when given as infusions.[75] This equates to a ratio of 1:30 when partitioning of alfentanil from whole blood to plasma is considered.[75] Mertens *et al.* estimated a relative potency of 1:31 for remifentanyl: alfentanil for ablation of response to surgical stimuli in the lower abdomen when data from two separate studies of similar methodology were pooled.[69] Similarly, Glass *et al.* estimated a relative potency of 1.2:30:1 for fentanyl: alfentanil: remifentanyl (correcting for co-administration of thiopental) for a 50% reduction in MAC of isoflurane.[253, 254] Estimates of relative potency for these opioids and various endpoints are summarised in Table 5.3.

There are some limitations to the work presented here. The data were pooled from two separate studies and consequently the populations studied are different, and this almost certainly impacts model prediction performance between studies. BIS data from the study reported in chapter 4 were collected during both a preoperative phase and surgery, while data from Bouillon *et al.* were collected from healthy volunteers in controlled conditions.[59] Variability ($\eta_{RUV,i}$) associated with the residual variability term was included in this analysis to reflect differences in data collection between the two

studies, although similar estimates were obtained for these (21% CV for study 1 and 16% CV for study 2). Predicted plasma concentrations taken at steady state were assumed to be proxies for those in the effect site for study 2. OBJ values obtained for the propofol-alfentanil dataset could not be compared directly with that of the pooled dataset as calculation of this value is dependent on the number of observations. However, the model reported in chapter 4 for propofol and alfentanil showed similar performance when applied directly to the propofol-remifentanil dataset. This, when taken alongside the similarity of parameter estimates of the propofol-alfentanil model with those published for propofol-remifentanil and those obtained during the estimation step for the pooled dataset, supports the idea that a pharmacodynamic model describing BIS response can be extrapolated between these phenyl-piperidine opioids.

	Endpoint	Relative potency
Egan <i>et al.</i> 1996 [75]	EEG	Remifentanil: alfentanil 1:30
Shafer <i>et al.</i> 1991 [72]		Alfentanil: fentanyl 70: 1
This study		Remifentanil: alfentanil 1:33
Glass <i>et al.</i> 1997 [253]	Reduction in MAC of isoflurane	Remifentanil: alfentanil: fentanyl 1: 30: 1.2
Lang <i>et al.</i> 1996 [169]		Remifentanil: alfentanil: fentanyl 1: 70: 1.2
Westmoreland <i>et al.</i> 1994 [167]		Alfentanil: fentanyl 58: 1
Mertens <i>et al.</i> 2003 [69]	Ablation of response to surgical stimuli	Remifentanil: alfentanil 1:31

Table 5.3

Estimates of relative potency for the phenyl-piperidine opioids remifentanil and alfentanil. EEG=electroencephalogram.

Summary

This study suggests that a model for propofol-alfentanil BIS response may be extrapolated to describe response for propofol in combination with other opioids of the phenyl-piperidine class. A relative potency of remifentanil: alfentanil of around 1:33 is estimated for extrapolation of models between these opioids from the populations included in this analysis. Measures of model performance reported in this analysis were good, probably due to the carefully controlled conditions in which both studies were conducted. This may not reflect model performance when tested prospectively during anaesthesia, or in a more diverse patient group. I investigate further the idea of model extrapolation between these opioids for a much wider patient population group undergoing surgery at Auckland City Hospital in the next chapter.

Chapter 6. Predictive performance of a response surface model for target controlled infusion during surgery

Background: Propofol with remifentanyl is commonly used for total intravenous anaesthesia (TCI). The performance of a pharmacokinetic-linked response surface model for TCI has not been tested.

Methods: This was a prospective study of model performance in adult patients undergoing surgery. Target-controlled infusions of propofol and remifentanyl were given using standard pharmacokinetic models linked to a response surface model. The targeted response was BIS. Model performance measures were bias (median performance error, MDPE), precision (median absolute performance error, MDAPE) and wobble (median PE-MDPE).

Results: Data from 45 patients, who had a mean (range) age of 48 (19-73) years, weight of 80 (45-169) kg and height of 166 (148-193) cm, were analysed. The model had MDPE 7% and MDAPE 21% across all time points, MDPE 14% and MDAPE 28% during the early phase and MDPE 5% and MDAPE 22% during maintenance. A retrospective analysis of the performance of Schnider's propofol and Minto's remifentanyl pharmacokinetic models teamed with the model reported in chapter 4 gave the lowest bias for all time points (MDPE 4%), but this was probably because of over-prediction during the early phase (0-20 min, MDPE 18%) and under-prediction during recovery (MDPE -7%). The pharmacokinetic model developed in chapter 4 of this thesis performed poorly in participants with $BMI \geq 35 \text{ kg.m}^{-2}$, although the propofol keo parameter (0.2 min^{-1} , $t_{1/2\text{keo}} 3.4 \text{ min}$) did improve model predictions during induction.

Conclusions: Response surface models, when linked to appropriate pharmacokinetic models, predict BIS response within limits regarded as clinically acceptable for current pharmacokinetic TCI systems. Further research is required to improve model performance in participants aged ≥ 60 y, and with a $BMI \geq 35 \text{ kg.m}^{-2}$. Use of a longer $t_{1/2\text{keo}}$ (3.4 min as opposed to 1.5 min as is commonly recommended) may better describe the onset of propofol effects as measured using BIS in this setting.

6.1. Introduction

I presented a response surface model for propofol with alfentanil and BIS in the previous chapters, and established a relative potency for application of that model to propofol-remifentanil data. Performance error was similar when a model describing the propofol-alfentanil relationship for BIS was used to describe that of propofol-remifentanil in these individuals, suggesting that models can be extrapolated between these drug pairs. However the data used were derived from carefully designed studies in controlled situations,[59] and performance might not be similar when used to predict response in less controlled conditions. A diverse patient population (for which influential covariates are unknown or poorly described), and factors such as a changing level of noxious stimulus during surgery, co-administration of other drugs, and pathology, may all impact model performance.

Propofol in combination with remifentanil is commonly used for total intravenous anaesthesia (TIVA) at Auckland City Hospital.[36] Automated pumps programmed with population-based pharmacokinetic models are used to infuse drugs to a targeted plasma or effect site concentration, a method called ‘Target Controlled Infusion’ (TCI). I describe in this chapter a prospective observational study of response surface model based TCI for TIVA. I also retrospectively assess my model for propofol-opioid BIS response in this dataset.

The aims of this study were therefore to;

1. prospectively test the bias and accuracy of a pharmacokinetic-linked response surface model when used to drive BIS targeted controlled infusion of propofol with remifentanil,
2. test the propofol-opioid response surface model developed in the previous chapters in a wider patient population receiving propofol and remifentanil during general surgery.

This is the first study, to my knowledge, of using pharmacokinetic models linked to response surface models to drive concomitant drug infusions.

6.2. Methods

This study received ethics committee approval by the Upper South B committee prior to commencing the study (URB/11/06/014, see Appendix 5), and was registered with the Australian and New Zealand Trials Registry (Ref: ACTRN12611000428965). A copy of the Ethics approval for this study is given in Appendix 5. The study was explained to potential participants and written informed consent was given by each participant before enrolment into the study.

6.2.1 Participants

Adult patients, aged 18-80 years with an American Society of Anesthesiologists physical status (ASA) of 1-2 and who were scheduled for surgery at Auckland City Hospital, were eligible to be studied. Only those patients for whom a total intravenous anaesthesia (TIVA) with neuromuscular blockade was planned were approached. Patients who: had an allergy or contraindication to the study drugs; had a history of chronic opioid consumption; used psychoactive medication (including high alcohol intake); had neurological dysfunction; or who required premedication before surgery were excluded.

I aimed to study 50 patients. Studies that assess pharmacokinetic model performance typically study between 20 and 50 individuals. The ‘Marsh’ model describing propofol pharmacokinetics (and now available in commercial TCI pumps) was prospectively tested in 20 children; model parameters were then refined before performance was again assessed in a further 10 children.[46] Varvel *et al.* demonstrated their methods for assessing model performance in 51 adults undergoing surgery.[249] Syroid *et al.* compared response surface model predictions for time to anaesthetic emergence, and probability of response to painful stimuli, with observations in 25 patients undergoing surgery. A sample size between 25 and 50 should therefore be sufficient for the current study. This was a sample of convenience as the presence of an anaesthetist appropriately familiarised with the protocol and study software was required for all participants.

6.2.2 Anaesthesia and study drugs

Participants received propofol and remifentanyl as a target controlled infusion (TCI). Propofol was given as a 10 mg.ml⁻¹ solution and remifentanyl was given as a 50 ng.ml⁻¹ solution. Anaesthetists were asked to refrain from administering other opioids, intravenous anaesthetics and volatiles, and from

giving adjuvants to anaesthetic agents (particularly those with actions at GABA_A or NMDA receptors or known to affect BIS response such as midazolam, ketamine, clonidine and dexmedetomidine). Analgesics for postoperative pain were administered on emergence from the anaesthetic (defined for this purpose as a BIS response > 90).

Study drugs were infused using Graseby 3400 syringe pumps connected to a dedicated laptop computer by the RS232C serial ports. The computer controlled pump rates using a program written by YH Tam (Department of Anaesthesia, Prince of Wales Hospital, The Chinese University of Hong Kong, Shatin, Hong Kong, China).[232] The program delivers drug using response surface model parameters linked to published pharmacokinetic parameters with effect site compartments. Pharmacokinetic models were that described by Minto *et al.* for remifentanyl,[73, 255] and that described by Schnider *et al.* for propofol.[54, 55] The pharmacodynamic model was that described by Bouillon *et al.* for propofol with remifentanyl and BIS.[59] The software allows the user to select both a target effect level and the ratio of propofol to remifentanyl. Drug ratios and target effect (BIS response) were selected and adjusted by anaesthetists throughout each anaesthetic according to their patient needs. Infusion rates and volumes, and predicted concentrations for all model compartments, were generated at 5 s epochs by the software.

6.2.3 Effect measurements

The site of electrodes was cleaned with alcohol prior to applying the BIS sensor. BIS response was recorded electronically at 30 second epochs throughout the study period using a BISTM Monitoring System (Aspect Medical Systems, Massachusetts, USA) with BISTM Quatro sensor. BIS data were extracted from the data file generated by the integrated drug administration system (IDAS) SaferSLEEP (Safer Sleep LLC, Nashville, TN), which automatically compiles drug administration data with monitored physiological data. Baseline BIS data were collected prior to beginning study drug infusions and during recovery until patients had opened their eyes in response to verbal command.

6.2.4 Data analysis

Pump generated and observed BIS data were reduced to one minute epochs. Only BIS values associated with a Signal Quality Index (SQI) ≥ 50 were used in the analysis.

6.2.4.1. Model performance measures

Model performance measures as described by Varvel *et al.* were used to assess how well the model predicted the observed BIS.[249] Performance error (PE) was calculated at each time point using weighted residuals i.e.

$$PE(\%) = \frac{Y - \hat{Y}}{\hat{Y}} \cdot 100$$

Equation 6.1

where Y is the measured BIS value and \hat{Y} is the model predicted BIS.[73, 202, 249] The median PE (MDPE) was calculated as a measure of bias for each individual i , i.e.

$$MDPE_i = \text{Median} \{PE_{ij}, j = 1, \dots, N_i\}$$

Equation 6.2

The median absolute PE (MDAPE) was used as a measure of model precision:

$$MDAPE_i = \text{Median} \{|PE_{ij}|, j = 1, \dots, N_i\}$$

Equation 6.3

Wobble, which measures within-individual variation in PE, was calculated as:

$$\text{Wobble}_i = \text{Median} \{|PE_{ij} - MDPE_i|, j = 1, \dots, N_i\}$$

Equation 6.4

Lower values of MDPE, MDAPE and wobble indicate better model performance. The above measures were calculated for the entire group across all time points, and also for defined time intervals to facilitate assessment of model performance during different stages of anaesthesia. These intervals were defined as: an ‘early phase’ (1-20 min from infusion start); a ‘maintenance phase’ (20 min from infusion start to the end of the infusion); and a ‘recovery phase’ (from the end of the propofol infusion until eye opening in response to verbal command). Commercial pharmacokinetic TCI models are considered to be within acceptable model performance limits if $MDPE < \pm 20\%$ and $MDAPE < \pm 30\%$ across all time points.[250-252] A similar definition of clinically acceptable performance has yet to be established for pharmacodynamic models.

6.2.4.2. Retrospective model performance

A further three pharmacokinetic-pharmacodynamic parameter sets (or ‘combinations’) were retrospectively tested in addition to the parameter set combination prospectively tested. Plasma and effect site concentrations at each time point were predicted from dosing and covariate data. Predictions were made in Excel 2010 and using PK–PD Tools for Excel© 2009, Version 1.31 (www.pkpdtools.com),[256] a suite of functions developed by Charles Minto and Thomas Schnider.

Combination 2 was that reported for the propofol-alfentanil dataset in chapter 4. The ‘Schnider model’ was used to describe propofol pharmacokinetics,[54, 55] and the ‘Minto model’ was used for remifentanil pharmacokinetics.[73, 255] The pharmacokinetic models for combination 2 were selected because of their wide availability in commercial TCI software, because their predictive performance in various populations has previously been studied,[49, 250, 257] and to enable comparison of performance with the prospectively tested model. Effect site concentrations of remifentanil were converted directly to alfentanil equivalents using a potency ratio of remifentanil: alfentanil 1:33 as was established in chapter 5. Effect predictions were made from the normalised units of alfentanil equivalents and propofol concentrations using the parameter set already reported (chapter 4).

Pharmacokinetic models developed with response surface models were used for combinations 3 and 4. Bouillon *et al.* reported both propofol and remifentanil pharmacokinetics (combination 3).[63] The study by Bouillon *et al.* was conducted during pseudo steady state conditions and keo values were not

reported.[59, 63] The keo parameter describes the rate of drug transfer out of the effect compartment^{iv} and so its value is dependent on the time course of drug in the plasma as predicted by the pharmacokinetic model.[51] Estimation of keo is usually made from a simultaneous (integrated) pharmacokinetic-pharmacodynamic analysis. An alternative method of linking independently derived pharmacokinetic and pharmacodynamic parameters is to use the Time-to-Peak-Effect (TTPE) method as described by Minto *et al.*[51] Using TTPE improves model predictions by adjusting keo values according to a model independent parameter (the time to peak effect, or ‘Tpeak’) and the underlying pharmacokinetic parameters sets. A Tpeak of 1.6 min has been reported for BIS pharmacodynamics following propofol.[51, 52, 55] Therefore the keo value was estimated for the propofol pharmacokinetic parameter set reported by Bouillon *et al.* using a Tpeak of 1.6 min.[51, 52, 55] A Tpeak of 1.4 min, as estimated by Minto *et al.*,[73] was used to calculate the keo for remifentanyl. The propofol model (and corresponding keo estimate) given in chapter 4 of this thesis was used for combination 4. Parameter sets are summarised in Table 6.1.

6.3. Results

Data were collected at Auckland City Hospital between February 2011 and January 2013. A total of 50 patients participated in the study. Five participants were excluded: four received premedication with midazolam (two of whom also received opioid doses additional to the study drugs); and data were unavailable for one participant because of a computer failure. There were 28 female and 17 male participants (total n= 45) included in the final analysis. Participants had a mean (range) age of 48 (19-73) years, weight of 80 (45-169) kg and the height of 166 (148-193) cm. Three participants initially scheduled to receive a TIVA with neuromuscular blockade did not receive neuromuscular blockade during their anaesthetic.

6.3.1 Prospectively tested model

The model tested prospectively had a MDPE of 7%, MDAPE 21% and wobble of 12% across all time points. Model performance was best during the maintenance and recovery phases of anaesthesia, although percentiles for each measure of model performance were wide. Measures of model performance for each phase of anaesthesia, and for the total study time, are summarised in Table 6.2.

^{iv} This rate is assumed to equal that of drug moving between plasma and effect site compartments at steady state.

Six participants had a body mass index (BMI) equal to, or greater than, 35 kg.m^{-2} . Two of these participants had a BMI exceeding 40 kg.m^{-2} . Participants were subsequently split according to BMI ($\text{BMI} < 35 \text{ kg.m}^{-2}$ *versus* $\text{BMI} \geq 35 \text{ kg.m}^{-2}$) and data re-analysed for all time points to give an idea of performance in this subgroup. Positive bias was observed in the $\text{BMI} \geq 35 \text{ kg.m}^{-2}$ group (Table 6.3). Twelve participants were aged between 60 and 73 years old. Propofol effects are known to vary with age, with propofol requirements for various anaesthetic endpoints generally reduced as age increases. The prospectively tested pharmacodynamic parameter set did not include age as a covariate effect. Participants were subsequently split according to age ($\text{age} < 60 \text{ y}$ *versus* $\text{age} \geq 60 \text{ y}$) and data re-analysed for all time points (Table 6.3). Plots of performance error for the entire group are given in Figure 6.1 and Figure 6.2, while predictions overlaid with observations are given for each individual in Figure 6.3.

Parameter combination	Propofol PK	Model link (keo)	Remifentanil PK	Model link (keo)	PD response surface
Prospectively tested:					
1	Schnider <i>et al.</i> [54]	0.46 min ⁻¹ keo (t _{1/2} keo 1.50 min)[55]	Minto <i>et al.</i> [73]	0.63* min ⁻¹ keo (t _{1/2} keo 1.10 min)[73]	Bouillon <i>et al.</i> [59]
Retrospectively tested:					
2	Schnider <i>et al.</i> [54]	0.46 min ⁻¹ keo (t _{1/2} keo 1.50 min)[55]	Minto <i>et al.</i> [73]	0.63* min ⁻¹ keo (t _{1/2} keo 1.10 min)[73]	Chapter 4
3	Bouillon <i>et al.</i> [63]	0.14 min ⁻¹ keo (t _{1/2} keo 4.90 min), from 1.60 min Tpeak [55]	Bouillon <i>et al.</i> [63]	1.40 min ⁻¹ keo (t _{1/2} keo 0.50 min), from 1.40 min Tpeak [73]	Bouillon <i>et al.</i> [59]
4	Chapter 4	0.2 min ⁻¹ keo (t _{1/2} keo 3.50 min) chapter 4	Minto <i>et al.</i> [73]	0.63* min ⁻¹ keo (t _{1/2} keo 1.10 min)[73]	Chapter 4

Table 6.1

Tested parameter set combinations. Combination 1 was implemented in the TCI software and tested prospectively, while models 2-4 were assessed retrospectively. *Keo value is adjusted for age, i.e. $0.595 - 0.007 \cdot (\text{AGE} - 40)$. [73] PK is pharmacokinetics, PD is pharmacodynamics. Keo values for combination 3 were calculated in PK-PD Tools for Excel© 2009 using the TTPE method and Tpeak estimates reported in the literature. [55, 73] Predicted effect site concentrations of remifentanil were converted to alfentanil equivalents for combinations 2 and 4 using a potency ratio of remifentanil: alfentanil of 1:33 (as estimated in chapter 5).

Phase of anaesthesia	MDPE (%)	MDAPE (%)	Wobble (%)
Early	14 (-30: 110)	28 (5: 110)	25 (4: 98)
Maintenance	5 (-31: 58)	22 (4: 58)	11 (2: 40)
Recovery	6 (-30: 50)	25 (4: 51)	12 (2: 40)
All time points	7 (-19: 37)	21 (13: 40)	12 (8: 23)

Table 6.2

Measures of model performance for the prospectively tested model for each stage of anaesthesia. Measures are: median bias, given as the median performance error (MDPE); median precision, given as the median absolute performance error (MDAPE); and median wobble, given as the PE-MDPE. Values are median percentage bias (10th-90th percentile). The prospectively tested model was standard pharmacokinetic models teamed with the response surface model reported by Bouillon *et al.*

	MDPE (%)	MDAPE (%)	Wobble (%)
BMI<35 kg.m ⁻²	4 (-18: 39)	22 (13: 40)	13 (8: 25)
BMI≥35 kg.m ⁻²	13 (-23: 198)	18 (14: 31)	11 (7: 15)
Age<60 y	11 (-15: 37)	21 (13: 39)	14 (8: 21)
Age≥60 y	-8 (-22: 21)	21 (14: 40)	11 (9: 33)

Table 6.3

Measures of model performance by body mass index (BMI, BMI<35 kg.m⁻² versus BMI≥35 kg.m⁻²) and by age (Age≥60 y versus Age<60 y) for the prospectively tested model. Measures are: bias, given as the median performance error (MDPE); precision, given as the median absolute performance error (MDAPE); and wobble, given as the PE-MDPE. Values are median percentage bias (10th-90th percentile). The prospectively tested model was standard pharmacokinetic models teamed with the response surface model reported by Bouillon *et al.*

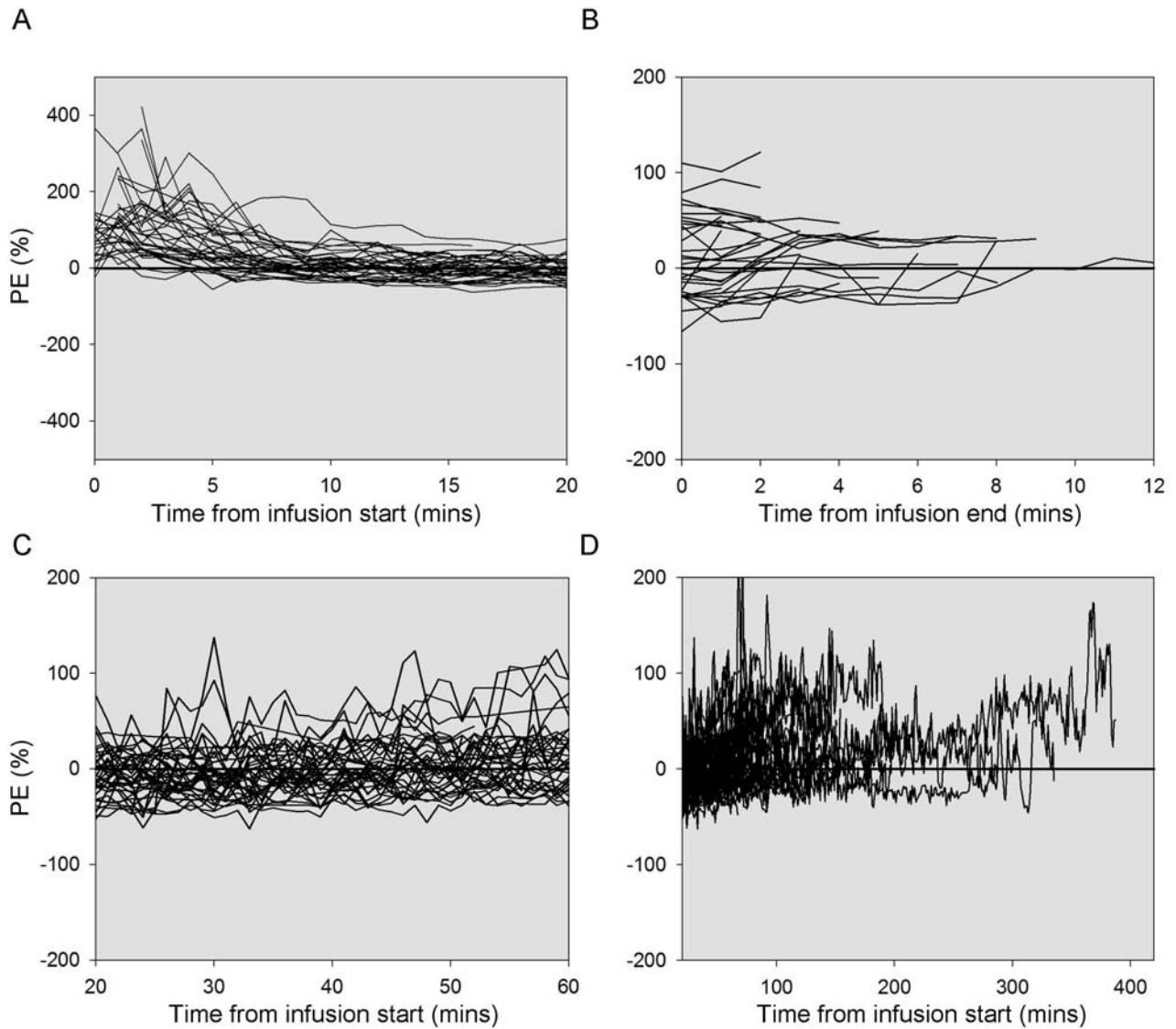


Figure 6.1

Performance error (PE, %) over time for the prospectively tested model (combination 1: standard pharmacokinetic models teamed with the response surface model reported by Bouillon *et al.*). Plots are: (A) PE during the early phase of anaesthesia (0-20 min post infusion start); (B) PE during the recovery phase (from when the infusion is halted at the end of the anaesthetic until the participant opens their eyes); (C) PE during the maintenance phase of anaesthesia (20 min post infusion start to the end of infusion, plot is truncated here at 60 min); and (D) PE during the maintenance and recovery phase of anaesthesia (20 min post infusion start to the end of data collection). Note the differences in scale of the y-axes (plot A).

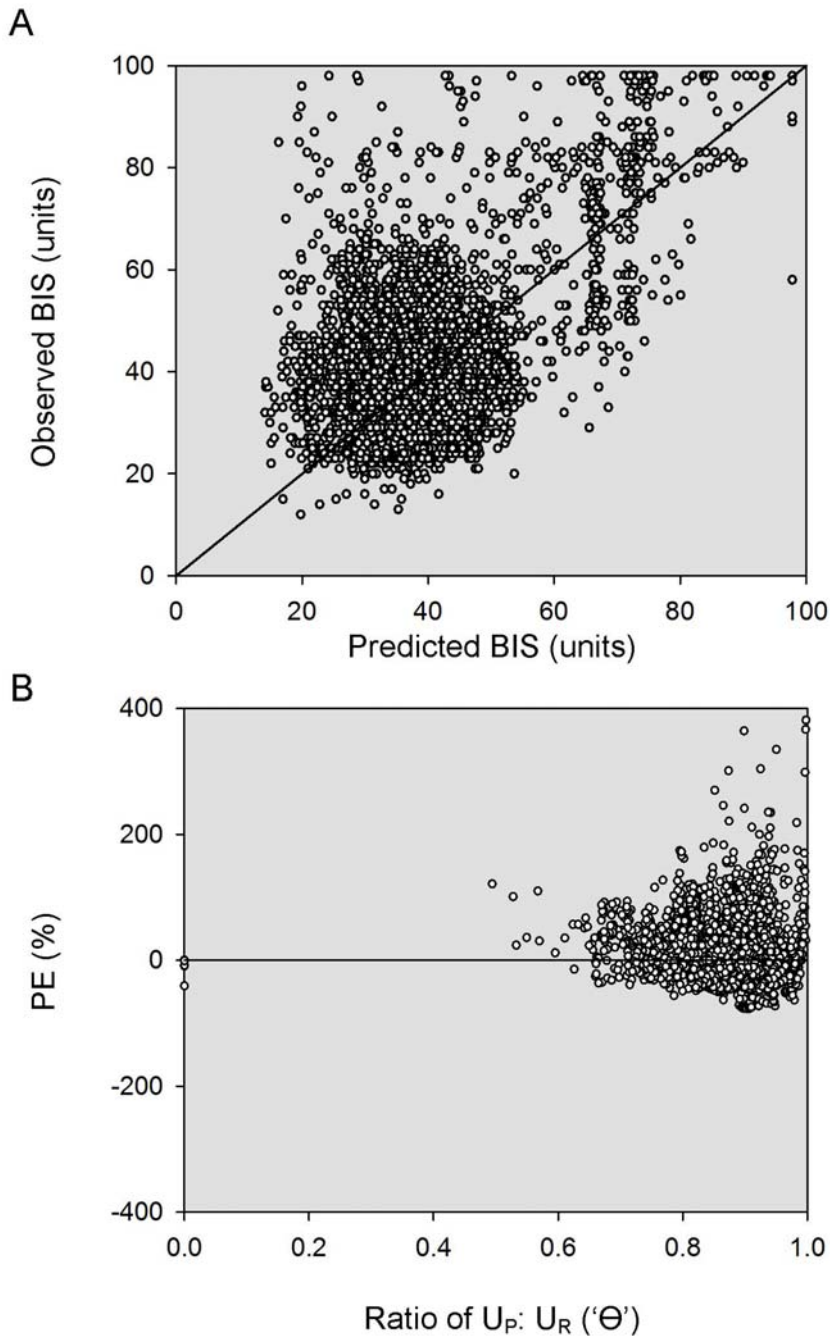


Figure 6.2

Quality of model predictions for the prospectively tested model (combination 1: standard pharmacokinetic models teamed with the response surface model reported by Bouillon *et al.*). Plots give: (A) predicted *versus* observed BIS, where units are BIS units 0-100 (BIS of 100 is resting and awake, BIS < 60 is recommended for surgical stimuli); and (B) performance error (PE, %) against the ratio of the normalised concentrations of propofol (U_P) to remifentanyl (U_R). The ratio, ' Θ ', is calculated as $U_P / (U_P + U_R)$. A Θ value equal to 0 means only remifentanyl is present, while a value of 1 means only propofol is present. The data predominantly fall in the upper range of Θ .

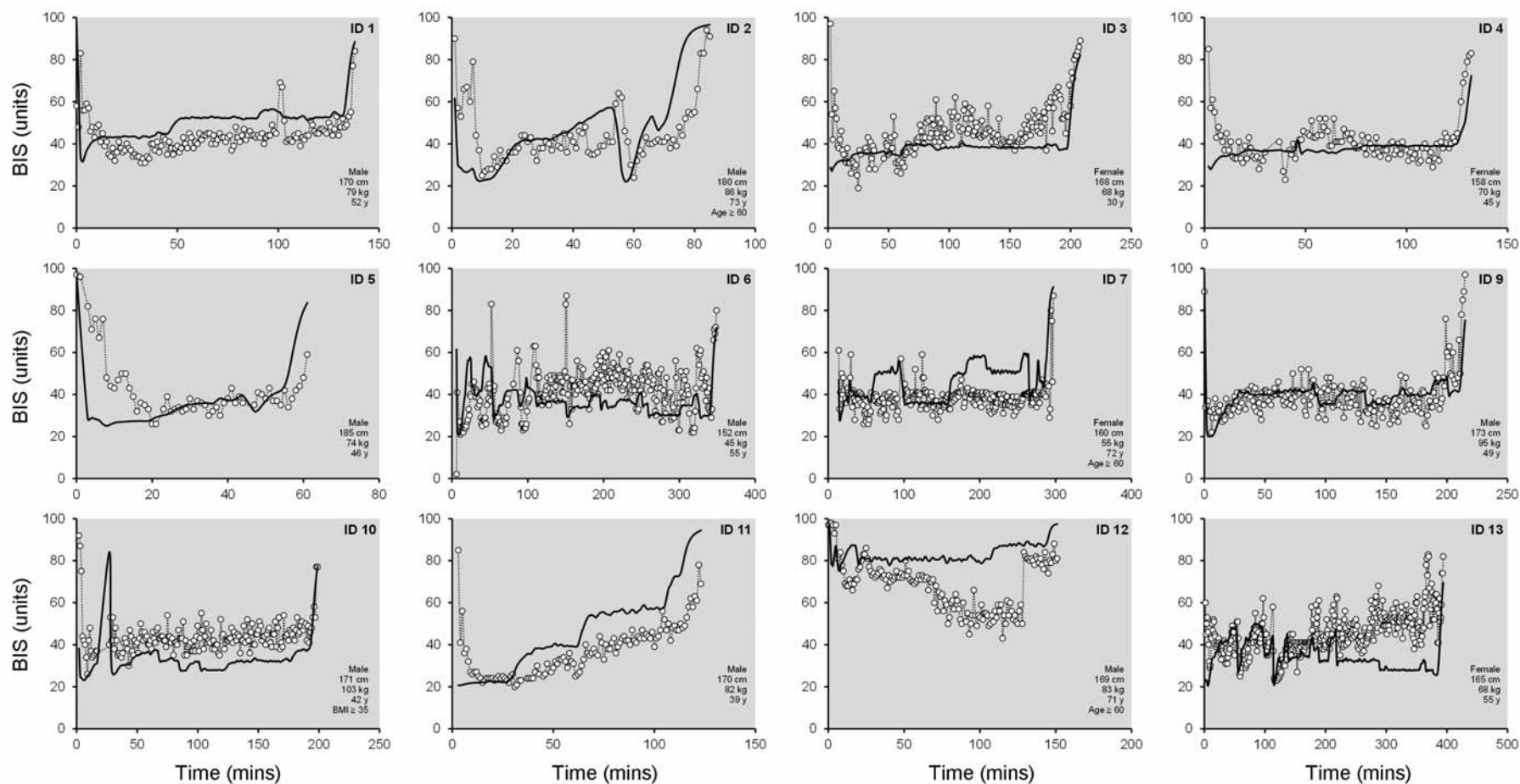


Figure 6.3

Plots of observed and predicted response over time for individuals. Open circles are observations and solid lines are the model predictions. Model predictions are made using the prospectively tested model (combination 1: standard pharmacokinetic models teamed with the response surface model reported by Bouillon *et al.*). BIS units are 0-100 (where 100 is resting and awake, and <60 is recommended for surgical stimuli).

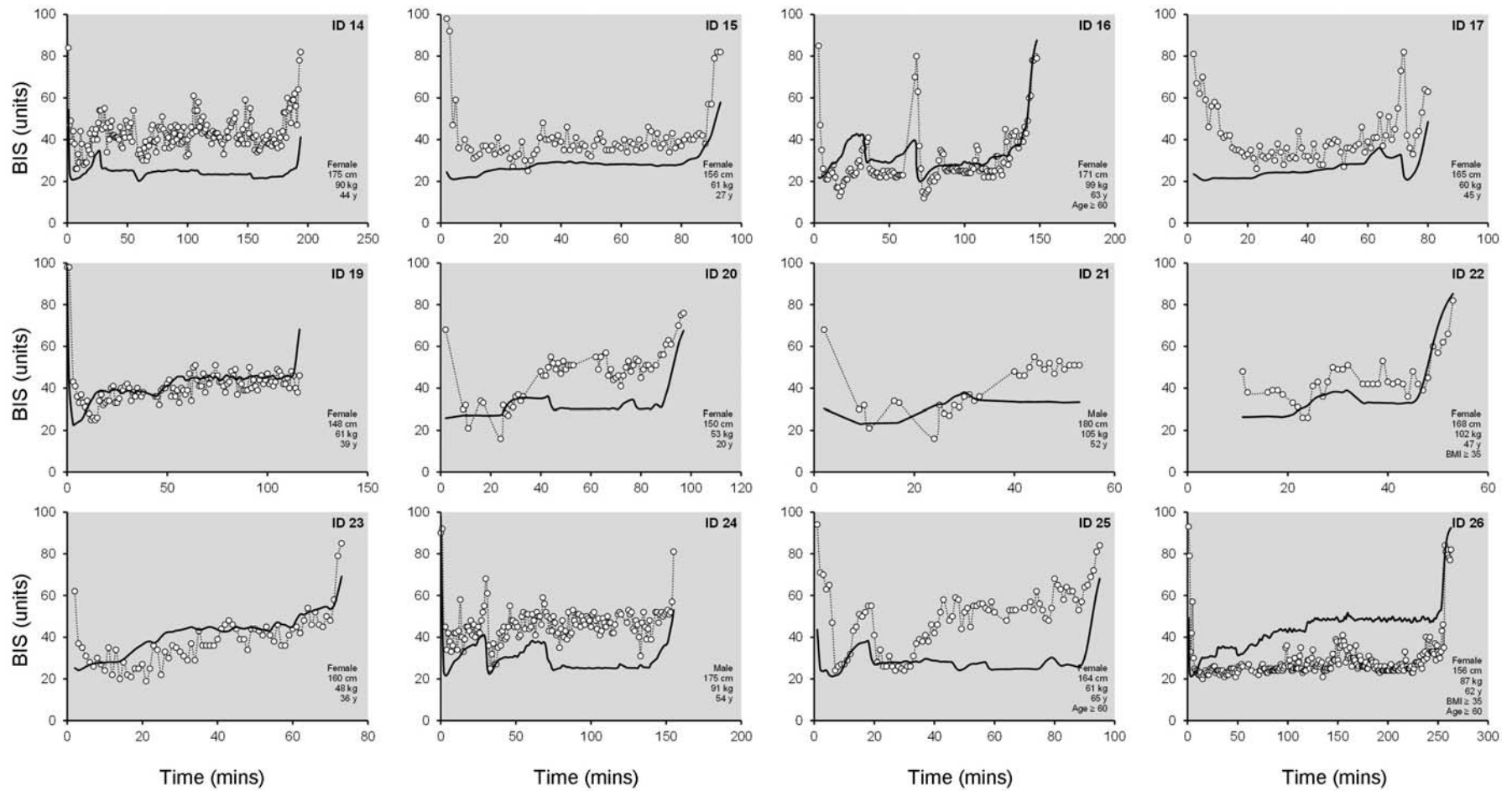


Figure 6.3 continued

Plots of observed and predicted response over time for individuals. Open circles are observations and solid lines are the model predictions. Model predictions are made using the prospectively tested model (combination 1: standard pharmacokinetic models teamed with the response surface model reported by Bouillon *et al.*). BIS units are 0-100 (where 100 is resting and awake, and <60 is recommended for surgical stimuli).

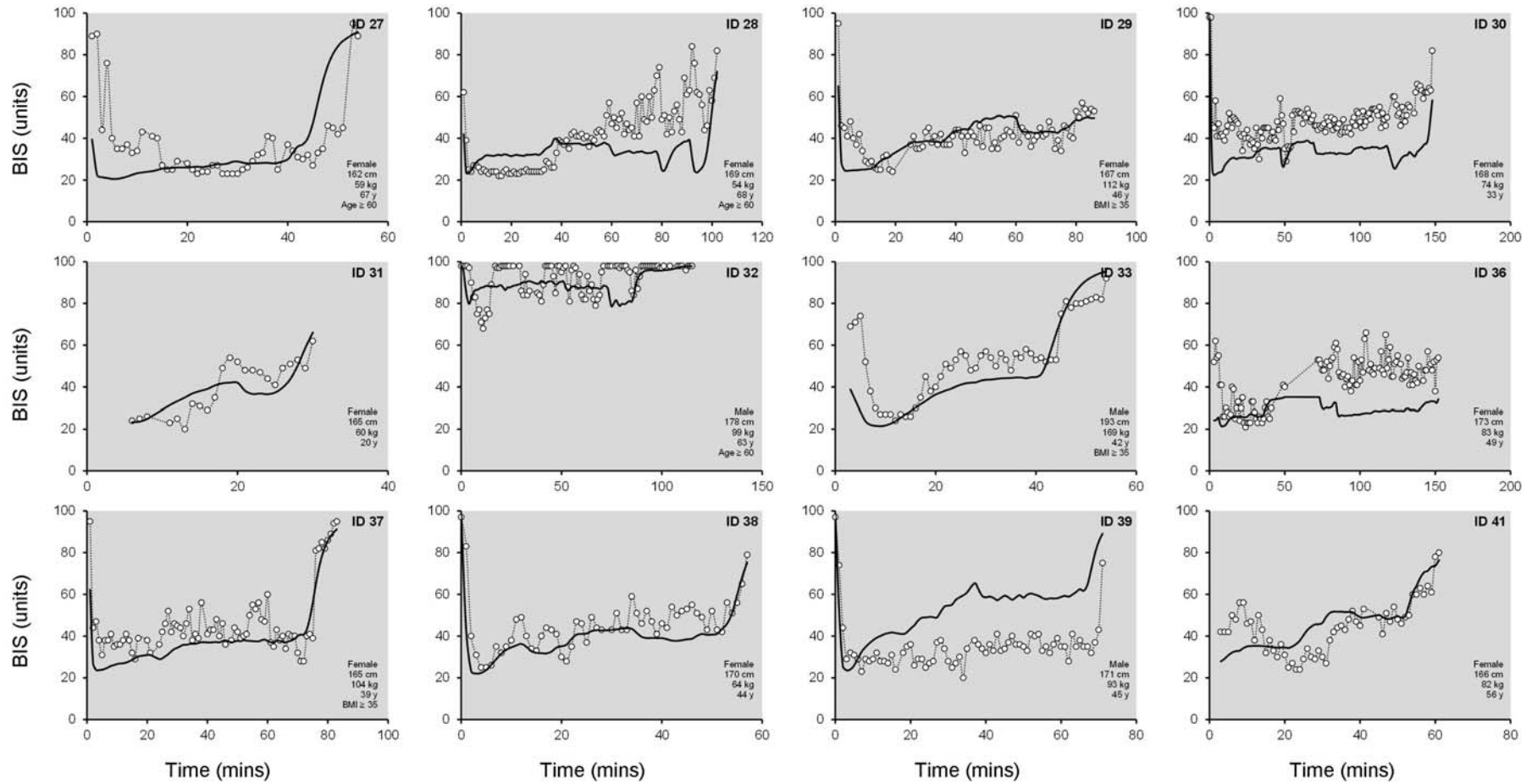


Figure 6.3 continued

Plots of observed and predicted response over time for individuals. Open circles are observations and solid lines are the model predictions. Model predictions are made using the prospectively tested model (combination 1: standard pharmacokinetic models teamed with the response surface model reported by Bouillon *et al.*). BIS units are 0-100 (where 100 is resting and awake, and <60 is recommended for surgical stimuli).

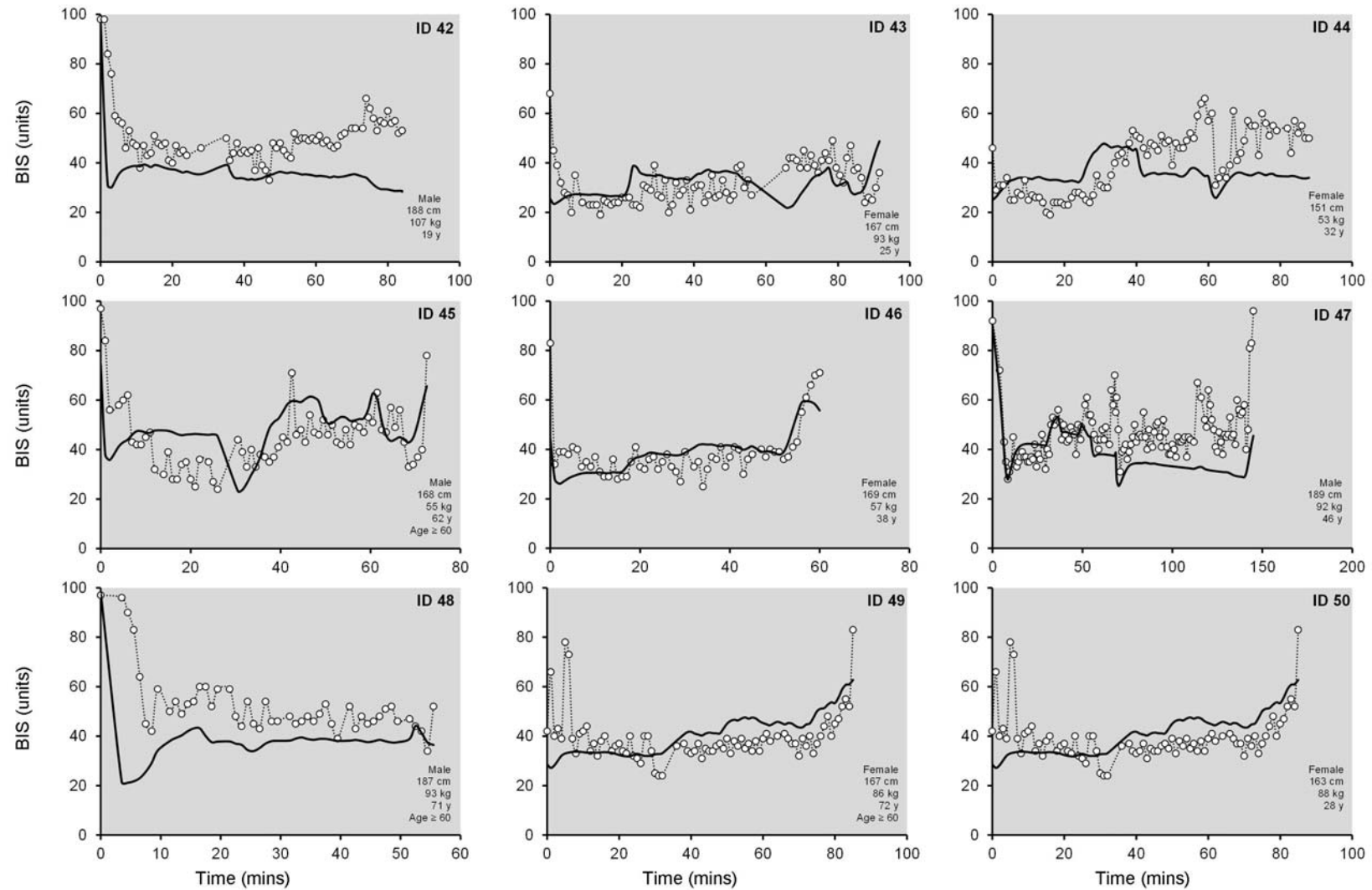


Figure 6.3 continued

Plots of observed and predicted response over time for individuals. Open circles are observations and solid lines are the model predictions. Model predictions are made using the prospectively tested model (combination 1: standard pharmacokinetic models teamed with the response surface model reported by Bouillon *et al.*). BIS units are 0-100 (where 100 is resting and awake, and <60 is recommended for surgical stimuli).

6.3.2 Retrospectively tested parameter combinations

Median measures of model performance taken across all time points showed $MDPE < \pm 20\%$ and $MDAPE < \pm 30\%$ for all three retrospectively tested parameter combinations. Percentiles were wide for all measures and often outside limits of ‘acceptable’ model performance defined for pharmacokinetic models (given in Section 1.2.4.1), as was observed with the prospectively tested model. The prospectively tested model (standard pharmacokinetic models [54, 73] with Bouillon’s pharmacodynamic model) [59] had the best median precision. Combination 2 (standard pharmacokinetic models [54, 73] with the pharmacodynamic model reported in chapter 4) had the lowest median bias across all time points ($MDP=4\%$); combination 3 (Bouillon’s pharmacokinetic and pharmacodynamic models)[59, 63] had the lowest wobble across all time points (wobble=9%). Combination 3 had the greatest median bias ($MDPE=-20\%$ for all time points) and performed poorly during the early ($MDPE=-22\%$, $MDAPE=27\%$) and maintenance phases ($MDPE=-18\%$, $MDAPE=26\%$) in particular. Combination 2 also performed poorly in the initial stages of anaesthesia ($MDPE=18\%$, $MDAPE=27\%$). Results for retrospectively tested parameter combinations for each phase of anaesthesia, and for the total study time, are given in Table 6.4. Results for the prospectively tested model are reiterated in the table for ease of comparison with retrospectively tested parameter sets.

Subjects were again split into two subgroups ($BMI < 35 \text{ kg.m}^{-2}$ versus $BMI \geq 35 \text{ kg.m}^{-2}$ and $Age \geq 60 \text{ y}$ versus $Age < 60 \text{ y}$) for re-analysis. Positive bias was observed in the $BMI \geq 35 \text{ kg.m}^{-2}$ group for all parameter combinations (Table 6.5). This was greatest when combination 4 (Minto’s remifentanyl model with propofol and pharmacodynamics as reported in chapter 4) was used to make predictions ($MDPE 77\%$). Combination 3 performed best with bias of just 3%. Median measures of model precision and wobble were best for combination 3 in the $BMI \geq 35 \text{ kg.m}^{-2}$ group. Under-prediction was seen for all models in the $Age \geq 60$ subgroup, indicating that observed BIS values were lower than those predicted by the model (Table 6.6). Combination 4 gave the least bias ($MDPE -1\%$) in the $Age \geq 60$ subgroup, while bias for combinations 2 was similar to that of the prospectively tested model (-11% versus -9% respectively). Measures of model precision and wobble were similar between participants in both groups.

	Prospectively tested*	2	3	4
Parameter sets (R/P/PD)	Minto/ Schnider/ Bouillon	Minto/ Schnider/ Chapter 4	Bouillon/ Bouillon/ Bouillon	Minto/ Chapter 4/ Chapter 4
MDPE (%)				
Early	14 (-30: 110)	18 (-25: 106)	-22 (-52: 17)	9 (-46: 80)
Maintenance	5 (-31: 58)	5 (-33: 69)	-18 (-46: 27)	6 (-36: 99)
Recovery	6 (-30: 50)	-7 (-40: 38)	8 (-33: 42)	15 (-24: 164)
All time points	7 (-19: 37)	4 (-19: 47)	-20 (-38: 18)	8 (-27: 93)
MDAPE (%)				
Early	28 (5: 110)	27 (5: 106)	27 (4: 55)	29 (5: 80)
Maintenance	22 (4: 58)	25 (5: 69)	26 (5 : 49)	29 (5: 99)
Recovery	25 (4: 51)	18 (3: 51)	23 (6: 47)	25 (5: 163)
All time points	21 (13: 40)	23 (13: 49)	24 (9: 40)	26 (10: 93)
Wobble (%)				
Early	25 (4: 98)	26 (5: 95)	14 (2: 39)	19 (3: 57)
Maintenance	11 (2: 40)	12 (2: 43)	9 (1: 31)	12 (2: 41)
Recovery	12 (2: 40)	20 (3: 43)	21 (3: 57)	21 (4: 74)
All time points	12 (8: 23)	13 (8: 25)	9 (5: 18)	13 (7: 25)

Table 6.4

Measures of model performance for each stage of anaesthesia for retrospectively tested combinations. Measures are: median bias, given as the median performance error (MDPE); median precision, given as the median absolute performance error (MDAPE); and median wobble, given as the PE–MDPE. Values are median percentage bias (10th-90th percentile). R indicates remifentanyl pharmacokinetic parameter set, P indicates propofol pharmacokinetic parameter set, and PD indicates pharmacodynamic parameter set. *Note that model performance for the prospectively tested model is reiterated here for ease of comparison.

	Prospectively tested*	2	3	4
Parameter sets (R/P/PD)	Minto/ Schnider/ Bouillon	Minto/ Schnider/ Chapter 4	Bouillon/ Bouillon/ Bouillon	Minto/ Chapter 4/ Chapter 4
MDPE (%)				
BMI<35 kg.m ⁻²	4 (-18: 39)	3 (-17: 51)	-21 (-37: 16)	5 (-29: 80)
BMI≥35 kg.m ⁻²	13 (-23: 198)	13 (-21: 29)	3 (-30: 30)	77 (26: 134)
All patients	7 (-19: 37)	4 (-21: 47)	-20 (-39: 15)	8 (-28: 91)
MDAPE (%)				
BMI<35 kg.m ⁻²	22 (13: 40)	23 (14: 51)	25 (14: 39)	22 (10: 80)
BMI≥35 kg.m ⁻²	18 (14: 31)	25 (14: 36)	11 (9: 54)	77 (44: 134)
All patients	21 (13: 40)	23 (12: 47)	24 (9: 39)	26 (10: 91)
Wobble (%)				
BMI<35 kg.m ⁻²	13 (8: 25)	13 (8: 28)	9 (5: 19)	13 (6: 24)
BMI≥35 kg.m ⁻²	11 (7: 15)	14 (8: 18)	8 (5: 13)	16 (7: 28)
All patients	12 (8: 23)	13 (7: 22)	9 (5: 16)	13 (7: 24)

Table 6.5

Measures of model performance by body mass index (BMI, BMI<35 kg.m⁻² versus BMI≥35 kg.m⁻²) for retrospectively tested combinations. Measures are: bias, given as the median performance error (MDPE); precision, given as the median absolute performance error (MDAPE); and wobble, given as the PE-MDPE. Values are median percentage bias (10th-90th percentile). Poor performance is seen for combination 4 (developed in chapter 4) for those individuals with a BMI ≥ 35 kg.m⁻². Measures of bias, precision and wobble for all patients across all time points, as given in Table 6.4, are repeated here for ease of comparison. R indicates remifentanyl pharmacokinetic parameter set, P indicates propofol pharmacokinetic parameter set, and PD indicates pharmacodynamic parameter set.

*Note that model performance for the prospectively tested model is reiterated here for ease of comparison.

	Prospectively tested*	2	3	4
Parameter sets (R/P/PD)	Minto/ Schnider/ Bouillon	Minto/ Schnider/ Chapter 4	Bouillon/ Bouillon/ Bouillon	Minto/ Chapter 4/ Chapter 4
MDPE (%)				
Age<60 y	11 (-15: 37)	15 (-16: 50)	-16 (-31: 21)	8 (-22: 97)
Age≥60 y	-8 (-22: 21)	-11 (-20: 25)	-28 (-41: 7)	-1 (-31: 33)
All patients	7 (-19: 37)	4 (-21: 47)	-20 (-39: 15)	8 (-28: 91)
MDAPE (%)				
Age<60 y	21 (13: 39)	26 (13: 50)	22 (10: 34)	26 (10: 97)
Age≥60 y	21 (14: 40)	21 (15: 39)	30 (10: 41)	23 (12: 43)
All patients	21 (13: 40)	23 (12: 47)	24 (9: 39)	26 (10: 91)
Wobble (%)				
Age<60 y	14 (8: 21)	15 (8: 22)	10 (6: 16)	13 (7: 24)
Age≥60 y	11 (9: 33)	11 (7: 35)	8 (5: 21)	10 (7: 26)
All patients	12 (8: 23)	13 (7: 22)	9 (5: 16)	13 (7: 24)

Table 6.6

Measures of model performance by age (Age≥60 y *versus* Age<60 y) for retrospectively tested combinations. Measures are: bias, given as the median performance error (MDPE); precision, given as the median absolute performance error (MDAPE); and wobble, given as the PE-MDPE. Values are median percentage bias (10th-90th percentile). Under-prediction (in the form of negative bias) is seen for all models in participants aged 60 years and older. Measures of bias, precision and wobble for all patients across all time points, as given in Table 6.4, are repeated here for ease of comparison. R indicates remifentanyl pharmacokinetic parameter set, P indicates propofol pharmacokinetic parameter set, and PD indicates pharmacodynamic parameter set. *Note that model performance for the prospectively tested model is reiterated here for ease of comparison.

6.4. Discussion

I prospectively tested the performance of a pharmacokinetic-linked response surface model to target BIS in patients undergoing surgery, and retrospectively tested performance of three other model combinations. The prospectively tested model predicted observed BIS with a bias of 7%, precision of 21% and wobble of 12%. Performance was best during maintenance and worst during induction (the ‘early’ phase). Performance measures for retrospectively tested models typically showed greater bias, imprecision and wobble than seen with the prospectively tested model. The range of performance was wide (for all models) and predictions during the first 20 minutes of anaesthesia were poor. Combination 2 (standard pharmacokinetic models,[54, 73] with the pharmacodynamic model reported in chapter 4) had the lowest bias across all time points but this was probably a result of over-prediction during the early phase and under-prediction during recovery. The models that performed best, i.e. the prospectively test model (combination 1) and combination 2, used standard pharmacokinetic models that are available in commercial TCI pumps and have been clinically validated.[54, 55, 73, 255] Notably, predicted effect site concentrations of remifentanyl were converted to alfentanil equivalents for combination 2 and combination 4 (Minto’s remifentanyl model with propofol and pharmacodynamics as reported in chapter 4) using a potency ratio of remifentanyl: alfentanil of 1:33 as was reported in chapter 5.

One limitation of this study is that concentration data were not collected. This means that performance of the pharmacokinetic component is unknown for each model and the true performance of the pharmacodynamic component remains unidentified. Performance has been assessed for several pharmacokinetic parameter sets available in commercial pumps and this helps to put these results into context. Each parameter set reflects the population from which it was developed and consequently performance varies when extrapolated to individuals who are dissimilar to this ‘learning’ group. For example the Marsh model, which was initially developed in children, predicts propofol plasma concentrations in adult patients with bias (MDPE) ranging from 1 to 16%, and precision (MDAPE) ranging from 25 to 29%.[49, 50, 257]

Performance is poor in young children aged 3 to 24 months, with an estimated MDPE -20.1% and MDAPE 23.4%. [258] The model described by Schnider *et al.*, [54] and used for combinations 1 and 2 in this study, was found to perform with -0.1% bias and 23.6% precision in patients with normal renal and hepatic function. [49] The authors of this study split their analysis into distinct stages of anaesthesia similar to those used here. [49] This revealed a bias of -20% for Schnider's model during the 21 minutes following infusion start, meaning concentrations predicted by the model were greater than the observed concentrations of propofol. Over-prediction of drug concentration may in turn lead to over-prediction of drug response. This might have been a contributing factor to the high response predictions seen in the early phase of this study for the prospectively tested model and combination 2, both of which used Schnider's parameter set to describe propofol pharmacokinetics. MDPE was 14% and 18% during the early phase for the prospectively test model and combination 2 respectively (shown as positive bias due to the inverted scale of BIS where 100 is baseline response and decreasing values indicate increasing depth of anaesthesia).

The pharmacodynamic relationship is also associated with variability. [259] Additive residual error associated with BIS predictions made using a pharmacodynamic models for propofol with alfentanil or remifentanil was 8 BIS units (see chapters 4 and 5). Others have estimated this can be as high as 14 BIS units in surgical patients. [245] Neither of the pharmacodynamic parameter sets assessed here included adjustment of the population model to an individual in the form of covariate effects. Propofol requirements for loss of consciousness in 25 year olds are nearly halved in 75 year olds. [54, 55] Twelve participants were aged 60 years or more in the current study. All models showed negative bias (or under-estimated the observed response) when used to make effect predictions in these individuals (Table 6.3 and Table 6.6). This directly contrasted with the positive bias seen in participants aged 59 years and under and in the population as a whole, suggesting that this is a patient subgroup for which drug effects are poorly described by the tested models. Age effects were included in both the pharmacokinetic models used for combinations 1 and 2 (standard pharmacokinetics with pharmacodynamics reported by Bouillon *et al.* and in chapter 4, respectively). [54, 55, 73, 255] Minto *et al.* also included age effects on the keo and Ce_{50} parameter for remifentanil effects on EEG response. [73, 255] Incorporating influential covariates such as age into response surface models might improve their accuracy when applied to more diverse populations like that studied here.

Performance of the models was reasonable, despite the lack of covariate models included in the response surface models. Minto *et al.* reported a bias of 7% and precision of 19%, expressed as a percentage of the pharmacodynamic range, for a remifentanil pharmacodynamic model of EEG effects measured using spectral edge frequency.[73, 255] Propofol pharmacodynamics as described by Schnider *et al.* have an estimated a bias of 5.5% and accuracy of 17% during induction in children and adults.[55, 200] Both these studies were conducted in volunteers during carefully controlled conditions, and plasma concentrations were sampled. Estimates of bias and precision in this study were higher (for example the prospectively tested model, standard pharmacokinetics with Bouillon's pharmacodynamics, had MDPE of 7% and MDAPE of 21%) but this is as expected when one considers that the participants were patients undergoing surgery and that the performance of the pharmacokinetic models used to make concentration predictions was unknown. Lui *et al.* reported median (range) MDPE, MDAPE and wobble estimates of -6.0 (-12.0 to -2.8)%, 10.5 (9.0 to 14.0)% and 8.0 (7.0 to 10.0)% respectively, for BIS guided propofol and remifentanil infusions administered using a closed loop controller.[260] Their system drives drug infusions to an initial effect site concentration selected by the anaesthetist and subsequently adjusts infusion rates to achieve a 'set-point' (in this case, a BIS of 50 units). Their study is interesting because both propofol and remifentanil infusions were used together in the one system and the study was conducted during anaesthesia (so participants received other co-administered drugs and varying noxious stimuli). Drug concentrations were not measured and so inaccuracies arising from the pharmacokinetic models are unknown, as was the case in the current study. Several other closed-loop control systems have also been reported that use BIS as a set-point to titrate pharmacokinetic models to the individual, though most are for single drugs. Absalom *et al.* reported bias, precision and wobble of 2.2%, 8.0% and 7.3% respectively for a closed loop propofol controller when used for adult patients undergoing orthopaedic surgery.[261] The controller was refined and performance retested in a younger patient population, which resulted in bias, precision and wobble estimates of -0.4%, 5.6% and 5.4% respectively.[262] Remifentanil was given alongside propofol as a manually controlled infusion. Similar performance was observed by Struys *et al.* for their closed-loop controller of propofol.[263] An advantage of including a second drug in these systems is that the ratio of drugs may be adjusted to influence other factors that are important intraoperatively in addition to the depth of anaesthesia.[264] For example, blood pressure and the level of analgesia may be better controlled with the addition of an opioid. Morely *et al.* investigated a controller for propofol and alfentanil in combination, although the two drugs were mixed together in single syringe so that the ratio of propofol to alfentanil was the same for all patients and at all stages of surgery.[265]

The propofol and remifentanyl models used for combination 3 (Bouillon's pharmacokinetic and pharmacodynamic parameters) were derived in 20 healthy volunteers with a median (range) age of 33 (20-43) years, and weight 70 (50-120) kg. Combination 3 showed the smallest bias in the BMI ≥ 35 kg.m⁻² group. This might be attributable to the wide range of weights of the patients studied either through the pharmacokinetic models, the pharmacodynamic models or both. Performance for combination 3 was poor in the age ≥ 60 group (MDPE -28% as opposed to MDPE -1 to -11% for the other combinations). Notably combination 4 (Minto's remifentanyl model with propofol and pharmacodynamics as reported in chapter 4) performed worst in the BMI ≥ 35 kg.m⁻² group. This is attributable to the propofol pharmacokinetic model and keo value developed in chapter 4 of this thesis, as all other components of the model were unchanged from combination 2. The mean weight of the participants in chapter 4 was 55 (range 43-71) kg, spanning just 28 kg. The propofol pharmacokinetic model is unlikely to predict concentrations well in a diverse population given the narrow range of demographics of the population from which it was derived, and this is reflected in the results reported here. The keo value used for combination 4 was 0.2 min⁻¹ (as given in chapter 4). This gives a $t_{1/2\text{keo}}$ of 3.4 min, which is longer than the $t_{1/2\text{keo}}$ 1.5 min (keo 0.46 min⁻¹) used for the other combinations. The longer keo value improved early model predictions; combination 4 had the lowest MDPE during the early phase of anaesthesia.

This study has several limitations. Multiple factors that probably impact on model performance were not controlled for. All patients experienced surgical stimulus and no attempt was made to limit the type of surgery observed. Pain types and intensities were therefore different between participants, influencing each individual's requirements for opioids. Patient demographics spanned a wide range of weights, heights and ages (45-169 kg, 148-193 cm and 20-70 years respectively). These are covariates known to influence pharmacokinetics and pharmacodynamics of both drugs.[54, 55, 73] However this in itself makes the study interesting, as we are able to gain an idea of model performance as it would typically be used by clinicians in an everyday setting. Bouillon *et al.* did not report keo values for their parameter sets and so these had to be extrapolated for combination 3 using TTPE methods and literature estimates of Tpeak. Three individuals did not receive neuromuscular blocking agents as part of their anaesthetic, which may have introduced artefact or signal disruption to EEG recordings. Only BIS values associated with a SQI >50 were retained for this analysis and so the effect of electromyography interference should be minimal. BIS measurements were a result of signal

processing occurring over 30 second epochs. None of the tested models included a lag time. This probably contributed to the poor model performance observed during the early anaesthetic phase, particularly in the first few minutes where the patient state is rapidly changing. This is nicely illustrated in the plots for individuals 2, 5 and 25, given in Figure 6.3, and supported by the observation that combination 4 (standard pharmacokinetic models with pharmacodynamics from chapter 4 with a long keo value) showed better model predictions in the early stages of anaesthesia.

Response surface models, when used together with carefully derived pharmacokinetic models, are good candidates for TCI during anaesthesia. The inclusion of a pharmacodynamic model theoretically offers advantages over a solely pharmacokinetic based system in that discrepancies between targeted and observed effects are directly observable throughout an anaesthetic, whereas targeted concentrations are unobservable in real time. This information can be used to incorporate adaptive control systems that adjust for the individual.[259] Although clinicians may consider pharmacokinetic and pharmacodynamic interactions of co-administered agents when selecting infusion targets, no adjustment is made for these in current automated TCI systems. Incorporating these models into existing TCI or closed loop adaptive systems would provide some adjustment for compounding drug actions.[264]

Summary

The parameter sets assessed here showed similar performance in a diverse patient population (for whom pathology, surgical types and durations, influential covariates differed widely) to other reports of pharmacodynamic models for single drugs assessed in more carefully controlled conditions. Both the prospectively tested model (standard pharmacokinetics with pharmacodynamics reported by Bouillon *et al.* for propofol and remifentanyl) and combination 2 (standard pharmacokinetic models with pharmacodynamics from chapter 4 for propofol and alfentanil) showed similar performance at all stages of anaesthesia; this was despite the conversion of remifentanyl concentrations to alfentanil equivalents using a conversion factor of 1:33 for combination 2. Further development is clearly required in the form of covariate effects and appropriate linking between pharmacokinetic and pharmacodynamic models (through the keo parameter). This work is continued in the next chapter, where I begin to develop a model for BIS response for multiple drug classes in patients undergoing general surgery.

Chapter 7. A model of combined BIS response for opioid, intravenous and inhalation anaesthetics

Background: There are numerous studies that describe two drug models for interactions between opioid, intravenous and inhalation anaesthetics. No models as yet describe combined BIS effects for all three drug classes when given together.

Methods: This was an observational study of BIS effects following bolus or infusion dosing of multiple drug classes in a diverse population of patients undergoing surgery. Demographic, drug dosing and BIS response data were collected. Standard pharmacokinetic models were used to predict plasma and effect site concentrations of each drug. Drug concentrations were normalised using their Ce_{50} values and expressed as total drug-class units. The model developed in chapters 4 and 5 was extended for three drugs classes: opioid, intravenous and inhalation anaesthetics.

Results: Data from 51 individuals (28 males and 23 females) were included in the analysis. Patients had a mean (range) age, weight and height of 44 (19-65) years, 70 (24-120) kg and 169 (143-192) cm, respectively. Alfentanil and remifentanil Ce_{50} parameters were fixed at earlier estimates (chapter 4), while that of isoflurane was fixed at literature reports. Estimated Ce_{50} parameters were fentanyl 9.0 mcg. Γ^1 , propofol 2.46 mg. Γ^1 , desflurane 3.94 %vol, and sevoflurane 1.32 %vol. The maximal effect (E_{MAX}) was 76 BIS units and the slope was 2.56. Effects of midazolam were also included (estimated Ce_{50} 0.264 mg. Γ^1). Additivity was assumed for pairwise interactions between opioid, intravenous anaesthetic and inhalation anaesthetic drug classes. A non-additive triple interaction parameter (describing the relationship between all three drug classes) did not further improve the model. The model suggested additivity exists between propofol and midazolam for BIS for the concentration ranges studied.

Conclusions: A model describing combined BIS response for multiple drug classes is given. The model includes representatives from the intravenous anaesthetic, phenyl-piperidine opioids and the inhalation anaesthetic drug classes. The model suggests additivity between these three drug classes for BIS effects in the dosing ranges studied. The effects of midazolam, a sedative, are also included and an additive relationship between propofol and midazolam suggested.

7.1. Introduction

The combination of a phenyl-piperidine opioid with an intravenous and inhalation anaesthetic drug is typical of most general anaesthetics. The relationships existing between drug pairs for various endpoints have been well described for opioid, intravenous and inhalation anaesthetic drug classes. Response surface models have been reported for drug combinations representing all three drug class pairs. Propofol-sevoflurane models have been reported for intravenous anaesthetic-inhalation anaesthetic combinations.[129, 143] Sevoflurane-alfentanil and sevoflurane-remifentanil models have been reported for opioid-inhalation anaesthetic combinations.[76, 128] Propofol-remifentanil models,[59, 146] and a propofol-alfentanil model (chapter 4), have been reported for intravenous anaesthetic-opioid combinations. A model for the combined effect of these drug classes on BIS has not been described.

The aim of this study was therefore to establish a basic structural model and some initial parameter estimates for a model describing BIS effect for phenyl-piperidine opioids, intravenous anaesthetics and inhalation anaesthetics.

7.1. Methods

Ethics committee approval was given by the Northern Y Regional Ethics Committee prior to commencing the study (NTY/10/EXP/002, see Appendix 6). This was an observational study of BIS effect following infusion and bolus dosing of three drug classes in a diverse population of patients undergoing surgery.

The three drug classes were defined for this study as:

1. Intravenous anaesthetic: propofol
2. Phenyl-piperidine opioids: alfentanil, fentanyl and remifentanil
3. Inhalation anaesthetics: desflurane, isoflurane and sevoflurane.

7.1.1 Participants

Adult patients, aged 18-65 years with an American Society of Anesthesiologists' physical status (ASA) of 1-2 and scheduled for surgery on Level 4 or Level 5 of Auckland City Hospital, were eligible to be studied. Only patients for whom EEG monitoring using BIS was planned could be studied. Patients who had a history of chronic opioid consumption or psychoactive medication use (including high alcohol intake), had neurological dysfunction, or who received intravenous anaesthetics or sedatives (other than propofol or midazolam) were not studied. Local ethics committee consent was gained for the study *via* the expedited review process. The need for participant consent was waived because data were observational and the study did not alter patient care in any way.

7.1.2 Data collection

I aimed to collect data for 60 individuals. Data collection was dependent on the availability of a study laptop, and on the attending anaesthetist's decision as to whether BIS would be monitored.

The site of electrodes was cleaned with alcohol prior to applying the BIS sensor. The BIS response was calculated using 10 second epochs of EEG and recorded electronically at 30 second epochs using a BISTM Monitoring System (see section 6.2.3) with BISTM Quatro sensor. Demographic, physiologic and drug dosing data were recorded automatically by the integrated drug administration system (IDAS) SaferSLEEP (see section 6.2.3). Drug dosing and BIS data were extracted from the data file generated by the IDAS at the end of each case. Drug administration data were collected directly for propofol and opioid infusions using a dedicated study laptop. The study laptop was connected to automated infusion pumps using the RS232C serial ports. The computer time was aligned to that of the operating room anaesthetic computer, and pump rates and volumes were recorded in real time using the software 'Monitor (for PC)' Version 5.0 (Department of Anaesthesia, Prince of Wales Hospital, The Chinese University of Hong Kong, Shatin, Hong Kong, China).[266] Demographic data for covariate analysis (sex, weight, height and age) were also recorded.

7.1.3 Data analysis

Observed BIS data were reduced to one minute epochs for the first twenty minutes of anaesthesia and then further reduced to five minute epochs following this to allow analysis using NONMEM. BIS values associated with a Signal Quality Index (SQI) < 50 were not included in the analysis.

Plasma and effect site concentrations of each drug were predicted from dosing and covariate data. Predictions were made in Excel 2010, using PK–PD Tools for Excel© 2009, Version 1.31 (www.pkpdtools.com), [14] and published parameter sets selected from the literature. Parameter sets that a) have been clinically validated in a patient population and shown to have reasonable performance, b) report an appropriate keo parameter for BIS (or EEG) response and c) include covariate models for known influential covariates were selected. Pharmacokinetic and keo parameter sets selected for each study drug are summarised in Table 7.1. End-tidal concentrations of inhalation anaesthetics were assumed proxies for plasma concentration and so only a keo value was required to describe transfer of drug from plasma to effect compartments for this drug class i.e.

$$\frac{dC_{\text{eff}}}{dt} = \text{keo} [C_{\text{ET}} - C_e]$$

Equation 7.1

where C_{ET} is the end tidal concentration and C_e is the effect site concentration of the inhalation anaesthetic.

Drug class*	Drugs included	Parameter set	Reason for selection
Inhalation anaesthetic	Desflurane	Kreur <i>et al.</i> 2009 [104]	keo for BIS response given
	Isoflurane	Kreur <i>et al.</i> 2009 [104]	keo for BIS response given
	Sevoflurane	Cortinez <i>et al.</i> 2008 [58]	keo for BIS response given, covariate inclusion (AGE)
Intravenous anaesthetic	Propofol	Schnider <i>et al.</i> 1998 [54, 55]	Clinically validated, keo for EEG response given, covariate inclusion (HT, WT, AGE, LBM)
Phenyl-piperidine opioids	Alfentanil	Scott <i>et al.</i> 1985 [71, 243]	Clinically validated, keo for EEG response given
	Fentanyl	Scott <i>et al.</i> 1985 [71, 243]	Clinically validated, keo for EEG response given
	Remifentanil	Minto <i>et al.</i> 1997 [73, 255]	Clinically validated, keo for EEG response given, covariate inclusion (AGE, LBM)

Table 7.1

Parameter sets selected from the literature and used to predict plasma and effect site concentrations from dosing information. *The three drug classes (and their representative drugs) are defined for this thesis as 1) intravenous anaesthetic (propofol); phenyl-piperidine opioids (alfentanil, fentanyl and remifentanil); and inhalation anaesthetics (desflurane, isoflurane and sevoflurane).

7.1.3.1. Modelling methods

The analysis described here builds on the work presented in earlier chapters. Data were modelled using the structural model identified in chapter 4: baseline BIS was fixed at 98.0 units, an E_{MAX} parameter was estimated, response was described using the model given by Minto *et al.*, [122] and a constraint model was used to ensure that E_{MAX} did not result in a negative BIS in each individual.

Response was modelled from estimated effect site concentrations and according to drug class. Effect site concentrations (C_e) of each drug were converted to normalised units (U) by dividing by the C_{e50} . Alfentanil and remifentanil C_{e50} parameters were fixed at 646 ng.l⁻¹ and 20 ng.l⁻¹ respectively (as in chapters 4 and 5), while the C_{e50} of fentanyl was estimated. C_{e50} parameters were also estimated for the inhalation anaesthetics and for propofol. Normalised units of drugs belonging to the same drug class were summed and expressed as total units of drug class. For example, units of alfentanil (U_A), fentanyl (U_F) and remifentanil (U_R) units were expressed as units of opioids (U_O), i.e.

$$U_O = U_A + U_F + U_R$$

Equation 7.2

Units of opioids (U_O), intravenous anaesthetics (U_P) and inhalation anaesthetics (U_I) were modelled in a response surface. A function describing the ratio of drugs present, and including an interaction parameter, was applied to drug potency as in earlier chapters. [122] The introduction of a third drug (or in this case, drug class) required extension of the function as described by Minto *et al.* [122] Firstly, the ratio of drugs present is expressed in relation to each drug class, i.e.

$$\theta_P = \frac{U_P}{U_P + U_O + U_I}, \quad \theta_O = \frac{U_O}{U_P + U_O + U_I}, \quad \theta_I = \frac{U_I}{U_P + U_O + U_I}$$

Equation 7.3

Just two of these terms are required for the model as by definition their sum is 1. [122] Ratios expressed against intravenous (θ_P) and inhalation (θ_I) anaesthetics were used in the following equations. Interaction parameters for each drug class pair are included (for example, β_{PO} describes the interaction between the intravenous anaesthetic and opioid classes; β_{PI} describes the interaction between the intravenous and inhalation anaesthetic classes; and β_{OI} describes the interaction between

the opioid and inhalation anaesthetic classes). A further interaction parameter, β_{POI} , describes that existing between all three drug class pairs. The function $U_{50}(\theta)$, given for two drugs in Equation 3.3, can be extended ($U_{50}(\theta_1, \theta_2)$) for three drug classes, i.e.

$$U_{50}(\theta_P, \theta_I) = 1 - \beta_{PO} \cdot \theta_P + \beta_{PO} \cdot \theta_P^2 - \beta_{PI} \cdot \theta_I + \beta_{PI} \cdot \theta_I^2 + (\beta_{PO} + \beta_{PI} - \beta_{OI}) \cdot \theta_P \cdot \theta_I + \beta_{POI} \cdot \theta_P \cdot \theta_I \cdot (1 - \theta_P - \theta_I)$$

Equation 7.4

This is a quadratic function that describes at most a parabola shaped surface.[122] More complex functions are possible but are not used here because, as suggested by Minto *et al.*, they are likely to be overly complex for the type of data in this analysis.[122] The function given in Equation 7.4 is then applied to normalised drug class units and response modelled as previously described, i.e.

$$R = E_0 - \left(E_{MAX} \cdot \frac{U^{slope}}{(1 + U)^{slope}} \right)$$

Equation 7.5

where R is response, E_0 is baseline BIS, slope is an estimated parameter determining the shape of the surface and U is given as;

$$U = \frac{U_P + U_O + U_I}{U_{50}(\theta_P, \theta_I)}$$

Equation 7.6

Prior knowledge of the pairwise interactions, denoted here by β_{PO} , β_{PI} and β_{OI} , suggests additivity exists for each (as has been reported in the literature and in chapter 4).[59, 76, 128, 129, 143, 146]. β_{PO} , β_{PI} and β_{OI} were therefore fixed at 0. Thus Equation 7.4 was reduced, i.e.

$$U_{50}(\theta_P, \theta_I) = 1 - \beta_{POI} \cdot \theta_P \cdot \theta_I \cdot (1 - \theta_P - \theta_I)$$

Equation 7.7

7.1.3.2. Population parameter estimates

Data were analysed using nonlinear mixed effects models (NONMEM 7.1, Globomax LLC, Hanover, MD, USA). Population parameters and variances were estimated using the first order conditional estimation method with interaction option. A user-defined PRED routine was used and equations were integrated within ADVAN=11. Convergence criterion was three significant digits. Between-subject variability (η) was described using exponential error models. Residual unknown error was described using an additive error model. Covariance between elements of η was included where appropriate. Inclusion of an additional parameter, covariate effect or non-additive interaction parameter required a statistically significant improvement in the NONMEM OBJ between nested models (a reduction in OBJ > 6.64 based on a Chi square distribution $\alpha < 0.01$).

7.2. Results

A total of 60 patients were studied. Data from nine individuals were excluded: the IDAS drug barcode scanner was not functioning during three cases and consequently drug dosing entries were inaccurate and incomplete; one individual was excluded due to excessive alcohol use; one patient was given an intraoperative infusion of dexmedetomidine (a sedative that causes a dose-dependent reduction in BIS); and a further four individuals were excluded because of incomplete dosing data (for example, failure of the computer software to collect infusion data or connection failure). A total of 51 patients were included in this analysis. Intraoperative doses of clonidine (another intravenous sedative with actions at the α_2 receptor) were given to four patients. Only data prior to clonidine doses were included in the analysis for these patients. Patient demographics, and a summary of drugs administered, are given in Table 7.2.

Patient demographics:		Mean (Range)			
Age (y)		44 (19-65)			
Sex (M:F)		28: 23			
Height (cm)		169 (143-192)			
Weight (kg)		70 (24-120)			
BMI (kg.m ⁻²)		24 (8-46)			
Intraoperative drug administrations:		Cases	Administrations	Mean (SD) dose per case	Estimated Ce range
Intravenous anaesthetic					
Propofol		49	68	123 (60) mg	0-11.96 mcg.ml ⁻¹
Phenyl-piperidine opioids					
Alfentanil		1	1	1 mg	0-91.85 ng.ml ⁻¹
Fentanyl		48	119	88 (54) mcg	0-5.85 mcg.ml ⁻¹
Remifentanyl		1	Constant infusion	0.1 mcg.kg.min ⁻¹	0-1.51 ng.ml ⁻¹
Inhalation anaesthetics					
Desflurane		11	-	-	0-7.83 %vol
Isoflurane		1	-	-	0-1.64 %vol
Sevoflurane		48	-	-	0-5.89 %vol
Sedative					
Midazolam		38	38	2.1 (0.6) mg	0-0.16 mcg.ml ⁻¹
NMBD		38			

Table 7.2

Patient demographics and drug administrations. ‘Cases’ are the total number of cases in which each drug was administered and ‘Administrations’ gives the total number of administrations for all patients and the final column. NMBD=Neuromuscular blockade drugs. BMI=Body mass index. Ce=concentration in the effect site compartment. Midazolam was given to 75% of patients. NMBD were atracurium (31 cases), rocuronium (2 cases), suxamethonium (8 cases) and vecuronium (3 cases). Thirteen individuals did not receive NMBD.

Effect site concentrations calculated in Excel 2010 using PK–PD Tools [256] were initially used to model BIS response. However, between-subject variability estimates associated with the propofol, fentanyl and sevoflurane C_{e50} estimates were inflated. These were the most frequently administered drugs of each class (see Table 7.2). The increased variability on pharmacodynamic parameters probably occurred because variability associated with the pharmacokinetic models (and consequently, plasma and effect site concentration predictions) was ignored. Dosing information for propofol and fentanyl was subsequently included in the dataset and concentration predictions for these drugs made in NONMEM. The pharmacokinetic parameter estimates, covariate effects and variability estimates were fixed at literature values.[54, 55, 71, 243] Including the dosing and pharmacokinetic information in this manner reduced the between-subject variability and improved the ability of the model to estimate the other parameters. Including age as a covariate on the sevoflurane C_{e50} significantly improved the model ($\Delta \text{OBJ} = -9$, $P = 0.003$).

Estimating the interaction parameter for all three drug class pairs (Equation 7.4 and Equation 7.7) suggested synergy ($\beta_{\text{POI}} = 0.761$) but the value was small and the OBJ increased ($\Delta \text{OBJ} = +11.438$) indicating no improvement in the model fit. Additivity was therefore selected as best describing the relationship between the three drug classes (phenyl-piperidine opioid, intravenous and inhalation anaesthetics). The equation describing drug response was therefore further reduced to;

$$R = E_0 - \left(E_{\text{MAX}} \cdot \frac{U^{\text{slope}}}{(1 + U)^{\text{slope}}} \right), \text{ where } U = U_P + U_O + U_I$$

Equation 7.8

Midazolam is a sedative with anxiolytic properties that causes dose dependent reductions in EEG measures such as BIS.[38, 39, 53] Participants who received midazolam were included in the study because of its frequent administration prior to anaesthetic induction (Table 1.2), and because this reflects the nature of clinical practice at our centre. Midazolam has an estimated E_{MAX} (maximum drug effect) of 40 BIS units and an estimated C_{e50} of 303 $\text{ng} \cdot \text{ml}^{-1}$ for BIS effects.[53] Midazolam was given to 75% of participants in this study to facilitate induction of anaesthesia (Table 7.2) and so its effects on BIS were also added to the model. Albrecht *et al.* investigated midazolam pharmacokinetics in two age groups (24-28 y and 67-81 y), giving separate pharmacokinetic and keo parameter sets for BIS response in each age group. The parameter set given for patients aged 67-81 y was used to estimate plasma and effect site concentrations in this analysis. Normalised concentrations of

midazolam (U_M) were initially introduced into the model under the assumption that additivity exists for BIS with all other drugs. Response was calculated as above using modified units of propofol ($U_{P'}$) i.e.

$$R = E_0 - \left(E_{MAX} \cdot \frac{U^{slope}}{(1 + U)^{slope}} \right), \text{ where } U = U_{P'} + U_O + U_I$$

Equation 7.9

where

$$U_{P'} = U_p + U_M$$

Equation 7.10

Including midazolam effects in this way resulted in a modest improvement in model fit for one additional parameter ($\Delta OBJ = -5.258, P < 0.0218$). Again variability associated with the midazolam Ce_{50} estimate was high and so dosing information was included in the data file and a three compartment model as reported by Albrecht *et al.* used to make concentration predictions.[39] Parameter and variability estimates were fixed at those reported by Albrecht *et al.*[39] This resulted in a large improvement in the model ($\Delta OBJ = -90.13, P < 0.0001$).

A non-additive relationship between midazolam and propofol concentrations, assuming additivity exists between midazolam and all other drug classes (as it does for propofol),[137, 267] was then investigated once parameter estimates had been refined. An interaction function as described by Minto *et al.* for two drugs was investigated,[122] i.e.

$$U_{50}(\theta_M) = 1 - \beta_{PM} \cdot \theta_M + \beta_{PM} \cdot \theta_M^2, \text{ where } \theta_M = \frac{U_M}{U_M + U_P}$$

Equation 7.11

where β_{PM} is the parameter describing the interaction between propofol and midazolam, and $U_{P'}$ is instead calculated for Equation 7.8 as:

$$U_{P'} = \frac{U_P + U_M}{U_{50}(\theta_M)}$$

Equation 7.12

Inclusion of a non-additive interaction in this manner suggested strong synergy ($\beta_{PM}=2.38$) between propofol and midazolam but, as this did not improve the model fit ($\Delta \text{OBJ}=+126.048$), additivity was selected for this drug class pair. Including age as a covariate on the fentanyl Ce_{50} significantly improved the model ($\Delta \text{OBJ}= -13.544$, $P =0.0002$), but this effect was negligible. A summary of the model development process is given in Table 7.3. Final estimates for parameters and associated variances are given in Table 7.4, while estimates for covariance between population parameter variability (where included) is given in Table 7.5. Graphs of residuals and visual predictive checks are given in Figure 7.1 and Figure 7.2 respectively. NONMEM code for the final model is given in Appendix 7.

Model	OBJ	N parameters	ΔOBJ
Baseline model: includes phenyl-piperidine opioids; intravenous anaesthetic (propofol); inhalation anaesthetics	6786.537		
Non-additive interaction parameter for β_{POI} (pairwise parameters β_{PO} , β_{PI} and β_{OI} assumed to equal 0)	6797.975	+ 1	+ 11.438
Add midazolam (previously calculated effect site concentrations [†])	6781.279	+ 1	- 5.258 ($P < 0.0218$)
As above but predict effect site concentrations in NONMEM [‡]	6691.149	+ 7*	- 90.13 ($P < 0.0001$)
Refine model parameters ($\beta_{PM}=0$)	6552.503		
Non-additive interaction between propofol and midazolam (β_{PM} estimated at 2.38)	6678.551	+ 1	+ 126.048

Table 7.3

Pharmacodynamic model development. OBJ is NONMEM's objective function. [†]Predicted effect site concentrations were calculated in the data file using Excel (see methods) and used in modelling. [‡]Midazolam dosing information was included in the data file and pharmacokinetic parameters and variability estimates reported by Albrecht *et al.* were used to make concentration predictions in NONMEM.[39] *Additional parameters entered for the pharmacokinetic model were not estimated but fixed at values in the literature.

Parameter estimate	Estimate	%CV	95% CI*
E0	98.0 FIX	0 FIX	-
Ce _{50,Propofol} (mcg.ml ⁻¹)	2.46	105.36	1.91, 3.40
keo _{Propofol} (min ⁻¹)	0.19	198.75	0.10, 0.21
t _{1/2} keo _{Propofol} (min)	3.65		
Ce _{50,Fentanyl} (mcg.ml ⁻¹)	9.0·(-0.00001·(AGE-46)+1)	141.42	8.99, 9.99
keo _{Fentanyl} (min ⁻¹)	0.085	0 FIX	0.07, 0.23
t _{1/2} keo _{Fentanyl} (min)	8.15		
Ce _{50,Sevoflurane} (% vol)	1.32·(-0.01·(AGE-46)+1)	46.26	0.97, 1.63
Ce _{50,Midazolam} (mcg.ml ⁻¹)	0.264	-	0.07, 0.80
keo _{Midazolam} (min ⁻¹)	0.154	0 FIX	0.01, 0.20
t _{1/2} keo _{Midazolam} (min)	4.50		
Ce _{50,Alfentanil} (ng.ml ⁻¹)	646 FIX	-	-
Ce _{50,Remifentanil} (ng.ml ⁻¹)	20.1 FIX	-	-
Ce _{50,Desflurane} (% vol)	3.94	-	2.61, 4.96
Ce _{50,Isoflurane} (% vol)	0.66 FIX	-	-
Beta _{Propofol-Midazolam} (β)	0 FIX	-	-
Slope (γ)	2.56	38.73	2.42, 3.9
E _{MAX}	75.8	32.87	73.0, 76.4
Err _{add}	7.32		

Table 7.4

Pharmacodynamic parameter estimates. CV is the coefficient of variability; CI is the confidence interval; Err_{add} is the residual variability estimated for BIS measurements using an additive error model; Ce_{50,x} is the effect site concentration of drug that causes 50% maximal drug effect; t_{1/2}keo_x is the equilibration half-time; and keo_x is the equilibration rate constant (or 0.69/ t_{1/2}keo_x) for drug moving between plasma and effect site compartments. Note the small effect of age on the Ce₅₀ estimate for fentanyl. *A total of 224 bootstraps were completed in the time available.

	E_{MAX}	Slope (γ)
E_{MAX}	1	
Slope (γ)	-0.943	1
	$keO_{Propofol}$	$Ce_{50,Propofol}$
$keO_{Propofol}$	1	
$Ce_{50,Propofol}$	0.989	1

Table 7.5

Correlation of population parameter variability for the pharmacodynamic model.

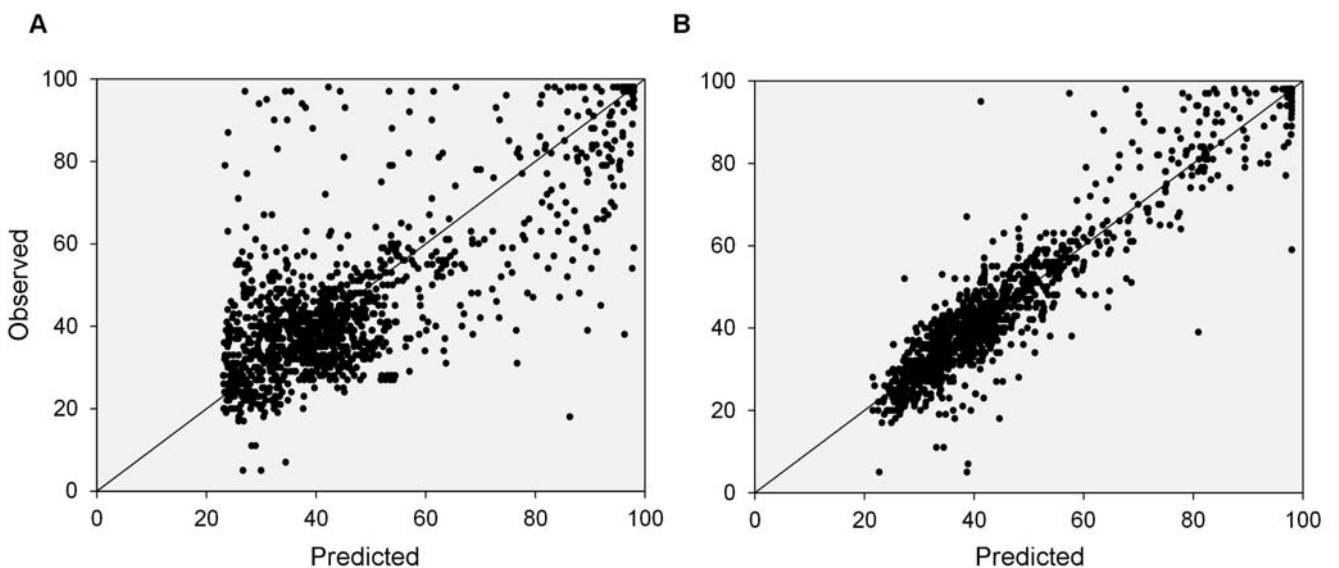


Figure 7.1

Quality of fit of the pharmacodynamic model for BIS response. Plots give (A) Population predictions for BIS against observed BIS values, and (B) individual Bayesian predictions for BIS based on adjusted parameters for the specific individual against observed BIS values. Units are BIS units (0-100, where 100 is resting and awake, and < 60 is recommended for surgical stimuli). A systematic trend in the population predictions can be seen (plot A) as a result of the maximal drug effect, E_{MAX} , which was estimated to be 76 BIS units.

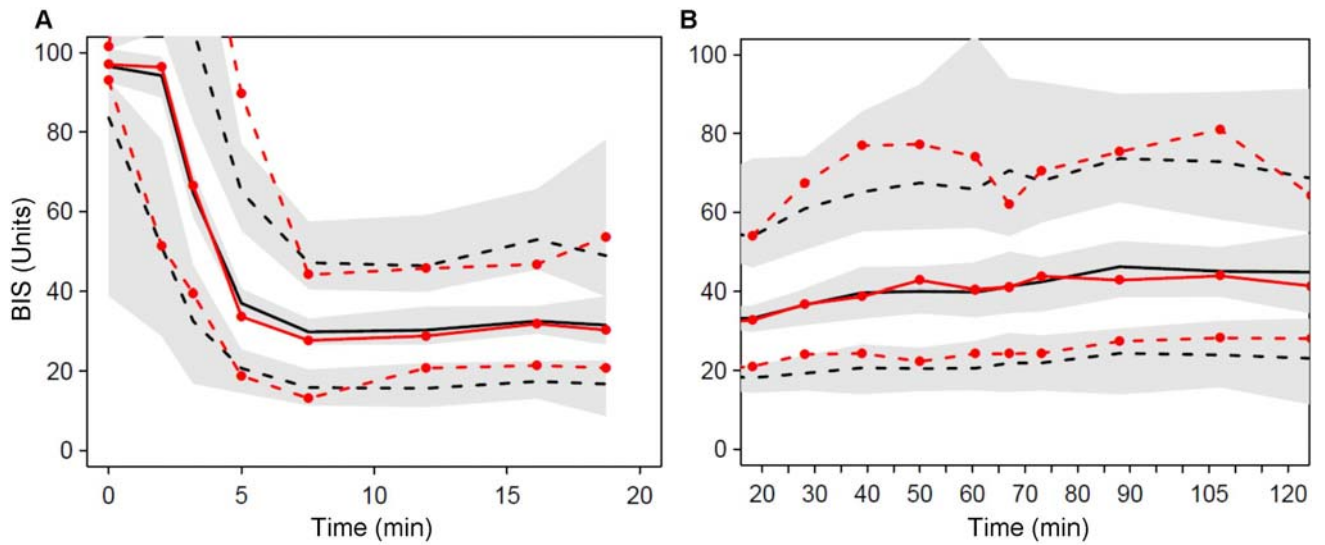


Figure 7.2

Prediction corrected visual predictive checks (PC-VPC) for pharmacodynamic model of BIS response. Plots give A) response over the first 20 min of anaesthesia (i.e. during the induction phase) and B) response from 20 min post induction to 120 min. The plots show median and 90% intervals (solid and dashed lines respectively). Prediction percentiles (10%, 50%, and 90%) for predictions (black lines) are overlaid with those of the observations (red lines with symbols). Grey shaded areas are 95% confidence intervals for the prediction percentiles.

7.3. Discussion

I have presented a model that describes BIS effect for any combination of several drugs that belong to the phenyl-piperidine opioid, intravenous and inhalation anaesthetic drug classes. The drugs include alfentanil, fentanyl and remifentanil (phenyl-piperidine opioids); propofol (intravenous anaesthetic); isoflurane, desflurane and sevoflurane (inhalation anaesthetics). The sedative midazolam was also included as it was frequently used as a premedicant, and 75% of participants received midazolam as an intravenous bolus. Additivity for BIS has been reported for phenyl-piperidine opioids with intravenous anaesthetics,[59, 146] phenyl-piperidine opioids with inhalation anaesthetics,[76, 128] and intravenous with inhalation anaesthetics.[129, 143] The interaction between midazolam and propofol was additive, although the interaction parameter suggested synergy. The predicted concentrations for midazolam were low in this study and investigating this relationship across a wider range of concentrations might lead to a non-additive interaction. The finding of additivity is dependent on the assumption that all other drug class pairs show additivity for BIS response, and that midazolam interacts with phenyl-piperidine opioids and inhalation anaesthetics in a manner similar to propofol (i.e. relationships are additive).

There are few reports in the anaesthetic literature of models that describe effects for more than two drugs in combination. Jeleazcov *et al.* assumed additivity between propofol, fentanyl and remifentanil for EEG measures and reported parameters for a three drug model of BIS response in children aged 1 to 16 years.[57] They used published pharmacokinetic models to predict plasma and effect site concentrations, as in the current analysis. Baseline BIS (E_0) in their study was 93.2 units with a maximal reduction in BIS (E_{MAX}) of 83 units. The authors estimated Ce_{50} parameters for each drug. An alternative method is to convert drugs to equivalents of another from the same class as was done by Johnson *et al.* and Syroid *et al.*[131, 132] These authors investigated time to emergence from anaesthesia for inhalation anaesthetics (isoflurane and sevoflurane) with phenyl-piperidine opioids (fentanyl and remifentanil), and used relative potencies from the literature to convert fentanyl concentrations to remifentanil equivalents. Propofol was used for induction of anaesthesia but residual concentrations remaining at emergence were low ($< 5.7 \text{ ng.ml}^{-1}$, associated with a Ramsey sedation score of 2). The authors assumed that propofol would not impact on the time to awakening at these levels and so did not include its effects in their analysis.[131]

The only combination of three drug classes that has been studied using methods like those reported in this analysis is that of alfentanil, midazolam and propofol for endpoints of hypnosis (defined as loss of response to verbal command) and anaesthesia (defined as loss of response to 5 s transcutaneous stimulus).[137] Short *et al.* found supra-additivity, or ‘synergism’, between each drug pair for these endpoints using the pharmacodynamic model described by Plummer and Short.[125] They could not demonstrate synergism for the three drug combination over that expected from the individual drug pairs, and this was later confirmed upon reanalysis of their data using the Minto model.[122] Vinik *et al.* also investigated loss of response to verbal command and confirmed synergism between alfentanil, midazolam and propofol.[139] These analyses correlated drug effect with administered dose,[122, 137, 139] i.e. pharmacokinetics were not considered and effects were not related to concentrations in the plasma or effect site. We now know that pharmacokinetic interactions exist between each of these drug pairs. For example, midazolam and propofol both reduce clearance of the other drug, and this can cause a 25% increase in propofol concentrations and a 30% increase in midazolam concentrations.[141, 142] Similarly, propofol concentrations increase by 18% when given with an infusion of alfentanil,[268] while propofol reduces alfentanil clearance by 15%. This led to a 10 fold increase in alfentanil plasma concentrations in one study.[90] These pharmacokinetic interactions potentially confound the results of the above pharmacodynamic studies (and might explain some of the observed synergy for anaesthetic endpoints), although the impact of each probably depends on the method of drug administration (infusion or bolus) and the doses given.[63]

The model developed in this study is dependent on the dose ranges studied, and on the parameter estimates used to predict plasma and effect site concentrations. A different choice of pharmacokinetic models may lead to different results. Midazolam plasma concentrations were predicted using the parameter set developed by Albrecht *et al.* in nine volunteers aged 67-81 y.[39] Parameters for volunteers aged 24-28 y were also available and may have been more appropriate for the population studied here.[39] The authors did not study individuals outside of these two distinct age groups and so it was not clear which parameter set was more appropriate for participants aged 29-66 y. I subsequently chose to use the parameter set for the older age group. Predicted plasma and effect site concentrations made using these two parameter sets are similar following a single 2 mg bolus dose of midazolam (as is typical of the patients in the current analysis) and so the impact of my selection is probably small. This is demonstrated in Figure 7.3 where predicted plasma concentrations for various midazolam pharmacokinetic models are depicted. Other models could have been used. For example, Greenblatt *et al.* also studied midazolam pharmacokinetics in healthy volunteers,[40] Maitre *et al.*

studied patients receiving midazolam for sedation[43] and Lichtenbelt *et al.* reported parameters for infusion data adjusted for co-administration of propofol.[142] The parameter set reported by Albrecht was ultimately selected because a keo of BIS response was reported and because predicted plasma and effect site concentrations were similar to those predicted by other reported parameter sets (refer to Figure 7.3).

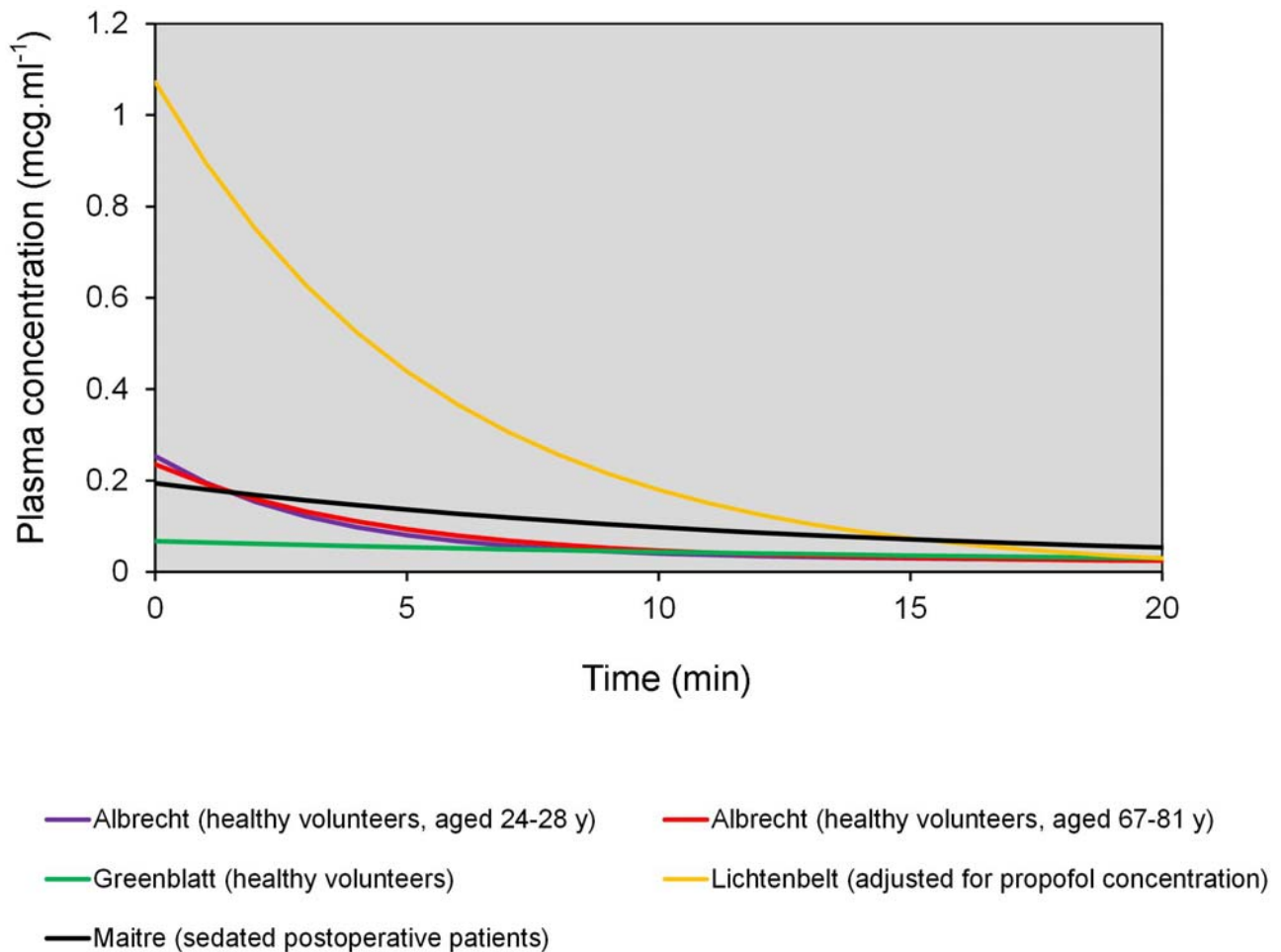


Figure 7.3

Predicted plasma concentrations of midazolam for different pharmacokinetic parameter sets. Concentration curves are for a single 2 mg bolus dose of midazolam in a 70 kg adult given at time=0 and assuming no co-administration of propofol. Concentration profiles are similar for pharmacokinetic models given by Albrecht *et al.*,[39] Greenblatt *et al.*,[40] and Maitre *et al.*,[43] with the exception of that described by Lichtenbelt *et al.* (see text for discussion).[142]

Only one participant received isoflurane for a short period. Isoflurane was given during induction and discontinued 13 min into the procedure. Sevoflurane was then used to maintain anaesthesia for the remainder of the case. The isoflurane C_{e50} parameter was unstable and influential on other model

parameters. This issue was expected given so few data and was resolved by fixing the parameter to literature estimates (0.7 %vol).[104, 105] One participant received remifentanyl as an infusion and one participant received alfentanil as a single bolus dose. The C_{e50} parameters for these drugs were also fixed at previously established estimates. Alfentanil and remifentanyl concentrations, normalised against these C_{e50} estimates, were summed with normalised concentrations of fentanyl to give the total opioid units for inclusion in the model. The C_{e50} used for alfentanil was that estimated in chapter 4 (646 ng.ml⁻¹) for infusion data and might not be appropriate for the individual in this study who received alfentanil as a bolus. The C_{e50} for fentanyl was estimated to be 9 ng.ml⁻¹, which is higher than those estimates reported by others for EEG effects (6.9-7.8 ng.ml⁻¹).[71, 243] The C_{e50} for fentanyl was associated with high variability (141.42 %CV), although other authors have made a similar observation when modelling opioid effects on EEG response.[71]

The C_{e50} estimate for propofol was 2.46 mcg.ml⁻¹. This is similar to that reported in chapter 4 (2.7 mcg.ml⁻¹). Others report a C_{e50} in the range of 2.3-4.5 mcg.ml⁻¹ for propofol effects on BIS when given alone,[38, 53, 59, 241, 242] and 2-5 mcg.ml⁻¹ when given in combination.[129, 143, 150, 155] The C_{e50} estimate for sevoflurane was 1.32 %vol. This is usually estimated to be between 1.12-1.70 vol%,[105-109, 111] although Dahan *et al.* reported a sevoflurane C_{e50} of 0.9 %vol using response surface methods.[76] Rheberg *et al.* investigated EEG slowing effects for inhalation anaesthetics and reported a C_{e50} for desflurane similar to that estimated in this study (3.48 %vol versus 3.94 %vol respectively).[105] The C_{e50} estimate for midazolam was 0.264 mcg.ml⁻¹. Albrecht *et al.* estimated a C_{e50} for midazolam effects on BIS of 0.2 mcg.ml⁻¹ in volunteers aged 67-81 y and 0.5 mcg.ml⁻¹ in volunteers aged 24-28 y.[39]

The maximal effect (E_{MAX}) was a reduction in BIS of 76 units and slope was 2.56. These estimates are similar to those reported in chapter 4 for alfentanil and propofol effects on BIS, where the E_{MAX} was 80 units and the slope was 3.1. As in chapter 4, a constraint model was used to estimate E_{MAX} while ensuring that it did not take on impossible values in each individual (i.e. negative values). Applying narrow constraints to parameters might force them to take on values that are not supported by the data, or influence those parameters with which there is correlation. Here the value of E_{MAX} was allowed to vary over a wide range of values and the constraint on negative values reflects reality so this probably had little effect on parameter estimation. Again, the impact of the E_{MAX} parameter is visible in the residual plots (Figure 7.1). Bruhn *et al.* suggested that BIS values less than 30 are linearly associated

with a burst suppression ratio greater than 40%,[269] which might explain why my model was unable to adequately describe this part of the concentration-response relationship. The choice to include an E_{MAX} parameter probably has little impact when taken in context of the typical clinical BIS range. An alternative way forward might be to include a composite sigmoidal model to describe these two apparently distinct phases of the BIS response (or algorithm).

Variability associated with model parameters was high. This was improved by including pharmacokinetic models for the three most commonly used intravenous drugs (fentanyl, propofol and midazolam, Table 7.2). Parameter and variability estimates were fixed at those reported in the literature.[39, 54, 71] Keo parameters for propofol and midazolam were estimated. The propofol keo estimate was 0.19 min^{-1} ($t_{1/2 \text{ keo}}$ of 3.7 min). This describes a similar onset of propofol effect as estimated in chapter 4 (keo 0.2 min^{-1} , $t_{1/2 \text{ keo}}$ 3.5 min), and for infusion data when a 10 s lag is included in the model (keo 0.17 min^{-1} , $t_{1/2 \text{ keo}}$ 4.1 min).[240] Struys *et al.* reported a $t_{1/2 \text{ keo}}$ 4.1 min (keo of 0.32 min^{-1}) for infusion and bolus data.[239] A keo of 0.14 min^{-1} ($t_{1/2 \text{ keo}}$ 4.8 min) has been recently reported for use with the Schnider parameter set for BIS response.[262] The time to peak effect (T_{peak}) for the Schnider parameter set when used with a keo of 0.14 min^{-1} is 2.45 min,[262] which is 51 s longer than the 1.6 min predicted with a keo of 0.456 min^{-1} (illustrated in Figure 7.4, green line). The effect profile for the current study (red line) fits somewhere between these estimates with a peak effect from propofol occurring at 2.2 min. Albrecht *et al.* estimated midazolam keo values of 0.11 min^{-1} ($t_{1/2 \text{ keo}}$ 6.3 min) in patients aged 24-28 y, and 0.08 min^{-1} ($t_{1/2 \text{ keo}}$ 8.7 min) in patients aged 67-81 y.[39] These estimates are contrasted by that of Billard *et al.* who reported a midazolam keo value of 0.02 min^{-1} ($t_{1/2 \text{ keo}}$ 33 min) for BIS effects in healthy adult volunteers.[53] A keo estimate of 0.15 ($t_{1/2 \text{ keo}}$ 4.5 min) in the current analysis is similar to that given by Albrecht *et al.* and so appears to be reasonable.

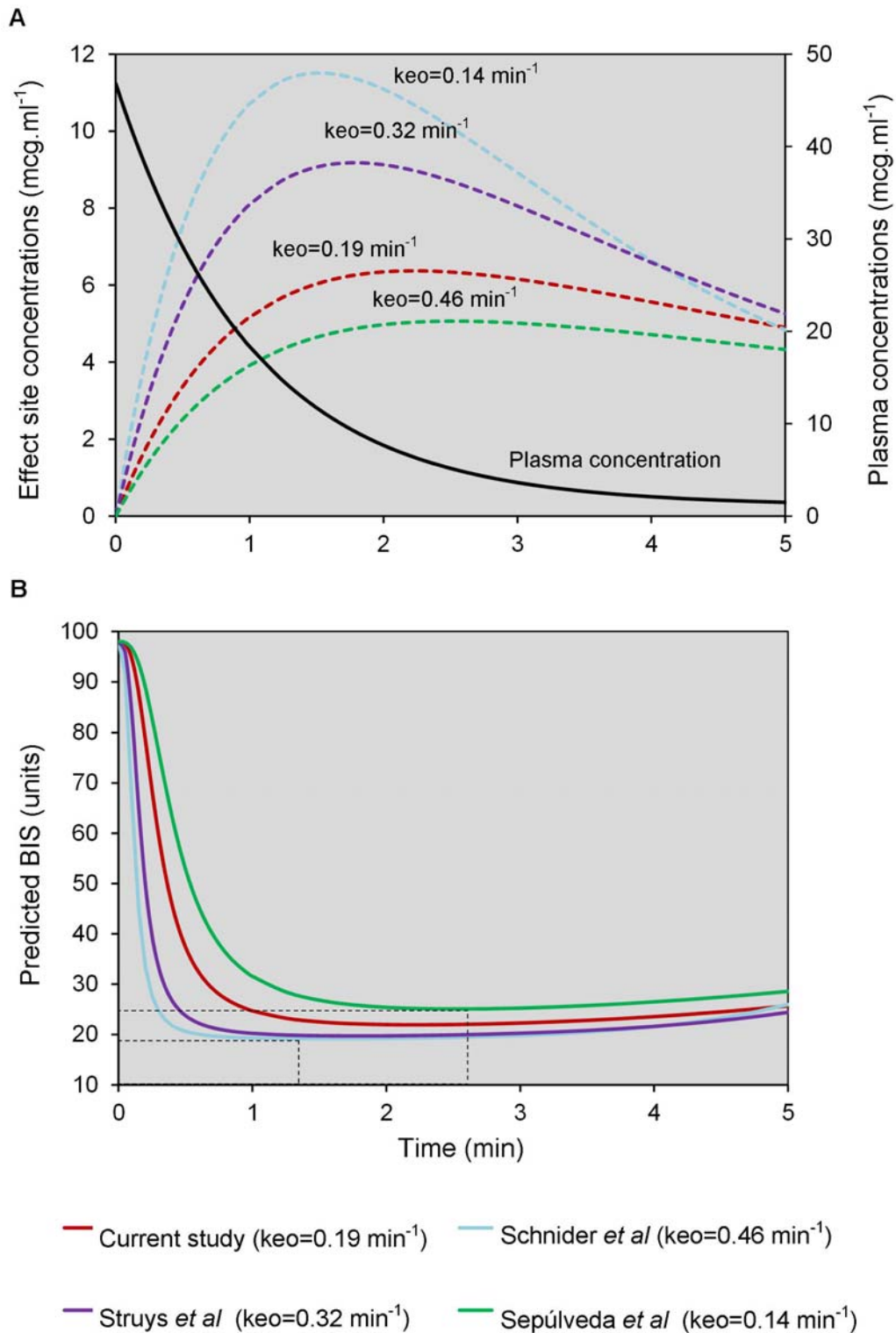


Figure 7.4

The effect of the keo parameter on the onset of BIS effect for propofol. Concentrations and effects are for a 70 kg, 170 cm, 40 y male given a 200 mg bolus of propofol (at time=0 min). A) Simulated effect site concentrations using the parameter set given by Schnider *et al.*,[54] for various keo estimates.[55, 239, 262] Simulated plasma concentrations are depicted also (solid black line in plot A). B) Simulated BIS effect corresponding to each effect site concentration profile. Time to peak effect is indicated by the broken line in plot B for keo parameters as given by Schnider *et al.* (T_{peak}=1.6 min),[54] and by Sepúlveda *et al.* (T_{peak}=2.45 min).[262] A T_{peak} of 2.2 min is calculated for this study.

The finding of an additive interaction between propofol and midazolam for BIS is interesting because this relationship has not been well studied. Synergism for this drug pair has been shown for sedation and loss of consciousness,[37, 122, 137, 139, 140] with the combination estimated to be 1.44 times as potent as either drug given alone.[37] It is important to note that the authors of these studies used larger doses than those given to the participants of the current study. For example, just two patients in this study received midazolam doses greater than 2 mg, while the remainder received doses ranging from 1-2 mg. A dose of 2 mg equates to 0.03 mg.kg^{-1} in a 70 kg adult, compared to doses $> 0.2 \text{ mg.kg}^{-1}$ midazolam given by Short *et al.*[137] Premedication with midazolam 20 minutes before induction of anaesthesia reduces the dose of propofol required to cause EEG burst suppression by 20%,[270] but whether this arises from an additive or non-additive interaction has yet to be determined. Additivity occurs when drugs exert their effects *via* the same mechanism but *in vivo* observations of additivity do not prove this.[119] Some interactions are considered synergistic by definition because one drug is incapable of causing the endpoint in question when given alone. The inability of midazolam to cause anaesthesia is a good example of this.[137] Both midazolam and propofol cause their effects (at least in part) by binding the inhibitory γ -aminobutyric acid (GABA) neurotransmitter, but they probably bind distinct receptor sites.[138] The binding site for midazolam is thought to be located between the γ_2 and α_1 subunits of the GABA_A receptor,[271] while *in vivo* studies in ‘knock-in’ mice implicate the β_3 subunit for the hypnotic effects of propofol (measured using the righting reflex).[272]

This is the first study in which a concentration-response curve for the effects of midazolam with propofol on BIS is provided, although the analysis also includes the effects of two other drug classes and the range of midazolam doses was small. The potential for pharmacokinetic interactions to confound the pharmacodynamic relationship between midazolam and propofol cannot be precluded as drug concentrations were not studied. Midazolam was incorporated into the model under the assumption that it behaves similarly to propofol with respect to its interaction with phenyl-piperidine opioids and the inhalation anaesthetics. This might not be the case although midazolam, like propofol, shows synergism when given with alfentanil and fentanyl to cause sedation.[122, 137, 139, 153, 273, 274] One study reported a synergistic relationship (by definition) between midazolam and halothane for an endpoint of MAC (minimum alveolar concentration required to prevent movement to noxious stimuli in 50% of patients).[138, 275] The results presented for the current analysis require confirmation with a carefully planned pharmacokinetic-pharmacodynamic study that investigates the relationship between propofol and midazolam across a wider range of midazolam doses.

I have grouped drugs according to their class for the purposes of this analysis. This has allowed me to model the effects of eight drugs in total. I have studied an endpoint of BIS, for which combined effects appear to be additive in the concentration ranges used clinically. Calculation of total units of combined drugs ('U', given in Equation 7.9) might be modified according to drug class. For example, I included midazolam in the calculation of U_p to give modified units of propofol, or $U_{p'}$. The decision to combine propofol and midazolam units in this model was based on several studies that suggest the midazolam - phenyl-piperidine opioids and the midazolam - inhalation anaesthetic relationships are similar to those shown for propofol with these drug classes.[137, 138, 267, 275] I have essentially combined propofol and midazolam into a single drug class for the purposes of the model, although I have classified these throughout this thesis as an intravenous anaesthetic and a sedative respectively to differentiate between their ability (or inability) to cause anaesthesia when given alone. Combining these drugs together also provided an opportunity to investigate potential interactions between propofol and midazolam which have been shown for other endpoints.[37, 122, 137, 139, 140] I used the interaction function given by Minto *et al.* to investigate a non-additive relationship between these drugs,[122] but I might also have used that described by Greco *et al.* (given in Equation 7.13), or a reduced version of this whereby a synergistic relationship is assumed (given Equation 7.14).[69, 119, 130] Similarly, these equations could be applied to describe non-additive relationships within other drug classes (such as the opioid or inhalation anaesthetic drug classes) should they be required.

$$U_{p'} = U_p + U_M \cdot \beta_{PM} \cdot U_p \cdot U_M$$

Equation 7.13

$$U_{p'} = U_p \cdot (1 + U_M)$$

Equation 7.14

My work is based on several assumptions; in particular I have assumed additivity between phenyl-piperidine opioid, intravenous and inhalation anaesthetic drugs. However, these assumptions are based on carefully designed studies of the interactions existing between these drug pairs in controlled study conditions and so they are well founded. The model I have presented might conceivably be adapted for more drugs or other drug combinations, although a solid understanding of how drug pairs interact for the endpoint in question would be required.

This study has several limitations, some of which have been discussed above. I did not attempt to control for the level of surgical stimuli experienced by each participant and this probably contributed to the high estimates of variability seen here. Arterial access was not considered standard care for any of the participants and it was not practical to measure drug concentrations (because of time and financial constraints). Plasma and effect site concentrations were instead estimated using reported parameters fixed at literature estimates. The parameter sets by Schnider *et al.*, Minto *et al.* and Scott *et al.* were used for propofol, remifentanyl, fentanyl and alfentanil respectively.[54, 71, 73, 255] These were chosen because they have been clinically validated although the performance of the Schnider parameter set is poor when used to predict propofol concentrations following a bolus dose.[49, 239, 261, 276] The Schnider and Minto parameter sets were linked to a response surface parameter set and used to drive drug infusions to BIS targets in chapter 6, so their use in the current analysis also follows logically from this work. End-tidal concentrations were assumed to be proxies for concentrations of inhalation anaesthetics in the plasma, and keo parameters were used to describe the transfer of drug from plasma to effect site compartments.[58, 104] An alternative approach is to use a physiologic model to describe sevoflurane kinetics,[101] as Johnson *et al.* did in their analysis.[131]

Summary

There are several future directions for the work presented here. Models of combined drug effects can be used to predict optimal dose combinations for clinically relevant endpoints. For example, the optimal effect site concentrations required to prevent movement to surgical stimuli, whilst still providing the shortest time to recovery, have been identified for alfentanil and remifentanil with propofol.[69, 277] This information can be incorporated into new displays that predict pharmacological profiles for anaesthetic drugs when given together. These displays, such as the Navigator Applications Suite (GE Healthcare, Finland), help anaesthetists to visualise the future ‘state’ of their patients and titrate drugs accordingly.[278] They might also be useful for students learning about pharmacology in anaesthesia. BIS monitoring gives no information on the analgesic state of the patient and so it cannot reliably predict responsiveness to noxious stimuli such as surgical incision, but it does provide a means to titrate drug dosing for depth of anaesthesia. Several authors have correlated BIS to clinical endpoints such as loss of consciousness and awakening,[38, 147] and BIS monitoring for dose titration during sedation has been identified as a promising area where combination models such as that given here might be useful.[279] Lastly, this model might be used for simulating depth of anaesthesia in a simulated patient currently used to for teaching and research in medicine. I focus on this idea in the next chapter.

Chapter 8. Using complex models to simulate anaesthesia

Background: The METI[®] HPS[™] is a sophisticated simulation tool that allows us to recreate complex anaesthetic and surgical scenarios for teaching, training and research. However, depth of anaesthesia is not typically simulated. The model developed in chapter 7 might be useful for simulating BIS response in this setting.

Methods: The model from chapter 7 was used to simulate two simple anaesthetic scenarios: a healthy adult female undergoing anaesthesia using target-controlled infusion of propofol and remifentanyl, followed by sevoflurane; and a healthy adult male undergoing anaesthesia with propofol, fentanyl and sevoflurane. Models from the literature that describe loss of responsiveness (LOR) and return of responsiveness (ROR) were used to construct probability curves for LOR and ROR. Between-subject variability (BSV) on pharmacokinetic and pharmacodynamic parameters, and residual error, were incorporated into simulations to demonstrate how realistic BIS responses might be achieved.

Results: Models describing loss of responsiveness (LOR) and return of responsiveness (ROR) based on propofol, sevoflurane and remifentanyl concentrations are available in the literature for these clinical endpoints. These models could be combined with the current model to provide simulated BIS values with automated eye closing and opening in the METI[®] HPS[™]. Residual variability of 7.7 BIS units or less (as reported in chapters 4 and 7) gives believable variation in BIS response while still ensuring that values fall within 10% of the population mean at all times.

Conclusions: The model presented in chapter 7 provides a framework for simulating BIS response to various drug interventions in the METI[®] HPS[™]. Variability can be adjusted to suit the purpose of the scenario and BIS response can be correlated to clinical endpoints of interest. This may be helpful in automating some responses (i.e. eye closure during anaesthetic induction).

8.1. Introduction

Over the course of my research I have developed a two-drug model for propofol with alfentanil, established a relative potency for alfentanil and remifentanil with propofol, prospectively tested a pharmacokinetic-pharmacodynamic model for combined response during surgical stimulus under anaesthesia, and developed a new model for combined response for multiple drug classes. This model for multiple drug classes includes the effects of phenyl-piperidine opioids, intravenous and inhalation anaesthetics, and also the effects of the commonly used sedative midazolam. It could be used to simulate BIS response for a range of drug interventions or anaesthetic scenarios.

The time spent at the Simulation Centre for Patient Safety, University of Auckland, represents their first experience in a surgical or anaesthesia setting for many undergraduate medical students. The METI[®] Human Patient Simulator (HPS)[™] (Medical Education Technologies, Inc; Sarasota, FL) breathes and expires anaesthetic gases using a mechanical lung model, demonstrates clinical signs (such as heart and chest sounds), and is programmed to respond to a wide range of clinical interventions and drugs. Our METI[®] HPS[™] is connected to real physiological clinical monitors, and set up in a fully integrated operating room with an anaesthetic machine and preoperative assessment area. The centre is used to acquaint students with operating rooms and teach basic life support skills, as well as for on-going education of experienced clinicians and clinical teams. Research is also conducted at the Simulation Centre for Patient Safety with a focus on human factors, team work and the provision of safe patient care. The METI[®] HPS[™] is marketed, amongst other things, as an anaesthetic simulator but does not come with the models required to simulate depth of anaesthesia or even EEG monitoring. Loss of consciousness is conveyed in our METI[®] HPS[™] by loss of verbal response and eye closing. Eye closing is not fully model-driven at our centre but is instead started and controlled by the person running the simulation. There are no indications of increasingly ‘light’ or ‘deep’ anaesthesia once the patient has been anaesthetised. Experienced clinicians who participated in educational courses at our simulation centre reported that they were often unsure of how deeply anaesthetised their simulated patient was, and that they predominantly relied on blood pressure monitoring to ensure adequate anaesthesia.[36] Physiological measures such as pulse and blood pressure are crude means of assessing depth of anaesthesia.

One way we might improve our simulation of depth of anaesthesia is to include a measure of processed EEG monitoring such as BIS. This would be a useful addition in the METI[®] HPS[™] for students and experienced clinicians alike. It gives a quantifiable marker of the depth of anaesthesia produced by their interventions in the simulator and supplements the information available on the patient state through other forms of monitoring (such as blood pressure and heart rate monitors) to convey adequate anaesthesia. I have used an endpoint of BIS throughout my work as this is a readily recognised, well-researched index of processed EEG that lends itself to use in simulated settings. BIS has the added benefit of being a regularly used form of monitoring that most medical students will encounter at some point during their training at the University of Auckland.

Several methods of simulating BIS exist. These include the screen-based BIS Titration SimulatOR 3.0 (Covidien Medical, Boulder, CO, USA)[280] and the ‘HPS interface’ (developed by AQAI Simulation Center Mainz, Mainz, Germany)[281]. The HPS interface provides a means of simulating BIS response in the METI[®] HPS[™]. The METI[®] HPS[™] software calculates plasma and effect site drug concentrations following infusion and bolus doses made by the user for simulation of its model-driven responses. The HPS interface calculates BIS from the outputted effect-site concentrations of propofol and remifentanyl. The interface software includes a ‘stimulus’ button *via* which technicians can cause a transient spike in BIS response to convey inadequate anaesthesia during noxious stimuli. The HPS interface has already been integrated into the METI[®] HPS[™] software at our centre. The effects of inhalation anaesthetics on BIS do not appear to be included in the simulation although the software has been designed so that the models may be modified as needed. Previous work in our department suggests that the current BIS response of the simulator following a standard bolus dose of propofol was unrealistic (a 100 mg bolus of propofol produced a maximal response to just 77 BIS units; we might expect loss of consciousness and lower BIS with this dose).[36] However, the software might provide a platform for implementing the current model in the METI[®] HPS[™] software.

The aim of the work I present in this chapter was to demonstrate how the model for BIS response for multiple drug classes (presented in chapter 7) might be applied to a simulation setting. I use the model to simulate patient responses for two basic anaesthetic scenarios. I demonstrate how the model might be correlated to loss of consciousness in the first scenario. I then discuss how variability in response might be included using the second scenario as an example. Implementing the model in the current METI[®] HPS[™] software is a matter of programming and is beyond the scope of this work.

8.2. Methods

8.2.1 The model

The following drugs are included in the model:

Desflurane (inhalation anaesthetic)

Isoflurane (inhalation anaesthetic)

Sevoflurane (inhalation anaesthetic)

Propofol (intravenous anaesthetic)

Midazolam (sedative)

Alfentanil (phenyl-piperidine opioid)

Fentanyl (phenyl-piperidine opioid)

Remifentanil (phenyl-piperidine opioid)

The following assumptions are made about the model:

1. Inhalation anaesthetics (desflurane, isoflurane and sevoflurane) behave similarly for BIS effects and can therefore be converted to inhalation anaesthetic equivalents in the model,[76, 128, 131, 132]
2. Phenyl-piperidine derivatives (alfentanil, fentanyl and remifentanil) behave similarly for BIS effects and can therefore be converted to opioid equivalents in the model,[59, 132, 146, 243]
3. Midazolam behaves similarly to propofol in the model with respect to its interaction with phenyl-piperidine opioids and inhalation anaesthetics,[37, 137]
4. The pharmacokinetics of each drug can be adequately described for simulation using published population-derived pharmacokinetic models,
5. End-tidal concentrations of inhalation anaesthetic are equivalent to concentrations in the plasma compartment,
6. Neuromuscular blocking drugs (NMBDs) do not affect anaesthetic depth as measured by BIS,
7. Antibiotics do not alter the pharmacokinetic or pharmacodynamic profiles of the modelled drugs.

Simulated patients are limited to a weight range of 40-120 kg, height range of 140-190 cm, body mass index (BMI) $<35 \text{ kg.m}^{-2}$ and age range of 18-90 y. These demographic ranges extend beyond those of the population used to develop the pharmacodynamic model (weight 24-99 kg; height 143-192 cm; age 19-65 y; and BMI $8\text{-}34 \text{ kg.m}^{-2}$, given in chapter 7), but should not cause unrealistic results when used in a simulation setting.

Pathology can have significant and varied effects on drug pharmacokinetics. Changes in plasma proteins, cardiac output, body water volume, and tissue pH (during sepsis for example) may alter drug distribution and clearance.[282, 283] Pathology of the liver reduces clearance of those drugs eliminated *via* hepatic pathways, by either decreased hepatic blood flow or reduced hepatic function.[284] Respiratory changes also impact drug pharmacokinetics by decreasing cardiac output and blood flow to organs such as the liver.[285]

For simplicity, the following assumptions are made about the patient:

1. Normal sympathetic tone exists at the start of the simulation,
2. The simulated patients have no pathology that would alter the pharmacokinetic or pharmacodynamic profiles of the modelled drugs,
3. Neuromuscular blockade is maintained through the procedure (using vecuronium, a NMBD with minimal effects on the cardiovascular system), and no pharmacokinetic or pharmacodynamic interactions exist between the NMBD and the drugs included in the model,
4. Respiration is controlled by mechanical ventilation.

Plasma concentrations for each drug administered were predicted using pharmacokinetic parameter sets from the literature. Parameter sets were those used in chapter 7, selected because they a) have been clinically validated in a patient population and shown to have reasonable performance, b) report an appropriate keo parameter for BIS or EEG response and c) include covariate models for those known to be important.

The METI[®] HPS[™] includes a sophisticated lung and gas model which is routinely used at our centre. End-tidal concentrations of volatiles expired by the simulator are measured by the anaesthetic machine and outputted to both the clinical displays and the control room software. End-tidal concentrations for inhalation anaesthetics generated by the METI[®] HPS[™] could be fed directly into the model and BIS effects calculated, but in this work, end-tidal concentrations were calculated using a two compartment model as described by Rietbrock *et al.*[286] Parameter estimates were those provided by Wissing *et al.* 2000.[103, 286] I assumed for the simulation that: fresh gas flow > tidal volume so that the concentration of inhalation anaesthetic delivered was equal to the concentration inspired by the patient; respiratory rate was equal to 10 breaths.min⁻¹ throughout; tidal volume was equal to 8 ml.kg⁻¹; and alveolar ventilation (\dot{V}_{alv}) was equal to tidal volume minus the dead space volume (set at 2.0 ml.kg⁻¹).[286] Uptake (U) of inhalation anaesthetic at time t was calculated as:

$$U(t) = \dot{V}_{alv} [F_I - A_1]$$

Equation 8.1

where F_I is the fraction of inhalation anaesthetic inspired and A_1 is the amount of inhalation anaesthetic in compartment 1.[286] A_1 was calculated as:

$$A_1 = A_1 + k_{21}A_2 - k_{12}A_1 + U(t)$$

Equation 8.2

where A_2 is the amount of inhalation anaesthetic in compartment 2. A_2 was calculated as:

$$A_2 = A_2 + k_{12}A_1 - k_{21}A_2$$

Equation 8.3

Amounts at time t were converted to concentrations by dividing by the volume (V) of the compartment,[286] i.e. for compartment 1:

$$C_{ET} = A_1/V_1$$

Equation 8.4

The pharmacokinetic parameter sets selected for each study drug are summarised in Table 6.4. Pharmacokinetic parameter estimates used for each drug included in the simulation are summarised in Table 8.2. Pharmacodynamic parameter estimates used in the simulation are given Table 4.4.

Drug class*	Drugs included	Parameter set	Covariates included
Inhalation anaesthetic [†]	Desflurane	Wissing <i>et al.</i> 2000 [103]	WT
	Isoflurane	Wissing <i>et al.</i> 2000 [103]	WT
	Sevoflurane	Wissing <i>et al.</i> 2000 [103]	WT
Intravenous anaesthetic	Propofol	Schnider <i>et al.</i> 1998 [54, 55]	HT, WT, AGE, LBM
Phenyl-piperidine opioids	Alfentanil	Scott <i>et al.</i> 1985 [71, 243]	
	Fentanyl	Scott <i>et al.</i> 1985 [71, 243]	
	Remifentanil	Minto <i>et al.</i> 1997 [73, 255]	AGE, LBM, SEX
Sedative	Midazolam	Albrecht <i>et al.</i> 1999* [39]	

Table 8.1

Parameter sets used to describe the pharmacokinetics of each drug allowed in the model. [†]End-tidal concentrations were calculated using a two-compartment model as described by Rietbrock *et al.* for this study,[286] although end-tidal concentrations generated by the METI[®] HPS[™] might be fed directly into the model (as was done in chapter 7 using observed end-tidal concentrations). I assumed for the simulation that: fresh gas flow>tidal volume so that the concentration of inhalation anaesthetic delivered=the concentration inspired by the patient; respiratory rate=10 breaths.min⁻¹; tidal volume=8 ml.kg⁻¹; and alveolar ventilation=tidal volume minus the dead space volume (set at 2.0 ml.kg⁻¹).[286] I also assumed that end-tidal concentrations of inhalation anaesthetic roughly represent the concentration in the plasma compartment. HT=height (cm), WT=weight (kg) and LBM=lean body mass (kg). *Albrecht *et al.* investigated midazolam pharmacokinetics in two age groups (24-28 y and 67-81 y), and gave two separate pharmacokinetic parameter sets; that given for the older age group was used in this analysis, see chapter 7 for discussion.

	V1 (l)	V2 (l)	V3 (l)	CL1 (l.min ⁻¹)	CL2 (l.min ⁻¹)	CL3 (l.min ⁻¹)
Propofol	4.27	18.90+scalar	238.00	1.89+scalar	1.29+scalar	0.84
Scalar		-.39·AGE-53		(TBW-77)·.05+(LBM-59)·-.07)+(HT-77)·.02	-.02·AGE-53	
Midazolam	8.50	18.57	63.03	0.30	0.95	0.44
Alfentanil	2.20	5.60	14.10	0.20	1.30	0.20
Fentanyl	12.70	49.30	296.90	0.70	4.70	2.30
Remifentanyl	5.10-scalar	9.82-scalar	5.42	2.60-scalar	2.05-scalar	0.08-scalar
Scalar	.02·Age-40+.07·LBM-55	.08·Age-40+.11·LBM-55		.02·Age-40+.02·LBM-55	.03·Age-40	.001·Age-40
Desflurane*	5.25	42.84	-	-	0.49	-
Isoflurane*	13.72	287.8	-	-	2.15	-
Sevoflurane*	7.42	114.38	-	-	0.91	-

Table 8.2

The pharmacokinetic parameters and covariate effects used for simulations. *Values given are for a 70 kg individual; note there is no clearance from the central compartment included in the model for inhalation anaesthetics (inter-compartmental clearance between compartments 1 and 2 is included only).

Parameter estimate	Estimate	Origin of parameter
$Ce_{50,Propofol}$ (mcg.ml ⁻¹)	2.46	Chapter 7
$ke_{OPropofol}$ (min ⁻¹)	0.19	Chapter 7
$Ce_{50,Midazolam}$ (mcg.ml ⁻¹)	0.26	Chapter 7
$ke_{OMidazolam}$ (min ⁻¹)	0.15	Chapter 7
$Ce_{50,Fentanyl}$ (mcg.ml ⁻¹)	9.0	Chapter 7
$ke_{OFentanyl}$ (min ⁻¹)	0.09	Chapter 7
$Ce_{50,Sevoflurane}$ (% vol)	$1.32 \cdot (-0.01 \cdot (AGE-46)+1)$	Chapter 7
$ke_{OSevoflurane}$ (min ⁻¹)	$0.38 \cdot (-0.008 \cdot (AGE-33.5)+1)$	Cortinez <i>et al.</i> 2008[58]
$Ce_{50,Alfentanil}$ (ng.ml ⁻¹)	646.00	Chapter 4
$ke_{OAlfentanil}$ (min ⁻¹)	0.77	Scott <i>et al.</i> 1985 [71, 243]
$Ce_{50,Remifentanil}$ (ng.ml ⁻¹)	20.10	Bouillon <i>et al.</i> 2004[59]
$ke_{ORemifentanil}$ (min ⁻¹)	$0.6-0.007 \cdot (AGE-40)$	Minto <i>et al.</i> 1997 [73, 255]
$Ce_{50,Desflurane}$ (% vol)	3.94	Chapter 7
$ke_{ODesflurane}$ (min ⁻¹)	0.5	Kreuer <i>et al.</i> 2009 [104]
$Ce_{50,Isoflurane}$ (% vol)	0.66	Kreuer <i>et al.</i> 2009, Rehberg <i>et al.</i> 1999[104, 105]
$ke_{OIsoflurane}$ (min ⁻¹)	0.2	Kreuer <i>et al.</i> 2009 [104]
$\text{Beta}_{Propofol-Midazolam}$ (β)	0	Chapter 7
Slope (γ)	2.56	Chapter 7
E_{MAX}	76	Chapter 7

Table 8.3

The pharmacodynamic parameters and covariate effects used for simulations. $Ce_{50,x}$ is the effect site concentration of drug that causes 50% maximal drug effect; and ke_{Ox} is the rate constant (or $0.69/t_{1/2}ke_{Ox}$) for drug moving between plasma and effect site compartments. Baseline BIS (E_0) was 98 units.

8.2.2 Method of simulation

The proposed method of simulating BIS response profiles is summarised below in Table 8.4. Simulations reported here were performed in Excel 2010 using PK–PD Tools for Excel© 2009 (see section 6.2.4.2).[256]

Steps to simulating BIS response profile	Comments
'Patient' selected (age, sex, height, weight)	Selected by the simulation technician
Selected drugs administered to patient	Given by the user
Pharmacokinetic models used to predict plasma concentrations of each drug <ul style="list-style-type: none"> - Exponential variability model included on pharmacokinetic parameters* - Covariate effect models included where applicable 	As given in Table 8.2, or as calculated by the simulation software (i.e. the METI® HPS™)
Transfer of drugs to effect site compartments using keo values (for an endpoint of BIS) <ul style="list-style-type: none"> - Exponential variability model included on keo parameters* - Covariate effect models included where applicable 	As given in Table 4.4
Concentrations of each drug in the effect compartment are normalised to 'units' of drug by division of the appropriate Ce ₅₀ estimate <ul style="list-style-type: none"> - Exponential variability model included on Ce₅₀ parameters* - Covariate effect models included where applicable 	As given in Table 4.4
Units of drugs belonging to the inhalation anaesthetic drug class are summed	
Units of drugs belonging to the phenyl-piperidine opioid drug class are summed	
Units of intravenous anaesthetic (propofol) and sedative (midazolam) are combined and modified according to the interaction parameter (β) and the ratio of propofol to midazolam present	As given in Table 4.4 and Chapter 7
Combined effects are predicted for resulting units of inhalation anaesthetic drug, phenyl-piperidine opioid, intravenous anaesthetic (propofol) and sedative (midazolam) <ul style="list-style-type: none"> - Baseline BIS response of 98 (awake patient) assumed 	As given in Chapter 7
Typical residual unknown error is added to response predictions	As given in Table 4.4

Table 8.4

Proposed method of using complex models to simulate depth of anaesthesia. Ce₅₀=effect site concentration associated with 50% the maximal effect. *Variability is included or adjusted to suit the requirements of the simulation or scenario.

8.3. Simulations

The simulated patients were: a healthy adult female undergoing anaesthesia using target-controlled infusion of propofol and remifentanyl followed by sevoflurane; a healthy adult male undergoing anaesthesia with propofol, fentanyl and sevoflurane.

8.3.1 Patient 1: TIVA followed by an inhalation anaesthetic

The simulated patient was a 30 y, 50 kg, 160 cm female. The anaesthetic protocol for this patient is given in Table 8.5. My aim here is to demonstrate how simulated effect site concentrations and BIS response might be correlated to the clinical endpoints of loss of consciousness, and return of consciousness. These endpoints are conveyed in the manikin by eye closure and are initiated by the person running the scenario at our centre. Models exist to automate eye closure in our METI[®] HPS[™] but these use the simulated concentration of NMBD to do this. One issue arising from simulating eye closure in this manner is that NMBD is not a mandatory part of anaesthesia. Consequently eye closure might not occur appropriately, or at all, in those simulations where NMBD are not used despite the patient being adequately anaesthetised (i.e. cases where patients spontaneously breathe with the help of a laryngeal mask airway). Alternatively, simulated patients might have their eyes closed because of NMBD levels but be ‘awake’ because of inadequate anaesthesia. A better way to simulate eye closure might be to use concentrations of the drugs that are responsible for loss of consciousness (i.e. intravenous and inhalation anaesthetics).

Population parameters for pharmacokinetic models give the concentration profiles depicted in Figure 8.1 for patient 1. Johnson *et al.* reported a model describing the probability of loss of responsiveness (LOR) for propofol with remifentanyl in a population of patients.[287] They used the Marsh model, teamed with a keo value of 0.51 min^{-1} , to describe propofol pharmacokinetics. The same authors later provided a model for probability of return of responsiveness (ROR) for patients emerging from remifentanyl-sevoflurane anaesthesia.[131] They defined LOR as an observer assessment of alertness/sedation (OAA/S) score decreasing from 2 to 1, and ROR as an OAA/S score greater than 1.[131, 287]

Time	Event	Drug (drug class)	Dose	Indication
1 min	Induction	Propofol (intravenous anaesthetic)	5 mcg.ml ⁻¹ *	Anaesthesia
		Remifentanil (phenyl-piperidine opioid)	6 ng.ml ⁻¹ †	Analgesia
		Vecuronium (NMBD)		Muscle relaxation
4 min	Intubation			
6 min	Maintenance	Propofol (intravenous anaesthetic)	3 mcg.ml ⁻¹ *	Anaesthesia
		Remifentanil (phenyl-piperidine opioid)	2 ng.ml ⁻¹ †	Analgesia
25 min	Propofol infusion stopped	Sevoflurane (inhalation anaesthetic)	2 %vol	Anaesthesia
40 min	Anaesthetic end			

Table 8.5

Anaesthetic protocol for patient 1. *Given *via* a target controlled infusion (TCI) pump used in plasma mode. †Given *via* a target controlled infusion (TCI) pump used in effect site mode. Ce is the concentration in the effect site compartment.

Parameters reported by the authors were used to predict probability of LOR and ROR based on the effect site concentrations of propofol, remifentanil and sevoflurane simulated for patient 1. Probability curves for LOR and ROR were superimposed over concentration profiles in Figure 8.1 to demonstrate how the time course of BIS response might relate to these important clinical outcomes in the simulator. The contributions of each drug to overall BIS response, as predicted by the model, are given in Figure 8.2. Probability curves for LOR and ROR were again indicated on the plots (shaded areas). We can see from Figure 8.2 that the point at which 50% of patients are expected to have lost responsiveness (vertical broken line on the left of plot B) occurs at a BIS value of 75 units. This is similar to that given for LOR by Lysakowski *et al.* for propofol with 6 ng.ml⁻¹ remifentanil (BIS value of 74 units, propofol EC₅₀ 1.6 mg.ml⁻¹).[247] The concentration in the effect site at LOR is 1.4 mg.ml⁻¹ propofol and 3.85 mg.ml⁻¹ remifentanil, as predicted using the parameters given by Johnson *et al.* Note that the propofol effect site concentrations predicted for the current model lag behind these somewhat due to the different keo parameter used, with LOR instead corresponding to a propofol concentration of 1.2 mg.ml⁻¹.

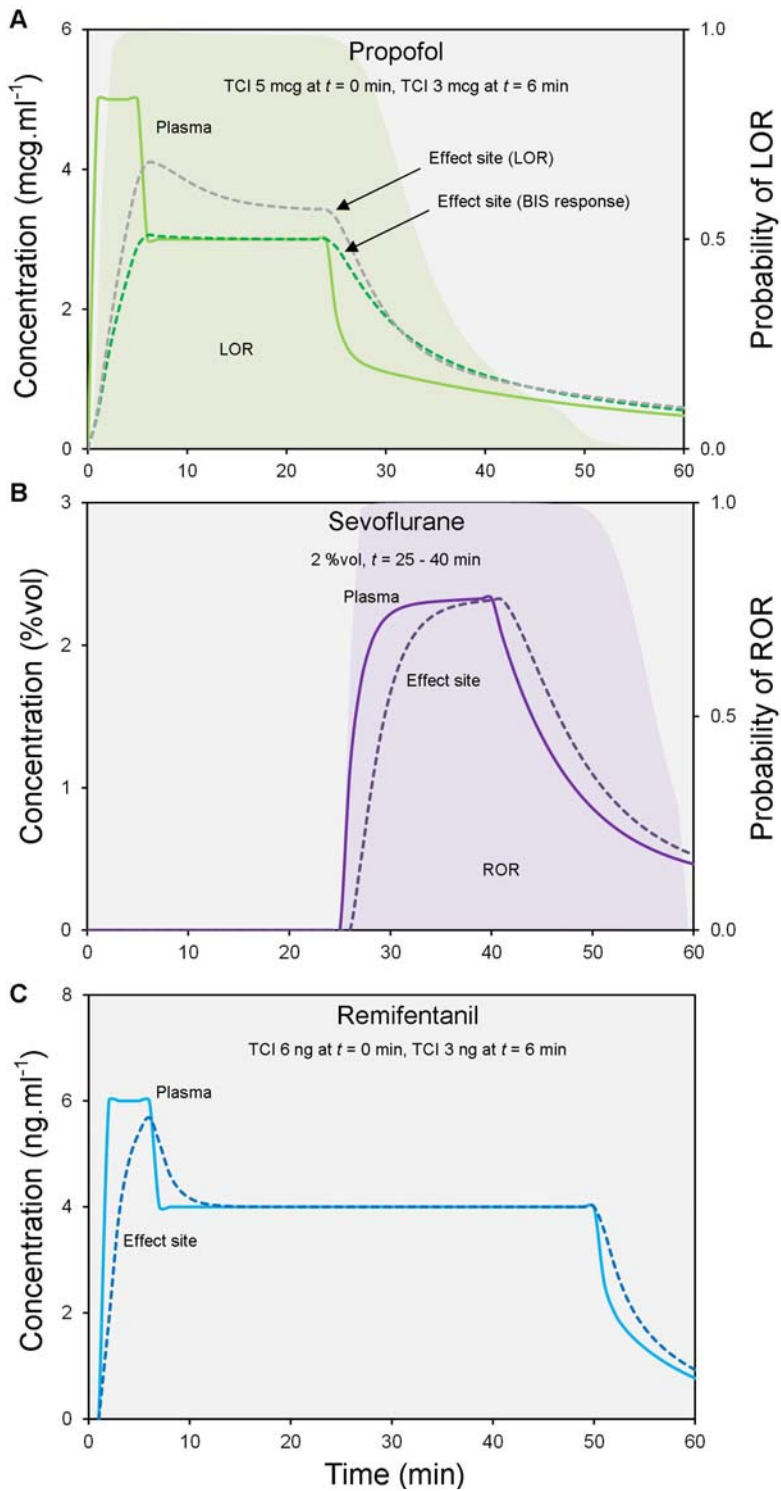


Figure 8.1

Simulated pharmacokinetic profiles for (A) propofol, (B) sevoflurane and (C) remifentanil for patient 1. Concentrations in the plasma (coloured lines in bold) and in the effect site (coloured broken lines) compartments are given. Probability of loss of responsiveness (LOR) and return of responsiveness (ROR) are overlaid on plots A and B (shaded areas). LOR and ROR are predicted from propofol-remifentanil concentrations and sevoflurane-remifentanil concentrations respectively.[131, 287] Propofol effect site concentrations as used for LOR predictions are given in plot A (grey broken lines), where the impact of the different k_{eo} values (0.19 min^{-1} BIS, 0.51 min^{-1} LOR) is visible.

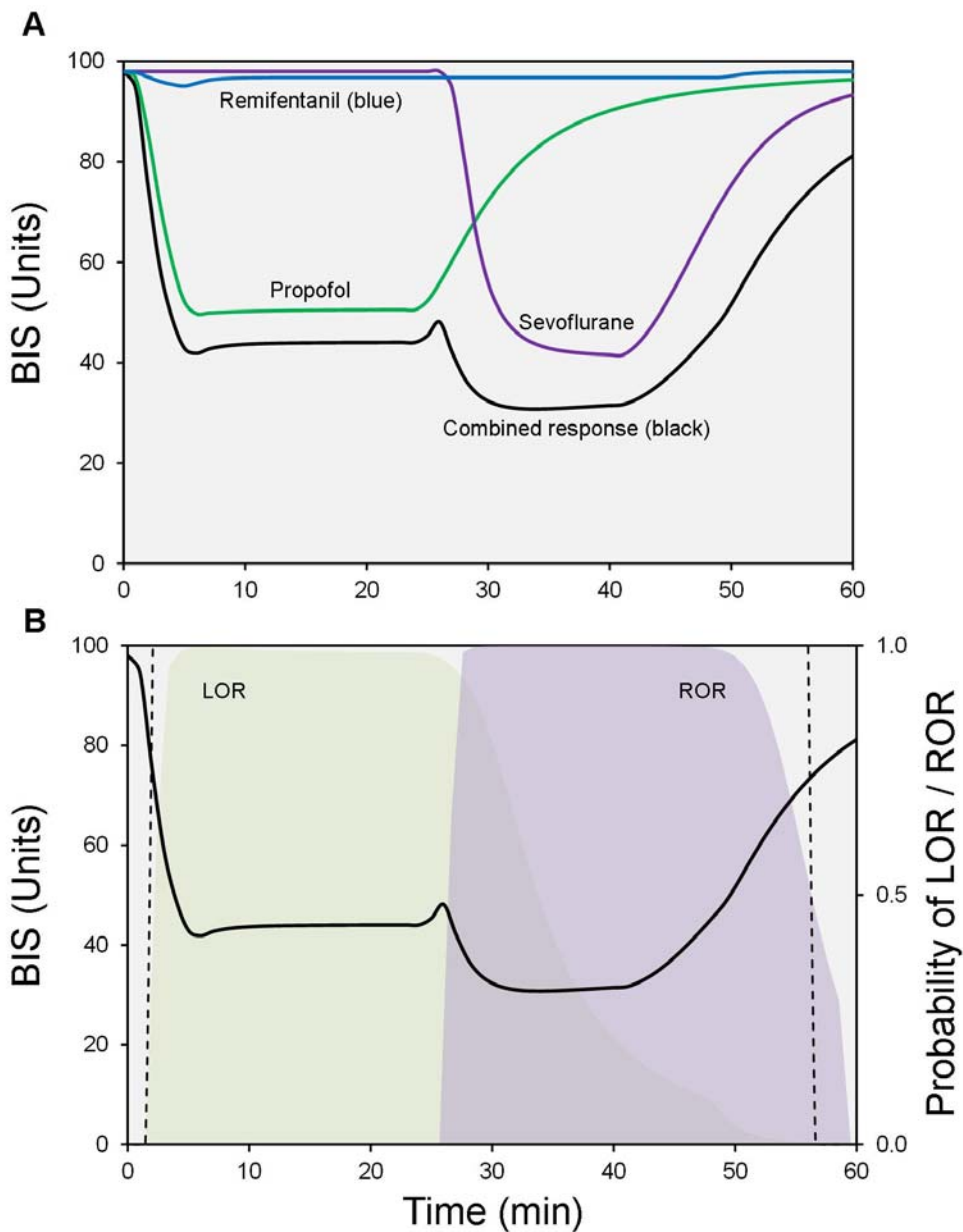


Figure 8.2

Simulated BIS response for patient 1. Plot (A) gives the contributions of each drug alone as well as the total combined response for all drugs (indicated on figure). The combined response is given in black. Plot (B) gives simulated response for the population (solid black line), with probability of loss of responsiveness (LOR) and return of responsiveness (ROR) overlaid on the plot (indicated on figure). LOR and ROR probabilities are predicted from propofol-remifentanyl concentrations (green shaded area) and sevoflurane-remifentanyl concentrations (purple shaded area) respectively and correspond to those given in Figure 8.1.[131, 287] During wash-out of propofol concentrations and wash-in of sevoflurane concentrations both drug pairs contribute to the probability that the patient is unresponsive (overlapping area). The point at which 50% of patients are expected to have lost responsiveness is shown by the vertical broken grey line on the left (plot B), while that at which 50% of patients are expected to have regained responsiveness is given by the vertical broken grey line on the right.

8.3.2 Patient 2: Bolus induction followed by inhalation anaesthetic

The simulations presented so far do not include variability. Simulated response without variation might be perceived as unrealistic by users, particularly those who are experienced clinicians. The smooth response generated when variability is ignored can be seen in Figure 8.2. Variability might be included in simulations using this model to create ‘believable’ patient response. This is my focus in the following simulation.

The simulated patient was a 55 y, 73 kg, 168 cm male. The anaesthetic protocol for this patient is given in Table 8.6. Parameters for pharmacokinetic models give the concentration profiles depicted in Figure 8.3 for patient 2. The contributions of each drug to overall BIS response, as predicted by the model, are given in Figure 8.4. Midazolam and fentanyl have minimal effects on BIS for the concentration ranges in this simulation (midazolam effect site concentrations < 0.05 mcg.ml⁻¹, fentanyl effect site concentrations < 2.56 mcg.ml⁻¹). BIS response predictions for simulated concentrations of midazolam alone, propofol alone and the two drugs together are given in Figure 8.5

Time	Event	Drug (Drug class)	Dose (method)	Indication
0 min		Midazolam (sedative)	2 mg (bolus)	Premedication
3 min	Induction	Fentanyl (phenyl-piperidine opioid)	100 mcg (bolus)	Analgesia
		Propofol (intravenous anaesthetic)	100 mg (bolus)	Anaesthesia
		Vecuronium (NMBD)	8 mg (bolus)	Muscle relaxation
6 min	Intubation			
7 min		Sevoflurane (inhalation anaesthetic)	2 %vol (inhalation)	Anaesthesia
23 min		Fentanyl (phenyl-piperidine opioid)	100 mcg (bolus)	Analgesia
55 min	Anaesthetic end			

Table 8.6

Anaesthetic protocol for patient 2.

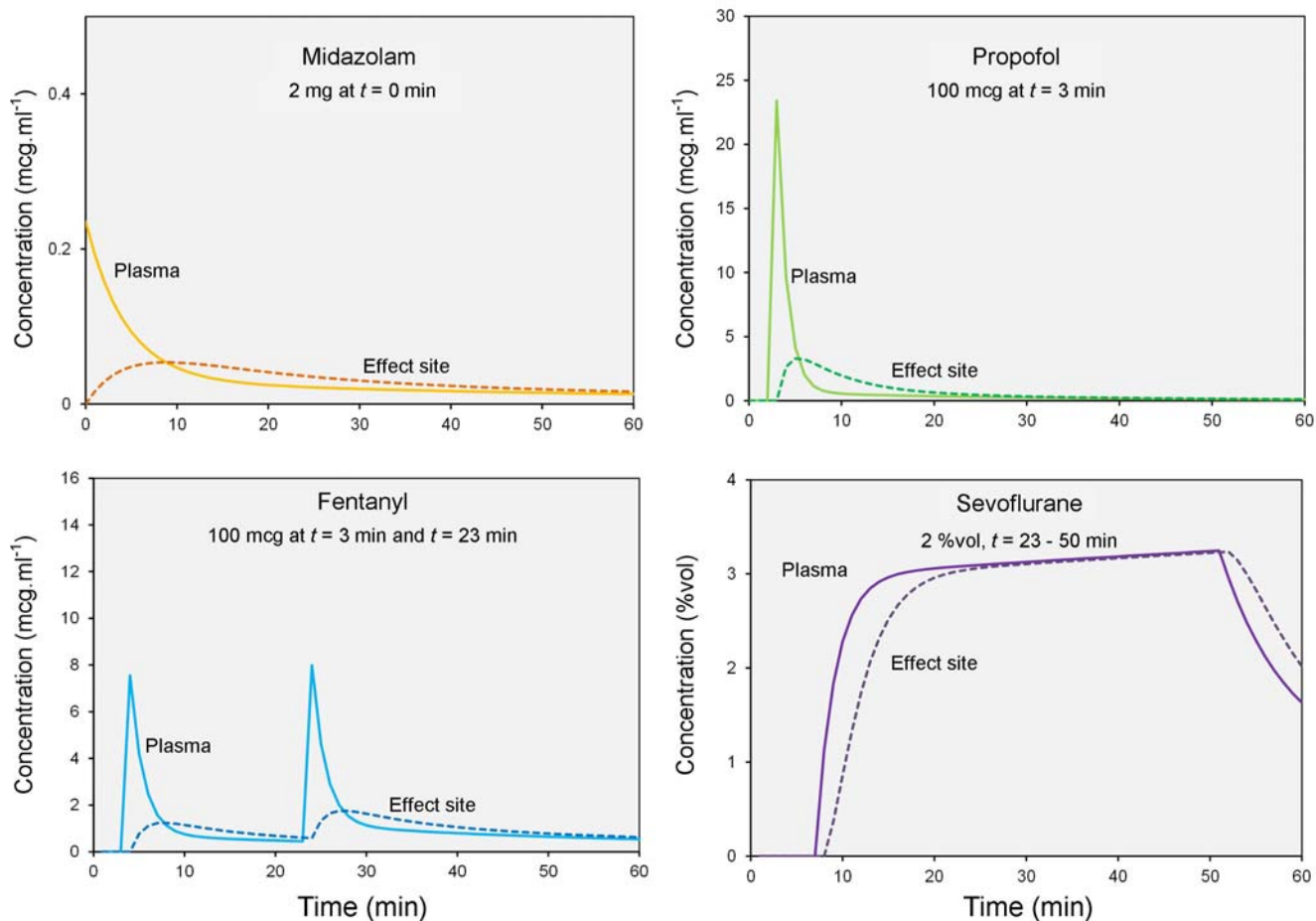


Figure 8.3

Simulated pharmacokinetic profiles for midazolam, propofol, fentanyl and sevoflurane for patient 2. Bold lines give the plasma concentration and broken lines give the effect site concentrations.

Estimates of between-subject and within-subject variability have been reported in the literature alongside pharmacokinetic and pharmacodynamic model parameters, as well as in chapters 4 and 7 of this thesis. Between-subject variability associated with the pharmacokinetic parameters of the models summarised in Table 8.2 are given below in Table 8.7. This illustrates the wide range of variability estimates. An approximate value for between-subject variability typically cited for pharmacokinetics is 20%, [15, 202, 288] and so this value was used in the current simulation for simplicity.

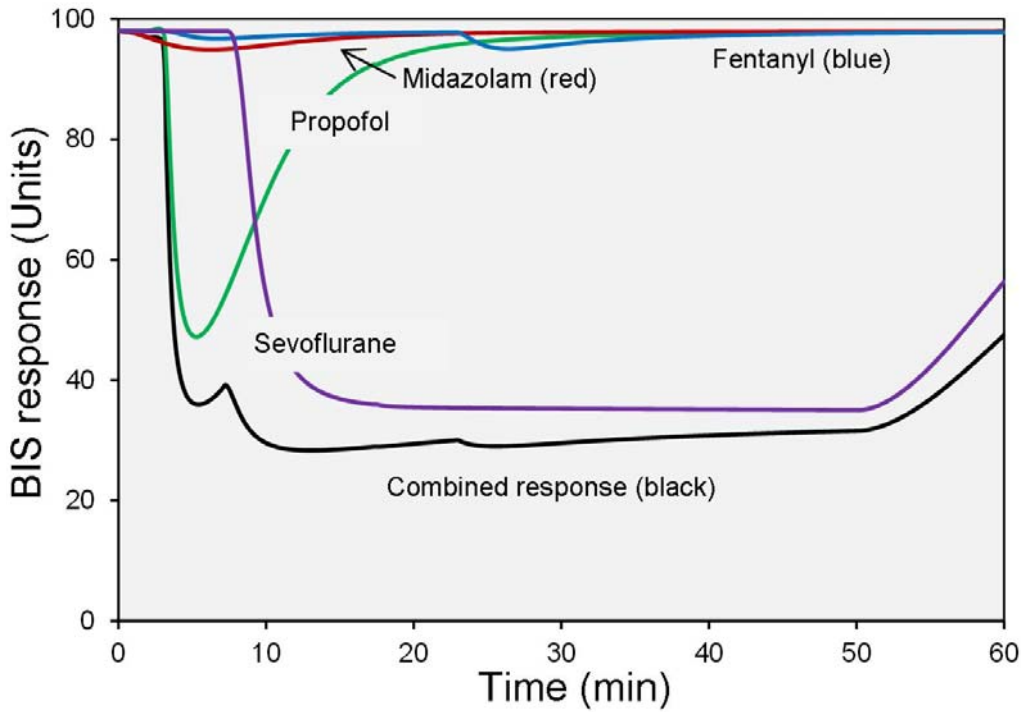


Figure 8.4

Simulated BIS response for patient 2. The contributions of each drug alone are depicted as well as the total combined response for all drugs (indicated on figure). The combined response is given in black.

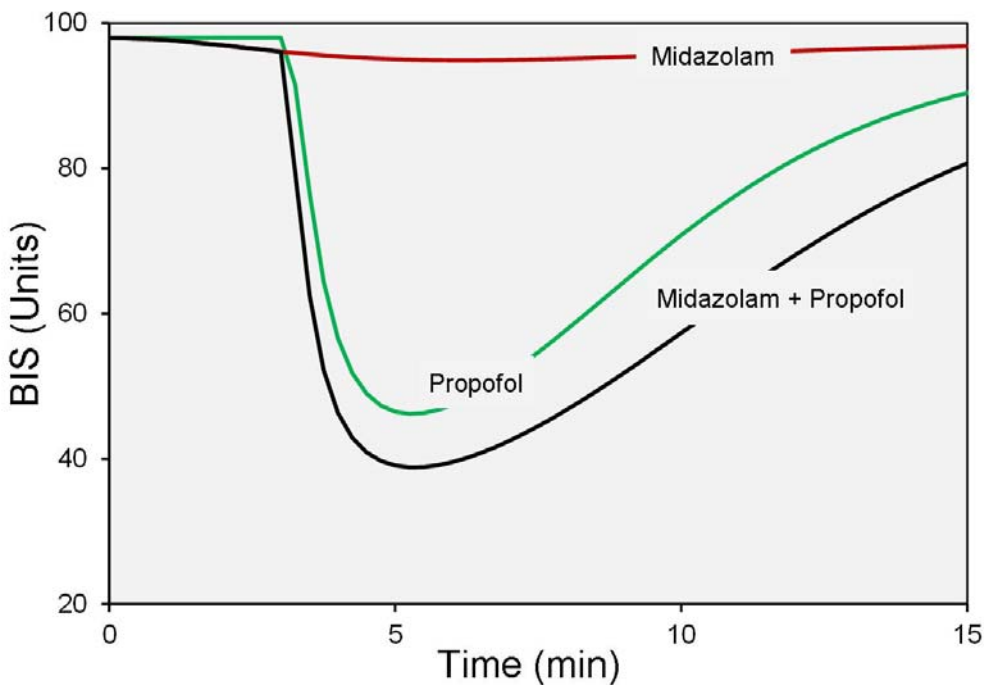


Figure 8.5

The contributions of midazolam and propofol to BIS response for patient 2. Note the small contribution of midazolam alone (given in red) but the increase in response for the combination (given in black) compared with propofol alone.

Five additional simulations were repeated for patient 2. A random number generator was used to simulate normally distributed between-subject variability with a mean of 0 and a variance (ω^2) of 0.20 (coefficient of variability of 20%) for pharmacokinetic parameters. An exponential error model was used i.e.

$$P_i = P_p e^{\eta^{\text{individual}}}$$

Equation 8.5

Plasma and effect site concentration profiles for these simulations are given in Figure 8.6. An approximate value for variability typically associated with pharmacodynamics is 30%. [15, 202, 288] BIS predictions were made from the effect site concentration profiles given in Figure 8.6 (between-subject variability of 20% associated with pharmacokinetics). A random number generator was used to simulate normally distributed between-subject variability with a mean of 0 and a variance (ω^2) of 0.30 (coefficient of variability of 30%) for pharmacodynamic parameters (using Equation 8.5).

We can ignore variability associated with drug concentration measurements when using the current model for simulation as we have no need to output simulated concentrations for users, but variability associated with BIS predictions might be included. A random number generator was used to simulate additive error for BIS measurements (± 7.7 units, chapter 4) for population predicted response i.e.

$$Y_i = Y + RUV_i$$

Equation 8.6

where Y is the response prediction, Y_i is the response prediction for the individual and RUV_i is the residual unknown variability for the individual. The effect of including residual error on BIS profiles is illustrated in plot A of Figure 8.7 (i.e. between-subject variability is not included). Plot B of Figure 8.7 shows the BIS response profiles when between-subject variability is included on both pharmacokinetic and pharmacodynamic parameters. Residual error for BIS response is also included here.

CV (%)	V1	V2	V3	CL1	CL2	CL3
Propofol [54]	4.04	<1.00	14.35	10.05	<1.00	11.79
Midazolam [39]*	20.00	Not reported	Not reported	9.70	Not reported	Not reported
Alfentanil [243]	86.00	Not reported	Not reported	19.50	126.60	22.40
Fentanyl [243]	590.00	Not reported	Not reported	21.40	230.00	139.00
Remifentanil [73]	26.00	29.00	66.00	14.00	36.00	41.00

Table 8.7

Variability associated with the pharmacokinetic parameters used for simulations. CV is the coefficient of variability (%).

*Authors reported pharmacokinetic models in terms of V1, CL1 and rate constants so variability associated with peripheral compartment volumes and clearances is unknown. Wissing *et al.* reported the range of individual parameter estimates across individuals for their analysis of desflurane, isoflurane and sevoflurane pharmacokinetics only.[103]

Including residual variability in BIS response only (plot A of Figure 8.7) results in BIS values that fluctuated within 10% of the population response (based on an additive error of ± 8 units and a pharmacodynamic range of 76 units). Including both pharmacokinetic and pharmacodynamic between-subject variability, and residual variability in BIS measurements, results in more systematic deviations for individuals from the population response (plot B of Figure 8.7). Note that no variability is included on the keo parameters in this figure. The effect of adding variability to the keo parameters is illustrated in Figure 8.8 where the response profile for patient 2 is given for two sets of twenty simulations. This method of incorporating variability more accurately portrays responses observed in the clinical setting but differences might become clinically important during induction and recovery phases. Including between-subject variability in the manner (and to the degree) that I have done here may cause repeated simulations to lack reproducibility and might not be suitable for some simulation purposes.

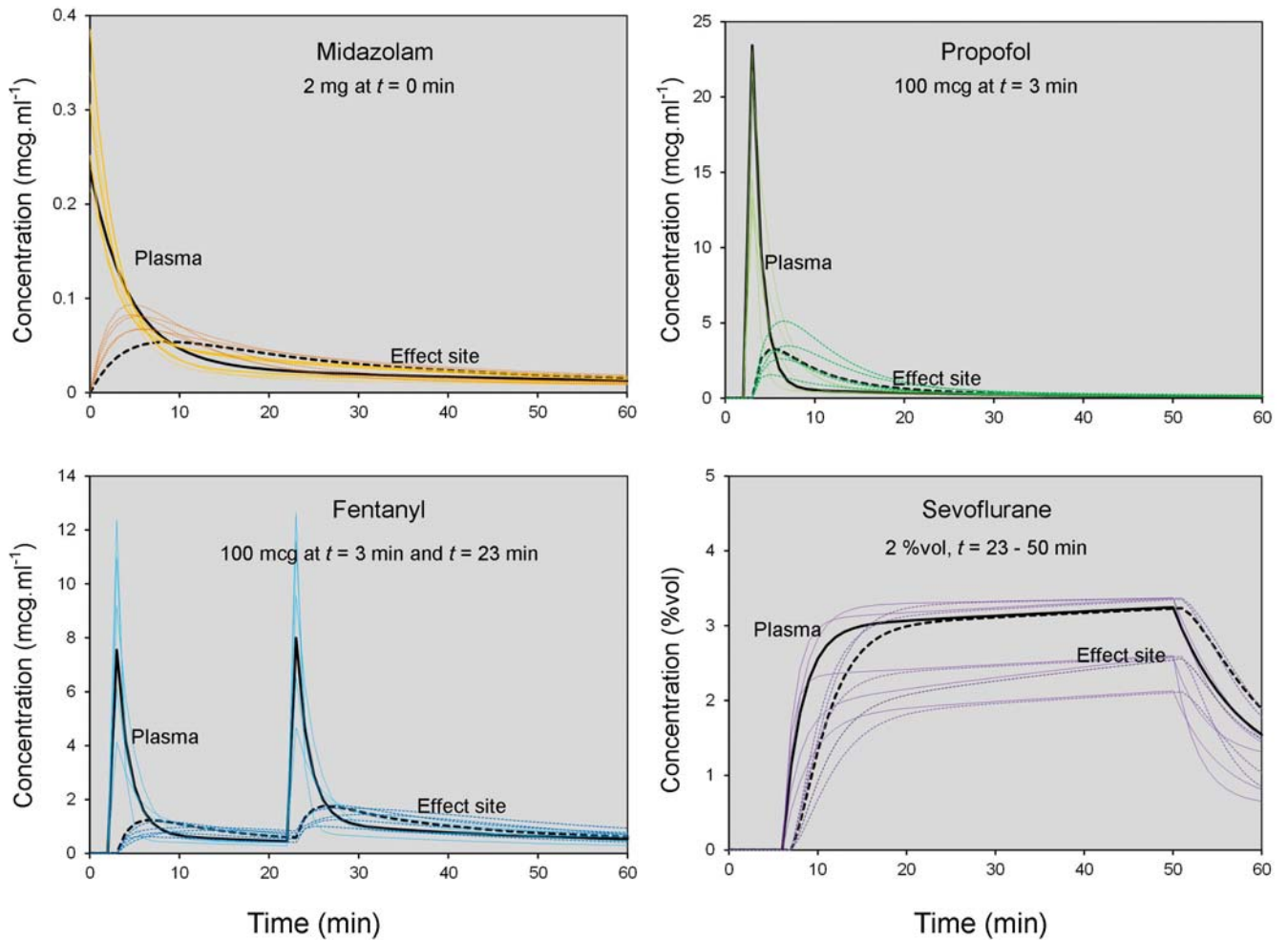


Figure 8.6

Simulated pharmacokinetic profiles for midazolam, propofol, fentanyl and sevoflurane for patient 2 assuming 20% between-subject variability. Solid lines give the plasma concentration and broken lines give the effect site concentrations. Population predictions (no variability) are given in black while those of the five simulations are given in colour.

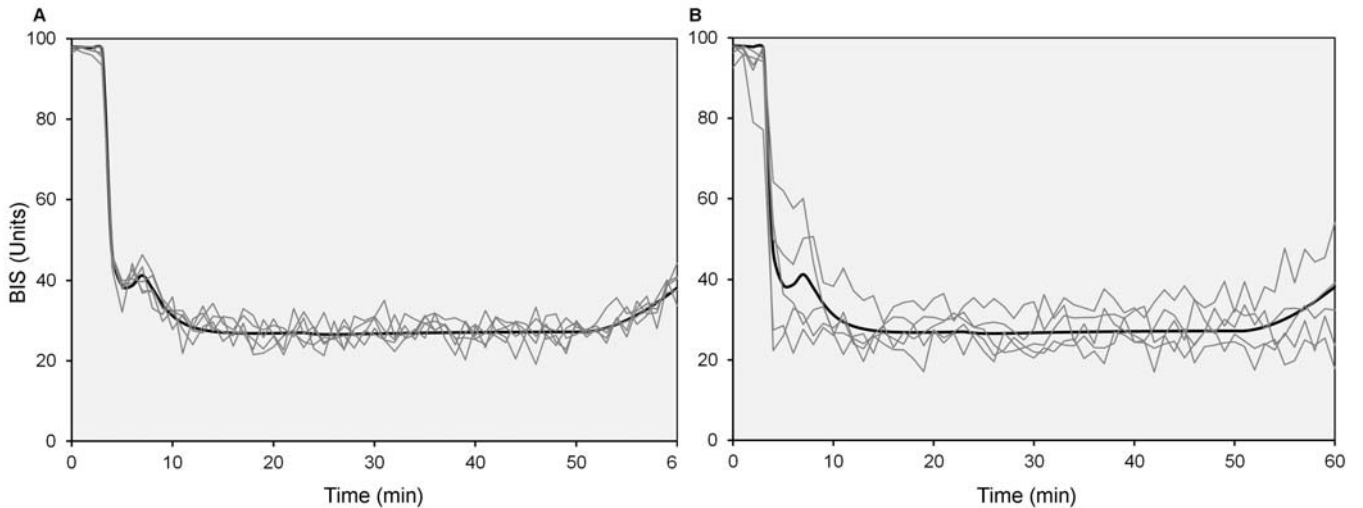


Figure 8.7

Simulated BIS response for patient 2 with variability. The plots show A) simulated response for population predictions of drug concentrations (given in Figure 8.6, black lines) assuming additive unknown error of 8 units only, and B) simulated response for predictions of drug concentrations with between-subject pharmacokinetic variability of 20% (given in Figure 8.6, coloured lines), between-subject pharmacodynamic variability of 30% and additive unknown error of 8 units. No variability is included on keo parameters. Response predictions for the population (no variability) are given in solid lines.

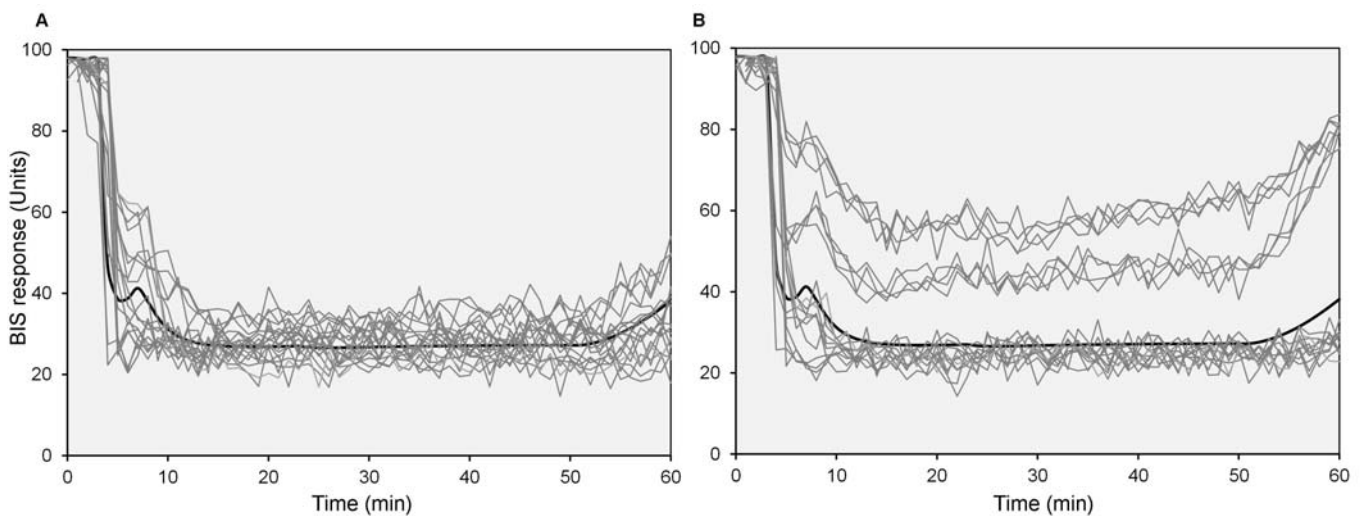


Figure 8.8

Simulated BIS response for patient 2 for twenty simulations each. Both plots are analogous to plot B of Figure 8.7 (five simulations) except that variability is also included on the keo parameters. This figure demonstrates the wide range of BIS response profiles possible when between-subject variability of just 20% is included on pharmacokinetics, 30% is included on pharmacodynamic parameters and a residual unknown error of 8 units is included on response predictions. Plot A gives one iteration of twenty simulations, all of which follow roughly a similar pattern. Plot B also gives one iteration of twenty simulations but a subset of these give a higher BIS trace (plus 20-30 units) which might become clinically important during the induction or recovery phases. Response predictions for the population (no variability) are given by the solid black lines.

8.4. Discussion

We use our METI[®] HPS[™] to simulate complex medical scenarios for various educational and research purposes. However, there are several aspects of our current simulation that require further development, particularly for those scenarios with an anaesthetic focus. Cues of inadequate anaesthesia in the clinical setting include sweating, increased blood pressure and respiratory rate, and purposeful movement (in patients who have not received NMBD). However, eye closure and loss of responsiveness are the only cues given to the user that the simulated patient is anaesthetised. Simulated EEG response is a useful addition to these. A method of simulating BIS has already been implemented into the METI[®] HPS[™] software at our centre (The HPS interface, AQAI Simulation Center)[281] but has limitations (i.e. effects of inhalation anaesthetics on depth of anaesthesia are not included; the appropriateness of simulated BIS response following an induction dose of propofol and at loss of consciousness has been questioned).[36] The model developed in chapter 7 might offer better predictions of BIS response. BIS predictions correlated well with literature estimates of BIS response at the time of loss of responsiveness and return of responsiveness (scenario 1). The model could be integrated into existing software to improve our simulation of depth of anaesthesia, and perhaps to automate some processes such as eye closure during induction.

BIS monitoring is useful for experienced clinicians using the simulator for immersive anaesthetic scenarios. It might also facilitate the teaching of some complex but important concepts relating to clinical pharmacology in a way that is both illustrative and memorable for students.[289] Examples of this include;

- the use of combinations to balance desired drug effects against adverse drug effects (e.g. adjusting the ratio of propofol to phenyl-piperidine opioids to maintain anaesthetic depth and control cardiovascular stability, without the need for vasopressor or antihypertensive agents);
- the need to titrate dose to individuals according to influential covariates that impact pharmacokinetics or pharmacodynamics (e.g. reductions in sevoflurane requirements with increasing age);
- the differences in response typically seen between similar patients for a given intervention (e.g. between-subject variability in time to loss of consciousness and BIS <60);

- the implications of suboptimal dosing (e.g. inadequate analgesia might lead to somatic responses during insertion of the endotracheal tube despite a BIS<60, overdosing might prolong times to wake up at the end of the procedure).

The HPS interface software is rather complex and the current BIS simulation requires further refinement. It is infrequently used at our centre as a result. However, HPS interface software has been designed to facilitate modifications and so it might provide a platform for implementing the current model in the METI[®] HPS[™] software. An advantage of the current model is the inclusion of three drug classes central to anaesthesia (propofol as an intravenous anaesthetic, phenyl-piperidine opioids and inhalation anaesthetics), and the allowance for midazolam as a sedative and popular supplement to anaesthesia. Several others have published preliminary reports of BIS simulators for educational purposes (available as abstracts),[290, 291] but few allow for more than two drug classes. A screen-based BIS simulator designed for education in BIS use is available from Covidien Medical. The BIS Titration SimulatOR 3.0, available at www.BISEducation.com, simulates BIS response for TIVA and TCI anaesthesia, and for inhalation anaesthetics.[280] The program allows administration of sevoflurane, propofol, remifentanyl and fentanyl (as well as the NMBD rocuronium, and cardiovascular modulating drugs such as labetalol). The simulator does not allow administration of midazolam but it does incorporate fluctuations in BIS during intraoperative stimulation. The impact of painful or unpleasant stimuli on BIS was not included in the development of the current model for two reasons; firstly, all patients were assumed to have adequate analgesia during insertion of the endotracheal tube and throughout their surgery, so a change in BIS as a result of pain was not expected; secondly, participants experienced different types and intensities of surgical stimuli which varied over the procedure. Both factors hinder quantification of the impact of pain on BIS response. Allowance for the effect of pain on BIS could be included if needed for simulation using literature estimates of response, as was used by Greenwald *et al.* for the BIS Titration SimulatOR,[292] and perhaps a ‘switch’ setting whereby levels of opioids (as the primary class of analgesics) must be below a known concentration associated with ablation of response to surgical incision before an effect on BIS is seen.

Simulation is becoming more popular for teaching and research in medicine. Cumin *et al.* listed several benefits of using simulation in a healthcare setting:[293] it provides an environment where students can practise manual skills without harming patients; training and assessment scenarios can be

standardised and repeatable; scenarios may be tailored to specific learning objectives; rare events may be artificially recreated; and behaviours of individuals or teams can be recorded, providing an opportunity to study aspects of clinical decision making, teamwork and communication.[293] The ability of a simulator or manikin to mimic reality is often termed ‘simulation fidelity’.[294] We increasingly require higher levels of simulation fidelity as we use our centre for more complex tasks and research initiatives. Several factors affect simulator fidelity, including the simulation environment itself, the physical look and feel of the simulator and the way in which the simulator responds to interventions made by the user.[294] The level of fidelity required is dependent on the purpose of the scenario.

One issue not yet resolved is how much variability is required for a simulated output.[293] Clearly, this depends on what one is simulating and for whom. Simulated response with low or absent variation might not be perceived as realistic by experienced clinicians during high-fidelity, immersive simulations. Large variations in response might make scenarios difficult to reproduce (i.e. a lack of ‘repeatability’) and result in users experiencing different ‘patients’, which might be unsuitable for assessments or research.[294] An advantage of using population-derived pharmacokinetic and pharmacodynamic models to describe drug response in simulation is that estimates of realistic variability can be easily obtained from the anaesthetic literature. Reporting between-subject and random variability is considered standard practice and many of the drugs commonly used during anaesthesia (and therefore included in our human patient simulator) have been well studied in various patient populations.

Dieckmann *et al.* stress that simulators are best considered as the sum of their parts, and that the focus of the user should be on the goals of the scenario as opposed to individual aspects of the physical simulator itself (often termed the ‘physical reality’).[294] However, the importance of different ‘realities’ changes with the aim of the scenario.[295] Anaesthesia is one simulation application in which participants might be less aware of the physical shortcomings of the patient simulator (for example, skin colour and feel, or the lack of patient movement) because they are instead immersed in the information conveyed through the various forms of monitoring. It is helpful for our purposes to improve our simulated responses that are outputted to monitors wherever possible. The aim of including variability in BIS response for immersive simulations at our centre is to allow experienced users to accept the BIS trace as valid, and to avoid shifting their focus away from scenario goals or

impeding their ability to ‘suspend disbelief’ about the authenticity of the simulated patient.[294, 295] Some authors have cited a lack of repeatability in some physiologic variables when a single scenario is repeated multiple times in the METI[®] HPS[™] (available as an abstract only),[296] although Cumin found that this observation was largely due to small differences in phase and frequency that were unlikely to be clinically important.[294] Retaining a fixed baseline BIS response of 98 units, and perhaps refraining from adding variability to keo parameters, is therefore a sensible way to achieve repeatable BIS simulations. Residual variability of 7.7 BIS units or less (as reported in chapters 4 and 7, and illustrated here) would give believable variation in BIS response while still ensuring that values fall within 10% of the population mean at all times. Between-subject variability on pharmacokinetic or pharmacodynamic parameters might be added for those scenarios where simulating realistic patient responses is essential and repeatability issues are less of a concern.

Closing and opening of the eyes during induction and recovery is always initiated manually at our centre, despite the provision of a model-based method to automate this. This has arisen because our simulation technicians find manual methods to be easier and more reliable than relying on the software, partly because this endpoint is dependent on simulated concentration of NMBD. A more rational way to simulate eye closure might be to consider concentrations of the drugs that are responsible for loss of consciousness (i.e. intravenous and inhalation anaesthetics), in addition to concentrations of NMBD. Many models describing probability of loss of consciousness, and time to wake up, now exist for combinations of each of the three primary drug classes involved in anaesthesia (intravenous anaesthetics, phenyl-piperidine opioids and inhalation anaesthetics).[59, 60, 69, 121, 122, 128-130, 132, 147-149] These have been incorporated into graphical displays on anaesthetic monitors which predict time to awakening for various drug combinations in real time.[289] These models could be implemented in the METI[®] HPS[™] software alongside the current model to automate eye opening and closing. Automaticity in simulation improves both repeatability and objectivity of scenarios. One of the great benefits of using simulation is that scenarios, or events, can be repeated so that each participant essentially experiences the same patient. In the clinical setting, factors such as patient pathology, procedure type and difficulty contribute to between-subject variability and may confound research and assessments. Simulation scenarios can be thought of as a chain of actions and reactions (i.e. the user makes an intervention, the simulated ‘patient’ responds, the user makes an intervention based on the simulated response, and so forth). Ensuring a consistent and objective response from the simulator at each step improves the value of the simulator for assessments and research. Responses that are driven by models are more consistent and objective than those initiated or controlled manually

by a simulator technician. ‘Driving’ the simulator is quite difficult and technicians are required to split their attention between many tasks. Automating eye closure during induction and eye opening during recovery could provide more consistent, objective and potentially realistic simulator responses while also freeing up technicians to do other tasks.

There are several avenues for future research into the integration, refinement and assessment of this model at our simulation centre. Predicted plasma concentrations are readily available in the METI[®] HPS[™] software from the pre-programmed pharmacokinetic models and could be used to integrate the current model into the simulation hardware. This is outside the scope of this thesis but it is clearly one direction in which my research could be continued. Further work is also required in the provision of modelled response for different patient subgroups. For example, pathology was treated as absent here but it would be useful to allow for it in some manner as we typically construct educational and research scenarios around a ‘difficult’ or unstable patient. Including pathology in the model would require review of the underlying pharmacokinetic models used in the METI[®] HPS[™] to assess the appropriateness of predicted drug concentrations for various patient groups (although any attempt to integrate the current model with the METI[®] HPS[™] will probably also require this). Another area for future research is validation of the model for the simulator. This might involve asking experienced clinicians to score the realism of the BIS response during scenarios, or to select the anaesthetic record they perceive to be ‘real’ from anaesthetic records generated in the clinical and simulated operating room setting in a modified format of the Turing test.[297] Alternatively, more quantitative methods might be appropriate: standards or limits within which we expect BIS response to reasonably lie might be defined for a distinct phase of the scenario or an intervention, i.e. induction of anaesthesia, and response simulated by the model evaluated against these.[293] The way in which we evaluate models for simulation in healthcare is an on-going debate and continues to be a focus for research in our department.[36, 293, 298]

Summary

The aim of the work presented in chapters 7 and 8 was to begin development of a model that could describe BIS response for those drug classes commonly combined in anaesthetic practice. This is currently the only model, of which I am aware, that includes the effects of midazolam on BIS alongside those of three other drug classes. Here I have demonstrated the use of the model for some simple anaesthetic scenarios, and discussed it in context of how it might be used in our METI[®] HPS[™]. Several interesting avenues of research have also been highlighted and may be investigated in future studies within our department. I hope that this work provides a framework upon which we can continue to develop an appropriate simulation of depth of anaesthesia that will ultimately add to the educational value of our simulator when used for teaching medical students, and contribute to the overall environment presented to experienced clinicians taking part in education or research scenarios.

Chapter 9. General discussion

Anaesthesia is a unique clinical setting. Patients are rapidly rendered unaware, a high level of analgesia is established, physiology is manipulated to provide optimal conditions for surgery and recovery at the end of the procedure is achieved quickly. These objectives are accomplished through the use of drug combinations that together contribute to clinical endpoints. Combining drugs in this manner requires an understanding of the pharmacological profile of each agent when given alone and alongside others. Pharmacokinetic and pharmacodynamic models provide a means of summarising complex drug relationships so they might be better understood and used to the benefit of patients.

Two distinct topics have been discussed in the work presented in this thesis: combinations for analgesia in a postoperative setting and combinations for depth of anaesthesia during surgery. The common theme between these topics is the use of pharmacokinetic and pharmacodynamic models to describe combined drug response. The way in which these models might be used for applications in anaesthesia has been my focus. I aim to summarise my major findings in this final chapter, and to tie the various threads of my work together in the context of the wider literature. I will also outline some potential directions for future research that extend from the work that I have presented.

9.1. Main findings and contributions to knowledge

9.1.1 Paracetamol and NSAIDs for postoperative analgesia in children

The use of paracetamol with the NSAIDs ibuprofen and diclofenac for postoperative pain relief in children was my focus in chapters 2 and 3. A two drug pharmacodynamic interaction model was used to demonstrate the analgesic properties of the drug combinations. I presented a ‘hypothesis generating’ study in chapter 2. This work helps us to interpret trends in studies that compare analgesia for paracetamol, ibuprofen or these drugs in combination.

The main findings were:

1. The addition of paracetamol to ibuprofen improves analgesia when the ibuprofen dose is less than 5 mg.kg^{-1} ; paracetamol has minimal analgesic effect when given with doses of ibuprofen exceeding 5 mg.kg^{-1} in the immediate postoperative period.
2. Discrepancies in reports on the comparative efficacy of ibuprofen, paracetamol and combinations of the two probably arise (at least in part) due to differences in dose and therefore the portion of the analgesic response curve studied; differences in the efficacy of single drugs are unlikely to be distinguishable from that of the combination if studied doses are those relating to the upper portion of the analgesic curve where response is already approaching its maximum.

The second finding in particular might seem logical when presented in this way, yet it is a point that appears to be underappreciated. Ong *et al.* identified six studies directly comparing efficacies of paracetamol or ibuprofen and the combination,[182] all of which evaluated single doses of ibuprofen predominantly in combination with high dose paracetamol.[183-188] Only one study investigated more than one dose of paracetamol (Gazal *et al.*, two doses).[188] These ‘snap shots’ of the dose or concentration response curve make it difficult to decipher whether a benefit in analgesia exists for the combination. Researchers continue to ask the question ‘does the combination of paracetamol with ibuprofen offer an analgesic benefit over either drug alone’ but a better question might be ‘what are the minimum concentrations of these two drugs that together gives us optimal analgesia’.

This question can be answered using models like that developed in chapter 3. This analysis provides for the first time some estimates of diclofenac pharmacodynamics for analgesia in children. An existing but unanalysed dataset was pooled with two datasets from published studies.[29, 33, 206, 208] The maximal effect for these drugs was a reduction in pain score as measured by a visual analogue scale (VAS) of 4.8 cm. A paracetamol concentration in the effect site compartment of 48 mg.l^{-1} ($>60 \text{ mg.kg}^{-1}$) would be required to achieve a VAS of 5.2 cm assuming baseline pain is equal to 10 cm. The same pain score of 5.2 cm could be achieved using a paracetamol concentration of 15 mg.l^{-1} (20 mg.kg^{-1}) with 2.3 mg.l^{-1} diclofenac. However, these doses are much larger than those typically used. A paracetamol concentration of 10 mg.l^{-1} (achievable at 1.15 h following a single oral dose of 12.5 mg.kg^{-1}) has been recommended as a safe target that is less likely to cause dose-dependent adverse effects.[29] The addition of 2 mg.kg^{-1} diclofenac results in an effect site concentration of 0.7 mg.ml^{-1} at the same time point, and will reduce the pain score from 8.6 cm (paracetamol alone) to 6.5 cm. A dose of 1 mg.kg^{-1} is currently recommended for diclofenac and analgesia in children,[206, 208] although this would give a pain score of 7.3 cm when combined with 10 mg.l^{-1} paracetamol as described above. The difference in analgesia initially seems small (a decrease in pain score of 0.8 cm despite doubling the dose of diclofenac) but in fact represents 17% of the maximal drug effect; an alternative way to view this is that doubling the dose gives a reduction in pain score that is almost 50% of the target effect of 2 cm. This illustrates how models such as that developed for diclofenac and paracetamol can be used to determine the doses that provide optimal drug effect while minimising the risk for adverse effects.

The main findings that come from the work I presented in chapter 3 were:

1. Diclofenac suspension has an EC_{50} of 1.2 mg.l^{-1} , and equilibration half-time ($t_{1/2\text{keo}}$) of 0.2 h, for postoperative analgesia in children following oral dosing.
2. Baseline pain over time (as described by the placebo model) is similar for children undergoing day stay surgery with a minimal pain score of 5 cm occurring at 4 h, after which pain begins to increase again.
3. Poorly controlled pain is a significant factor for study dropout and should be considered during planning of analgesic studies.

The placebo model in this analysis indicates large changes in baseline pain over time. This is a consideration that should be incorporated in studies of analgesia. The peak of the placebo effect occurs at 3 to 4 h postoperatively (as estimated in this work and in an earlier study of a similar design).[29] This probably results from children being distracted from their pain in the postoperative room by their parents, watching television or some other activity, or by preparing to go home. It might be difficult to detect differences between analgesic efficacies at this time point where baseline pain is at its lowest. These large changes in baseline pain might also explain why some studies have detected differences in efficacy for a combination of paracetamol with ibuprofen over monotherapy outside the immediate postoperative recovery period.[186] This was a second hypothesis generated by the simulation study I reported in chapter 2.

9.1.2 Intraoperative drug classes and BIS effects

BIS monitoring is readily recognised, well-researched and is the only type of EEG monitor available to clinicians at Auckland City Hospital. The pharmacodynamic relationship for BIS response has been studied for many drugs alone and in combination for anaesthesia. BIS response has also been correlated to clinically relevant endpoints such as loss of consciousness, return to consciousness, and loss of responsiveness to painful stimuli such as intubation or surgical incision.

There are several gaps in the literature, despite the wealth of clinical research focusing on BIS monitoring in anaesthesia. For example, it has been shown that a model describing remifentanyl-sevoflurane effects can be extrapolated to describe those of fentanyl and isoflurane for an endpoint of return to consciousness,[132] but this has not been confirmed for other endpoints such as BIS. A three drug model for BIS has been reported for propofol with fentanyl and remifentanyl,[57] but this encompasses just two of the three drug classes predominantly used during the induction and maintenance of anaesthesia. Notably, the relationship between midazolam and propofol for BIS response has received little attention. The work that I have presented in the second part of this thesis fills some of these gaps.

I began by establishing a model for the effects of propofol with alfentanil on BIS in surgical patients, using a pre-existing, unanalysed dataset. The work is based on the idea that pharmacodynamic relationships between propofol and opioids of the phenyl-piperidine drug class are similar for endpoints of loss of consciousness and ablation of response to noxious stimuli. I sought to validate this assumption for BIS response before developing a three drug class model.

The main findings from the work which I presented in chapters 4 to 7 were:

1. Additivity between propofol and alfentanil for BIS is confirmed; a model describing this relationship can be extrapolated to describe that for propofol with remifentanil using a relative potency of remifentanil: alfentanil of 1:33.
2. Response surface models, when linked to appropriate pharmacokinetic models, can be used for target controlled infusion (TCI) systems; a k_{eo} of 0.2 min^{-1} ($t_{1/2}$ 3.5 min), as opposed to 0.45 min^{-1} ($t_{1/2}$ 1.6 min) as is commonly recommended, better captures propofol effects on BIS in the early stages of anaesthesia (using Schnider's pharmacokinetic model).[54]
3. A model is presented for the combined effects of four drug classes on BIS; the model includes the effects of eight drugs in total and can be used to realistically simulate BIS response as a means of simulating depth of anaesthesia.
4. The interaction between midazolam and propofol is additive for an endpoint of BIS in the concentration ranges studied (plasma propofol $<12 \text{ mcg.ml}^{-1}$ and midazolam $<0.16 \text{ mcg.ml}^{-1}$).

There are few reports in the anaesthetic literature of models that describe effects for more than two drug classes in combination using pharmacokinetic-pharmacodynamic analyses. Three exist for an endpoint of loss of responsiveness.[122, 137, 139] The model I have presented in chapter 7 is unique in that it not only describes the effects of three drug classes (phenyl-piperidine opioids, intravenous and inhalation anaesthetics), but it also includes the effects of the sedative midazolam. No studies have investigated combined response for propofol and midazolam on BIS using similar methods. This is surprising given the frequent co-administration of these agents. My work suggests an additive relationship between propofol and midazolam but this requires verification in a specifically designed clinical study. Recently we have seen an increase in modelling combined drug effects in anaesthesia as authors seek to identify optimal drug ratios to achieve specific endpoints. Midazolam and propofol are often combined for light sedation. BIS has been proposed as a useful way of measuring sedation as opposed to observer ratings which by nature require that the assessor rouse or stimulate the patient

(i.e. speaking their name loudly) to assess responsiveness. An OAA/S scale > 2 and < 3 , or a BIS between 70 and 80, is a reasonable definition of light sedation without loss of consciousness.[38, 299] The model can be used to predict dose combinations of propofol and midazolam that together will achieve this. For example, a BIS of 70 might be achieved using an effect site concentration of 1.98 mcg.ml^{-1} propofol alone or 0.21 mcg.ml^{-1} midazolam alone (Figure 9.1). Kazama *et al.* estimated a propofol C_{e50} for blood pressure changes of 2 mcg.ml^{-1} in patients aged 70-85 y.[135] A combination of 1 mcg.ml^{-1} propofol with 0.10 mcg.ml^{-1} midazolam would give an appropriate level of sedation (BIS of 70), anti-emesis and minimal changes in blood pressure, as predicted by the model.[38, 135, 299, 300]

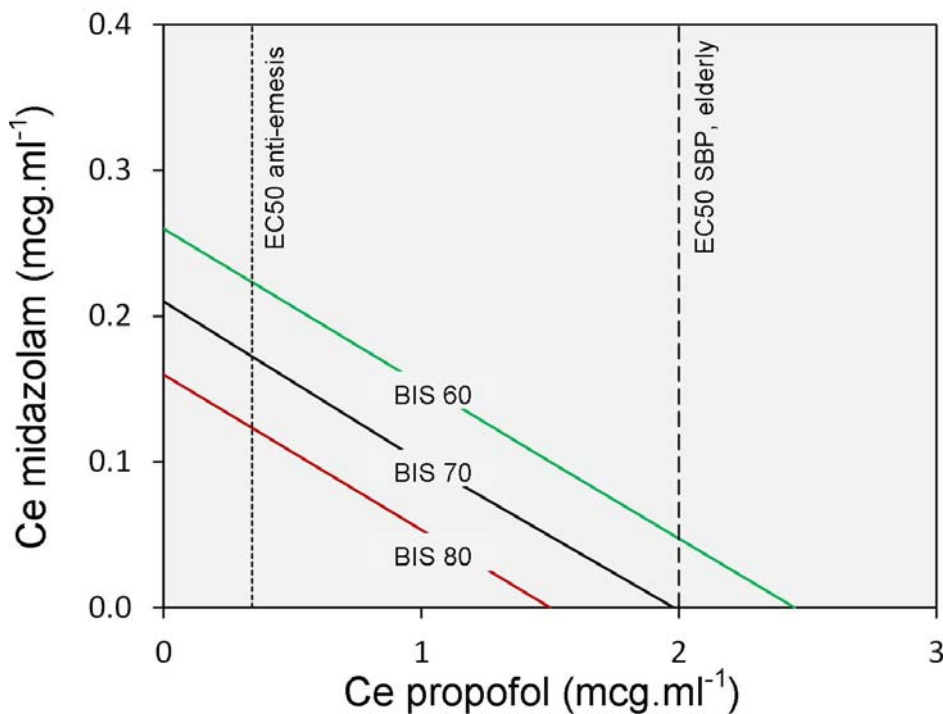


Figure 9.1

BIS levels associated with propofol-midazolam concentration pairs. The figure shows the concentration pairs in the effect site (C_e) required to produce a BIS of 60 (green line), a BIS of 70 (black line) and BIS of 80 (red line) as predicted by the model. BIS values between 70 and 80 are associated with an OAA/S scale > 2 and < 3 suitable for light sedation.[38, 299] The propofol C_{e50} for anti-emesis in adults ($0.343 \text{ mcg.ml}^{-1}$),[300] and systolic blood pressure changes in patients aged 70-85 y,[135] are indicated by the broken vertical lines.

The model that I presented in chapter 7 can be applied to the simulation setting. I have illustrated this in chapter 8 using simulated scenarios. Our METI[®] Human Patient Simulator (HPS)[™] is used for teaching, research and assessments. The anaesthetist is often the leading participant in our scenarios yet our simulation of anaesthetic depth is limited. Eye closure and loss of verbal response are the primary cues that the simulated patient is anaesthetised. Software has been integrated to allow model-based simulation of BIS but this is infrequently used because of its unrealistic response. A key feature of our simulator is that model-based response is outputted to real patient monitors identical to those used at Auckland City Hospital but the outward appearance of these monitors alone is not sufficient; we also require monitor traces to be sufficiently realistic, allowing anaesthetists to accept the data as real and to ‘buy in’ to the simulated patient. The current model can be used to simulate BIS response in this setting, providing a measure of anaesthetic depth. This would contribute to the realism of the simulated patient as perceived by the anaesthetist, whose focus is often centred on the information portrayed through the various monitors (as opposed to directly observing the patient). The model might also be useful for controlling eye closing and opening. The model-driven control of eye closure currently available is often over-ridden by simulation technicians at our centre because they have found this aspect of the software to be unreliable. Automating responses, such as BIS or eye closure during anaesthetic induction, provides greater consistency and objectivity than manual control. Removing variation introduced by simulation technicians improves the value of the simulator for research and assessments, where our ability to reliably reproduce sequences of events is a major advantage over the clinical setting.

Simulation in healthcare is an emerging field and many questions have yet to be answered. I address some of these areas for future research in the following section.

9.2. Directions for future research

Several directions for future research arise from the work I have presented in this thesis.

The optimal dose (or concentration) ratio for paracetamol with ibuprofen or diclofenac has yet to be established for postoperative analgesia. I have made some initial suggestions about how we might better use these drugs together but these require confirmation using clinical studies. Neither the simulation study in chapter 2, nor the analysis in chapter 3, addresses the type of interaction between paracetamol and these NSAIDs *in vivo*. The studies were not designed in a way that would allow identification or quantification of an interaction, if present, with sufficient precision. Both models supported additivity but this was a result of the limited data available. A recent animal study reported a synergistic interaction between paracetamol and various NSAIDs for analgesia.[203] There are no studies in humans that support this observation yet but this might be an interesting direction for future research.

Future studies that investigate differences in efficacy for combinations of paracetamol with a NSAID over either drug alone should do so with some consideration of the concentration-effect response relationship, and the postoperative window in which analgesia is studied. The model and simulations presented in chapter 2 suggest that benefits are more likely to be discernible using modest doses that relate to the mid portion of the response curve, and that analgesia might be prolonged for the combination. These observations might be allowed for in future trial designs. Clinical trials are costly and time consuming. Studies of paediatric populations in particular are challenging. Clinical trial simulation is fast becoming a routine and necessary part of study design. The observations described above and the model presented in chapter 3 might be useful for future trial design. The impact of placebo effects and study drop out are important factors that should be considered for analgesic studies. The placebo and dropout models given in chapter 3 should be broadly generalisable to similar populations (i.e. children undergoing day stay surgeries).

Parameter sets for combined drug response, like that given in chapter 4, are suitable for target controlled infusion (TCI) systems. This would require further refinement and validation in diverse patient populations. It makes sense to build on previous research by linking these parameter sets to

established pharmacokinetic models. Both of the pharmacodynamic models tested in chapter 6 performed best when linked to standard pharmacokinetic models. BIS predictions were also improved during induction when a shorter keo value was used (0.2 min^{-1} as opposed to 0.456 min^{-1}). This observation is supported by Sepúlveda *et al.*, who suggest using a keo of 0.14 min^{-1} ($t_{1/2}$ 4.9 min) in combination with Schnider's model for BIS response,[262] and by a propofol keo estimate of 0.19 min^{-1} given in chapter 7. Another area for future research is the use of combined response models for TCI in children.[301] A recent review noted that there are no models that allow TCI administration of opioids in children.[302] This is just one patient group for whom current TCI systems are known to perform poorly. Others include elderly and obese patients. Hopefully our ability to titrate drug dosing to individuals will improve once the best size descriptors have been identified for the key drugs used in anaesthesia. Better understanding of the sources of variability will also improve drug titration. One such source of variability is time of day. I have not considered the impact of circadian rhythms in my work, but Cheeseman *et al.* demonstrated that the duration of rocuronium induced muscle relaxation fluctuates with time of day.[303] Time of day is a covariate that has received little attention but does warrant further investigation.[304, 305]

The study presented in chapter 7 is the first to investigate BIS response for midazolam with propofol, albeit in combination with other drug classes. The finding of additivity between propofol and midazolam for BIS should be validated as my study was not designed to quantify this interaction and the midazolam concentration range was small. The work I have presented in this thesis only includes the effects of propofol but other intravenous anaesthetics exist that might also be investigated. The model might be useful in new pharmacokinetic-pharmacodynamic displays that give clinicians a graphical display of their patient's current state (in terms of sedation and analgesia). The models used in these monitors also give predictions on the patient state in the future, for example the level of sedation expected in ten minutes time. This type of application helps clinicians to optimise recovery times and avoid overdosing.

Several directions for future research in simulation exist. I have not attempted to integrate my model with the METI[®] HPS[™] software as this would probably require another thesis in itself. Integrating the model with the software would require extensive review of the underlying pharmacokinetic models programmed into the manikin, and an iterative cycle of simulation assessments and refinements. The model could be further developed to include some simulation of lightening anaesthesia in response to

inadequate analgesia, as has been done for the AQAI HPS interface [281] or the online BIS simulation tool provided by Covidien Medical.[280] Simulation for teaching and research is an expanding field in medicine and many of the standards for simulation in healthcare have yet to be established. The question of how much variability to simulate has not been addressed for many manikin ‘responses’. Variability is needed to simulate realistic patient response but this must be balanced against the need to create repeatable scenarios that are comparable to one another. I have made some suggestions in chapter 8 as to how to simulate realistic BIS response. This is another area in which the model might be further developed and one which would be beneficial to the wider simulation community as more centres adapt their commercial simulators for research initiatives and face similar issues.

Clinical practice in anaesthesia draws on knowledge slowly accumulated over decades of clinical research. The ability to draw all these threads of information together helps us to use drug combinations to the best advantage of patients. Pharmacokinetic and pharmacodynamic models that describe complex pharmacology can be used to guide clinical use, and for applications in teaching and research such as medical simulation. I hope my contribution will improve patient care both through everyday clinical applications in dosing and, eventually, through education and research at our simulation centre.

“The purpose of models is not to fit the data, but to sharpen the question.”

Samuel Karlin, Evolutionary Geneticist (20 April 1983).

Appendices

- Appendix 1** NONMEM code for the analysis of morphine and morphine-6-glucuronide effects on respiratory depression in a child with kidney failure (Chapter 1, Section 1.3.2)
- Appendix 2** NONMEM code for the analysis of ibuprofen and paracetamol effects on pain relief following wisdom tooth extraction (Chapter 2, Section 2.3)
- Appendix 3** NONMEM code for the pharmacokinetic-pharmacodynamic analysis of diclofenac and paracetamol effects on pain relief following tonsillectomy in children (Chapter 3, Section 3.3)
- Appendix 4.1** NONMEM code for the first stage of the pharmacokinetic-pharmacodynamic analysis of alfentanil and propofol effects on BIS; initial estimation of effect site concentrations using loop collapsing (Chapter 4, Section 4.2.1.2)
- Appendix 4.2** Final NONMEM code for the pharmacokinetic-pharmacodynamic analysis of alfentanil and propofol effects on BIS; simultaneous analysis (Chapter 4, Section 4.2.1.2)
- Appendix 5** Ethics approval for the study described in Chapter 6
- Appendix 6** Ethics approval for the study described in Chapter 7
- Appendix 7** Final NONMEM code for the model of combined BIS response for multiple drug classes in a population of patients undergoing anaesthesia for surgery (Chapter 7)

Appendix 1. Model code for morphine-M6G respiratory effects

```

$PROB MORPHINE 12YR OLD CHILD ON DIALYSIS
$DATA ...\M6GLUCdatafile2.csv IGNORE#
$INPUT ID TIME AMT DV CMT DVID MDV DIA AGE WT
$ESTIM MAXEVAL=9999 SIGDIG=3 PRINT=1 NOABORT METHOD=1
MSFO=morphine_metab_2effect_ec_hill_data2.msf
$COV
$THETA
(0, 64.3, 300)  FIX ; CL2M3
(0, 3.63, 100)  FIX ; CL2M6
(0,17.4,  50)  FIX ; CLM3G
(0, 3.0, 1000)      ; CLM6GD
0.001          FIX ; CLM6G0
(0, 3.12,  50)  FIX ; CLEX
(50, 136, 1000) FIX ; V
(1,23.,200)    FIX ; V3M
(1,30.,200)    FIX ; V6M
(0.002, 0.109, 2) ; TEQM
(0.01, 7.78,  20) ; TEQM6
0 FIX          ; EMAX
(10, 21.6, 30)  ; E0
(0.1, 1.87, 4)  ; HILL
(.01, 0.162, 400) ; EC50M

$OMEGA
0 FIX ; PPVCL2M3
0 FIX ; PPVCL2M6
0 FIX ; PPVCLM3G
0 FIX ; PPVCLM6G
0 FIX ; PPVV
0 FIX ; PPVCLEX
0 FIX ; PPVTEQ
0 FIX ; PPVE50
0 FIX ; PPVHL
0 FIX ; PPVEMX
0 FIX ; PPVE0

$$SIGMA
5.05 ; SDEFF

$$SUBR ADVAN6 TOL=5
$MODEL
  COMP ( CP )
  COMP ( CM3G )
  COMP ( CM6G )
  COMP ( CE6G )
  COMP ( CEM )

$PK
LN2=LOG(2)
IF (AMT.GT.0) DOSE=AMT
FSZVD=WT/70 ; Size models, allometric scaling of V, CL and Teq parameters
FSZCL=FSZVD**.75
FSZT=FSZVD**0.25

```

```
CLM6GD=FSZCL*CLM6GD*EXP(PPVCLM6G)
CLM6G0=FSZCL*CLM6G0*EXP(PPVCLM6G)
  IF (DIA.EQ.1) THEN                ; dialysis, indicated in data file
CLM6G=CLM6GD
  ELSE
CLM6G=CLM6G0
  ENDIF
CLM3G=FSZCL*CLM3G*EXP(PPVCLM3G)
CL2M6=FSZCL*CL2M6*EXP(PPVCL2M6)
CL2M3=FSZCL*CL2M3*EXP(PPVCL2M3)
CLEX=FSZCL*CLEX*EXP(PPVCLEX)
CLT=CL2M6+CL2M3+CLEX
V=FSZVD*V*EXP(PPVV)
V3M=FSZVD*V3M
V6M=FSZVD*V6M
TEQM=FSZT*TEQM
TEQM6=FSZT*TEQM6*EXP(PPVTEQ)
E0=E0*EXP(PPVE0)
EMAX=EMAX*EXP(PPVEMX)
EC50M=EC50M*EXP(PPVE50)
HILL=HILL*EXP(PPVHL)

$DES
KEQM=LN2/TEQM
KEQM6=LN2/TEQM6

DCP=A(1)/V
DCM3G=A(2)/V3M
DCM6G=A(3)/V6M
DCEM6G=A(4)
DCEM=A(5)

DADT(1)= -CLT*DCP
DADT(2)= CL2M3*DCP-CLM3G*DCM3G
DADT(3)= CL2M6*DCP-CLM6G*DCM6G
DADT(4)= KEQM6*(DCM6G - DCEM6G)
DADT(5)= KEQM*(DCP-DCEM)

$ERROR
CP=A(1)/V
CM3G=A(2)/V3M
CM6G=A(3)/V6M
CEM6G=A(4)
CEM=A(5)

CEPM=CEM**HILL
C50PM=EC50M**HILL
FXM=CEPM/(C50PM+CEPM)                ; effect of morphine
CENM6=CEM6G**HILL
C50NM6=EC50M**HILL
FXM6=CENM6/(C50NM6+CENM6) ; effect of M6G
FX=E0-(E0-EMAX)*(FXM+FXM6)          ; additive effects for morphine and M6G
Y=FX + SDEFF

$TABLE ID TIME WT DVID Y CP CM3G CEM6G
NOPRINT ONEHEADER FILE=morphine_metab_2effect_ec_hill_data2.fit
```

Appendix 2. Model code for ibuprofen-paracetamol analgesia

```
$PROB IBUPROFEN AND PARACETAMOL COMBINATION
$DATA ...\Mehlich_dose_plac.csv IGNORE=#
$INPUT ID TIME MDV MDVD AMT CMT DV
$ESTIM MAXEVAL=9999 SIGDIG=3 PRINT=1 NOABORT METHOD=1 INTERACTION
MSFO=ibu_para_beta0_plac.msf
$COV
```

```
$THETA
```

```
; Paracetamol pharmacokinetic parameters
```

```
(5, 15, 25)    FIX ; CLP
(10, 55, 100)  FIX ; VP
(.1, .2, .8)   FIX ; TABSP
(.1, .136, 5)  ; TEQP
```

```
; Ibuprofen pharmacokinetic parameters
```

```
(1, 3.6, 25)   FIX ; CLI
(1, 10, 100)   FIX ; VI
(.1, .25, .8)  FIX ; TABSI
(.1, 1.1, 5)   ; TEQI
(.01, .3, 5)   ; TPLAC
```

```
; Pharmacodynamic parameters
```

```
(1, 14.4, 25) ; C5OPAR
(1, 5.13, 25) ; C5OIBU
(2, 4.06, 15) ; EMAX
(.3, 1.96, 10) ; HILL
0 FIX ; BETA
```

```
$OMEGA
```

```
; Pharmacokinetic BSV
```

```
0 FIX ; PPVCLP
0 FIX ; PPVVP
0 FIX ; PPVTBP
0 FIX ; PPVTQP
0 FIX ; PPVCLI
0 FIX ; PPVVI
0 FIX ; PPVTBI
0 FIX ; PPVTQI
```

```
; Pharmacodynamic BSV
```

```
0.923 ; PPV501
0.0362 ; PPV502
0.0201 ; PPVEMX
0 FIX ; PPVEO
0 FIX ; PPVHIL
```

```
$$SIGMA
```

```
0.0321; SD
0 FIX ; CV
```

```
$$SUBR ADVAN6 TOL=5
```

\$MODEL

COMP (GUT, PARA)
 COMP (CENTRAL, PARA)
 COMP (EFFECT SITE, PAR)
 COMP (GUT, IBU)
 COMP (CENTRAL, IBU)
 COMP (EFFECT SITE, IBU)

\$PK

LN2=LOG(2)
 IF (AMT.GT.0) DOSE=AMT

CLP=CLP*EXP(PPVCLP)
 VP=VP*EXP(PPVVP)
 TABSP=TABSP*EXP(PPVTBP)
 KAP=LN2/TABSP
 TEQP=TEQP*EXP(PPVTQP)

CLI=CLI*EXP(PPVCLI)
 VI=VI*EXP(PPVVI)
 TABSI=TABSI*EXP(PPVTBI)
 KAI=LN2/TABSI
 TEQI=TEQI*EXP(PPVTQI)

\$DES

; Paracetamol pharmacokinetics

DCP=A(2)/VP
 DCEP=A(3)
 KEQP=LN2/TEQP
 DADT(1)=-KAP*A(1)
 DADT(2)=KAP*A(1)-CLP*DCP
 DADT(3)=KEQP*(DCP-DCEP)

; Ibuprofen pharmacokinetics

DCI=A(5)/VI
 DCEI=A(6)
 KEQI=LN2/TEQI
 DADT(4)=-KAI*A(4)
 DADT(5)=KAI*A(4)-CLI*DCI
 DADT(6)=KEQI*(DCI-DCEI)

\$ERROR

CP=A(2)/VP
 PARA=A(3)
 CI=A(5)/VI
 IBU=A(6)

; Model for combined response

C50PAR=C50PAR*EXP(PPV501)
 C50IBU=C50IBU*EXP(PPV502)
 E0= E0*EXP(PPVE0)
 EMAX=EMAX*EXP(PPVEMX)
 HILL= HILL+(PPVHIL
 BETA = BETA

; Normalise drug concentrations to units

U1=PARA/C50PAR
 U2=IBU/C50IBU

```
CONC =U1+U2

; compute 'Q' for Minto equation
IF(CONC.EQ.0) THEN
  Q = 0
ELSE
  Q=U2/CONC
ENDIF

; Minto equation
CON = CONC / (1-BETA*Q+BETA*Q**2)
CGAM=CON**HILL

; Describe changes in baseline pain using placebo model
E0=1-EXP(-TIME*LN2/TPLAC)

; Calculate effect for sigmoidal response curve
EFF=E0 + EMAX*(CGAM/(1+CGAM))

Y= EFF*EXP(CV)+SD

$TABLE ID TIME Y PARA IBU
ONEHEADER NOPRINT FILE=ibu_para_beta0_plac.fit
```

Appendix 3. Model code for diclofenac-paracetamol analgesia

```

$PROB DICLOFENAC AND PARACETAMOL COMBINATION
$INPUT ID AMT CMT TIME DV DVID MDV SEX WT AGE FORM SDY EVID OCC ENDS VOM RESC
$DATA ..\Copy_dataset_dropout_interval2.csv IGNORE #
$ESTIM MAXEVAL=9999 SIGDIG=5 PRINT=1 NOABORT METHOD=1 INTERACTION LAPLACE NUMERICAL SLOW
MSFO=DiclofenacParacetamol_intensored_drop_dp2.msf
$COV SLOW

```

```
$THETA
```

```
;Paracetamol pharmacokinetics
```

```

(5, 11.7, 25) ; CLP
(30, 56, 100) ; VP
(0.1, .495, 2) ; TEQP
(.001, .127, 2) ; TABSPO
(.1, .538, 6) ; TABSPR
(.1, .499, 5) ; LAGPR
(.1, .579, 1) ; FPR

```

```
;Diclofenac pharmacokinetics
```

```

(.5, 53.2, 500) ; CLD
(1, 16.0, 500) ; VDD
(.05, .23, 2) ; TEQD
(.01, 1.09, 2) ; TABSD

```

```
; Pharmacodynamics
```

```

(1, 13.3, 25) ; C50P
(.001, 1.21, 20) ; C50D
(.1, .489, 1) ; EMAX
10 FIX ; EO
1 FIX ; HILL
0 FIX ; BETA

```

```
; Placebo (describing changes in baseline pain over time)
```

```

(.01, 1.75, 10) ; BETAPL 11
(.01, 2.65, 10) ; TEQPL 12
(.01, 2.97, 10) ; TELPL 13

```

```
; Hazard of dropping out of the study over time
```

```

(.00001, 0.0152, 10) ; BASHAZ
.308 ; BASFX 1/PAIN SCORE
0 FIX ; BETGOM

```

```
; Pharmacokinetic BSV
```

```

$OMEGA BLOCK (2)
.194 ; PPVCLP
-.0163 .192 ; PPVVP

```

```
$OMEGA BLOCK (3)
```

```

0.045 ; BSVCLD
-0.00404 0.195 ; BSVVDD
0.0971 0.103 0.308 ; PPVTBD

```

```
$OMEGA
```

```
.0004 ; PPVTPR
```

```
.0662 ; PPVTPO
$OMEGA BLOCK(2)
0.0342 ; BOVCL1
0.008 0.458 ; BOVV1

$OMEGA BLOCK(2) SAME
;.0846 ; BOVCL2
;.01 .0477 ; BOVV2

; Pharmacodynamic BSV
$OMEGA BLOCK (3)
1.18 ; PPVEMX
.663 1.89 ; PPV501
.00552 .0499 1.52; PPV502

$OMEGA
0 FIX ; PPVTQP
0 FIX ; PPVTQD
0 FIX ; PPVEO
0 FIX ; PPVHIL
0 FIX ; PPVBET
.00013 ; CVBETAP

$OMEGA BLOCK (2)
.259 ; CVTEQP
-.0399 .549 ; CVTELP

$$SIGMA
; Residual error for effect predictions
1.41 ; SDFX
; Residual error for diclofenac concentrations
.0001 ; SDCD additive error
.214 ; CVCD proportional error
; Residual error for paracetamol concentrations
1.38 ; SDCP additive error
.00809 ; CVCP proportional error

$SUBR ADVAN13 TOL=9
$MODEL
  COMP ( GUT, PARA )
  COMP ( CENTRAL, PARA )
  COMP ( EFFECT SITE, PARA )
  COMP ( GUT, DICL )
  COMP ( CENTRAL, DICL )
  COMP ( EFFECT SITE, DICL )
  COMP (CUMHAZ)

$ABBREVIATED DERIV2=NO
$PK
OBS = DV
IF (NEWIND.LE.1) SURVL = 1 ; at the start, the hazard of dropping out is 0 and the likelihood of survival is 1

IF (AMT.GT.0) THEN
  DOSE=AMT
  LN2=LOG(2)
ENDIF
```

FSZCL=(WT/70)**.75 ; Size models – allometric scaling for V, CL and Teq parameters
 FSZV=WT/70
 FSZT=FSZV**.25

; Between occasion variability for those individuals in Study 3 that were studied on more than one occasion

IF (OCC.EQ.1) THEN ; indicated in the data file

BOVCL=BOVCL1

BOVV =BOVV1

ENDIF

IF (OCC.EQ.2) THEN

BOVCL=BOVCL2

BOVV =BOVV2

ENDIF

CLP=FSZCL*CLP*EXP(PPVCLP)

VP=FSZV*VP*EXP(PPVVP)

TEQP=FSZT*TEQP*EXP(PPVTQP)

TABSPO=TABSPO*EXP(PPVTPO)

TABSPR=TABSPR*EXP(PPVTPR)

CLD=FSZCL*CLD*EXP(BSVCLV+BOVCL)

VDD=FSZV*VDD*EXP(BSVVDV+BOVV)

TEQD=FSZT*TEQD*EXP(PPVTQD)

TABSD=TABSD*EXP(PPVTBD)

IF (FORM.EQ.3) THEN ; Oral formulation of paracetamol, indicated in data file

ALAG1=0

F1=1

ENDIF

IF (FORM.EQ.1) THEN ; Rectal formulation of paracetamol, indicated in data file

ALAG1=LAGPR ; Lag for rectal dose absorption

F1=FPR ; Fraction bioavailability relative to oral formulation

ENDIF

IF (FORM.EQ.2) THEN ; Oral formulation of diclofenac, indicated in data file

ALAG4=0

F4=1

ENDIF

; Formulation specific KA parameters

IF (FORM.EQ.3) THEN ; Oral paracetamol

TABSPO = TABSPO

ELSE

TABSPO = 1

ENDIF

IF (FORM.EQ.1) THEN ; Rectal paracetamol

TABSPR = TABSPR

ELSE

TABSPR = 1

ENDIF

TABS = TABSPO * TABSPR

KA=LN2/TABS

KADICL=LN2/TABSD

C50P=C50P*EXP(PPV501)

```

C50D=C50D*EXP(PPV502)
E0=E0*EXP(PPVE0)

TNOW=TIME-ENDS ; ENDS is end of surgery, indicated in the data file
IF (TNOW.LE.0) THEN
  ISPFX=0
  TNOW=0 ; Avoids exp overflows
ELSE
  ISPFX=1
ENDIF

BETAPL=BETAPL*EXP(CVBETAP)
TEQPL=TEQPL*EXP(CVTEQP)
TELPL=TELPL*EXP(CVTELP)

; EMAX constraint model, avoids negative values
TVEMAX=EMAX
LGEMAX=LOG(TVEMAX/(1-TVEMAX))
EXEMAX=EXP(LGEMAX+PPVEMX)
EMAX=EXEMAX/(1+EXEMAX)

; Placebo effect over time
KEQPL=LN2/TEQPL
KELPL=LN2/TELPL

P1=EXP(-KELPL*TNOW)-EXP(-KEQPL*TNOW)
PFX=ISPFX*BETAPL*KEQPL/(KEQPL-KELPL)*P1

$DES
; Paracetamol pharmacokinetics
DCP=A(2)/VP
DPARA=A(3)
KEQP=LN2/TEQP
DADT(1)=-KA*A(1)
DADT(2)=KA*A(1)-CLP*DCP
DADT(3)=KEQP*(DCP-DPANA)

; Diclofenac pharmacokinetics
DCD=A(5)/VDD
DDICL=A(6)
KEQD=LN2/TEQD
DADT(4)=-KADICL*A(4)
DADT(5)=KADICL*A(4)-CLD*DCD
DADT(6)=KEQD*(DCD-DDICL)

; Normalise concentrations of both drugs to units using Ce50
DU1=DPARA/C50P
DU2=DDICL/C50D
DCONC = DU1 + DU2
; Compute 'theta' and response for Minto model
IF(DCONC.EQ.0) THEN
  DQ = 0 ; theta
ELSE
  DQ=DU2/DCONC
ENDIF

; Calculate 'U' as given in Equation 3.4.
DCON = DCONC / (1-BETA*DQ+BETA*DQ*DQ)

```

```

; Dose response curve
IF (DCON.LE.0) THEN
  DCGAM=0
ELSE
  DCGAM=DCON**HILL
ENDIF

; Calculate out drug effect
DDRGFX=1 - EMAX* (DCGAM/(1+DCGAM))

; Calculate out response including placebo (or baseline pain) and drug effects
DFX=E0*(1-PFX)*DDRGFX

; Hazard accumulating in compartment 7, dependent on time and pain score
DADT(7)=BASHAZ*EXP(BASFX*DFX + BETGOM*T)

$ERROR
; Paracetamol pharmacokinetics
CP=A(2)/VP
PARA=A(3)
; Diclofenac pharmacokinetics
CD=A(5)/DVD
DICL=A(6)

; Cumulative hazard at time=t
CUMHAZT=A(7)

; repeat calculations outside of $DES for model predictions ($ERROR)
; Normalise concentrations of both drugs to units using Ce50
U1=PARA/C50P
U2=DICL/C50D
CONC = U1 + U2

; Compute 'theta' and response for Minto model
IF(CONC.EQ.0) THEN
  Q = 0 ; theta
ELSE
  Q=U2/CONC
ENDIF

; Calculate 'U' as given in Equation 3.4.
CON = CONC / (1-BETA*Q+BETA*Q*Q)

; dose response curve
IF(CON.LE.0) THEN
  CGAM =0
ELSE
  CGAM=CON**HILL
ENDIF

; Calculate out drug effect
DRGFX=1 - EMAX* (CGAM/(1+CGAM))

; Calculate out response including placebo (or baseline pain) and drug effects
EFX=E0*(1-PFX)*DRGFX

; Model predictions

```

```
IF (DVID.EQ.1) THEN ; Pain score
  F_FLAG=0 ; Indicates that this is a prediction
  Y = EFX+SDFX
ENDIF

IF (DVID.EQ.2) THEN ; Paracetamol concentration
  F_FLAG=0 ; Indicates that this is a prediction
  Y = CP*EXP(CVCP)+SDCP
ENDIF

IF (DVID.EQ.3) THEN ; Diclofenac concentration
  F_FLAG=0 ; Indicates that this is a prediction
  Y = CD*EXP(CVCD)+SDCD
ENDIF

; relate cumulative hazard to likelihood of survival
IF (CUMHAZT.LT.0) THEN
  SURVT=1
ELSE
  SURVT=EXP(-CUMHAZT)
ENDIF

IF (DVID.EQ.4.AND.DV.EQ.0) THEN ; Dropout entry in dataset, 0 indicates no dropout (individual still participating)
  F_FLAG=1 ; Indicates that this is a likelihood
  Y=SURVT ; Likelihood of an event at this time
ENDIF

IF (DVID.EQ.4.AND.DV.EQ.1) THEN ; Dropout entry in dataset, 1 indicates individual has dropped out of study
  F_FLAG=1 ; Indicates that this is a likelihood
  Y=(SURVL - SURVT) ; Likelihood of an survival = survival at last observation minus survival at time t
ENDIF

IF (DVID.EQ.6) THEN ; Indicates last observation for individual in dataset
  SURVL = SURVT ; Retains survival at this time for calculation of survival at time of next scheduled assessment
ELSE
  SURVL = SURVL
ENDIF

$TABLE ID TIME Y EFX TABSD TABSPO TABSPR CD CP PARA DICL DVID
ONEHEADER NOPRINT FILE= diclofenac_paracetamol_intensored_model1.fit

$TABLE ID TIME DV DVID PRED OBS MDV WT AGE SEX FORM SDY Y
NOAPPEND ONEHEADER NOPRINT FILE=diclofenac_paracetamol_intensored_model2.fit
```

Appendix 4.1 Model code for alfentanil-propofol: loop collapsing

The following code was used to establish some initial pharmacodynamic parameter estimates for the analysis presented in chapter 4, using the pharmacokinetic models for propofol and alfentanil (developed independently of response data in the first instance). All parameters were then refined in a simultaneous pharmacokinetic-pharmacodynamic analysis. Code for the final analysis is given in Appendix 4.2.

```

$PROB GAIN INITIAL ESTIMATE OF EFFECT SITE CONCS FOR ALFENTANIL PROPOFOL BIS EFFECTS
$DATA ..\concBIS_16aug_richPDdata.csv
$INPUT ID TIME PROP ALF DV DVID POPA INDA POPP INDP BASE MDV AGE M0F1 WT HT
$ESTIMATION NSIG=3 SIGL=9 MAX=1999 PRINT=1 METHOD=1 NOABORT
MSFO=minto_cedata1_emax_add.msf
$COV

$THETA
841 ; EC50A
2530 ; EC50P
1.4 ; GAMMA
98 FIX ; BASELN
0 FIX ; BETA
(70, 78.9, 98) ; EMAX
.212 ; KEOP
.7 FIX ; KEOA

$OMEGA
.812 ; PPVGAM
0 FIX ; PPVE0

.0257 ; PPVKP
.0312 ; PPVC5P

$OMEGA BLOCK(3)
.913 ; PPVEMX
.762 .976 ; PPVC5A
1.23 1.06 1.68 ; PPVKA

$SIGMA
81.7 ; SDEFX

$PRED
; Individual Bayesian predictions for concentrations from pharmacokinetic models developed in initial stage
CPA=INDA ; alfentanil
CPP=INDP ; propofol

C50A= EC50A*EXP(PPVC5A)
C50P= EC50P*EXP(PPVC5P)
SLOPE = GAMMA*EXP(PPVGAM)
E0= BASELN*EXP(PPVE0)

```

```

KEOP=KEOP*EXP(PPVKP)
KEOA=KEOA*EXP(PPVKA)

; EMAX constraint model
TVEMAX=EMAX/100
LGEMAX=LOG(TVEMAX/(1-TVEMAX))
EXEMAX=EXP(LGEMAX+PPVEMX)
EMAX=EXEMAX*100/(1+EXEMAX)

IF (TIME.EQ.0) THEN ; At t=0, all values = 0
  CEP = 0
  CEA = 0
  PTIME = 0
  PCPA = 0
  PCEA = 0
  PCPP = 0
  PCEP = 0
ENDIF

DT=TIME-PTIME ; Establishes a d/dt interval

IF (DT.EQ.0) THEN ; Avoids issues with nested statements
  DT1=1
ELSE
  DT1=DT
ENDIF

; Alfentanil
IF (CPA.GE.PCPA) THEN ; concentrations increasing
  SLOPEA = (CPA-PCPA)/DT1
  DELTAA=DT1*SLOPEA+(KEOA*PCPA-SLOPEA)*(1-EXP(-KEOA*DT1))/KEOA
ELSE
  SLOPEA = (LOG(CPA)-LOG(PCPA))/DT1; concentrations decreasing
  DELTAA=PCPA*KEOA/(KEOA+SLOPEA)*(EXP(DT1*SLOPEA)-EXP(-KEOA*DT1))
ENDIF

; Propofol
IF(CPP.GE.PCPP) THEN
  SLOPEP = (CPP-PCPP)/DT1; concentrations increasing
  DELTAP=DT1*SLOPEP+(KEOP*PCPP-SLOPEP)*(1-EXP(-KEOP*DT1))/KEOP
ELSE
  SLOPEP = (LOG(CPP)-LOG(PCPP))/DT1; concentrations decreasing
  DELTAP=PCPP*KEOP/(KEOP+SLOPEP)*(EXP(DT1*SLOPEP)-EXP(-KEOP*DT1))
ENDIF

; calculate effect site concentrations
IF (DT.GT.0) THEN
  CEA = PCEA*EXP(-KEOA*DT)+DELTAA
  CEP = PCEP*EXP(-KEOP*DT)+DELTAP
ELSE
  CEA = PCEA
  CEP = PCEP
ENDIF

; normalise drug concentrations according to EC50
UA=CEA/C50A
UP=CEP/C50P
CONCC=UA+UP

```

```
IF(CONCC.EQ.0) THEN
  RESPN = 0
ELSE
  Q = UP/CONCC
  CON = CONCC / (1-BETA*Q+BETA*Q*Q)
  CGAM=CON**SLOPE
  RESPN=CGAM/(1+CGAM)
ENDIF

EFX= E0 - (EMAX * RESPN)

Y=EFX + SDEFX

; Retain values of variables for use at the next iteration
PTIME = TIME ; Prior time
PCPA = CPA ; Prior plasma concentration
PCPP = CPP
PCEA = CEA ; Prior effect site concentration
PCEP = CEP

$TABLE ONEHEADER NOPRINT FILE=minto_cedata1_emax_add.fit
ID TIME Y DV INDA INDP CPA CPP CEA CEP KEOA KEOP EFX CGAM RESPN
```

Appendix 4.2 Model code for alfentanil-propofol: simultaneous PKPD analysis

```

$PROB ALFENTANIL PROPOFOL SIMULTANEOUS PKPD ANALYSIS FOR BIS EFFECTS
$INPUT ID TIME DV DVID CMT MDV AMT RATE AGE MOF1 WT HT COAD STDY ESTCPA ESTCPP ALFOB
$DATA ..\8Dec2012_PABISjh.csv IGNORE #
$ESTIM MAXEVAL=9999 SIGDIG=3 PRINT=0 METHOD=CONDITIONAL INTERACTION NOABORT
MSFO=all_minto_final.msf
$COV

```

```
$THETA
```

```
; Alfentanil pharmacokinetics
```

```
(0, 6.29, 200) ; V1A
(0, 16.3, 200) ; V2A
(0, .456, 8) ; CL1A
(0, .596, 8) ; CL2A
(.01, 4.44, 10) ; TEQA
```

```
; Propofol pharmacokinetics
```

```
(0, 7.63, 50) ; V4P
(0, 13.2, 500) ; V5P
(0, 68.5, 100) ; V6P
(0, 2.13, 100) ; CL4P
(0, 1.76, 100) ; CL5P
(0, 1.12, 100) ; CL6P
(.01, 3.39, 10) ; TEQP
```

```
; Pharmacodynamics
```

```
(0, 562, 1200) ; EC50A
(0, 2640, 5000) ; EC50P
(0, 2.98, 6) ; GAMMA
(95, 98, 100) FIX ; BASELN
0 FIX ; BET
(70, 76.3, 98) ; EMAX
```

```
(0, .177,) ; RUV_CVA
(0, .0335,) ; RUV_SDA
(0, .229,) ; RUV_CVP
(0, .0114,) ; RUV_SDP
```

```
7.98 ; RUV_SDFX
0 FIX ; RUV_CVFX
```

```
$OMEGA
```

```
;BSV alfentanil pharmacokinetics
```

```
0.064 ;PPVCL2A
0.0615 ;PPVV2A
0.708 ; PPVTQA
```

```
$OMEGA BLOCK(2)
```

```
0.5 ;PPVV1A
0.1 0.5 ; PPVCL1A
```

```
;BSV propofol pharmacokinetics
$OMEGA BLOCK(4)
0.5 ; PPVV4P
0.1 0.5 ; PPVCL4P
0.1 0.1 0.5 ; PPVV5P
0.1 0.1 0.1 0.5 ; PPVCL5P

$OMEGA
0.00022 ; PPVV6P
0.0357 ; PPVCL6P
0.00547 ; PPVTQP

; BSV pharmacodynamics
0.0308 ; PPVC5P
0 FIX ; PPVE0

$OMEGA BLOCK(3)
0.5 ; PPVEMX
0.1 0.5 ; PPVC5A
0.1 0.1 0.5 ; PPVGAM

; variability associated with residual error terms
0.0361 ; PPV_FX
0.0735 ; PPV_RUVP
0.406 ; PPV_RUVA

$SIGMA
1. FIX ; EPS1
1. FIX ; EPS2

$SUBR ADVAN13 TOL=9

$MODEL
COMP(CENTRAL, ALF) ; Two compartments
COMP(P1, ALF)
COMP(EFFECT SITE, ALF)
COMP(CENTRAL, PROP) ; Three compartments
COMP(P1, PROP)
COMP(P2, PROP)
COMP(EFFECT SITE, PROP)

$PK
IF (AMT.GT.0) THEN
DOSE=AMT
ENDIF

LN2=LOG(2)

FSZCL=(WT/70)**0.75 ; Size models, allometric scaling on V, CL and TEQ parameters
FSZV =WT/70
FSZT=FSZV**0.25

V1A=V1A *FSZV *EXP(PPVV1A)
V2A=V2A *FSZV *EXP(PPVV2A)
CL1A=CL1A *FSZCL *EXP(PPVCL1A)
CL2A=CL2A *FSZCL *EXP(PPVCL2A)

TEQA=TEQA* FSZT*EXP(PPVTQA)
```

KEQA=LN2/TEQA

V4P = V4P *FSZV *EXP(PPVV4P)

V5P = V5P *FSZV *EXP(PPVV5P)

V6P = V6P *FSZV *EXP(PPVV6P)

CL4P = CL4P *FSZCL *EXP(PPVCL4P)

CL5P = CL5P *FSZCL *EXP(PPVCL5P)

CL6P = CL6P *FSZCL *EXP(PPVCL6P)

TEQP=TEQP*FSZT*EXP(PPVTQP)

KEQP = LN2/TEQP

S1=V1A

S4=V4P

; Pharmacodynamics

C50A = EC50A*EXP(PPVC5A)

C50P = EC50P*EXP(PPVC5P)

SLOPE= GAMMA*EXP(PPVGAM)

E0 = BASELN*EXP(PPVE0)

BETA = BET

; E_{MAX} constraint model

TVEMAX=EMAX/100

LGEMAX=LOG(TVEMAX/(1-TVEMAX))

EXEMAX=EXP(LGEMAX+PPVEMX)

EMAX=EXEMAX*100/(1+EXEMAX)

\$DES

; Alfentanil pharmacokinetics

DCA1=A(1)/V1A

DCA2=A(2)/V2A

DCEA=A(3)

DADT(1) = DCA2*CL2A-DCA1*(CL1A+CL2A)

DADT(2) = CL2A*(DCA1-DCA2)

DADT(3) = KEQA*(DCA1-DCEA)

; Propofol pharmacokinetics

DCP1=A(4)/V4P

DCP2=A(5)/V5P

DCP3=A(6)/V6P

DCEP=A(7)

DADT(4) = DCP2*CL5P+DCP3*CL6P-DCP1*(CL4P+CL5P+CL6P)

DADT(5) = CL5P*(DCP1-DCP2)

DADT(6) = CL6P*(DCP1-DCP3)

DADT(7) = KEQP*(DCP1-DCEP)

\$ERROR

CPA = A(1)/V1A

ALF = A(3)

CPP = A(4)/V4P

PROP= A(7)

; Normalise drug concentrations to units using Ce₅₀

UA=ALF/C50A

```

UP=PROP/C50P

CONCC=UA+UP

; Calculate 'theta' for Minto model
IF(UP.EQ.0) THEN
  Q = 0
ELSE
  Q = UP/CONCC
ENDIF

; Calculate drug effects
IF(CONCC.EQ.0) THEN
  CON = 0
  CGAM = 0
  RESPN = 0
ELSE
  CON = CONCC / (1-BETA*Q+BETA*Q*Q)
  CGAM=CON**SLOPE
  RESPN=CGAM/(1+CGAM)
ENDIF

; Calculate effects
EFX = E0 - (EMAX * RESPN)

; Add variability associated with residual error - Effects
BISP=EFX*RUV_CVFX
BISA=RUV_SDFX
SDFX=SQRT(BISP*BISP+BISA*BISA)*EXP(PPV_FX)

IF (DVID.EQ.1) THEN ; Effect prediction (BIS)
  Y=EFX +SDFX*EPS2
ENDIF

; Add variability associated with residual error – Alfentanil concentrations
PROPA=CPA*RUV_CVA ;
ADDA=RUV_SDA
SDA=SQRT(PROPA*PROPA+ADDA*ADDA)*EXP(PPV_RUVA)

; Add variability associated with residual error – Propofol concentrations
PROPP=CPP*RUV_CVP
ADDP=RUV_SDP
SDP=SQRT(PROPP*PROPP+ADDP*ADDP)*EXP(PPV_RUVP)

IF (DVID.EQ.2) THEN ; Alfentanil concentrations
  Y=CPA+SDA*EPS1
ENDIF

IF (DVID.EQ.3) THEN ; Propofol concentrations
  Y=CPP+SDP*EPS1
ENDIF

$TABLE ID TIME CPA CPP EFX RESPN DVID Y PROP ALF CON CGAM Q
ONEHEADER NOPRINT FILE=prop_alf_cond_err_nmVII.fit

```

Appendix 4.3 PK covariate screening summary

The following table provides a summary of the initial covariate screening process for pharmacokinetic models. COAD=co-administration of alfentanil, OBJ= Objective function. In the early stages of the analysis, inclusion of age resulted in a significant improvement in our model fit for propofol pharmacokinetics (inclusion on V_1 parameter = Δ OBJ 12.1, $P < 0.001$). However, when this covariate effect was tested again at a later stage, its removal did not affect the model fit and so it was excluded. In the final stage of model development, it was again investigated but was ultimately excluded (propofol V_1 parameter = Δ OBJ 3.67, $P < 0.055$).

ALFENTANIL COVARIATE SEARCH - RUN# 120517-091229						
Covariate Search	THETA	Covariate	Implemented As	SigDigits	OBJ	Δ OBJ
0	-	-	Normal Run	3.5	899.3788762	-
1	1	WT	(THETA(1) * (WT / 55) ** (THETA(5) - 1))	3.8	895.4837995	-3.90
2	2	WT	(THETA(2) * (WT / 55) ** (THETA(5) - 1))	3.2	897.8732388	-1.51
3	4	WT	(THETA(4) * (WT / 55) ** (THETA(5) - 1))	3.4	898.8833534	-0.50
4	5	WT	(THETA(5) * (WT / 55) ** (THETA(5) - 1))	3.5	899.3788762	0.00
5	1	HT	(THETA(1) * (HT / 160) ** (THETA(5) - 1))	4.0	898.255788	-1.12
6	2	HT	(THETA(2) * (HT / 160) ** (THETA(5) - 1))	3.5	893.5660919	-5.81
7	4	HT	(THETA(4) * (HT / 160) ** (THETA(5) - 1))	3.2	898.2303453	-1.15
8	5	HT	(THETA(5) * (HT / 160) ** (THETA(5) - 1))	3.5	899.3788762	0.00
9	NA	AGE		3.5	899.3788762	0.00
10	1	AGE	(THETA(1) * (AGE / 40) ** (THETA(5) - 1))	3.8	898.2485988	-1.13
11	2	AGE	(THETA(2) * (AGE / 40) ** (THETA(5) - 1))	3.2	898.7293435	-0.65
12	4	AGE	(THETA(4) * (AGE / 40) ** (THETA(5) - 1))	3.6	906.5696692	7.19
13	5	AGE	(THETA(5) * (AGE / 40) ** (THETA(5) - 1))	3.5	899.3788762	0.00

PROPOFOL COVARIATE SEARCH - RUN# 120705-134816						
Covariate Search	THETA	Covariate	Implemented As	SigDigits	OBJ	Δ OBJ
0	-	-	Normal Run	3.1	4631.762632	-
1	1	COAD	(THETA(1) * (COAD / 1) ** (THETA(7) - 1))	3.9	4628.131027	-3.63
2	2	COAD	(THETA(2) * (COAD / 1) ** (THETA(7) - 1))	3.7	4631.496701	-0.27
3	3	COAD	(THETA(3) * (COAD / 1) ** (THETA(7) - 1))	3.3	4631.520942	-0.24
4	4	COAD	(THETA(4) * (COAD / 1) ** (THETA(7) - 1))	3.2	4631.148515	-0.61
5	5	COAD	(THETA(5) * (COAD / 1) ** (THETA(7) - 1))	3.9	4631.582023	-0.18
6	6	COAD	(THETA(6) * (COAD / 1) ** (THETA(7) - 1))	3.5	4631.541029	-0.22
7	1	HT	(THETA(1) * (HT / 160) ** (THETA(7) - 1))	3.3	4631.576424	-0.19
8	2	HT	(THETA(2) * (HT / 160) ** (THETA(7) - 1))	3.4	4628.330261	-3.43
9	3	HT	(THETA(3) * (HT / 160) ** (THETA(7) - 1))	3.7	4629.535282	-2.23
10	4	HT	(THETA(4) * (HT / 160) ** (THETA(7) - 1))	4.3	4628.346444	-3.42
11	5	HT	(THETA(5) * (HT / 160) ** (THETA(7) - 1))	3.3	4631.592872	-0.17
12	6	HT	(THETA(6) * (HT / 160) ** (THETA(7) - 1))	3.6	4630.780476	-0.98
13	1	AGE	(THETA(1) * (AGE / 38) ** (THETA(7) - 1))	3.1	4619.695824	-12.07
14	2	AGE	(THETA(2) * (AGE / 38) ** (THETA(7) - 1))	3.4	4631.149052	-0.61
15	3	AGE	(THETA(3) * (AGE / 38) ** (THETA(7) - 1))	3.5	4630.988199	-0.77
16	4	AGE	(THETA(4) * (AGE / 38) ** (THETA(7) - 1))	3.6	4628.948417	-2.81
17	5	AGE	(THETA(5) * (AGE / 38) ** (THETA(7) - 1))	3.2	4630.915516	-0.85

Implemented using PLT Tools, version 4.4.2 and R, version 2.13.1

Appendix 7. Model code for BIS response for multiple drug classes

```

$PROB MULTIPLE DRUG CLASS MODEL FOR BIS EFFECTS IN SURGICAL PATIENTS
$INPUT ID TIME CESE CEDE CEIS CERE CEAL M1F2 HT WT AGE DV MDV DVID AMT LBM CMT
$DATA MultidrugDat.csv
$ESTIMATION SIGDIG=7 MAX=500 PRINT=1 METHOD=1 NOABORT
MSFO=a_3brun_additive_openfentkeo.msf
$COV
$THETA
; Fentanyl pharmacokinetics, taken from Scott et al (all parameters and BSV estimates fixed)
12.7 FIX ; V1F
49.3 FIX ; V2F
297. FIX ; V3F
0.71 FIX ; CL1F
4.74 FIX ; CL2F
2.29 FIX ; CL3F
(.05, 0.1, .50) ; KEOF

; Propofol pharmacokinetics, taken from Schnider et al (all parameters and BSV estimates fixed, but keo estimated)
4.27 FIX ; V5P
18.9 FIX ; V6P
238. FIX ; V7P
1.89 FIX ; CL5P
1.29 FIX ; CL6P
0.836 FIX ; CL7P
(.1, 0.204) ; KEOP

; Midazolam pharmacokinetics, taken from Absalom et al (all parameters and BSV estimates fixed, but keo estimated)
8.5 FIX ; V1M
18.6 FIX ; V2M
63. FIX ; V3M
0.3 FIX ; CL1M
0.95 FIX ; CL2M
0.44 FIX ; CL3M
(.01,0.156, 0.3) ; KEOM

; Pharmacodynamics
(0.5, 1.37, 5) ; EC50S
(0, 3.89, 5) ; EC50D
(0, 2.16, 5) ; EC50P
(0, 0.258, 1.5) ; EC50M
(0, 8.99, 10) ; EC50F

(0, 2.65, 4) ; GAMMA
(95, 98, 100) FIX ; BASELN
(70, 76.4, 98) ; EMAX

; Parameter describing the interaction between propofol and midazolam
0 FIX ; BETPM

;variability associated with residual error estimates
(0, 6.8, ) ; RUV_SDFX
0 FIX ; RUV_CVFX

; Covariate effects, pharmacodynamics

```

(-.01,-0.00999, 0) ; AGES
0 FIX; AGEF
(-.01,-0.00001, 0); AGEF

\$OMEGA

; Fentanyl BSV for pharmacokinetics, taken from Scott et al

0.2 FIX ; PPVV1F

0.1 FIX ; PPVV2F

0.38 FIX ; PPVV3F

0.32 FIX ; PPVCL1F

0.1 FIX ; PPVCL2F

0.34 FIX ; PPVCL3F

; Propofol BSV for pharmacokinetics, taken from Schnider et al

0.2 FIX ; PPVV5P

0.1 FIX ; PPVCL5P

0.38 FIX ; PPVV6P

0.32 FIX ; PPVCL6P

0.1 FIX; PPVV7P

0.34 FIX ; PPVCL7P

; Midazolam BSV for pharmacokinetics, taken from Absalom et al

0.2 FIX ; PPVV1M

0.1 FIX ; PPVV2M

0.38 FIX ; PPVV3M

0.32 FIX ; PPVCL1M

0.1 FIX ; PPVCL2M

0.34 FIX ; PPVCL3M

; BSV on residual error estimates

0.0427 ; PPV_FX

; BSV for pharmacodynamics

0.243 ; PPVC5S

0 FIX ; PPVKEOM

0 FIX ; PPVC5M

0 FIX ; PPVKEOF

1.82 ; PPVC5F

\$OMEGA BLOCK(2)

2.68 ; PPVKEOP

1.35 0.702 ; PPVC5P

\$OMEGA BLOCK(2)

0.0793; PPVEMX

-0.15 0.299; PPVGAM

\$SIGMA

1 FIX ; EPS1

```

$SUBR ADVAN13 TOL=9
$MODEL
COMP(FENC) ; 3 compartment fentanyl pharmacokinetics
COMP(FENP1)
COMP(FENP2)
COMP(FEFFCT)
COMP(PROPC) ; 3 compartments propofol pharmacokinetics
COMP(PROPP1)
COMP(PROPP2)
COMP(PEFFCT)
COMP(MDZC) ; 3 compartments midazolam pharmacokinetics
COMP(MDZP1)
COMP(MDZP2)
COMP(MDZEFFCT)

$PK
IF (AMT.GT.0) THEN
DOSE=AMT
ENDIF

; scaling parameters for size
FSZCL=(WT/70)**0.75
FSZV =WT/70
FSZT = FSZV**.25

LN2=LOG(2)

; Scott et al pharmacokinetic model for fentanyl
V1F = (V1F/70*WT) *EXP(PPVV1F)
V2F = (V2F/70*WT) *EXP(PPVV2F)
V3F = (V3F/70*WT) *EXP(PPVV3F)
CL1F = (CL1F/70*WT) *EXP(PPVCL1F)
CL2F = (CL2F/70*WT) *EXP(PPVCL2F)
CL3F = (CL3F/70*WT) *EXP(PPVCL3F)
KEOF= KEOF *EXP(PPVKEOF)

; Schnider et al pharmacokinetic model for propofol (note covariate effects)
V5P =V5P*EXP(PPVV5P)
V6P =(V6P+(-0.391*(AGE-53)))*EXP(PPVV6P)
V7P =V7P*EXP(PPVV7P)
CL5P =(CL5P+(0.0456*(WT-77))+(-0.0681*(LBM-59))+(0.0264*(HT-177)))*EXP(PPVCL5P)
CL6P =(CL6P+(-0.024*(AGE-53)))*EXP(PPVCL6P)
CL7P =CL7P*EXP(PPVCL7P)
KEOP=KEOP*EXP(PPVKEOP)

; Absalom et al pharmacokinetic model for midazolam
V1M =(V1M/70*WT)*EXP(PPVV1M)
V2M =(V2M/70*WT)*EXP(PPVV2M)
V3M =(V3M/70*WT)*EXP(PPVV3M)
CL1M =(CL1M/70*WT)*EXP(PPVCL1M)
CL2M =(CL2M/70*WT)*EXP(PPVCL2M)
CL3M =(CL3M/70*WT)*EXP(PPVCL3M)
KEOM=KEOM*EXP(PPVKEOM)

```

```

; Pharmacodynamic models
C50S = EC50S*EXP(PPVC5S) *(1+AGES*(AGE-46))
C50D = EC50D
C50P = EC50P*EXP(PPVC5P)*(1+AGEP*(AGE-46))
C50F = EC50F*EXP(PPVC5F)*(1+AGEF*(AGE-46))
C50M = EC50M*EXP(PPVC5M)
SLOPE = GAMMA*EXP(PPVGAM)
E0 = BASELN

; EMAX constraint model
TVEMAX=EMAX/100
LGEMAX=LOG(TVEMAX/(1-TVEMAX))
EXEMAX=EXP(LGEMAX+PPVEMX)
EMAX=EXEMAX*100/(1+EXEMAX)

$DES
; Differential equations for movement of drug between compartments
; Fentanyl
DCF1=A(1)/V1F
DCF2=A(2)/V2F
DCF3=A(3)/V3F
DCEF=A(4)

DADT(1) = DCF2*CL2F+DCF3*CL3F-DCF1*(CL1F+CL2F+CL3F)
DADT(2) = CL2F*(DCF1-DCF2)
DADT(3) = CL3F*(DCF1-DCF3)
DADT(4) = KEOF*(DCF1-DCEF)

; Propofol
DCP1=A(5)/V5P
DCP2=A(6)/V6P
DCP3=A(7)/V7P
DCEP=A(8)

DADT(5) = DCP2*CL6P+DCP3*CL7P-DCP1*(CL5P+CL6P+CL7P)
DADT(6) = CL6P*(DCP1-DCP2)
DADT(7) = CL7P*(DCP1-DCP3)
DADT(8) = KEOP*(DCP1-DCEP)

; Midazolam
DCM1=A(9)/V1M
DCM2=A(10)/V2M
DCM3=A(11)/V3M
DCEM=A(12)

DADT(9) = DCM2*CL2M+DCM3*CL3M-DCM1*(CL1M+CL2M+CL3M)
DADT(10) = CL2M*(DCM1-DCM2)
DADT(11) = CL3M*(DCM1-DCM3)
DADT(12) = KEOM*(DCM1-DCEM)

$ERROR
; Plasma and effect site concentration, Fentanyl
CPF = A(1)/V1F
FENT = A(4)
; Plasma and effect site concentration, Propofol
CPP = A(5)/V5P
PROP = A(8)
; Plasma and effect site concentration, Midazolam

```

CPM = A(9)/V1M

MIDZ = A(12)

; Normalise effect site concentrations for each drug class

UO = (CERE/20.1) + (FENT/C50F) + (CEAL/646) ; opioid drug class, CE₅₀ from Ch 4&5 for alfentanil and remifentanil

UV = (CESE/C50S) + (CEDE/C50D) + (CEIS/0.66) ; inhalation drug class, CE₅₀ from literature for isoflurane

UM = MIDZ/C50M ; Propofol and midazolam units for combining

UP = PROP/C50P

; Calculate ratio of propofol to midazolam according to Minto et al

IF (UP.EQ.0)THEN

Q = 0

ELSE

Q = UP / (UP + UM)

ENDIF

; Calculate function for interaction parameter and ratio of propofol to midazolam

U50= 1- BETPM*Q + BETPM*Q*Q

; Note all other interactions are assumed to be additive

; Needed to ensure NONMEM can calculate drug response in the absence of any propofol or midazolam

UH =UM+UP

IF(UH.EQ.0)THEN

UQM = 0

ELSE

; incorporate U50 term

UQM = (UP+UM) / U50

ENDIF

; Needed to ensure NONMEM can calculate drug response in the absence of any drug

UALL = UP + UV + UO + UM

IF(UALL.EQ.0)THEN

CGAM =0

RESPN =0 ; if no drug then drug response is 0

ELSE

CGAM=(UQM+UV+UO)**SLOPE ; Combine all drug units, including modified propofol units (denoted as UQM)

RESPN=CGAM/(1+CGAM)

ENDIF

; Calculate BIS response

EFX = E0 - (EMAX * RESPN)

; Variability model

BISP=EFX*RUV_CVFX

BISA=RUV_SDFX

SDFX=SQRT(BISP*BISP+BISA*BISA)*EXP(PPV_FX)

; Response predictions

Y=EFX +SDFX*EPS1

\$TABLE ONEHEADER NOPRINT FILE=corrected_3run1_4drug_4mar_2.fit

ID TIME DV RESPN EFX Y PRED

References

1. J.W. Chiu, *Nonopioid intravenous anesthesia*, in *Clinical Anesthesia*, P.G. Barash, B.F. Cullen, and R.K. Stoelting, Editors. 2001, Lippincott Williams & Wilkins: Philadelphia. p. 339.
2. P.S. Glass, *Anesthetic drug interactions: An insight into general anesthesia - Its mechanism and dosing strategies*. *Anesthesiology*, 1998. **88**(1): p. 5-6.
3. J.S. Lundy, *Balanced anesthesia*. Minnesota Medical, 1926. **9**: p. 399-404.
4. C.T. Gray and J.G. Rees, *Role of apnoea in anaesthesia for major surgery*. *BMJ*, 1952. **2**: p. 891-92.
5. T.C. Gray, *The use of d-Tubocurarine chloride in anaesthesia: lecture delivered at The Royal College of Surgeons of England on 17th April, 1947*. *Ann. R. Coll. Surg. Engl.*, 1947. **1**(4): p. 191-203.
6. B.J. Anderson, A.L. Potts and D.W. Herd, *Problems and pitfalls performing pharmacokinetic studies in children*. *Paediatr Perinat Drug Ther*, 2007. **8**(1): p. 4-17.
7. A.M. Lynn, M.K. Nespeca, K.E. Opheim and J.T. Slattery, *Respiratory effects of intravenous morphine infusions in neonates, infants, and children after cardiac surgery*. *Anesth Analg*, 1993. **77**(4): p. 695-701.
8. L.L. Christrup, *Morphine metabolites*. *Acta Anaesthesiol Scand*, 1997. **41**(1 Pt 2): p. 116-22.
9. National Ethics Advisory Committee, *Ethical Guidelines for Intervention Studies: Revised edition*. 2012, Ministry of Health: Wellington.
10. Bouwmeester NJ, Anderson BJ, Tibboel D and Holford NH, *Developmental pharmacokinetics of morphine and its metabolites in neonates, infants and young children*. *Br J Anaesth*, 2004. **92**(2): p. 208-17.
11. C.J. Hull, H.B. Van Beem, K. McLeod, A. Sibbald and M.J. Watson, *A pharmacodynamic model for pancuronium*. *Br J Anaesth*, 1978. **50**(11): p. 1113-23.
12. A. Hill, *The possible effects of the aggregation of the molecules of haemoglobin on its dissociation curves*. *J Physiol*, 1910. **40**(Suppl): p. i-vii.
13. T.M. Post, J.I. Freijer, B.A. Ploeger and M. Danhof, *Extensions to the visual predictive check to facilitate model performance evaluation*. *J Pharmacokinet Pharmacodyn*, 2008. **35**(2): p. 185-202.
14. W.J. Sam, S.C. MacKey, J. Lotsch and D.R. Drover, *Morphine and its metabolites after patient-controlled analgesia: considerations for respiratory depression*. *J Clin Anesth.*, 2011. **23**(2): p. 102-6.
15. B.J. Anderson, *My child is unique; the pharmacokinetics are universal*. *Paediatr Anaesth*, 2012. **22**(6): p. 530-38.
16. A. Dahan, R. Romberg, L. Teppema, E. Sarton, H. Bijl and E. Olofsen, *Simultaneous measurement and integrated analysis of analgesia and respiration after an intravenous morphine infusion*. *Anesthesiology*, 2004. **101**(5): p. 1201-9.
17. C.E. Inturrisi and W.A. Colburn, *Application of pharmacokinetic-pharmacodynamic modeling to analgesia*, in *Advances in Pain Research and Therapy. Opioid Analgesics in the Management of Clinical Pain*, K.M. Foley and C.E. Inturrisi, Editors. 1986, Raven Press: New York. p. 441-452.
18. E.L. van Dorp, R. Romberg, E. Sarton, J.G. Bovill and A. Dahan, *Morphine-6-glucuronide: morphine's successor for postoperative pain relief?* *Anesth Analg*, 2006. **102**(6): p. 1789-97.

19. N.J. Bouwmeester, J.N. van den Anker, W.C. Hop, K.J. Anand and D. Tibboel, *Age- and therapy-related effects on morphine requirements and plasma concentrations of morphine and its metabolites in postoperative infants*. Br J Anaesth, 2003. **90**(5): p. 642-52.
20. R.J. Bray, C. Beeton, W. Hinton and J.A. Seviour, *Plasma morphine levels produced by continuous infusion in children*. Anaesthesia, 1986. **41**(7): p. 753-5.
21. A.M. Lynn, K.E. Opheim and D.C. Tyler, *Morphine infusion after pediatric cardiac surgery*. Crit Care Med, 1984. **12**(10): p. 863-6.
22. R. Romberg, E. Olofsen, E. Sarton, L. Teppema and A. Dahan, *Pharmacodynamic effect of morphine-6-glucuronide versus morphine on hypoxic and hypercapnic breathing in healthy volunteers*. Anesthesiology, 2003. **99**(4): p. 788-98.
23. J. Lotsch, C. Skarke, H. Schmidt, S. Grosch and G. Geisslinger, *The transfer half-life of morphine-6-glucuronide from plasma to effect site assessed by pupil size measurement in healthy volunteers*. Anesthesiology, 2001. **95**(6): p. 1329-38.
24. H. Kehlet, *Surgical stress: the role of pain and analgesia*. Br J Anaesth, 1989. **63**(2): p. 189-95.
25. K. Toussaint, X.C. Yang, M.A. Zielinski, K.L. Reigle, S.D. Sacavage, S. Nagar, et al., *What do we (not) know about how paracetamol (acetaminophen) works?* Journal of Clinical Pharmacy and Therapeutics, 2010. **35**(6): p. 617-638.
26. B.J. Anderson, *Paracetamol (Acetaminophen): mechanisms of action*. Paediatr Anaesth, 2008. **18**(10): p. 915-21.
27. G.G. Graham and K.F. Scott, *Mechanism of action of paracetamol*. Am J Ther, 2005. **12**(1): p. 46-55.
28. H.S. Smith, *Potential analgesic mechanisms of acetaminophen*. Pain Physician, 2009. **12**(1): p. 269-80.
29. B.J. Anderson, G.A. Woollard and N.H. Holford, *Acetaminophen analgesia in children: placebo effect and pain resolution after tonsillectomy*. Eur J Clin Pharmacol, 2001. **57**(8): p. 559-69.
30. B.J. Anderson, N.H. Holford, G.A. Woollard and P.L. Chan, *Paracetamol plasma and cerebrospinal fluid pharmacokinetics in children*. Br J Clin Pharmacol, 1998. **46**(3): p. 237-43.
31. B. Kis, J.A. Snipes and D.W. Busija, *Acetaminophen and the cyclooxygenase-3 puzzle: sorting out facts, fictions, and uncertainties*. J Pharmacol Exp Ther, 2005. **315**(1): p. 1-7.
32. L.F. Prescott, *Paracetamol (Acetaminophen) A critical bibliographic review*. 2nd ed. 1996, London: Taylor & Francis Publishers. p 205-214.
33. B.J. Anderson, N.H. Holford, G.A. Woollard, S. Kanagasundaram and M. Mahadevan, *Perioperative pharmacodynamics of acetaminophen analgesia in children*. Anesthesiology, 1999. **90**(2): p. 411-21.
34. R.D. Brown, J.T. Wilson, G.L. Kearns, V.F. Eichler, V.A. Johnson and K.M. Bertrand, *Single-dose pharmacokinetics of ibuprofen and acetaminophen in febrile children*. J Clin Pharmacol, 1992. **32**(3): p. 231-41.
35. E. Sigel, *Mapping of the benzodiazepine recognition site on GABA(A) receptors*. Curr Top Med Chem, 2002. **2**(8): p. 833-9.
36. Y. Al-Tiay, *Validation of the pharmacokinetic and pharmacodynamic drug models in a full scale anaesthetic simulator*, in *Department of Anaesthesiology*. 2007, University of Auckland: Auckland. p. 33.
37. T.G. Short and P.T. Chui, *Propofol and midazolam act synergistically in combination*. Br J Anaesth, 1991. **67**(5): p. 539-45.
38. P.S. Glass, M. Bloom, L. Kearse, C. Rosow, P. Sebel and P. Manberg, *Bispectral analysis measures sedation and memory effects of propofol, midazolam, isoflurane, and alfentanil in healthy volunteers*. Anesthesiology, 1997. **86**(4): p. 836-47.

39. S. Albrecht, H. Ihmsen, W. Hering, G. Geisslinger, J. Dingemanse, H. Schwilden, et al., *The effect of age on the pharmacokinetics and pharmacodynamics of midazolam*. Clin Pharmacol Ther, 1999. **65**(6): p. 630-9.
40. D.J. Greenblatt, B.L. Ehrenberg, J. Gunderman, A. Locniskar, J.M. Scavone, J.S. Harmatz, et al., *Pharmacokinetic and electroencephalographic study of intravenous diazepam, midazolam, and placebo*. Clin Pharmacol Ther, 1989. **45**(4): p. 356-65.
41. J. Barr, K. Zomorodi, E.J. Bertaccini, S.L. Shafer and E. Geller, *A double-blind, randomized comparison of i.v. lorazepam versus midazolam for sedation of ICU patients via a pharmacologic model*. Anesthesiology, 2001. **95**(2): p. 286-98.
42. M. Buhner, P.O. Maitre, O. Hung and D.R. Stanski, *Electroencephalographic effects of benzodiazepines. I. Choosing an electroencephalographic parameter to measure the effect of midazolam on the central nervous system*. Clin Pharmacol Ther, 1990. **48**(5): p. 544-54.
43. P.O. Maitre, B. Funk, C. Crevoisier and H.R. Ha, *Pharmacokinetics of midazolam in patients recovering from cardiac surgery*. Eur J Clin Pharmacol, 1989. **37**(2): p. 161-6.
44. K. Zomorodi, A. Donner, J. Somma, J. Barr, R. Sladen, J. Ramsay, et al., *Population pharmacokinetics of midazolam administered by target controlled infusion for sedation following coronary artery bypass grafting*. Anesthesiology, 1998. **89**(6): p. 1418-29.
45. L.I. Cortínez, B.J. Anderson, A. Penna, L. Olivares, H.R. Muñoz, N.H.G. Holford, et al., *Influence of obesity on propofol pharmacokinetics: derivation of a pharmacokinetic model*. Br J Anaesth, 2010. **105**(4): p. 448-456.
46. B. Marsh, M. White, N. Morton and G.N. Kenny, *Pharmacokinetic model driven infusion of propofol in children*. Br J Anaesth, 1991. **67**(1): p. 41-8.
47. E. Gepts, F. Camu, I.D. Cockshott and E.J. Douglas, *Disposition of propofol administered as constant rate intravenous infusions in humans*. Anesth Analg, 1987. **66**(12): p. 1256-1263.
48. M. White, G.N. Kenny and S. Schraag, *Use of target controlled infusion to derive age and gender covariates for propofol clearance*. Clin Pharmacokinet, 2008. **47**(2): p. 119-27.
49. J.B. Glen and F. Servin, *Evaluation of the predictive performance of four pharmacokinetic models for propofol*. Br J Anaesth, 2009. **102**(5): p. 626-32.
50. C.F. Swinhoe, J.E. Peacock, J.B. Glen and C.S. Reilly, *Evaluation of the predictive performance of a 'Diprifusor' TCI system*. Anaesthesia, 1998. **53 Suppl 1**: p. 61-7.
51. C. Minto, T.W. Schnider, K. Gregg, T. Henthorn and S. Shafer, *Using the time of maximum effect site concentration to combine pharmacokinetics and pharmacodynamics*. Anesthesiology, 2003. **99**(2): p. 324-333.
52. M.M. Struys, T. De Smet, B. Depoorter, L.F. Versichelen, E.P. Mortier, F.J. Dumortier, et al., *Comparison of plasma compartment versus two methods for effect compartment-controlled target-controlled infusion for propofol*. Anesthesiology, 2000. **92**(2): p. 399-406.
53. V. Billard, P. Gambus, N. Chamoun, D. Stanski and S. Shafer, *A comparison of spectral edge, delta power, and bispectral index as EEG measures of alfentanil, propofol, and midazolam drug effect*. Clin Pharmacol Ther, 1997. **61**(1): p. 45-58.
54. Schnider T. W., Minto C. F., Gambus P. L., Andresen C., Goodale D. B., Shafer S. L., et al., *The influence of method of administration and covariates on the pharmacokinetics of propofol in adult volunteers*. Anesthesiology, 1998. **88**(5): p. 1170-1182.
55. Schnider T.W., Minto C.F., Shafer S.L., Gambus P.L., Andresen C., Goodale D.B., et al., *The influence of age on propofol pharmacodynamics*. Anesthesiology, 1999. **90**(6): p. 1502-16.
56. B.J. Anderson and G.H. Meakin, *Scaling for size: some implications for paediatric anaesthesia dosing*. Paediatr Anaesth, 2002. **12**(3): p. 205-19.
57. C. Jeleazcov, H. Ihmsen, J. Schmidt, C. Ammon, H. Schwilden, J. Schuttler, et al., *Pharmacodynamic modelling of the bispectral index response to propofol-based anaesthesia during general surgery in children*. Br J Anaesth, 2008. **100**(4): p. 509-16.

58. L.I. Cortinez, I.F. Troconiz, R. Fuentes, P. Gambus, Y.W. Hsu, F. Altermatt, et al., *The influence of age on the dynamic relationship between end-tidal sevoflurane concentrations and bispectral index*. *Anesth Analg*, 2008. **107**(5): p. 1566-72.
59. T.W. Bouillon, J. Bruhn, L. Radulescu, C. Andresen, T.J. Shafer, C. Cohane, et al., *Pharmacodynamic interaction between propofol and remifentanyl regarding hypnosis, tolerance of laryngoscopy, bispectral index, and electroencephalographic approximate entropy*. *Anesthesiology*, 2004. **100**(6): p. 1353-72.
60. S.E. Kern, G. Xie, J.L. White and T.D. Egan, *A response surface analysis of propofol-remifentanyl pharmacodynamic interaction in volunteers*. *Anesthesiology*, 2004. **100**(6): p. 1373-81.
61. C. Smith, A.I. McEwan, R. Jhaveri, M. Wilkinson, D. Goodman, L.R. Smith, et al., *The interaction of fentanyl on the Cp50 of propofol for loss of consciousness and skin incision*. *Anesthesiology*, 1994. **81**(4): p. 820-8; discussion 26A.
62. A. Shafer, V.A. Doze, S.L. Shafer and P.F. White, *Pharmacokinetics and pharmacodynamics of propofol infusions during general anesthesia*. *Anesthesiology*, 1988. **69**(3): p. 348-56.
63. T. Bouillon, J. Bruhn, L. Radu-Radulescu, E. Bertaccini, S. Park and S. Shafer, *Non-steady state analysis of the pharmacokinetic interaction between propofol and remifentanyl*. *Anesthesiology*, 2002. **97**(6): p. 1350-62.
64. B.K. Kataria, S.A. Ved, H.F. Nicodemus, G.R. Hoy, D. Lea, M.Y. Dubois, et al., *The pharmacokinetics of propofol in children using three different data analysis approaches*. *Anesthesiology*, 1994. **80**(1): p. 104-122.
65. J. Schuttler and H. Ihmsen, *Population pharmacokinetics of propofol: a multicenter study*. *Anesthesiology*, 2000. **92**(3): p. 727-38.
66. F. Servin, R. Farinotti, J.-P. Haberer and J.-M. Desmots, *Propofol Infusion for maintenance of anesthesia in morbidly obese patients receiving nitrous oxide: A clinical and pharmacokinetic study*. *Anesthesiology*, 1993. **78**(4): p. 657-665.
67. T.G. Short, C.S. Aun, P. Tan, J. Wong, Y.H. Tam and T.E. Oh, *A prospective evaluation of pharmacokinetic model controlled infusion of propofol in paediatric patients*. *Br J Anaesth*, 1994. **72**(3): p. 302-6.
68. R.M. Tackley, G.T.R. Lewis, C. Prys-Roberts, R.W. Boaden, J. Dixon and J.T. Harvey, *Computer controlled infusion of propofol*. *Br J Anaesth*, 1989. **62**(1): p. 46-53.
69. M.J. Mertens, E. Olofsen, F.H. Engbers, A.G. Burm, J.G. Bovill and J. Vuyk, *Propofol reduces perioperative remifentanyl requirements in a synergistic manner: response surface modeling of perioperative remifentanyl-propofol interactions*. *Anesthesiology*, 2003. **99**(2): p. 347-59.
70. J.W. Sear, *Recent advances and developments in the clinical use of i.v. opioids during the perioperative period*. *Br J Anaesth*, 1998. **81**(1): p. 38-50.
71. J.C. Scott and D.R. Stanski, *Decreased fentanyl and alfentanil dose requirements with age. A simultaneous pharmacokinetic and pharmacodynamic evaluation*. *J Pharmacol Exp Ther*, 1987. **240**(1): p. 159-66.
72. S.L. Shafer and J.R. Varvel, *Pharmacokinetics, pharmacodynamics, and rational opioid selection*. *Anesthesiology*, 1991. **74**(1): p. 53-63.
73. C.F. Minto, T.W. Schnider, T.D. Egan, E. Youngs, H.J. Lemmens, P.L. Gambus, et al., *Influence of age and gender on the pharmacokinetics and pharmacodynamics of remifentanyl. I. Model development*. *Anesthesiology*, 1997. **86**(1): p. 10-23.
74. P.O. Maitre, S. Vozeh, J. Heykants, D.A. Thomson and D.R. Stanski, *Population pharmacokinetics of alfentanil: the average dose-plasma concentration relationship and interindividual variability in patients*. *Anesthesiology*, 1987. **66**(1): p. 3-12.

75. T.D. Egan, C.F. Minto, D.J. Hermann, J. Barr, K.T. Muir and S.L. Shafer, *Remifentanil versus alfentanil: comparative pharmacokinetics and pharmacodynamics in healthy adult male volunteers*. *Anesthesiology*, 1996. **84**(4): p. 821-33.
76. A. Dahan, D. Nieuwenhuijs, E. Olofsen, E. Sarton, R. Romberg and L. Teppema, *Response surface modeling of alfentanil-sevoflurane interaction on cardiorespiratory control and bispectral index*. *Anesthesiology*, 2001. **94**(6): p. 982-91.
77. M. Niesters, A. Dahan, B. Kest, J. Zacny, T. Stijnen, L. Aarts, et al., *Do sex differences exist in opioid analgesia? A systematic review and meta-analysis of human experimental and clinical studies*. *Pain*, 2010. **151**(1): p. 61-8.
78. E. Sarton, E. Olofsen, R. Romberg, J. den Hartigh, B. Kest, D. Nieuwenhuijs, et al., *Sex differences in morphine analgesia: an experimental study in healthy volunteers*. *Anesthesiology*, 2000. **93**(5): p. 1245-54; discussion 6A.
79. L. Barvais, F. Cantraine, A. D'Hollander and E. Coussaert, *Predictive accuracy of continuous alfentanil infusion in volunteers*. *Anesth Analg*, 1993. **77**(4): p. 801-810.
80. T. Bouillon, C. Schmidt, G. Garstka, D. Heimbach, D. Stafforst, H. Schwilden, et al., *Pharmacokinetic-pharmacodynamic modeling of the respiratory depressant effect of alfentanil*. *Anesthesiology*, 1999. **91**(1): p. 144-55.
81. S. Bower and C.J. Hull, *Comparative pharmacokinetics of fentanyl and alfentanil*. *Br J Anaesth*, 1982. **54**(8): p. 871-7.
82. A.G. Burm, M.E. Ausems, J. Spierdijk and D.R. Stanski, *Pharmacokinetics of alfentanil administered at a variable rate during three types of surgery*. *Eur J Anaesthesiol*, 1993. **10**(4): p. 241-51.
83. R.J. Fragen, L.H. Booij, G.J. Braak, T.B. Vree, J. Heykants and J.F. Crul, *Pharmacokinetics of the infusion of alfentanil in man*. *Br J Anaesth*, 1983. **55**(11): p. 1077-81.
84. C. Meistelman, C. Saint-Maurice, M. Lepaul, J.C. Levron, J.P. Loose and K. Mac Gee, *A comparison of alfentanil pharmacokinetics in children and adults*. *Anesthesiology*, 1987. **66**(1): p. 13-6.
85. M.P. Persson, A. Nilsson and P. Hartvig, *Pharmacokinetics of alfentanil in total i.v. anaesthesia*. *Br J Anaesth*, 1988. **60**(7): p. 755-61.
86. A. Shafer, M.-L. Sung and P.F. White, *Pharmacokinetics and pharmacodynamics of alfentanil infusions during general anesthesia*. *Anesth Analg*, 1986. **65**(10): p. 1021-1028.
87. H. Van Beem, A. Van Peer, R. Gasparini, R. Woestenborghs, J. Heykants, H. Noorduyn, et al., *Pharmacokinetics of alfentanil during and after a fixed rate infusion*. *Br J Anaesth*, 1989. **62**(6): p. 610-5.
88. J.G. Bovill, P.S. Sebel, C.L. Blackburn and J. Heykants, *The pharmacokinetics of alfentanil (R39209): a new opioid analgesic*. *Anesthesiology*, 1982. **57**(6): p. 439-43.
89. F. Camu, E. Gepts, M. Rucquoi and J. Heykants, *Pharmacokinetics of alfentanil in man*. *Anesth Analg*, 1982. **61**(8): p. 657-61.
90. M.J. Mertens, J. Vuyk, E. Olofsen, J.G. Bovill and A.G. Burm, *Propofol alters the pharmacokinetics of alfentanil in healthy male volunteers*. *Anesthesiology*, 2001. **94**(6): p. 949-57.
91. A. Petros, N. Dunne, R. Mehta, C.J. Dore, A. Van Peer, C. Gillbe, et al., *The pharmacokinetics of alfentanil after normothermic and hypothermic cardiopulmonary bypass*. *Anesth Analg*, 1995. **81**(3): p. 458-64.
92. D.A. McClain and C.C. Hug, Jr., *Intravenous fentanyl kinetics*. *Clin Pharmacol Ther*, 1980. **28**(1): p. 106-14.
93. S.L. Shafer, J.R. Varvel, N. Aziz and J.C. Scott, *Pharmacokinetics of fentanyl administered by computer-controlled infusion pump*. *Anesthesiology*, 1990. **73**(6): p. 1091-102.

94. J. Lötsch, C. Skarke, H. Schmidt, J. Liefhold and G. Geisslinger, *Pharmacokinetic modeling to predict morphine and morphine-6-glucuronide plasma concentrations in healthy young volunteers*. Clin Pharmacol Ther, 2002. **72**(2): p. 151-62.
95. E. Olofsen, E. van Dorp, L. Teppema, L. Aarts, T.W. Smith, A. Dahan, et al., *Naloxone reversal of morphine- and morphine-6-glucuronide-induced respiratory depression in healthy volunteers: a mechanism-based pharmacokinetic-pharmacodynamic modeling study*. Anesthesiology, 2010. **112**(6): p. 1417-27.
96. R. Romberg, E. Olofsen, E. Sarton, J. den Hartigh, P.E. Taschner and A. Dahan, *Pharmacokinetic-pharmacodynamic modeling of morphine-6-glucuronide-induced analgesia in healthy volunteers: absence of sex differences*. Anesthesiology, 2004. **100**(1): p. 120-33.
97. T.D. Egan, B. Huizinga, S.K. Gupta, R.L. Jaarsma, R.J. Sperry, J.B. Yee, et al., *Remifentanil pharmacokinetics in obese versus lean patients*. Anesthesiology, 1998. **89**(3): p. 562-73.
98. T.D. Egan, H.J. Lemmens, P. Fiset, D.J. Hermann, K.T. Muir, D.R. Stanski, et al., *The pharmacokinetics of the new short-acting opioid remifentanil (GI87084B) in healthy adult male volunteers*. Anesthesiology, 1993. **79**(5): p. 881-92.
99. W.W. Mapleson, *Effect of age on MAC in humans: a meta-analysis*. Br J Anaesth, 1996. **76**(2): p. 179-185.
100. J.G. Lerou and L.H. Booij, *Model-based administration of inhalation anaesthesia. 1. Developing a system model*. Br J Anaesth, 2001. **86**(1): p. 12-28.
101. J.G. Lerou and J. Mourisse, *Applying a physiological model to quantify the delay between changes in end-expired concentrations of sevoflurane and bispectral index*. Br J Anaesth, 2007. **99**(2): p. 226-236.
102. R.R. Kennedy, R.A. French and C. Spencer, *Predictive accuracy of a model of volatile anesthetic uptake*. Anesth Analg, 2002. **95**(6): p. 1616-21.
103. H. Wissing, I. Kuhn, S. Rietbrock and U. Fuhr, *Pharmacokinetics of inhaled anaesthetics in a clinical setting: comparison of desflurane, isoflurane and sevoflurane*. Br J Anaesth, 2000. **84**(4): p. 443-9.
104. S. Kreuer, J. Bruhn, W. Wilhelm, U. Grundmann, H. Rensing and S. Ziegeler, *Comparative pharmacodynamic modeling of desflurane, sevoflurane and isoflurane*. J Clin Monit Comput, 2009. **23**(5): p. 299-305.
105. B. Rehberg, T. Bouillon, J. Zinserling and A. Hoeft, *Comparative pharmacodynamic modeling of the electroencephalography-slowng effect of isoflurane, sevoflurane, and desflurane*. Anesthesiology, 1999. **91**(2): p. 397-405.
106. R.K. Ellerkmann, V.M. Liermann, T.M. Alves, I. Wenningmann, S. Kreuer, W. Wilhelm, et al., *Spectral entropy and bispectral index as measures of the electroencephalographic effects of sevoflurane*. Anesthesiology, 2004. **101**(6): p. 1275-82.
107. J. Mourisse, J. Lerou, M. Struys, M. Zwarts and L. Booij, *Multi-level approach to anaesthetic effects produced by sevoflurane or propofol in humans: 1. BIS and blink reflex*. Br J Anaesth, 2007. **98**(6): p. 737-745.
108. E. Olofsen, J.W. Sleight and A. Dahan, *The influence of remifentanil on the dynamic relationship between sevoflurane and surrogate anesthetic effect measures derived from the EEG*. Anesthesiology, 2002. **96**(3): p. 555-64.
109. M. Soehle, R.K. Ellerkmann, M. Grube, M. Kuech, S. Wirz, A. Hoeft, et al., *Comparison between bispectral index and patient state index as measures of the electroencephalographic effects of sevoflurane*. Anesthesiology, 2008. **109**(5): p. 799-805.
110. R.R. Kennedy, C. Minto and A. Seethepalli, *Effect-site half-time for burst suppression is longer than for hypnosis during anaesthesia with sevoflurane*. Br J Anaesth, 2008. **100**(1): p. 72-7.

111. I.D. McKay, L.J. Voss, J.W. Sleight, J.P. Barnard and E.K. Johannsen, *Pharmacokinetic-pharmacodynamic modeling the hypnotic effect of sevoflurane using the spectral entropy of the electroencephalogram*. *Anesth Analg*, 2006. **102**(1): p. 91-7.
112. T. Matsuura, Y. Oda, K. Tanaka, T. Mori, K. Nishikawa and A. Asada, *Advance of age decreases the minimum alveolar concentrations of isoflurane and sevoflurane for maintaining bispectral index below 50*. *Br J Anaesth*, 2009. **102**(3): p. 331-5.
113. S. Loewe, *The problem of synergism and antagonism of combined drugs*. *Arzneimittelforschung*, 1953. **3**(6): p. 285-90.
114. C.I. Bliss, *The toxicity of poisons applied jointly*. *Ann Appl Biol*, 1939. **26**(3): p. 585-615.
115. M.C. Berenbaum, *Criteria for analyzing interactions between biologically active agents*. *Adv Cancer Res*, 1981. **35**: p. 269-335.
116. M.C. Berenbaum, *What is synergy? [published erratum appears in Pharmacol Rev 1990 Sep;41(3):422]*. *Pharmacol Rev*, 1989. **41**(2): p. 93-141.
117. W.H. Carter, Jr., *Relating isobolograms to response surfaces*. *Toxicology*, 1995. **105**(2-3): p. 181-8.
118. P.K. Gessner, *Isobolographic analysis of interactions: an update on applications and utility*. *Toxicology*, 1995. **105**(2-3): p. 161-179.
119. W.R. Greco, G. Bravo and J.C. Parsons, *The search for synergy: a critical review from a response surface perspective*. *Pharmacol Rev*, 1995. **47**(2): p. 331-85.
120. R.J. Tallarida, *An overview of drug combination analysis with isobolograms*. *J Pharmacol Exp Ther*, 2006. **319**(1): p. 1-7.
121. C.D. LaPierre, K.B. Johnson, B.R. Randall, J.L. White, T.D. Egan, L. Yang, et al., *An exploration of remifentanil-propofol combinations that lead to a loss of response to esophageal instrumentation, a loss of responsiveness, and/or onset of intolerable ventilatory depression*. *Anesth Analg*, 2011. **113**(3): p. 441-3.
122. C.F. Minto, T.W. Schnider, T.G. Short, K.M. Gregg, A. Gentilini and S.L. Shafer, *Response surface model for anesthetic drug interactions*. *Anesthesiology*, 2000. **92**(6): p. 1603-16.
123. W.H. Carter, C. Gennings, J.G. Staniswalis, E.D. Campbell and K.L. White, *A statistical approach to the construction and analysis of isobolograms*. *Int J of Toxicology*, 1988. **7**(7): p. 963-973.
124. C. Gennings, W.H. Carter, E.D. Campbell, J.G. Staniswalis, T.J. Martin, B.R. Martin, et al., *Isobolographic characterization of drug interactions incorporating biological variability*. *J Pharmacol Exp Ther*, 1990. **252**(1): p. 208-217.
125. J.L. Plummer and T.G. Short, *Statistical modeling of the effects of drug combinations*. *J Pharmacol Methods*, 1990. **23**(4): p. 297-309.
126. S.G. Machado and G.A. Robinson, *A direct, general approach based on isobolograms for assessing the joint action of drugs in pre-clinical experiments*. *Stat Med*, 1994. **13**(22): p. 2289-309.
127. W.R. Greco, H.S. Park and Y.M. Rustum, *Application of a new approach for the quantitation of drug synergism to the combination of cis-diamminedichloroplatinum and 1-beta-D-arabinofuranosylcytosine*. *Cancer Res*, 1990. **50**(17): p. 5318-27.
128. S.C. Manyam, D.K. Gupta, K.B. Johnson, J.L. White, N.L. Pace, D.R. Westenskow, et al., *When is a bispectral index of 60 too low? Rational processed electroencephalographic targets are dependent on the sedative-opioid ratio*. *Anesthesiology*, 2007. **106**(3): p. 472-483.
129. P.M. Schumacher, J. Dossche, E.P. Mortier, M. Luginbuehl, T.W. Bouillon and M.M. Struys, *Response surface modeling of the interaction between propofol and sevoflurane*. *Anesthesiology*, 2009. **111**(4): p. 790-804.
130. B. Heyse, J.H. Proost, P.M. Schumacher, T.W. Bouillon, H.E. Vereecke, D.J. Eleveld, et al., *Sevoflurane remifentanil interaction: comparison of different response surface models*. *Anesthesiology*, 2012. **116**(2): p. 311-23.

131. K.B. Johnson, N.D. Syroid, D.K. Gupta, S.C. Manyam, N.L. Pace, C.D. LaPierre, et al., *An evaluation of remifentanil-sevoflurane response surface models in patients emerging from anesthesia: Model improvement using effect-site sevoflurane concentrations*. *Anesth Analg*, 2010. **111**(2): p. 387-94.
132. N.D. Syroid, K.B. Johnson, N.L. Pace, D.R. Westenskow, D. Tyler, F. Bruhschwein, et al., *Response surface model predictions of emergence and response to pain in the recovery room: An evaluation of patients emerging from an isoflurane and fentanyl anesthetic*. *Anesth Analg*, 2010. **111**(2): p. 380-6.
133. C.D. LaPierre, K.B. Johnson, B.R. Randall, J.L. White and T.D. Egan, *An exploration of remifentanil-propofol combinations that lead to a loss of response to esophageal instrumentation, a loss of responsiveness, and/or onset of intolerable ventilatory depression*. *Anesth Analg*, 2011. **113**(3): p. 490-9.
134. T. Kazama, K. Ikeda and K. Morita, *The pharmacodynamic interaction between propofol and fentanyl with respect to the suppression of somatic or hemodynamic responses to skin incision, peritoneum incision, and abdominal wall retraction*. *Anesthesiology*, 1998. **89**(4): p. 894-906.
135. T. Kazama, K. Ikeda, K. Morita, M. Kikura, M. Doi, T. Ikeda, et al., *Comparison of the effect-site $k(e)0$ s of propofol for blood pressure and EEG bispectral index in elderly and younger patients*. *Anesthesiology*, 1999. **90**(6): p. 1517-27.
136. J. Vuyk, F.H. Engbers, A.G. Burm, A.A. Vletter, G.E. Griever, E. Olofsen, et al., *Pharmacodynamic interaction between propofol and alfentanil when given for induction of anesthesia*. *Anesthesiology*, 1996. **84**(2): p. 288-99.
137. T.G. Short, J.L. Plummer and P.T. Chui, *Hypnotic and anaesthetic interactions between midazolam, propofol and alfentanil*. *Br J Anaesth*, 1992. **69**(2): p. 162-7.
138. J.F.A. Hendrickx, E.I. Eger, J.M. Sonner and S.L. Shafer, *Is synergy the rule? A review of anesthetic interactions a producing hypnosis and immobility*. *Anesth Analg*, 2008. **107**(2): p. 494-506.
139. H.R. Vinik, E.L. Bradley, Jr. and I. Kissin, *Triple anesthetic combination: propofol-midazolam-alfentanil*. *Anesth Analg*, 1994. **78**(2): p. 354-8.
140. S. McClune, A.C. McKay, P.M. Wright, C.C. Patterson and R.S. Clarke, *Synergistic interaction between midazolam and propofol*. *Br J Anaesth*, 1992. **69**(3): p. 240-5.
141. J. Vuyk, B.J. Lichtenbelt, E. Olofsen, J.W. van Kleef and A. Dahan, *Mixed-effects modeling of the influence of midazolam on propofol pharmacokinetics*. *Anesth Analg*, 2009. **108**(5): p. 1522-30.
142. B.J. Lichtenbelt, E. Olofsen, A. Dahan, J.W. van Kleef, M.M.R.F. Struys and J. Vuyk, *Propofol reduces the distribution and clearance of midazolam*. *Anesth Analg*, 2010. **110**(6): p. 1597-1606.
143. J.C. Diz, R. Del Rio, A. Lamas, M. Mendoza, M. Duran and L.M. Ferreira, *Analysis of pharmacodynamic interaction of sevoflurane and propofol on Bispectral Index during general anaesthesia using a response surface model*. *Br J Anaesth*, 2010. **104**(6): p. 733-9.
144. M. Luginbuhl, P.M. Schumacher, P. Vuilleumier, H. Vereecke, B. Heyse, T.W. Bouillon, et al., *Noxious stimulation response index: A novel anesthetic state index based on hypnotic-opioid interaction*. *Anesthesiology*, 2010. **112**(4): p. 872-80.
145. L. Yang, B. Wei, L.P. Zhang, S.S. Bi, W. Lu and X.Y. Guo, *Pharmacodynamic interaction between propofol and remifentanil on the tolerance response to electrical tetanus stimuli*. *Beijing Da Xue Xue Bao*, 2010. **42**(5): p. 547-53.
146. D.J.F. Nieuwenhuijs, E. Olofsen, R.R. Romberg, E. Sarton, D. Ward, F. Engbers, et al., *Response surface modeling of remifentanil-propofol Interaction on cardiorespiratory control and Bispectral Index*. *Anesthesiology*, 2003. **98**(2): p. 312-322.

147. J. Bruhn, T.W. Bouillon, L. Radulescu, A. Hoeft, E. Bertaccini and S.L. Shafer, *Correlation of approximate entropy, bispectral index, and spectral edge frequency 95 (SEF95) with clinical signs of "anesthetic depth" during coadministration of propofol and remifentanil*. *Anesthesiology*, 2003. **98**(3): p. 621-627.
148. S.C. Manyam, D.K. Gupta, K.B. Johnson, J.L. White, N.L. Pace, D.R. Westenskow, et al., *Opioid-volatile anesthetic synergy: a response surface model with remifentanil and sevoflurane as prototypes*. *Anesthesiology*, 2006. **105**(2): p. 267-78.
149. H.L. Wang, L. Yang, X.Y. Guo, L.P. Zhang, S.S. Bi and W. Lu, *Response surface analysis of sevoflurane-remifentanil interactions on consciousness during anesthesia*. *Chin Med J (Engl)*, 2012. **125**(15): p. 2682-7.
150. I.A. Iselin-Chaves, R. Flaishon, P.S. Sebel, S. Howell, T.J. Gan, J. Sigl, et al., *The effect of the interaction of propofol and alfentanil on recall, loss of consciousness, and the Bispectral Index*. *Anesth Analg*, 1998. **87**(4): p. 949-955.
151. D.J.M. Pavlin, B.M. Coda, D.D.P. Shen, J.P. Tschanz, Q.B. Nguyen, R.M. Schaffer, et al., *Effects of combining propofol and alfentanil on ventilation, analgesia, sedation, and emesis in human volunteers*. *Anesthesiology*, 1996. **84**(1): p. 23-37.
152. I. Ben-Shlomo, J. Finger, E. Bar-Av, A.Z. Perl, A. Etchin and M. Tverskoy, *Propofol and fentanyl act additively for induction of anaesthesia*. *Anaesthesia*, 1993. **48**(2): p. 111-3.
153. I. Ben-Shlomo, H. abd-el-Khalim, J. Ezry, S. Zohar and M. Tverskoy, *Midazolam acts synergistically with fentanyl for induction of anaesthesia*. *Br J Anaesth*, 1990. **64**(1): p. 45-7.
154. D.R. Drover, C. Litalien, V. Wellis, S.L. Shafer and G.B. Hammer, *Determination of the pharmacodynamic interaction of propofol and remifentanil during esophagogastroduodenoscopy in children*. *Anesthesiology*, 2004. **100**(6): p. 1382-1386.
155. J. Fechner, W. Hering, H. Ihmsen, T. Palmaers, J. Schuttler and S. Albrecht, *Modelling the pharmacodynamic interaction between remifentanil and propofol by EEG-controlled dosing*. *Eur J Anaesthesiol*, 2003. **20**(5): p. 373-9.
156. H. Ropcke, M. Konen-Bergmann, M. Cuhls, T. Bouillon and A. Hoeft, *Propofol and remifentanil pharmacodynamic interaction during orthopedic surgical procedures as measured by effects on bispectral index*. *J Clin Anesth*, 2001. **13**(3): p. 198-207.
157. L.L. Luo, L.X. Zhou, J. Wang, R.R. Wang, W. Huang and J. Zhou, *Effects of propofol on the minimum alveolar concentration of sevoflurane for immobility at skin incision in adult patients*. *J Clin Anesth*, 2010. **22**(7): p. 527-32.
158. R.S. Harris, O. Lazar, J.W. Johansen and P.S. Sebel, *Interaction of propofol and sevoflurane on loss of consciousness and movement to skin incision during general anesthesia*. *Anesthesiology*, 2006. **104**(6): p. 1170-1175.
159. A. Luo and K. Sugiyama, *Additive potentiation by co-application of propofol and sevoflurane on GABA-induced chloride current in cultured neurons from rat dorsal root ganglia*. *Chin Med J (Engl)*, 1999. **112**(12): p. 1138-42.
160. L.E. Sebel, J.E. Richardson, S.P. Singh, S.V. Bell and A. Jenkins, *Additive effects of sevoflurane and propofol on gamma-aminobutyric acid receptor function*. *Anesthesiology*, 2006. **104**(6): p. 1176-83.
161. P.S. Garcia, S.E. Kolesky and A. Jenkins, *General anesthetic actions on GABA(A) receptors*. *Curr Neuropharmacol*, 2010. **8**(1): p. 2-9.
162. T. Katoh, Y. Suguro, T. Kimura and K. Ikeda, *Morphine does not affect the awakening concentration of sevoflurane*. *Can J Anesth*, 1993. **40**(9): p. 825-8.
163. J.B. Gross and C.M. Alexander, *Awakening concentrations of isoflurane are not affected by analgesic doses of morphine*. *Anesth Analg*, 1988. **67**(1): p. 27-30.
164. C.L. Lake, C.A. DiFazio, J.C. Moscicki and J.S. Engle, *Reduction in halothane MAC: comparison of morphine and alfentanil*. *Anesth Analg*, 1985. **64**(8): p. 807-10.

165. H. Ropcke, H. Lier, A. Hoefl and H. Schwilden, *Isoflurane, nitrous oxide, and fentanyl pharmacodynamic interactions in surgical patients as measured by effects on median power frequency*. J Clin Anesth, 1999. **11**(7): p. 555-62.
166. P.S. Sebel, P.S. Glass, J.E. Fletcher, M.R. Murphy, C. Gallagher and T. Quill, *Reduction of the MAC of desflurane with fentanyl*. Anesthesiology, 1992. **76**(1): p. 52-9.
167. C.L. Westmoreland, P.S. Sebel and A. Gropper, *Fentanyl or alfentanil decreases the minimum alveolar anesthetic concentration of isoflurane in surgical patients*. Anesth Analg, 1994. **78**(1): p. 23-8.
168. T. Katoh, S. Kobayashi, A. Suzuki, T. Iwamoto, H. Bito and K. Ikeda, *The effect of fentanyl on sevoflurane requirements for somatic and sympathetic responses to surgical incision*. Anesthesiology, 1999. **90**(2): p. 398-405.
169. E. Lang, A. Kapila, D. Shlugman, J.F. Hoke, P.S. Sebel and P.S. Glass, *Reduction of isoflurane minimal alveolar concentration by remifentanyl*. Anesthesiology, 1996. **85**(4): p. 721-8.
170. T. Kazama, K. Ikeda and K. Morita, *Reduction by fentanyl of the Cp50 values of propofol and hemodynamic responses to various noxious stimuli*. Anesthesiology, 1997. **87**(2): p. 213-27.
171. J. Vuyk, T. Lim, F.H. Engbers, A.G. Burm, A.A. Vletter and J.G. Bovill, *The pharmacodynamic interaction of propofol and alfentanil during lower abdominal surgery in women*. Anesthesiology, 1995. **83**(1): p. 8-22.
172. J. Yumura, Y. Koukita, K. Fukuda, Y. Kaneko and T. Ichinohe, *Low dose of fentanyl reduces predicted effect-site concentration of propofol for flexible laryngeal mask airway insertion*. J Anesth, 2009. **23**(2): p. 203-8.
173. E. Jacqz-Aigrain and B.J. Anderson, *Pain control: Non-steroidal anti-inflammatory agents*. Semin Fetal Neonatal Med, 2006. **11**(4): p. 251-259.
174. I. Cattabriga, D. Pacini, G. Lamazza, F. Talarico, R. Di Bartolomeo, G. Grillone, et al., *Intravenous paracetamol as adjunctive treatment for postoperative pain after cardiac surgery: a double blind randomized controlled trial*. Eur J Cardiothorac Surg, 2007. **32**(3): p. 527-531.
175. I.F. Troconiz, S. Armenteros, M.V. Planelles, J. Benitez, R. Calvo and R. Dominguez, *Pharmacokinetic-Pharmacodynamic Modelling of the antipyretic effect of two oral formulations of ibuprofen*. Clin Pharmacokinet, 2000. **38**(6): p. 505-18.
176. J.G. Wagner, K.S. Albert, G.J. Szpunar and G.F. Lockwood, *Pharmacokinetics of ibuprofen in man IV: Absorption and disposition*. J Pharmacokinet Pharmacodyn, 1984. **12**(4): p. 381-399.
177. H. Li, J. Mandema, R. Wada, S. Jayawardena, P. Desjardins, G. Doyle, et al., *Modeling the onset and offset of dental pain relief by ibuprofen*. J Clin Pharmacol, 2011. **52**(1): p. 89-101.
178. N.M. Davies, *Clinical pharmacokinetics of ibuprofen. The first 30 years*. Clin Pharmacokinet, 1998. **34**(2): p. 101-54.
179. A.F. Merry, R.D. Gibbs, J. Edwards, G.S. Ting, C. Frampton, E. Davies, et al., *Combined acetaminophen and ibuprofen for pain relief after oral surgery in adults: a randomized controlled trial*. Br J Anaesth, 2010. **104**(1): p. 80-88.
180. C.A. Pierce and B. Voss, *Efficacy and safety of ibuprofen and acetaminophen in children and adults: a meta-analysis and qualitative review*. Ann Pharmacother, 2010. **44**(3): p. 489-506.
181. D.A. Perrott, T. Piira, B. Goodenough and G.D. Champion, *Efficacy and safety of acetaminophen vs ibuprofen for treating children's pain or fever: a meta-analysis*. Arch Pediatr Adolesc Med, 2004. **158**(6): p. 521-6.

182. C.K. Ong, R.A. Seymour, P. Lirk and A.F. Merry, *Combining paracetamol (acetaminophen) with nonsteroidal antiinflammatory drugs: a qualitative systematic review of analgesic efficacy for acute postoperative pain*. *Anesth Analg*, 2010. **110**(4): p. 1170-9.
183. V. Dahl, T. Dybvik, T. Steen, A.K. Aune, E.K. Rosenlund, aelig, et al., *Ibuprofen vs. acetaminophen vs. ibuprofen and acetaminophen after arthroscopically assisted anterior cruciate ligament reconstruction*. *Eur J Anaesthesiol*, 2004. **21**(06): p. 471-475.
184. S.R. Ianiro, B.G. Jeansonne, S.F. McNeal and P.D. Eleazer, *The effect of preoperative acetaminophen or a combination of acetaminophen and Ibuprofen on the success of inferior alveolar nerve block for teeth with irreversible pulpitis*. *J Endod*, 2007. **33**(1): p. 11-4.
185. K.A. Menhinick, J.L. Gutmann, J.D. Regan, S.E. Taylor and P.H. Buschang, *The efficacy of pain control following nonsurgical root canal treatment using ibuprofen or a combination of ibuprofen and acetaminophen in a randomized, double-blind, placebo-controlled study*. *Int Endod J*, 2004. **37**(8): p. 531-41.
186. H. Viitanen, N. Tuominen, H. Vaaraniemi, E. Nikanne and P. Annila, *Analgesic efficacy of rectal acetaminophen and ibuprofen alone or in combination for paediatric day-case adenoidectomy*. *Br J Anaesth*, 2003. **91**(3): p. 363-7.
187. A.E. Pickering, H.S. Bridge, J. Nolan and P.A. Stoddart, *Double-blind, placebo-controlled analgesic study of ibuprofen or rofecoxib in combination with paracetamol for tonsillectomy in children*. *Br J Anaesth*, 2002. **88**(1): p. 72-7.
188. G. Gazal and I.C. Mackie, *A comparison of paracetamol, ibuprofen or their combination for pain relief following extractions in children under general anaesthesia: a randomized controlled trial*. *Int J Paediatr Dent*, 2007. **17**(3): p. 169-77.
189. B.J. Anderson, *Comparing the efficacy of NSAIDs and paracetamol in children*. *Paediatr Anaesth*, 2004. **14**(3): p. 201-17.
190. N.H. Holford and L.B. Sheiner, *Understanding the dose-effect relationship: clinical application of pharmacokinetic-pharmacodynamic models*. *Clin Pharmacokinet*, 1981. **6**(6): p. 429-53.
191. D.R. Mehlich, S. Aspley, S.E. Daniels, K.A. Southerden and K.S. Christensen, *A single-tablet fixed-dose combination of racemic ibuprofen/paracetamol in the management of moderate to severe postoperative dental pain in adult and adolescent patients: a multicenter, two-stage, randomized, double-blind, parallel-group, placebo-controlled, factorial study*. *Clin Ther*, 2010. **32**(6): p. 1033-49.
192. Quadtech Associates. *GraphExtract*. [cited 2011 March 10]; version 2.1:[Available from: <http://quadtechassociates.com/9101.html>].
193. B. Anderson, G. Woollard and N. Holford, *Acetaminophen analgesia in children: placebo effect and pain resolution after tonsillectomy*. *Eur J Clin Pharmacol*, 2001. **57**(8): p. 559-569.
194. B.J. Anderson, G.A. Woollard and N.H.G. Holford, *A model for size and age changes in the pharmacokinetics of paracetamol in neonates, infants and children*. *Br J Clin Pharmacol*, 2000. **50**(2): p. 125-134.
195. L.F. Prescott, *Paracetamol (acetaminophen). A Critical Bibliographic Review*. 2nd ed. 2000, London: Taylor and Francis Publishers.
196. B. Efron and R. Tibshirani, *Bootstrap methods for standard errors, confidence intervals, and other measures of statistical accuracy*. *Statistical Science*, 1986. **1**(1): p. 54-77.
197. D.C. Brater, *Effects of nonsteroidal anti-inflammatory drugs on renal function: focus on cyclooxygenase -2-selective inhibition*. *Am J Med*, 1999. **107**(6, Supplement 1): p. 65-70.
198. G. Ciabattini, G.A. Cinotti, A. Pierucci, B.M. Simonetti, M. Manzi, F. Pugliese, et al., *Effects of sulindac and ibuprofen in patients with chronic glomerular disease. Evidence for the dependence of renal function on prostacyclin*. *N Engl J Med*, 1984. **310**(5): p. 279-83.

199. M.T. Kelley, P.D. Walson, J.H. Edge, S. Cox and M.E. Mortensen, *Pharmacokinetics and pharmacodynamics of ibuprofen isomers and acetaminophen in febrile children*. Clin Pharmacol Ther, 1992. **52**(2): p. 181-9.
200. A. Rigouzzo, F. Servin and I. Constant, *Pharmacokinetic-pharmacodynamic modeling of propofol in children*. Anesthesiology, 2010. **113**(2): p. 343-352
201. P. Jacqmin, E. Snoeck, E.A. van Schaick, R. Gieschke, P. Pillai, J.L. Steimer, et al., *Modelling response time profiles in the absence of drug concentrations: Definition and performance evaluation of the K-PD model*. J Pharmacokinet Pharmacodyn, 2007. **34**(1): p. 57-85.
202. T.G. Short, T.Y. Ho, C.F. Minto, T.W. Schnider and S.L. Shafer, *Efficient trial design for eliciting a pharmacokinetic-pharmacodynamic model-based response surface describing the interaction between two intravenous anesthetic drugs*. Anesthesiology, 2002. **96**(2): p. 400-8.
203. H.F. Miranda, M.M. Puig, J.C. Prieto and G. Pinardi, *Synergism between paracetamol and nonsteroidal anti-inflammatory drugs in experimental acute pain*. Pain, 2006. **121**(1-2): p. 22-8.
204. A.H. Thomson and H.L. Elliott, *Designing simple PK-PD studies in children*. Pediatr Anesth, 2011. **21**(3): p. 190-6.
205. J.A. Hannam and B.J. Anderson, *Explaining the acetaminophen-ibuprofen analgesic interaction using a response surface model*. Paediatr Anaesth, 2011. **21**(12): p. 1234-1240.
206. J.F. Standing, D. Tibboel, R. Korpela and K.T. Olkkola, *Diclofenac pharmacokinetic meta-analysis and dose recommendations for surgical pain in children aged 1-12 years*. Pediatr Anesth, 2011. **21**(3): p. 316-324.
207. C.D. van der Marel, B.J. Anderson, J. Romsing, E. Jacqz-Aigrain and D. Tibboel, *Diclofenac and metabolite pharmacokinetics in children*. Paediatr Anaesth, 2004. **14**(6): p. 443-51.
208. J.F. Standing, R.F. Howard, A. Johnson, I. Savage and I.C. Wong, *Population pharmacokinetics of oral diclofenac for acute pain in children*. Br J Clin Pharmacol, 2008. **66**(6): p. 846-53.
209. J. Rømsing, D. Østergaard, T. Senderovitz, D. Drozdiewicz, J. Sonne and G. Ravn, *Pharmacokinetics of oral diclofenac and acetaminophen in children after surgery*. Pediatr Anesth, 2001. **11**(2): p. 205-213.
210. B.P. Schachtel, J.M. Fillingim, W.R. Thoden, A.C. Lane and R.I. Baybutt, *Sore throat pain in the evaluation of mild analgesics*. Clin Pharmacol Ther, 1988. **44**(6): p. 704-11.
211. S. Olsen, M.F. Nolan and S. Kori, *Pain measurement. An overview of two commonly used methods*. Anesthesiol Rev, 1992. **19**(6): p. 11-5.
212. R.S. Hannallah, L.M. Broadman, A.B. Belman, M.D. Abramowitz and B.S. Epstein, *Comparison of caudal and ilioinguinal/iliohypogastric nerve blocks for control of post-orchiopey pain in pediatric ambulatory surgery*. Anesthesiology, 1987. **66**(6): p. 832-4.
213. L.M. Rusy, C.S. Houck, L.J. Sullivan, L.A. Ohlms, D.T. Jones, T.J. McGill, et al., *A double-blind evaluation of ketorolac tromethamine versus acetaminophen in pediatric tonsillectomy: analgesia and bleeding*. Anesth Analg, 1995. **80**(2): p. 226-229.
214. Summary: Ministerial Inquiry into the Auckland Power Supply Failure, in The New Zealand Herald. 1998: Auckland, NZ. Available from: http://www.nzherald.co.nz/energy/news/article.cfm?c_id=37&objectid=3400502.
215. B.J. Anderson and N.H. Holford, *Mechanism-based concepts of size and maturity in pharmacokinetics*. Annu Rev Pharmacol Toxicol, 2008. **48**: p. 303-32.
216. T. Bouillon, *Hypnotic and opioid anesthetic drug interactions on the CNS, focus on response surface models*, in *Modern Anesthetics. Handbook of Experimental Pharmacology 182*, J. Schuttler and H. Schwilden, Editors. 2008, Springer - Verlag: Berlin. p. 480-481.
217. J.A. Hannam and B.J. Anderson, *Contribution of morphine and morphine-6-glucuronide to respiratory depression in a child*. Anaesth Intensive Care, 2012. **40**(5): p. 861-6.

218. M.A. Björnsson and U.S. Simonsson, *Modelling of pain intensity and informative dropout in a dental pain model after naproxen, naproxen and placebo administration*. Br J Clin Pharmacol, 2011. **71**(6): p. 899-906.
219. M.C. Wu and R.J. Carroll, *Estimation and comparison of changes in the presence of informative right censoring by modeling the censoring process*. Biometrics, 1988. **44**(1): p. 175-188.
220. C. Hu and M.E. Sale, *A joint model for nonlinear longitudinal data with informative dropout*. J Pharmacokinet Pharmacodyn, 2003. **30**(1): p. 83-103.
221. P. Patel, H. Mulla, S. Tanna and H. Pandya, *Facilitating pharmacokinetic studies in children: a new use of dried blood spots*. Archives of disease in childhood, 2010. **95**(6): p. 484-7.
222. S. Suraseranivongse, U. Santawat, K. Kraiprasit, S. Petcharatana, S. Prakkamodom and N. Muntraporn, *Cross-validation of a composite pain scale for preschool children within 24 hours of surgery*. Br J Anaesth, 2001. **87**(3): p. 400-5.
223. D.C. Tyler, A. Tu, J. Douthit and C.R. Chapman, *Toward validation of pain measurement tools for children: a pilot study*. Pain, 1993. **52**(3): p. 301-309.
224. J.E. Montgomery, C.J. Sutherland, I.G. Kestin and J.R. Sneyd, *Morphine consumption in patients receiving rectal paracetamol and diclofenac alone and in combination*. Br J Anaesth, 1996. **77**(4): p. 445-7.
225. B. Munishankar, P. Fettes, C. Moore and G.A. McLeod, *A double-blind randomised controlled trial of paracetamol, diclofenac or the combination for pain relief after caesarean section*. Int J Obstet Anesth, 2008. **17**(1): p. 9-14.
226. S.M. Siddik, M.T. Aouad, M.I. Jalbout, L.B. Rizk, G.H. Kamar and A.S. Baraka, *Diclofenac and/or propacetamol for postoperative pain management after cesarean delivery in patients receiving patient controlled analgesia morphine*. Reg Anesth Pain Med, 2001. **26**(4): p. 310-5.
227. R.W. Matthews, C.M. Scully and B.G. Levers, *The efficacy of diclofenac sodium (Voltarol) with and without paracetamol in the control of post-surgical dental pain*. Br Dent J, 1984. **157**(10): p. 357-9.
228. E.K. Breivik, P. Barkvoll and E. Skovlund, *Combining diclofenac with acetaminophen or acetaminophen-codeine after oral surgery: a randomized, double-blind single-dose study*. Clin Pharmacol Ther, 1999. **66**(6): p. 625-35.
229. W. Riad and A. Moussa, *Pre-operative analgesia with rectal diclofenac and/or paracetamol in children undergoing inguinal hernia repair*. Anaesthesia, 2007. **62**(12): p. 1241-5.
230. L.B. Sheiner, *A new approach to the analysis of analgesic drug trials, illustrated with bromfenac data*. Clin Pharmacol Ther, 1994. **56**(3): p. 309-22.
231. H. Schwilden, J. Fechner, S. Albrecht, W. Hering, H. Ihmsen and J. Schuttler, *Testing and modelling the interaction of alfentanil and propofol on the EEG*. Eur J Anaesthesiol, 2003. **20**(5): p. 363-72.
232. Y.H. Tam, *CCIP (Computer Controlled Infusion Pump) Version 2.4*. 2012, Department of Anaesthesia and Intensive Care, The Chinese University of Hong Kong.
233. T. Gin, M.A. Gregory, K. Chan, T. Buckley and T.E. Oh, *Pharmacokinetics of propofol in women undergoing elective caesarean section*. Br J Anaesth, 1990. **64**(2): p. 148-153.
234. B.D. Lacroix, L.E. Friberg and M.O. Karlsson, *Evaluation of IPPSE, an alternative method for sequential population PK/PD analysis*. J Pharmacokinet Pharmacodyn, 2012. **39**(2): p. 177-93.
235. L. Zhang, S.L. Beal and L.B. Sheiner, *Simultaneous vs. sequential analysis for population PK/PD data I: best-case performance*. J Pharmacokinet Pharmacodyn, 2003. **30**(6): p. 387-404.

236. J.E. Ahn, M.O. Karlsson, A. Dunne and T.M. Ludden, *Likelihood based approaches to handling data below the quantification limit using NONMEM VI*. J Pharmacokinet Pharmacodyn, 2008. **35**(4): p. 401-21.
237. S.L. Beal, *Ways to fit a PK model with some data below the quantification limit*. J Pharmacokinet Pharmacodyn, 2001. **28**(5): p. 481-504.
238. M. Bergstrand, A.C. Hooker, J.E. Wallin and M.O. Karlsson, *Prediction-corrected visual predictive checks for diagnosing nonlinear mixed-effects models*. Aaps J, 2011. **13**(2): p. 143-51.
239. M.M. Struys, M.J. Coppens, N. De Neve, E.P. Mortier, A.G. Doufas, J.F. Van Bocxlaer, et al., *Influence of administration rate on propofol plasma-effect site equilibration*. Anesthesiology, 2007. **107**(3): p. 386-96.
240. A.G. Doufas, M. Bakhshandeh, A.R. Bjorksten, S.L. Shafer and D.I. Sessler, *Induction speed is not a determinant of propofol pharmacodynamics*. Anesthesiology, 2004. **101**(5): p. 1112-21.
241. R.K. Ellerkmann, M. Soehle, T.M. Alves, V.-M. Liermann, I. Wenningmann, H. Roepcke, et al., *Spectral Entropy and Bispectral Index as measures of the electroencephalographic effects of propofol*. Anesth Analg, 2006. **102**(5): p. 1456-1462.
242. M.G. Irwin, T.W.C. Hui, S.E. Milne and G.N.C. Kenny, *Propofol effective concentration 50 and its relationship to bispectral index*. Anaesthesia, 2002. **57**(3): p. 242-248.
243. J.C. Scott, K.V. Ponganis and D.R. Stanski, *EEG quantitation of narcotic effect: the comparative pharmacodynamics of fentanyl and alfentanil*. Anesthesiology, 1985. **62**(3): p. 234-41.
244. M. Soehle, M. Kuech, M. Grube, S. Wirz, S. Kreuer, A. Hoeft, et al., *Patient state index vs bispectral index as measures of the electroencephalographic effects of propofol*. Br J Anaesth, 2010. **105**(2): p. 172-8.
245. P. Wiczling, A. Bienert, P. Sobczynski, R. Hartmann-Sobczynska, K. Bieda, A. Marcinkowska, et al., *Pharmacokinetics and pharmacodynamics of propofol in patients undergoing abdominal aortic surgery*. Pharmacol Rep, 2012. **64**(1): p. 113-22.
246. G.A. Campbell, D.J. Morgan, K. Kumar and D.P. Crankshaw, *Extended blood collection period required to define distribution and elimination kinetics of propofol*. Br J Clin Pharmacol, 1988. **26**(2): p. 187-90.
247. C. Lysakowski, L. Dumont, M. Pellégrini, F. Clergue and E. Tassonyi, *Effects of fentanyl, alfentanil, remifentanil and sufentanil on loss of consciousness and bispectral index during propofol induction of anaesthesia*. Br J Anaesth, 2001. **86**(4): p. 523-527.
248. American Society of Anesthesiologists. *Pharmacodynamic Interaction between Propofol and Remifentanil Regarding Hypnosis, Tolerance of Laryngoscopy, Bispectral Index, and Electroencephalographic Approximate Entropy*. 2004 [cited 2012 23 August]; Available from:
http://journals.lww.com/anesthesiology/Fulltext/2004/06000/Pharmacodynamic_Inte_raction_between_Propofol_and.6.aspx.
249. J.R. Varvel, D.L. Donoho and S.L. Shafer, *Measuring the predictive performance of computer-controlled infusion pumps*. J Pharmacokinet Biopharm, 1992. **20**(1): p. 63-94.
250. K. Masui, R.N. Upton, A.G. Doufas, J.F. Coetzee, T. Kazama, E.P. Mortier, et al., *The performance of compartmental and physiologically based recirculatory pharmacokinetic models for propofol: a comparison using bolus, continuous, and target-controlled infusion data*. Anesth Analg, 2010. **111**(2): p. 368-79.
251. P.S. Glass, S.L. Shafer and J.G. Reves, *Intravenous drug delivery systems*, in *Miller's anesthesia*, R. Miller, Editor. 2005, Elsevier (Churchill Livingstone): Philadelphia, Pennsylvania. p. 439-80.

252. J. Vuyk, F.H. Engbers, A.G. Burm, A.A. Vletter and J.G. Bovill, *Performance of computer-controlled infusion of propofol: an evaluation of five pharmacokinetic parameter sets*. *Anesth Analg*, 1995. **81**(6): p. 1275-82.
253. P.S. Glass, T.J. Gan, S. Howell and B. Ginsberg, *Drug Interactions: Volatile anesthetics and opioids*. *J Clin Anesth*, 1997. **9**(6, Supplement 1): p. 18S-22S.
254. M.D. Brunner, P. Braithwaite, R. Jhaveri, A.I. McEwan, D.K. Goodman, L.R. Smith, et al., *MAC reduction of isoflurane by sufentanil*. *Br J Anaesth*, 1994. **72**(1): p. 42-6.
255. Minto C. F., Schnider T. W. and S.S. L., *Pharmacokinetics and pharmacodynamics of remifentanil. II. Model application*. *Anesthesiology*, 1997. **86**(1): p. 24-33.
256. C. Minto. *PK PD Tools for Excel*. 2009 20 April 2011 [cited 2012 22 October]; Available from: <http://pkpdtools.com/doku.php/downloads:start>.
257. J.F. Coetzee, J.B. Glen, V.A. Wium and L. Boshoff, *Pharmacokinetic model selection for target controlled infusions of propofol: Assessment of three parameter sets*. *Anesthesiology*, 1995. **82**(6): p. 1328-1345.
258. P. Sepúlveda, L.I. Cortínez, C. Sáez, A. Penna, S. Solari, I. Guerra, et al., *Performance evaluation of paediatric propofol pharmacokinetic models in healthy young children*. *Br J Anaesth*, 2011. **107**(4): p. 593-600.
259. P.S. Glass and I.J. Rampil, *Automated anesthesia: fact or fantasy?* *Anesthesiology*, 2001. **95**(1): p. 1-2.
260. N. Liu, T. Chazot, S. Hamada, A. Landais, N. Boichut, C. Dussaussoy, et al., *Closed-loop coadministration of propofol and remifentanil guided by Bispectral Index: A randomized multicenter study*. *Anesth Analg*, 2011. **112**(3): p. 546-557.
261. T. Kazama, K. Morita, T. Ikeda, T. Kurita and S. Sato, *Comparison of predicted induction dose with predetermined physiologic characteristics of patients and with pharmacokinetic models incorporating those characteristics as covariates*. *Anesthesiology*, 2003. **98**(2): p. 299-305.
262. P. Sepúlveda and X. Mora, *Reevaluation of the time course of the effect of propofol described with the Schnider pharmacokinetic model*. *Rev Esp Anestesiología Reanim*, 2012. **59**(10): p. 542-8.
263. M.M. Struys, T. De Smet, L.F. Versichelen, S. Van De Velde, R. Van den Broecke and E.P. Mortier, *Comparison of closed-loop controlled administration of propofol using Bispectral Index as the controlled variable versus "standard practice" controlled administration*. *Anesthesiology*, 2001. **95**(1): p. 6-17.
264. A. Absalom, R. De Keyser and M. Struys, *Closed loop anesthesia: Are we getting close to finding the holy grail?* *Anesth Analg*, 2011. **112**(3): p. 516-518.
265. A. Morley, J. Derrick, P. Mainland, B.B. Lee and T.G. Short, *Closed loop control of anaesthesia: an assessment of the bispectral index as the target of control*. *Anaesthesia*, 2000. **55**(10): p. 953-9.
266. Y.H. Tam, *Monitor (for PC) Version 5.0*. 2012, Department of Anaesthesia and Intensive Care, The Chinese University of Hong Kong.
267. T.G. Short, D.C. Galletly and J.L. Plummer, *Hypnotic and anaesthetic action of thiopentone and midazolam alone and in combination*. *Br J Anaesth*, 1991. **66**(1): p. 13-9.
268. M.J. Mertens, E. Olofsen, A.G. Burm, J.G. Bovill and J. Vuyk, *Mixed-effects modeling of the influence of alfentanil on propofol pharmacokinetics*. *Anesthesiology*, 2004. **100**(4): p. 795-805.
269. J. Bruhn, T.W. Bouillon and S.L. Shafer, *Bispectral index (BIS) and burst suppression: revealing a part of the BIS algorithm*. *Journal of clinical monitoring and computing*, 2000. **16**(8): p. 593-6.

270. O.G. Wilder-Smith, P. Ravussin, L. Decosterd, P. Despland and B. Bissonnette, *Midazolam premedication reduces propofol dose requirements for multiple anesthetic endpoints*. *Can J Anesth*, 2001. **48**(5): p. 439-445.
271. E. Sigel and B.P. Luscher, *A closer look at the high affinity benzodiazepine binding site on GABAA receptors*. *Curr Top Med Chem*, 2011. **11**(2): p. 241-6.
272. R. Jurd, M. Arras, S. Lambert, B. Drexler, R. Siegwart, F. Crestani, et al., *General anesthetic actions in vivo strongly attenuated by a point mutation in the GABAA receptor β 3 subunit*. *FASEB J*, 2002. **17**(2): p. 250-2.
273. I. Kissin, H.R. Vinik, R. Castillo and E.L. Bradley, Jr., *Alfentanil potentiates midazolam-induced unconsciousness in subanalgesic doses*. *Anesth Analg*, 1990. **71**(1): p. 65-9.
274. H.R. Vinik, E.L. Bradley, Jr. and I. Kissin, *Midazolam-alfentanil synergism for anesthetic induction in patients*. *Anesth Analg*, 1989. **69**(2): p. 213-217.
275. Y. Inagaki, K. Sumikawa and I. Yoshiya, *Anesthetic interaction between midazolam and halothane in humans*. *Anesth Analg*, 1993. **76**(3): p. 613-7.
276. P. Sepúlveda, L.I. Cortínez, A. Recart and H. Muñoz, *Predictive ability of propofol effect-site concentrations during fast and slow infusion rates*. *Acta Anaesthesiol Scand*, 2010. **54**(4): p. 447-452.
277. J. Vuyk, M.J. Mertens, E. Olofsen, A.G. Burm and J.G. Bovill, *Propofol anesthesia and rational opioid selection: determination of optimal EC50-EC95 propofol-opioid concentrations that assure adequate anesthesia and a rapid return of consciousness*. *Anesthesiology*, 1997. **87**(6): p. 1549-62.
278. T. Gin, *Clinical pharmacology on display*. *Anesth Analg*, 2010. **111**(2): p. 256-258.
279. B.J. Lichtenbelt, M. Mertens and J. Vuyk, *Strategies to optimise propofol-opioid anaesthesia*. *Clin Pharmacokinet*, 2004. **43**(9): p. 577-93.
280. *BIS Titration SimulatOR*, in *BIS EDUCATION*. 2011, Covidien: Boulder, CO, USA.
281. *HPS interface; Simulation interface software*, AQAI Simulation Center: Mainz, Germany.
282. P. De Paepe, F.M. Belpaire and W.A. Buylaert, *Pharmacokinetic and pharmacodynamic considerations when treating patients with sepsis and septic shock*. *Clin Pharmacokinet*, 2002. **41**(14): p. 1135-51.
283. B.A. Boucher, G.C. Wood and J.M. Swanson, *Pharmacokinetic changes in critical illness*. *Crit Care Clin*, 2006. **22**(2): p. 255-271.
284. T. Johnson, K. Boussery, K. Rowland-Yeo, G. Tucker and A. Rostami-Hodjegan, *A semi-mechanistic model to predict the effects of liver cirrhosis on drug clearance*. *Clin Pharmacokinet*, 2010. **49**(3): p. 189-206.
285. C. Richard, A. Berdeaux, F. Delion, B. Riou, A. Rimailho, J.F. Giudicelli, et al., *Effect of mechanical ventilation on hepatic drug pharmacokinetics*. *Chest*, 1986. **90**(6): p. 837-41.
286. S. Rietbrock, H. Wissing, I. Kuhn and U. Fuhr, *Pharmacokinetics of inhaled anaesthetics in a clinical setting: description of a novel method based on routine monitoring data*. *Br J Anaesth*, 2000. **84**(4): p. 437-42.
287. K.B. Johnson, N.D. Syroid, D.K. Gupta, S.C. Manyam, T.D. Egan, J. Huntington, et al., *An evaluation of remifentanil propofol response surfaces for loss of responsiveness, loss of response to surrogates of painful stimuli and laryngoscopy in patients undergoing elective surgery*. *Anesth Analg*, 2008. **106**(2): p. 471-479.
288. C. Van Boxtel, Holford N.H. and M. Danhof, eds. *In vivo study of drug action*. 1992, Elsevier: Amsterdam. p. 402-405.
289. M. Struys, T. De Smet and E.P. Mortier, *Simulated drug administration: An emerging tool for teaching clinical pharmacology during anesthesiology training*. *Clin Pharmacol Ther*, 2008. **84**(1): p. 170-174.
290. N. de Beer, W. van Meurs, M. Grit, M. Good and D. Gravenstein, *Educational simulation of the electroencephalogram (EEG)*. *Technol Health Care*, 2001. **9**: p. 237-56.

-
291. A. Castro, E. Amadeu, P. Sa Couto, P. Amorim and C. Nunes, *Educational software for Bispectral Index simulation [Abstract]*, in American Society of Anesthesiologists. 2008. Available from: <http://www.asaabstracts.com/strands/asaabstracts/abstract.htm;jsessionid=715D4C8E EB8AACA10F9AE0CA25F8E1D9?year=2008&index=7&absnum=1745>.
292. S. Greenwald, S. Mersrobian and S. Kelley, *BIS-SIM: A new EEG simulator for demonstrating the effects of anesthesia on the brain [Abstract]*, in International Meeting on Medical Simulation. 2003. San Diego, CA.
293. D. Cumin, J.M. Weller, K. Henderson and A.F. Merry, *Standards for simulation in anaesthesia: creating confidence in the tools*. Br J Anaesth, 2010. **105**(1): p. 45-51.
294. P. Dieckmann, D. Gaba and M. Rall, *Deepening the theoretical foundations of patient simulation as social practice*. Simul Healthc, 2007. **2**(3): p. 183-93.
295. J.W. Rudolph, R. Simon and D.B. Raemer, *Which reality matters? Questions on the path to high engagement in healthcare simulation*. Simul Healthc, 2007. **2**(3): p. 161-3.
296. S. Mudumbai, G. Lighthall, C. Sun, K. Harrison, F. Davies and S. Howard, *Reproducibility of a model driven simulator and sensitivity to initial conditions*. Simul Healthc, 2007. **2**(1): p. 58.
297. A. Turing, *Computing machinery and intelligence*. Mind, 1950. **59**: p. 433-60.
298. D. Cumin, A.F. Merry and J.M. Weller, *Standards for simulation*. Anaesthesia, 2008. **63**(12): p. 1281-1284.
299. N.A. Sandler, J. Hodges and M.L. Sabino, *Assessment of recovery in patients undergoing intravenous conscious sedation using bispectral analysis*. J Oral Maxillofac Surg, 2001. **59**(6): p. 603-611.
300. T.J. Gan, P.S. Glass, S.T. Howell, A.T. Canada, A.P. Grant and B. Ginsberg, *Determination of plasma concentrations of propofol associated with 50% reduction in postoperative nausea*. Anesthesiology, 1997. **87**(4): p. 779-84.
301. B.J. Anderson, *Pediatric models for adult target-controlled infusion pumps*. Paediatr Anaesth, 2010. **20**(3): p. 223-32.
302. M. Struys, M. Sahinovic, B. Lichtenbelt, H. Vereecke and A. Absalom, *Optimizing intravenous drug administration by applying pharmacokinetic/pharmacodynamic concepts*. Br J Anaesth, 2011. **107**(1): p. 38-47.
303. J.F. Cheeseman, A.F. Merry, M.D.M. Pawley, R.L. De Souza and G.R. Warman, *The effect of time of day on the duration of neuromuscular blockade elicited by rocuronium*. Anaesthesia, 2007. **62**(11): p. 1114-1120.
304. A.L. Potts, J.F. Cheeseman and G.R. Warman, *Circadian rhythms and their development in children: implications for pharmacokinetics and pharmacodynamics in anesthesia*. Paediatr Anesth, 2011. **21**(3): p. 238-246.
305. M.Y.M. Peeters, S.A. Prins, C.A.J. Knibbe, J. DeJongh, R.H.N. van Schaik, M. van Dijk, et al., *Propofol pharmacokinetics and pharmacodynamics for depth of sedation in nonventilated Infants after major craniofacial surgery*. Anesthesiology, 2006. **104**(3): p. 466-474.